UNIVERSIDADE FEDERAL DE PERNAMBUCO
CENTRO DE CIÊNCIAS EXATAS E DA NATUREZA
PROGRAMA DE PÓS-GRADUAÇÃO EM ESTATÍSTICA

CÉSAR LEONARDO BARBOSA DA SILVA

A STUDY ON THE FRACTIONAL BILINEAR TRANSFORMATION AND THE THEORY OF NEW DISTRIBUTIONS

Recife

2023

CÉSAR LEONARDO BARBOSA DA SILVA

A STUDY ON THE FRACTIONAL BILINEAR TRANSFORMATION AND THE THEORY OF NEW DISTRIBUTIONS

Tese apresentada ao Programa de Pós-Graduação em Estatística do Centro de Ciências Exatas e da Natureza na Universidade de Federal de Pernambuco, para a obtenção de Título de Doutor em Ciências, na Área de Estatística.

Área de Concentração: Estatística Aplicada.

Orientadora: Profa. Maria do Carmo Soares de Lima.

Recife

2023

Catalogação na fonte
Bibliotecária Monick Raquel Silvestre da S. Portes, CRB4-1217

S586s Silva, César Leonardo Barbosa da
A study on the fractional bilinear transformation and the theory of new distributions / César Leonardo Barbosa da Silva. – 2023.
165 f.: il., fig, tab.

Orientadora: Maria do Carmo Soares de Lima.
Tese (Doutorado) – Universidade Federal de Pernambuco. CCEN, Estatística, Recife, 2023.
Inclui referências e apêndices.

1. Estatística aplicada. 2. Probabilidade. 3. Epidemiologia. I. Lima, Maria do Carmo Soares de (orientadora). II. Título.

310 CDD (23. ed.) UFPE - CCEN 2023-72

CÉSAR LEONARDO BARBOSA DA SILVA

A STUDY ON THE FRACTIONAL BILINEAR TRANSFORMATION AND THE THEORY OF NEW DISTRIBUTIONS

Tese apresentada ao Programa de Pós-Graduação em Estatística da Universidade Federal de Pernambuco, como requisito parcial para a obtenção do título de Doutorado em Estatística.

Aprovada em: 23 de janeiro de 2023.

BANCA EXAMINADORA

_____

Profa. Dra. Maria do Carmo Soares de Lima - (orientadora) - Presidente - UFPE

_____

Profº. Dr. Hemílio Fernandes - (Titular Externo) - UFPB

_____

Prof. Dr. Marcelo Bourguignon - (Titular Externo) - UFRN

_____

Prof. Dr. Frank Sinatra - (Titular Externo) - UFRPE

_____

Prof. Dr. Cícero Carlos Brito - (Titular Externo) -IFPE

I dedicate this work to my parents, wife and friends, as well as the ones who wants to enter in the wide range of mathematics and its applications.

ACKNOWLEDGEMENTS

First of all, i thank to The Creator Power, without which, nothing who is, would be, for, far off is true existence, and very deep; who may have knowledge of it?

I thank to my parents, José Roberto and Ana Maria to help me since the beginning of my first steps to now, and then, when they shall live completely in my heart. Through the faith the fight echoes in the unseen worlds. My two sisters, Roberta and Bethânia, for the love and care.

I also thank to my lovely wife, for the support, when the path came with much stones. Without her, the journey would be harder. I still thank for the patience in leading with the absence and the periods of loneliness that i imposed to myself, reflecting on her.

I thank to my honorable adviser, Dra. Maria do Carmo, who reached out me the hand when i was alone in the battle. If i could make a choice, into the set of eligibles, i certainly would select her to be by my side in battlefield for, surely, his spirit is not the one who left behind. Thank you very much.

Worth of saying are the mentions to friends, old and new ones. I've count with veterans, Carlos Eduardo, Igor and Krishnamurti, who helped me, while in conversations about technicalities from Statistics and interactions with Physics. Lucas Miranda, Darlisson Jesus, José Jairo, Lucas Davi -Curaçá-, Daniel Matos and Saul, colleagues of classes and discussions. Thank you. The professors whose knowledge and dedication served to inspire me into the theory of Probability, branch of mathematics of wonderful applications. Finally, i recognise and thank the financial support given by CAPES during the process of research.

ABSTRACT

This work, in the area of Probability and Mathematical Statistics, has its nucleus based on the Theory of New Distributions, its properties and applications. A sequence of facts is established, ranging from a brief introductory summary, dealing with the need for new distributions, to the proposition of a class of transformations, among which, the well-known Marshal-Olkin, whose expression can be derived. This class, then, is applied according to the aforementioned transformation, to known distributions such as, for example, Exponential, Weibull, among others. Some properties are studied following the ideas behind a odd log-logistic geometric family, as well as a geometric emphasis associated with the classification of the risk function on the distributions under analysis and making references to regions where their curves - of the risk functions -, are immersed, according to a criterion developed by Qian, (QIAN, 2012). Before, however, the actual applications, some mathematical properties related to moment calculations are presented making reference to canonical methods, as well as methods under development, using non-canonical techniques and the use of the special Spence functions, (SPENCE, 1809) when solving a particular case, while integrating a function for getting expected value. The applications, an essential part of the work, are interdisciplinary in nature, moving between epidemiological data from the current global sanitary crisis, due to COVID-19, passing through physical systems that demand statistical treatment as, for example, the problem of turbulence, as well as the astrophysics problem concerning sunspots. Times of transitions from hydrodynamic regimes to turbulence are analyzed. These studies play an important role in theoretical science and applications ranging from the construction of airplanes and ships, to biological processes involving the dynamics of blood in the heart.

Keywords: epidemiology; hydrodynamics; sunspots; probability distributions; risk functions; Spence function.

RESUMO

Este trabalho, na área de Probabilidade e Estatística Matemática, tem seu núcleo baseado na Teoria de Novas Distribuições, suas propriedades e aplicações. É estabelecida uma sequência de fatos que vão, desde um breve resumo introdutório, tratando da necessidade de novas distribuições, até à proposição de uma classe de transformações, dentre as quais, a conhecida Marshal-Olkin, cuja expressão pode ser derivada. Essa classe, então, é aplicada segundo à referida transformação, a distribuições conhecidas como, por exemplo, Exponencial, Weibull, entre outras. Algumas propriedades são estudadas seguindo as ideias relacionadas a uma família geométrica log-logística, bem como uma ênfase geométrica associada à classificação da função de risco, das distribuições em análise, segundo as regiões nas quais suas curvas- das funções de risco-, estão imersas, em referência a um critério desenvolvido por Qian, (QIAN, 2012). Antes, porém, das aplicações propriamente ditas, algumas propriedades matemáticas relacionadas aos cálculos de momentos são apresentadas, fazendo-se referência a métodos canônicos, bem como métodos em desenvolvimento, usando técnicas não-canônicas, e uso de funções especiais de Spence, (SPENCE, 1809) para se resolver um caso especial de integração com o intuito de se obter o valor esperado. As aplicações, parte essencial do trabalho, têm caráter interdisciplinar, transitando entre dados epidemiológicos oriundos da atual crise sanitária mundial, devido à COVID-19, passando por aplicações em sistemas físicos que demandam tratamento estatístico como, por exemplo, o problema da turbulência, bem como o problema de astrofísica sobre manchas solares. Tempos de transições de regimes hidrodinâmicos para a turbulência são analisados. Esses estudos desempenham importante papel na ciência teórica e aplicações que vão desde a construção de aviões e navios, até processos biológicos envolvendo a dinâmica do sangue no coração.

Palavras-chaves: distribuições de probabilidade; epidemiologia; funções de risco; função de Spence; hidrodinâmica; manchas solares.

LIST OF FIGURES

LIST OF TABLES

LIST OF SYMBOLS

EXP	Exponential distribution;
EXP-EXP	Exponentiated Exponential distribution;
F	Distribution function generated by M-transform;
f	Probability density function generated by M-transform;
Ga	Gamma distribution;
Ga-FE	Gamma Frechet distribution;
KW-W	Kumaraswamy Weibull distribution;
KW-EXP	Kumaraswamy Exponential distribution;
L_x, L_y	Length defining the geometry containing the fluids;
L-EXP	Lindley Exponential distribution;
W	Weibull distribution;
EXP-W	Exponentiated Weibull distribution;
B-W	Beta Weibull distribution;
$\mathbb{R}\|_{[0,1]}$	Restriction of $\mathbb{R}$ to $[0,1]$;
Re	Reynolds number. A combination of the characteristic region size $l[cm]$, characteristic velocity $v[cms^{-1}]$ and kinematic viscosity $\nu[cm^2s^{-1}]$, $Re = \frac{lv}{\nu}$;
μ	Measure;
$\mathscr{F}$	A class of subsets of Ω called a field. In particular, it will be a σ-field if Ω is finite, meaning that it contains all the subsets of it;
$\rho_{\pm}$	Densities of heavier and lighter fluids;
X	Real measurable random variable;

CONTENTS

1 INTRODUCTION

In the field of probability distribution functions, the search for new distributions is a trend while trying to understand the behaviour of data describing a broad range of phenomena, typically of physical origins, but not always, (KOUKOULOPOULOS, 2020), when random components are present on such phenomena. Over many years, different probability distributions have been studied in terms of their structures of probability density (or mass) and cumulative distribution functions (ALZAATREH CARL LEE, 2013), as well as to their various applications in science, technology, medicine and social affairs, in order to gain insight about the underlying reality carried by the data, found in these fields. Alongside, computational advances have become even more important, both from a scientific point of view, and in the perspective of the need imposed by society to find solutions for different types of problems. Furthermore, data are arriving in ever-increasing *volume, speed and variety*. One calls this "phenomenon"*Big Data*.

Along the last decade, the vehement work in the field of developing new models has unleashed, indeed, new classes of distributions, leading to a wide growth in this branch of mathematics. The process of generating new distributions, itself, is simple under some few reasonable assumptions, and will be considered later on the text. The main ideas behind the process include the conception of a distribution generator, which give rise to a *family of distribution*. Then, starting with a given known distribution, henceforth termed *baseline* distribution, the process of developing new distributions is initiated. Of course the properties inherent from probability theory, in his initial conception, must be verified.

Additionally, the ideas carried by the transformation theory applied to ordinary functions are extended to functions of random variables, whereas its effects are then, studied. In this spirit, some transformations are imposed over distribution functions and, over data, in an attempt to turn them more readable, in some sense, (OSBORNE, 2005). The primordial questions that arise is the impact of these transformations, as can be seen, for example, in the Jansen inequality, (BILLINGSLEY, 1995). Then, once the class of transformations has been defined, the development of the class of new distributions that emerges from these, are studied. For this purpose, the ordinary strategy performed by the experts in this field, follows the path:

- A family of known distributions is selected to be used, or a new one is proposed;
- A baseline is designated to be immersed into the family previously chosen;

- The mathematical properties of the proposed distribution are verified in its consistency with the underlying theory and all the calculational consequences, such as generating functions, moments, etc, are expected to be exactly solved, when possible, or have their terms given by series expansions, when appropriate;

- The estimation process is performed by the method of maximum likelihood, Rohatgi (2003), for example;

- The asymptotic properties of estimators, through the inferential method chosen, is verified by simulation studies;

- When real data are applied to the distribution at hand, in order to test the flexibility of the proposed model, natural comparisons are made to other models in the literature.

It is possible to list several types of data sets, and current works, that have been used in the context of new distributions. Some examples follow,

- Survival analysis is one of the most active branch of Statistics in the field of new distributions theory -, (REIS; CORDEIRO; LIMA, 2022); (KUMAR et al., 2022); In this branch, real data are achieved from medical and biological sciences, among others. Some problems like time-to-effect in drugs administration, lifetime after a general surgery, survival statistics of cancer patients, (DEVI, 2015) and (RICHARD, 1974) are common arena for applications.

- Engineering, or applied sciences, make uses of pure science to implement devices and stuffs for enhancing the experience of human activity. On their diverse applicabilities, damage analysis and crack propagation make uses of fatigue analysis in materials, leading to estimate of its lifetime. This implicate, directly, in security of the systems under investigation, (VASSILOPOULOS; KELLER, 2011), (DAVIES, 1999), (BALAKRISHNAN N.; KUNDU, 2018).

- Physics. The idea and uses of *time* in Physics is fundamental. The processes and way where it enters in the description of the Laws of Nature, as Laws of Physics, (MITTELSTAEDT, 2005), depend on the branch of the latter, with which one is dealing with. In the case where the tools of Mathematical Statistics are, indeed, applied to Physics, a field called Statistical Mechanics emerge. The objective of the latter is to predict the *macroscopic* properties of systems, by using a minimal set of reasonable assumptions

concerning the *microscopic* compositions of the system under analysis. As examples, one can be lead to consider the time necessary for reaching equilibrium, in physical systems like hydrodynamical one, (FALKOVICH GREGORY; SREENIVASAN, 2006b) and governed by Fermi-Pasta-Ulam theory, (FERMI et al., 1955), (KIMMOUN, 2016). As a motivation for the transformation theory in physics, the *symmetry* concept leads to amazing results concerning conservation of some properties which can be seen, when possible, as *invariance* of those, (WEINBERG C. N. YANG, 1991). The idea, therefore, is to induce these transformations to Statistics and study the consequences of them. For example, what means to the distribution a process of inversion? What is the reflection of the latter on the mean and variance of the given distribution?

Hence, as one is introduced to the study of Probability and Statistics, the necessity for treating known probability distributions of a given set of random variables is a matter of fact. By supposing that the experiments are made such that the conditions can closely lead to approximate a known distribution $F = F(x; \boldsymbol{\xi}; \boldsymbol{\tau})$, the problem is reduced to estimate $\boldsymbol{\xi}; \boldsymbol{\tau}$- the parameter vectors of the model-, from the data by using some test, (LEHMANN, 2005), to verify the agreement with mathematical model and the data. However, in general, it is not possible to know prior information about $F(x; \boldsymbol{\xi}; \boldsymbol{\tau})$ once, in general, the conditions describing a physical experiment are complex enough, (LORENZ, 1963). In that case one tries to estimate the underlying distribution function or density function, (FRANK, 2009).

One reasonable question that could arise is concerned to the necessity of investing some effort in developing new distributions. In few words, one could defend the position, just by invoking, as a matter of fact, that the manifold of natural and experimental phenomena cannot be, in all of their magnitude, described by known distributions, remaining to the scientist the continuous search for new distributions, that can improve the results one is dealing with. An example of such an event was the problem encountered by Einstein, and described in the introduction of (COHEN, 2003), when criticizing the probabilistic nature of Boltzmann theory, concerning the entropic dynamics of thermodynamic systems. After all, once one is dealing with models, and that ones are simplifications of reality, the attempt to fit the data describing the observable phenomena is a key problem in the majority of applied sciences. In terms of statistical description, one says that the phenomena are fitted by the model. Hence, on inverse terms, the distribution that a random variable (rv) follows, determines what kind of problem it can fit.

There are cases of discrete rv's and which are suitable for situations where the observations/data belong to the set of integers. The observations belonging to the set of real numbers have the continuous rv's for their description. One still have cases in which one manages to compose discrete rv's with continuous ones, where, for example, one convex-composes continuous known distributions, W_1, W_2, with a discrete, such as, Bernstein's,

$$\begin{aligned} Y &= XW_1 + (1-X)W_2 \\ X &\sim Bern(p). \end{aligned}$$

In this sense, the proposition of new distributions has been a way to describe, besides its ordinary duty, that is to say, construct the path and pave it, in order to realize the random phenomena one encounters in Nature, and in other branches where humanity is immersed in, to describe a greater amount of database types generated from these environments. This need also comes from the fact that the scientists are increasingly interested in studying databases with a large number of observations and that portray solutions in the most diverse areas of knowledge. In Brazil, for example, the publicly traded company that operates in the energy sector, called Petrobrás, has been investing in the creation of projects and programs that can help on its innovation. Such projects incorporate, for example, digital technologies (Big Data, Machine Learning and Artificial Intelligence) in the search for solutions that make them keep up with the constantly growing development of the business.

It is important to mention certain methods and examples of how to generate new distributions, in order to give tools for the framework in which the current work will be developed. As a starting point, it is possible to present new distributions by proposing generalizations such as the one made on standard exponential distribution, leading to a new class of the later with general properties and applications, (GUPTA; GUPTA; GUPTA, 1998). In this process the modification was performed by exponentiating the aforementioned distribution leading to interesting mathematical properties, (KUNDU, 2001), giving rise to alternative possibilities because of the similarity they acquire to gamma family, for example. In (CORDEIRO; ORTEGA; CUNHA, 2013) is presented a class that extends this type of distribution leading, among other things, to tractable properties that are, indeed, desirable when simulating, specially, when treating quantile functions construction. Note that, in these constructions the parameter set is increased by the composition induced by the process and this, by itself, constitutes a new method, (MARSHALL; OLKIN, 1997). It's well known but, worth of saying, that exponential distributions play a central role in processes that time of duration of events or, stuffs, are the kernel of research. For

applications in theoretical Physics and Financial Physics, the use of superposition of Gaussian distributions, (JIZBA; KLEINERT, 2008) is a technique endorsing the simplification of equations in this field of study. In a general way, a method of convex compose distributions has profound mathematical meaning linking concepts from the topology of spaces, where the distributions are immersed, with properties derived thereof.

From those there are calculational implications in the probability density functions and quantile functions, as well as in the conceptual meaning of independence of events, (JIZBA; KLEINERT, 2008), (COZMAN, 2012). A class of problems where superpositions of statistics are applied are termed *superstatistics*, (COHEN, 2003), (BECK, 2009).

1.1 GOALS

Following the ideas just described, the main goals of this text are to develop a class of distributions by mean of a general transformation, over the Real numbers, $\mathbb{R}$, leading to interesting results with some interdisciplinary applications. For some values of parameters, a well known transformation emerges as a particular case and the classical features are extracted when applied to current new distributions over canonical baselines such, Exponential, Weibull, etc. Some properties like moments are presented in a new approach and, for some cases, in terms of analytical known special functions. In some cases, particular solutions are presented and his generalizations are proposed, without demonstration, leading it for future work. A new method for computing moments is presented, although the formal mathematical bases are under development.

Along the the research some knowledge were brought from different branches of sciences, such as Physics and Astrophysics. In the former case, when treating the phenomena of turbulence and, in the latter one, when analysing and describing the natural processes of sunspot and its associated solar blasts, as well as its potential consequences. Another issue addressed in this text will be the current pandemic. When treating the COVID-19 virus spreading, the analysis followed a specific line, say, the information captured by data disposed by State Government of Santa Catarina, even though some other approaches and techniques would have been applied during the period of pandemic by other researchers.

As an example, an interesting study in the field of distribution theory applied to the efforts related to tracking and modeling of COVID-19 spreading, is made, among many others, by Hawryluk (HAWRYLUK, 2020). The authors have shown, among other things, that the

Gamma distribution exhibited a better adjustment to the *time until death*, when compared to Weibull and log-normal distributions, among others, to in-patients affected by COVID-19. The data base used in the research came from the Brazilian Sistema de Informação de Vigilância Epidemiológica da Gripe. Additionally, when the investigation focused on the *time until the in-patients*, the authors have shown that there were strong indications that the generalized log-normal distribution would be the best among the ones under consideration.

In the same spirit, but through another approach, some models were produced by using nonlinear differential equations of the type-like SIR models for disease spreading, (FRANCO; DUTRA, 2021), (MOEIN et al., 2021); the last one pointing up to an inadequacy for the approach at hand. In any case, what matter is the endeavor of several scientists and mathematicians in order to provide relevant information for decision-makers.

Concerning the turbulence investigation two physical phenomena are simulated: the Taylor-Green and Rayleigh-Taylor processes. The simulations follow the governing equations and the data are provided and statistically analysed in order to gain insight of the underlying phenomena for potential technological applications. For Astrophysics case, the data are processed, applied to the developed distributions, as well as the other ones above in the respective cases, so that forecasts processes can be made, for future works.

The developed distributions are submitted to comparison tests with canonical ones, and recent known distributions in order to identify best adequacy to data. It is worth of saying that, as the amount of experiments in all branches of sciences increases, a huge amount of complex data is available for analysis, since elementary to advanced one. One recent example comes from LHC, The Large Hadron Collider, (Are you up for the TrackML challenge?, 2018), where a huge amount of data, (CHALLENGE, 2018), is provided.

1.2 COMPUTING PLATFORM

Throughout this text the computational platforms have been balanced between Anaconda Navigator, (ANACONDA..., 2022), through Python 3, (ROSSUM; DRAKE, 2009), on platform Spyder 5.0.5, (RAYBAUT, 2009), and RStudio environment through R software version 1.3.959, (R Core Team, 2020). The graphs of the function appearing along the pages are performed with Python graphical libraries such as matplotlib and seaborn, as well as R software graphical tools. The code implementing the hydrodynamical systems solutions are made on Python language by using the traditional libraries associated to it, with modifications on the Python

modulus pysph, (RAMACHANDRAN et al., 2021). Additional details follows at corresponding chapter addressing the simulation.

1.3 TEXT ORGANIZATION

The whole text is divided into seven main chapters and some appendices, when necessary. The second operational chapter, say, is concerned with general tools and properties associated to the family generator, by a given transformation, and some of its consequences. To be more emphatic, a class of transformations with real parameters is introduced by means of a known bilinear fractional operator, defined in $\mathbb{R}$. The parameters do assume determined values whose impacts, on probability distributions, are investigated. The results arise as reflexes on the calculus of expected values and can be extended in order to obtain higher order moments, without the need of integration process, canonical method for this end.

The third chapter deals with the family studied in this thesis work, addressing some of its main mathematical properties. It extends the family proposed by (LIMA et al., 2019) and is generated by a method which is not the same as the one addressed there. Albeit some similarities can emerge, these are indeed coincidence driven by the choices one made for the parameter values of the transformation. Different choices of parameter values would lead to different and more general types of distributions. The reason by which these values was selected was just because of the benchmark allowed by the similitude induced by the former, and to induce the nested nature of the transformation, making reference to Marshal-Olkin. Furthermore, despite of the structure between the family here pondered and the one proposed by Lima et. al (2019) bear, however, some resemblance, the reader will perceive that the additional parameter, entitled here as θ, in fact differs structurally, from the one addressed in the cited article: $(1-p)$, i.e. there's a parametric interpretation and, also, in the way on the family was built up. Some important properties are obtained, as well as the power series expansion of the probability density and cumulative distribution functions. Parameter estimation was performed using the maximum likelihood method. Some geometric properties arising from the hazard function are obtained and disposed as quadrants driving the behaviour of the data, as expressed through the mentioned function. The quantile function and moment generating function are given and some methods are discussed. The general method of estimation is presented and particularized for the concrete case, as the baselines are chosen.

The fourth chapter brings two new models using Exponential and Weibull distributions as

baselines. The Birnbaum-Saunders and Burr-XII models were used as baselines in the next two chapters, totaling four studied models of the family in question. The maximum likelihood method was used in all chapters in order to estimate the parameters involved. Additionally, simulation studies were carried out to verify the asymptotic properties of the maximum likelihood estimators for the proposed models. Finally, applications in different areas, including physics and epidemiology- for COVID-19 spreading -, were carried out to show the performance of the proposed models when compared with others existing in the literature.

A final chapter, summarizing the objects figuring in the text, as well as making reference to future works, is included. A mathematical assertive is presented with the aim of fill the potential lack of measure-preserving structure due to the wide window of possibilities for the parameter set, ϖ of M, which, in counterpart, would increase the accuracy of values for the moments calculated along the text, via the transform method. Unfortunately, it is not possible to developed all the formal mathematics concerning it, due to question of time.

Some particular applications related to the astrophysics of Sun-Earth system is encouraged as well as the the understanding of the relation of control and turbulence, via statistical times involved in the fluid flow, specially, the hypersonic one.

It is worth mentioning that, each chapter was built up in an independent way and the results here presented are of own authorship, at least out of obvious trivialities.

2 FRACTIONAL BILINEAR TRANSFORMATION

2.1 INTRODUCTION

The uses of transformations in mathematics have important consequences in solving several, formal and applied problems, (GZYL, 1983), (WESTRöM, 1971), (HUNTSVILLE., 2021). Much of them are related to geometry, for example, when one treats congruence preservation, or isometry. In some cases, the uses of transformations lead to reduction in problem dimensions which turn the problem at hand, more tractable. When dealing with coordinate transformations, canonical transformations in physics, for example, the idea is to turn the operations relatively easier, preserving structures, as always as possible. In Statistics the idea follows the same purpose and is one of the keys of these writings. When one performs a transformation, say, of logarithm type, this one is intended, among other things, to facilitate relationship between data and the functional form at hand, since the logarithmic scales reduce wide-ranging quantities to smaller scopes. Examples can be given in Chemistry when defining pH of a solution and the measure of decibels, in acoustics. However, for the probability theory, one is interested in transformations that, beside the reduction of difficult that can rise from the complexity of functional relation, it leads to new classes of distributions. In what follows a class of transformations is presented and their consequences in applications to probability and statistics, are studied.

2.2 DEFINITIONS, PROPERTIES AND PARTICULAR CASES

When one treats multiparametric transformations of one given type, they are referred to as a class of transformations, once, depending on the parameter values, one has a particular transformation at hand, as will be seen forward. One such example are *canonical transformations* appearing in dynamics and in the theory of differential equations, (R., 1987), (ALZAATREH CARL LEE, 2013). In a general way, one can use the well-known concept from linear algebra, for formal definition. In this sense, one has a

Definition 1 *Let M:* $\mathbb{R} \to \mathbb{R}$ *be a function such that,*

$$M\left(y;\boldsymbol{\varpi}\right) = \frac{ay+b}{cy+d} \tag{2.1}$$

with a, b, c and d the components of $\boldsymbol{\varpi}$, the parameter space of the transformation with elements in $\mathbb{R}$ and $ad - bc \neq 0$. It's worth of saying that, in the case where the latter vanish, that is to say, $ad - bc = 0$, an uninteresting constant mapping erupts sending $\forall y \in \mathbb{R}$ to the same image $\frac{a}{c}$, which is an exceptional trivial case called, singular, in counterpart to the former case, where it is termed no-singular. Furthermore, by the $\mathbb{R}$-linear isomorphism between $\mathbb{R}^2$ and $\mathbb{C}$, one can identify, with $y \leftrightarrow z$, $ad - bc$ as the determinant of the M representation matrix, M_{2x2}.

Proposition 1 *If M is given by 2.1 above, then*

$$\begin{aligned} M(\infty; \cdot) &= \frac{a}{c} \in \mathbb{R}, \\ M(0; \cdot) &= \frac{b}{d} \in \mathbb{R}. \end{aligned}$$

More generally, this mapping defines a bijection of the extended complex plane onto itself, from what follows that,

$$M(\mathbb{R}_\infty; \cdot) = \mathbb{R}_\infty = M(\infty; \cdot).$$

Note that, as a consequence of the latter,

$$M^{-1}(\infty; \cdot) = -\frac{d}{c}, \tag{2.2}$$

where M^{-1} stands for the inverse of M. In what follows, a restricted map is defined for the case where some values of the parameters a, b, c or d, can vanish. For the case where $c = 0$, the relation (2.2) implies

$$M^{-1}_{c=0}(0; \cdot) = M^{-1}(0; \cdot).$$

This is called Alexandroff extension, in $\mathbb{R}$. When extended to complex spaces, M has many beautiful properties with varied applications, despite their apparent simplicity, one of which, connected with Einstein's Theory of Relativity, (COXETER, 1967).

Theorem 1 *Let M: $\mathbb{R} \to \mathbb{R}$ be a smooth function. Let $\mathcal{F}(x; \boldsymbol{\xi}; \boldsymbol{\tau})$ be a real valued distribution function with parameter vector $\boldsymbol{\xi}$, and $\mathcal{G}(x; \boldsymbol{\tau})$ the baseline distribution with parameter vector $\boldsymbol{\tau}$, such that the following properties hold:*

$$\begin{aligned} \mathcal{G}(x; \boldsymbol{\tau}) = \mu((-\infty, x]; \boldsymbol{\tau}) &= P\left[X \leq x\right], \\ \mathcal{G}(x-; \boldsymbol{\tau}) = \mu((-\infty, x); \boldsymbol{\tau}) &= P\left[X < x\right], \end{aligned}$$

with

$$\mathcal{G}(x;\boldsymbol{\tau}) - \mathcal{G}(x-;\boldsymbol{\tau}) = \mu\{x\} = P[X = x],$$

where μ *is a measure on a field* $\mathscr{F}$*, leading to*

$$\begin{aligned}\lim_{x\mapsto-\infty}\mathcal{G}(x;\boldsymbol{\tau}) &= 0,\\ \lim_{x\mapsto\infty}\mathcal{G}(x;\boldsymbol{\tau}) &= 1.\end{aligned}$$

By using (LIMA et al., 2019) extended distribution function with additional parameters $m_i \in (0,1)$*,* $i = 1,\cdots,n$*,*

$$\mathcal{F}(x;\boldsymbol{\xi},\boldsymbol{\tau}) = \frac{\mathcal{G}^{\alpha}(x;\boldsymbol{\tau})}{\mathcal{G}^{\alpha}(x;\boldsymbol{\tau}) + \prod_{i=1}^{n}(1-m_i)\left[1-\mathcal{G}(x;\boldsymbol{\tau})\right]^{\alpha}}. \tag{2.3}$$

If the action of M *over* $\mathcal{F}$ *reads*

$$M(y;\boldsymbol{\varpi})\circ\mathcal{F}(x;\boldsymbol{\xi},\boldsymbol{\tau}) = M(\mathcal{F}(x;\boldsymbol{\xi},\boldsymbol{\tau});\boldsymbol{\varpi}) = F(x;\boldsymbol{\xi},\boldsymbol{\tau}),$$

with $\mathcal{G}(x;\boldsymbol{\tau}) \xrightarrow{M} G(x;\boldsymbol{\xi},\boldsymbol{\tau})$ *then,*

$$F(x;\boldsymbol{\xi},\boldsymbol{\tau}) = \left(\frac{a+b}{c+d}\right)\frac{G^{\alpha}(x;\boldsymbol{\tau}) + \frac{b}{a+b}\prod_{i=1}^{n}(1-m_i)\left[1-G(x;\boldsymbol{\tau})\right]^{\alpha}}{G^{\alpha}(x;\boldsymbol{\tau}) + \frac{d}{c+d}\prod_{i=1}^{n}(1-m_i)\left[1-G(x;\boldsymbol{\tau})\right]^{\alpha}} \tag{2.4}$$

is the distribution induced by M*, with* $\boldsymbol{\varpi}$ *absorbed by* $\boldsymbol{\xi}$*.*

Dem. 1 *It's enough to use the definition and a straightforward algebra.* □

The transformation M induces a $\boldsymbol{\varpi}$-parametric invariance class under a suitable choice of the elements of $\boldsymbol{\varpi}$, whose properties are shown in the corollary below:

Corollary 1 *For suitable choices of the parameter vector* $\boldsymbol{\varpi}$*, one obtains,*

1. *Translation for* $a = 1$, $c = 0$ *and* $d = 1$*. The parameter* b *is free and stands for magnitude of translation;*
2. *Rotation/Homothety for* $b = c = 0$, $d = 1$,
3. *Inversion/Reflection for* $a = 0$, $b = 1$, $c = 1$ *and* $d = 0$.

Dem. 2 *1.* $\boldsymbol{\varpi} = (1, b, 0, 1) \quad \Rightarrow$

$$\begin{aligned}F(x;\boldsymbol{\xi},\boldsymbol{\tau}) &= (1+b)\left\{\frac{(1+b)G^{\alpha}(x;\boldsymbol{\tau}) + b\prod_{i=1}^{n}(1-m_i)\left[1-G(x;\boldsymbol{\tau})\right]^{\alpha}}{(1+b)\left[G^{\alpha}(x;\boldsymbol{\tau}) + \prod_{i=1}^{n}(1-m_i)\left[1-G(x;\boldsymbol{\tau})\right]^{\alpha}\right]}\right\},\\ &= \frac{G^{\alpha}(x;\boldsymbol{\tau}) + b\left\{G^{\alpha}(x;\boldsymbol{\tau}) + \prod_{i=1}^{n}(1-m_i)\left[1-G(x;\boldsymbol{\tau})\right]^{\alpha}\right\}}{G^{\alpha}(x;\boldsymbol{\tau}) + \prod_{i=1}^{n}(1-m_i)\left[1-G(x;\boldsymbol{\tau})\right]^{\alpha}},\\ &= \frac{G^{\alpha}(x;\boldsymbol{\tau}) + b\frac{G^{\alpha}(x;\boldsymbol{\tau})}{\mathcal{F}(x;\boldsymbol{\xi},\boldsymbol{\tau})}}{\frac{G^{\alpha}(x;\boldsymbol{\tau})}{\mathcal{F}(x;\boldsymbol{\xi},\boldsymbol{\tau})}},\\ &= \mathcal{F}(x;\boldsymbol{\xi},\boldsymbol{\tau}) + b; \qquad \square\end{aligned}$$

The same follows for the other statements,

2. $\varpi = (a, 0, 0, 1) \quad \Rightarrow |a|\mathcal{F}(x; \boldsymbol{\xi}, \boldsymbol{\tau})$;

3. $\varpi = (0, 1, 1, 0) \quad \Rightarrow \frac{1}{\mathcal{F}(x;\boldsymbol{\xi},\boldsymbol{\tau})}$.

Remark 1 *It's worth of saying that, if* $M : \mathbb{C} \to \mathbb{C}$ *and* $\varpi \in \mathbb{C}$*, then,*

1. $|a| = 1$ *implies in pure rotations,*

2. $|a| > 1$ *implies in homothety.*

Figure 1 – Example under the $TMOE$ model, which will be defined on (4.2) and M_X transform for general values of parameter set $\{a, b, c, d\}$, as a consequence of (1).

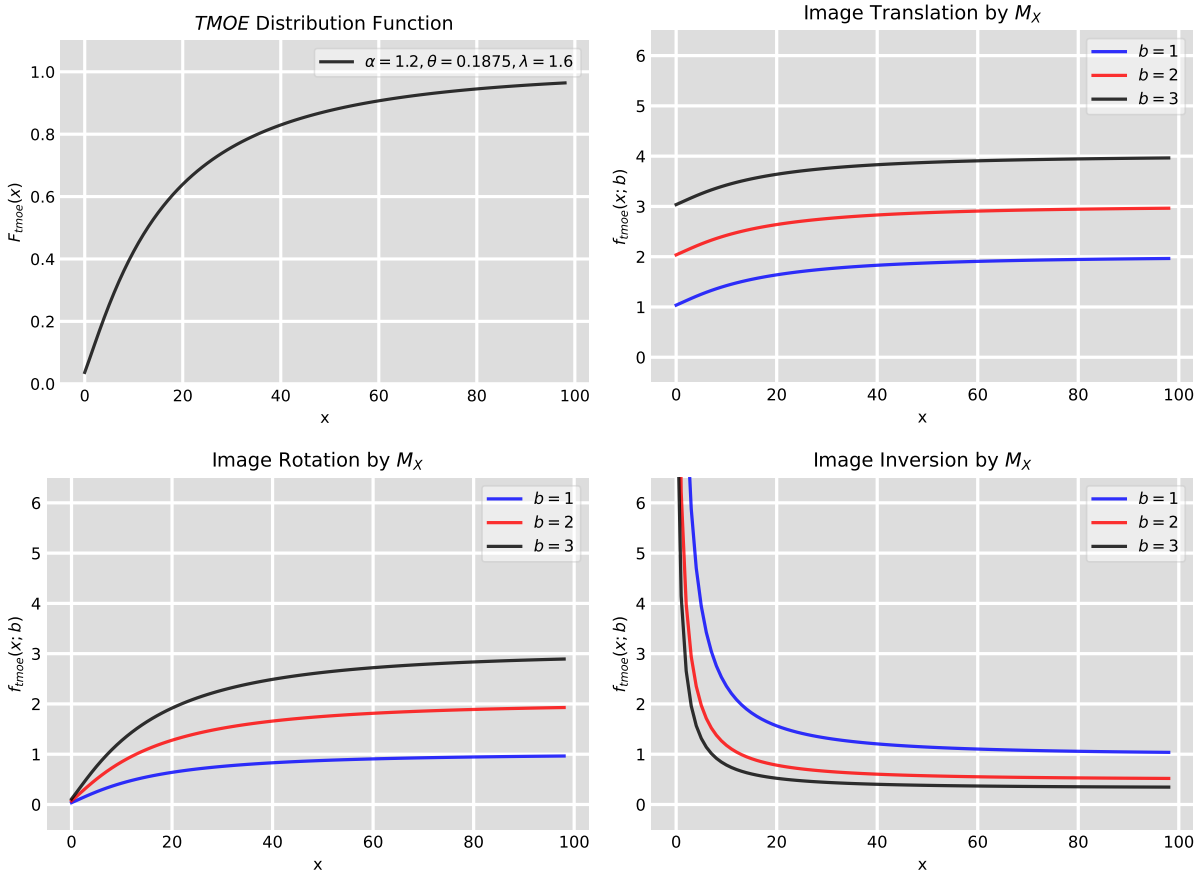

Source: the own author.

The figures appearing at (1) are of qualitative appeals, i.e., unless the translation case, the others are not referred to, for example, in the rotation case, to the angle. For a more quantitative analysis, it is developed, through complexification, a method to describe it.

Theorem 2 *Let $1 \leq i \leq k$, $k \in \mathbb{N}$. Let*

$$\begin{aligned} G(x;\boldsymbol{\tau}) = \mu((-\infty, x];\boldsymbol{\tau}) &= P\left[X \leq x\right], \\ G(x-;\boldsymbol{\tau}) = \mu((-\infty, x);\boldsymbol{\tau}) &= P\left[X < x\right], \end{aligned}$$

with

$$G(x;\boldsymbol{\tau}) - G(x-;\boldsymbol{\tau}) = \mu\left\{x\right\} = P\left[X = x\right],$$

where μ is a measure on a field $\mathscr{F}$ and such that

$$\begin{aligned} \lim_{x \mapsto -\infty} G(x;\boldsymbol{\tau}) &= 0, \\ \lim_{x \mapsto \infty} G(x;\boldsymbol{\tau}) &= 1. \end{aligned}$$

There exists $n \in \mathbb{N}$ such that,

$$\underbrace{F\left(F\left(F\left(\cdots\right)\right)\right)}_{n \text{ times}} = \frac{(n+1)G^{\alpha}(x;\boldsymbol{\tau}) + n\prod_{i=1}^{k}(1-m_i)\left[1-G(x;\boldsymbol{\tau})\right]^{\alpha}}{G^{\alpha}(x;\boldsymbol{\tau}) + \prod_{i=1}^{k}(1-m_i)\left[1-G(x;\boldsymbol{\tau})\right]^{\alpha}}$$

Dem. 3 *Indeed, it's enough to take $a = 1$, $b = n$ (and so, it proves the existence part, on the assertion), $c = 0$ and $d = 1$, in Equation (2.4).* □

In particular, for finite n, the statement of the previous theorem asserts that finite iterations leads to nondecreasing $F(x;\boldsymbol{\xi},\boldsymbol{\tau})$ what is expected for cumulative distribution functions.

Corollary 2 *Note that,*

$$\begin{aligned} \lim_{n \mapsto 0} \quad & \frac{(n+1)G^{\alpha}(x;\boldsymbol{\tau}) + n\prod_{i=1}^{k}(1-m_i)\left[1-G(x;\boldsymbol{\tau})\right]^{\alpha}}{G^{\alpha}(x;\boldsymbol{\tau}) + \prod_{i=1}^{k}(1-m_i)\left[1-G(x;\boldsymbol{\tau})\right]^{\alpha}} = \\ = \quad & \frac{G^{\alpha}(x;\boldsymbol{\tau})}{G^{\alpha}(x;\boldsymbol{\tau}) + \prod_{i=1}^{k}(1-m_i)\left[1-G(x;\boldsymbol{\tau})\right]^{\alpha}} \end{aligned}$$

Moreover, corroborating with the commentary in (1), above, in matrix terms one conceives,

$$\begin{aligned} F^{n} &= \begin{pmatrix} 1 & n \\ & \\ 0 & 1 \end{pmatrix} = M\left(\mathcal{F}\begin{pmatrix} 1 & n \\ & \\ 0 & 1 \end{pmatrix};\cdot\right) \\ &= \begin{pmatrix} 1 & 0 \\ & \\ 0 & 1 \end{pmatrix} = M\left(\mathcal{F}\begin{pmatrix} 1 & 0 \\ & \\ 0 & 1 \end{pmatrix};\cdot\right) \end{aligned} \tag{2.5}$$

which shows that, by starting from

$$M\left(\mathcal{F}\begin{pmatrix} 1 & 1 \\ & \\ 0 & 1 \end{pmatrix};\cdot\right) = \frac{2G^{\alpha}(x;\boldsymbol{\tau}) + \prod_{i=1}^{k}(1-m_i)\left[1-G(x;\boldsymbol{\tau})\right]^{\alpha}}{G^{\alpha}(x;\boldsymbol{\tau}) + \prod_{i=1}^{k}(1-m_i)\left[1-G(x;\boldsymbol{\tau})\right]^{\alpha}} \tag{2.6}$$

leading to a periodic system in the integers mod n, that is to say, in the Ring $\mathbb{Z}/n\mathbb{Z}$. Note, however that, in the

$$\lim_{m_1 \mapsto 1} M\left(\mathcal{F}\begin{pmatrix} 1 & 1 \\ & \\ 0 & 1 \end{pmatrix}; \cdot\right) \tag{2.7}$$

the system must be normalized to

$$\lim_{m_1 \mapsto 1} \frac{1}{2} M\left(\mathcal{F}\begin{pmatrix} 1 & 1 \\ & \\ 0 & 1 \end{pmatrix}; \cdot\right) \qquad 1 \leq i \leq k \in \mathbb{N}, \tag{2.8}$$

in order to the properties of G to be satisfied.

Remark 2 *As is done above, in 3, ϖ is chosen to be $(1, n, 0, 1)$. On the other hand, the definition that asserts the validity of 2.5 is, indeed, $M(y; \varpi) \circ \mathcal{F}(x, \boldsymbol{\xi}, \boldsymbol{\tau}) = F(x, \boldsymbol{\xi}, \boldsymbol{\tau})$. When one sees M as a representation matrix corresponding to the transformation, in the canonical basis, the result is straightforward.*

With the results of theorem (2) and corollary (2), one obtains a kind of periodic homography for the class of transformations appearing in theorem (1) which indicates that the transformations one may implement, under a given $\mathcal{F}$, is such that the results are homothety. In the case where there exist a dilation, this will be, indeed, the normalized factor calculated above, for the case at hand. As a consequence of these results, a finite number of composition, or generation of new distribution function, is allowed. All the one that may follow are representations of the class and periodicity conditions.

2.2.1 Particular Cases

Among many possibilities, two cases are presented and one is under investigation,

1. $\varpi = (1, 0, p, 1 - p)$;
2. $\varpi = (r, 1 - r, p, 1 - p)$.

In the first case, one reads

$$M_p(y; \cdot) = \frac{y}{py + (1 - p)} = \frac{y}{1 - p(1 - y)} \tag{2.9}$$

and, in the second one,

$$M_{p,r}(y;\cdot) = \frac{ry + (1-r)}{py + (1-p)} = \frac{y}{1 - p(1-y)} = M_{p,1}(y.\cdot). \tag{2.10}$$

Note that, for $r = 1$, $M_{p,r}(y;\cdot) \equiv M_p(y;\cdot)$. The transformation given at (2.9) will be recognized later, on Chapter 3. In 2.9 and 2.10, the indices $\{p\}$ and $\{r, p\}$ do refer to the choices made in the first and second cases above, 2.2.1, respectively.

Proposition 2 *Let M: $\mathbb{R} \mapsto \mathbb{R}$ be as given by (2.9). Let*

$$\mathcal{F}(x;\boldsymbol{\xi},\boldsymbol{\tau}) = \frac{\mathcal{G}^{\alpha}(x;\boldsymbol{\xi},\boldsymbol{\tau})}{\mathcal{G}^{\alpha}(x;\boldsymbol{\xi},\boldsymbol{\tau}) + (1-m)\left[1 - \mathcal{G}(x;\boldsymbol{\xi},\boldsymbol{\tau})\right]^{\alpha}}.$$

Applying M_p onto $\mathcal{F}(x;\boldsymbol{\xi},\boldsymbol{\tau})$, one has

$$\begin{aligned} M_p(y;\cdot) \circ \mathcal{F}(x;\boldsymbol{\xi},\boldsymbol{\tau}) &= M_p(\mathcal{F}(x;\boldsymbol{\xi},\boldsymbol{\tau});\cdot) \\ &= F(x;\boldsymbol{\xi},\boldsymbol{\tau}) \\ &= \frac{G^{\alpha}(x;\boldsymbol{\tau})}{G^{\alpha}(x;\boldsymbol{\tau}) + (1-p)(1-m)\left[1 - G(x;\boldsymbol{\tau})\right]^{\alpha}}. \end{aligned} \tag{2.11}$$

Remark 3 *Note that, in the context of general theory of functions, there is only one requirement under the equation 2.11: the denominator must be nonzero for it to make sense. However, in the context of probability distributions, note that the equation characterizes an accumulated distribution function (cdf). By checking the conditions under G, 2, then extending them to F, one verifies that the latter is, indeed, a distribution function. In fact, F has the mentioned inherited properties for all G, since the composition of continuous functions is continuous.*

Notwithstanding, a situation worth of attention is as follow: the image of a given random variable $x \in \mathbb{R}$ by F, must be unique in order to represent a function, at first. Then, the values assumed for $(1-p)(1-m)$ must ensure this condition. But this is not always the case.

To avoid situations like that, one denotes $(1-p)(1-m) = \theta$, for example, where θ is a new parameter, in principal, belonging to $\mathbb{R}$. This condition allows different settings of (α, θ, τ) to result in different distributions, avoiding an identifiability problem.

2.2.1.1 Properties

In addition to the inherent properties concerning the distribution functions, some hidden characteristics may emerge suggesting interesting consequences relative to the underlying symmetry carried by the parameter set, from both, M and $\mathcal{F}$.

From the concept of functions, it is read that, some points in the domain may not to be mapped to all points in the range, occasion where it is said that the relation is a injection, that is not bijection. When this relation is one-to-one, it is said that there exist a bijection.

It is possible for a function to have the same image for different points in the domain. When it happens, it is onto but not a bijection. One trivial example of such function is $f(x) = x^2$. For $x \in \{-1, 1\}$, the same $y = f(x)$ is obtained. In group theory, (ARMSTRONG, 1988), some class of symmetry is discussed as well as some of its consequences. In Nature, when a system exhibits some symmetry, hidden or not, a conservation of some physical dynamical quantity, or property, is observed, (NOETHER, 1971), (NEUENSCHWANDER, 2011).

2.2.1.2 Symmetry

The term symmetry occurs in both, Mathematics and Physics, meaning that one shape, in the former case, is identical to the other shape when it is translated, rotated, or flipped. In the latter case, some physical quantity, for example, like angular momentum, is conserved, when dynamical variables are at stake. In both cases, the theme is related to geometry.

There exist four basic types of symmetry, that is to say:

1. Translational symmetry;
2. Rotational symmetry;
3. Reflexive symmetry and
4. Glide symmetry.

The last one is a composition of a translation and a reflection. It is possible, however, that a transformation lead to a break of symmetry, when evolving. This is the case when, for example, a contraction is present. In what follows some cases are described.

2.2.1.3 Invariance for (p, m)-parametric permutation

Theorem 3 *Let M be according to the proposition (2). With*

$$\mathcal{F}(x; \boldsymbol{\xi}, \boldsymbol{\tau}) = \frac{G^{\alpha}(x; \boldsymbol{\tau})}{G^{\alpha}(x; \boldsymbol{\tau}) + \prod_{i=1}^{n}(1 - m_i)\left[1 - G(x; \boldsymbol{\tau})\right]^{\alpha}},$$

and

$$\begin{aligned} M_p(y;\cdot)\circ\mathcal{F}(x;\boldsymbol{\xi},\boldsymbol{\tau}) &= M_p(\mathcal{F}(x;\boldsymbol{\xi},\boldsymbol{\tau});\cdot) \\ &= F(x;\boldsymbol{\xi},\boldsymbol{\tau}) \\ &= \frac{G^{\alpha}(x;\boldsymbol{\tau})}{G^{\alpha}(x;\boldsymbol{\tau})+(1-p)\prod_{i=1}^{n}(1-m_i)\left[1-G(x;\boldsymbol{\tau})\right]^{\alpha}}, \end{aligned}$$

then, the distribution induced by M is (p, m_i)-parametric invariant under an even permutation, for $i = 1, \ldots, n$.

Dem. 4 *In effect, just keep p fixed and, for each i, $i = 1, \ldots, n$, the assumptions in the proposition (3), follows. Then, the theorem is valid for $n = 1$. Suppose it is, rather, valid for $n = k$ and let one show that it is valid for $n = k + 1$. It follows*

$$\begin{aligned} n=k+1 \;\Rightarrow\; & \frac{G^{\alpha}(x;\boldsymbol{\tau})}{G^{\alpha}(x;\boldsymbol{\tau})+(1-p)\prod_{i=1}^{n=k+1}(1-m_i)\left[1-G(x;\boldsymbol{\tau})\right]^{\alpha}} \\ = & \frac{G^{\alpha}(x;\boldsymbol{\tau})}{G^{\alpha}(x;\boldsymbol{\tau})+(1-p)(1-m)\prod_{i=1}^{n=k}(1-m_i)\left[1-G(x;\boldsymbol{\tau})\right]^{\alpha}} \\ = & \frac{G^{\alpha}(x;\boldsymbol{\tau})}{G^{\alpha}(x;\boldsymbol{\tau})+(1-\underbrace{m-p+pm}_{\tilde{p}})\prod_{i=1}^{n=k}(1-m_i)\left[1-G(x;\boldsymbol{\tau})\right]^{\alpha}} \\ = & \frac{G^{\alpha}(x;\boldsymbol{\tau})}{G^{\alpha}(x;\boldsymbol{\tau})+(1-\tilde{p})\prod_{i=1}^{n=k}(1-m_i)\left[1-G(x;\boldsymbol{\tau})\right]^{\alpha}} \Leftarrow n=k, \end{aligned}$$

It was shown that the principle is valid for $n = 1$. Supposed to be true for $n = k$, and, in virtue of the Principle of Finite Induction, that it is also true for $n = k + 1$. □

Proposition 3 *Let $p, m \in \mathbb{R}$ and consider (2.11). It's not hard to see that, under permutation on p and m, M preserves structure.*

Indeed, p and m are dummy parameters, i.e, they can be changed for, say, l and q and the image of M will be invariant. Take, for example, $p = 1/2$ and $m = 2$. One reads,

$$\begin{aligned} M(\mathcal{F};1/2,2) &= \frac{G^{\alpha}(x;\boldsymbol{\tau})}{G^{\alpha}(x;\boldsymbol{\tau})-\frac{1}{2}\left[1-G(x;\boldsymbol{\tau})\right]^{\alpha}} \\ &= M(\mathcal{F};2,1/2). \end{aligned}$$

Remark 4 *Here, the term dummy is the one encountered in matrix and tensor analysis, (MCCONNELL, 1957). Not to be confused with dummy variables in Statistics.*

Definition 2 *One says that the transformation induced by M leads to an invariance for the image of the distribution, if it preserves structure. Moreover, that the distribution has a (p, m)-parametric reflexive symmetry if interchanging p and m, the distribution maintains its characteristics.*

Conjecture 1 *Once that behind a symmetry of a dynamical variable there exist a conserved quantity, it is conjectured that, for the case of the reflexive symmetry seen above, some mathematical property related to the distribution function- endowed with a time parameter-, is hidden and is eligible to come to surface. It could be a result related to mean, variance, or other statistical property. The idea can be extended to involve the other symmetries.*

2.2.1.4 Contraction

In what follows a case is exhibited where the action of M does preserve structure, leading to interesting results.

Proposition 4 *Let $\boldsymbol{\varpi} = (a, b, c, d)$ with $a, b \in \mathbb{R}|_{(0,1)}$, where the symbol $|$ means restriction to. If $a \mapsto \alpha p + \beta$, with α, β, p such that $0 < \alpha p + \beta < 1$, then,*

$$F_{\boldsymbol{\varpi}_{\alpha p+\beta}} = \frac{\alpha p + \beta}{(1+b)^2} F_{\boldsymbol{\varpi}},$$

where,

$$\begin{aligned} F_{\boldsymbol{\varpi}_{\alpha p+\beta}} &= M\left(y; \boldsymbol{\varpi}_{\alpha p+\beta}\right) \circ \mathcal{F}(x; \boldsymbol{\xi}, \boldsymbol{\tau}) = M\left(\mathcal{F}(x; \boldsymbol{\xi}, \boldsymbol{\tau}); \boldsymbol{\varpi}_{\alpha p+\beta}\right), \\ F_{\boldsymbol{\varpi}} &= M\left(y; \boldsymbol{\varpi}\right) \circ \mathcal{F}(x; \boldsymbol{\xi}, \boldsymbol{\tau}) = M\left(\mathcal{F}(x; \boldsymbol{\xi}, \boldsymbol{\tau}); \boldsymbol{\varpi}\right). \end{aligned} \tag{2.12}$$

Dem. 5 *By applying M to 2.11 and considering the notation given by 2.12 one has,*

$$\frac{(1+b)(c+d)}{\alpha p + \beta} F_{\boldsymbol{\varpi}_{\alpha p+\beta}} = \left\{ \frac{G^\alpha + \frac{b}{1+b}\theta\left[1-G\right]^\alpha}{G^\alpha + \frac{d}{c+d}\theta\left[1-G\right]^\alpha} \right\}, \tag{2.13}$$

$$\frac{(c+d)}{(a+b)} F_{\boldsymbol{\varpi}} = \left\{ \frac{G^\alpha + \frac{b}{a+b}\theta\left[1-G\right]^\alpha}{G^\alpha + \frac{d}{c+d}\theta\left[1-G\right]^\alpha} \right\}. \tag{2.14}$$

Dividing 2.13 by 2.14 and taking the limit,

$$\begin{aligned}\lim_{a\to 1}\left[\frac{\frac{(1+b)(c+d)}{\alpha p+\beta}F_{\varpi_{\alpha p+\beta}}}{\frac{(c+d)}{(a+b)}F_{\varpi}}\right] &= \lim_{a\to 1}\left[\frac{\left\{\frac{G^{\alpha}+\frac{b}{1+b}\theta[1-G]^{\alpha}}{G^{\alpha}+\frac{d}{c+d}\theta[1-G]^{\alpha}}\right\}}{\left\{\frac{G^{\alpha}+\frac{b}{a+b}\theta[1-G]^{\alpha}}{G^{\alpha}+\frac{d}{c+d}\theta[1-G]^{\alpha}}\right\}}\right],\\ \frac{\frac{(1+b)(c+d)}{\alpha p+\beta}F_{\varpi_{\alpha p+\beta}}}{\frac{(c+d)}{(1+b)}F_{\varpi}} &= 1.\end{aligned}$$

such that,

$$F_{\varpi_{\alpha p+\beta}} = \frac{\alpha p+\beta}{(1+b)^2}F_{\varpi}. \qquad \square$$

Corollary 3

$$\lim_{b\to 0}\frac{F_{\varpi_{\alpha p+\beta}}}{F_{\varpi}} = \alpha p+\beta.$$

In particular, corollary 3 implies that the quotient of both distributions, $F_{\varpi_{\alpha p+\beta}}$ and F_{ϖ} is a well defined nondecreasing distribution function, since $0<\alpha p+\beta<1$, by hypothesis.

2.3 RESULTS

In what follows some results are presented as consequences of the theory described above. The idea is to apply the concepts in statistics as well as to develop tools in this branch of mathematics.

Definition 3 *Let $M_X(x)$ a smooth function as given by (1) and $\mathcal{F}(x)$ a distribution function. Once $M_X(x)\circ\mathcal{F}(x)$ is smooth, one defines*

$$\begin{aligned}T\left(M_X(x)\circ\mathcal{F}(x)\right)(x) &= \left\{M_X\mathcal{F},x\right\},\\ &= \epsilon_X(x),\end{aligned}$$

the generating function for the probability distribution function.

Definition 4 *On the Definition (3), the operator T is such that*

$$T(\cdot) = \frac{D^3}{D} - \left(\frac{3}{2}\right)\left(\frac{D^2}{D}\right)^2, \tag{2.15}$$

where D is the canonical differential operator and the exponents, akin to D, are the order of the derivative.

Proposition 5 *Let $M_X: \mathbb{R} \mapsto \mathbb{R}$ as given on (3) and consider the Schwartz derivative of $M_X \circ \mathcal{F}(x)$ relative to x, $T\left(M_X\mathcal{F}(x)\right)(x) = \{M_X\mathcal{F}, x\} = \epsilon_X(x)$, as defined by (3), and $M_X \circ \mathcal{F}_{X^2}(x) = \{M_X\mathcal{F}_{X^2}, x\} = \epsilon_{X^2}(x)$. If*

$$\begin{aligned} M_X(\mathcal{F}(x; \boldsymbol{\xi}, \boldsymbol{\tau})) &= F_{exp}(x; \cdot; \lambda) \\ M_X(\mathcal{F}_{X^2}(x; \boldsymbol{\xi}, \boldsymbol{\tau})) &= F^2_{exp}(x; \cdot; \lambda) \end{aligned}$$

where F_{exp} is the M-transformed exponential distribution, then,

$$E(X) = \lim_{x\to\infty} \frac{1}{\sqrt{-2\epsilon_X(x)}} = \frac{1}{\lambda} \tag{2.16}$$

$$E(X^2) = \lim_{x\to\infty} \frac{1}{-\epsilon_{X^2}(x)} \tag{2.17}$$

$$Var(X) = E(X^2) - E(X)^2, \tag{2.18}$$

where

$$\begin{aligned} T\left(M_X\mathcal{F}_{X^2}\right)(x) &= T(F^2(x)) \\ &= \epsilon_{X^2}(x) \end{aligned}$$

Indeed, with $\mathcal{F}(x) = 1 - e^{-\lambda x}$, one has

$$\begin{aligned} M_X\mathcal{F}_X &= \frac{a\left(1 - e^{-\lambda x}\right) + b}{c\left(1 - e^{-\lambda x}\right) + d}, \\ T\left(M_X\mathcal{F}_X\right) &= -\frac{\lambda^2}{2}, \end{aligned}$$

so that,

$$\begin{aligned} \lim_{x\to\infty} \frac{1}{\sqrt{-2\epsilon_X(x)}} &= \lim_{x\to\infty} \frac{1}{\sqrt{-2\left(-\frac{\lambda^2}{2}\right)}} \\ &= \lim_{x\to\infty} \frac{1}{\sqrt{\lambda^2}} = \frac{1}{\lambda} \end{aligned}$$

For the variance, $Var(X)$, one has,

$$\begin{aligned} Var_X(x) &= E(X^2) - E^2(X) \\ &= \lim_{x\to\infty} \frac{1}{-\epsilon_{X^2}(x)} - \frac{1}{\lambda^2} \\ &= \frac{2}{\lambda^2} - \frac{1}{\lambda^2} \\ &= \frac{1}{\lambda^2} \end{aligned}$$

Proposition 6 *Let M_X: $\mathbb{R} \mapsto \mathbb{R}$ as given on proposition (5) with $\mathcal{F}_X$ the $TMOE$ model distribution, that is to say,*

$$\mathcal{F}_X = \frac{\left(1 - e^{-\lambda x}\right)^{\alpha}}{(1 - e^{-\lambda x})^{\alpha} + \theta e^{-\alpha \lambda x}}$$

then,

$$\begin{aligned} T\left(M_X \mathcal{F}_X(x; \boldsymbol{\xi}, \boldsymbol{\tau})\right)(x) &= \frac{1}{2} \frac{2e^{\lambda x} - \alpha^2 e^{2\lambda x} - 1}{e^{2\lambda x} - 2e^{\lambda x} + 1} \\ &= \epsilon_X(x) \end{aligned}$$

so that,

$$\begin{aligned} E(X) &= \lim_{x \to \infty} \frac{1}{\sqrt{-2\epsilon_X(x)}} = \frac{0.707106781186548\sqrt{2}}{\alpha\lambda} \\ Var(X) &= E(X^2) - E^2(X) = E(X^2) - (\frac{0.707106781186548\sqrt{2}}{\alpha\lambda})^2 \end{aligned}$$

2.4 CONCLUSIONS

In this chapter, the concept of fractional bilinear transformation was applied and some concepts and properties were introduced inside the branch of probability theory. Despite the extension lacks up-dated formal mathematical sources- for it is under development-, the ideas and methods are worth of studying. The tools presented are interesting and show potential applications in several fields of, pure and applied, mathematics. In data science, for example, some enquire can be made about the applicability of the symmetry behind the theory, in similar tools as that of PCA, *principal component analysis*, (JOLLIFFE, 2010).

3 GENERAL PROPERTIES OF $\mathbf{M_p}$: THE MARSHALL-OLKIN TRANSFORMATION

3.1 INTRODUCTION

Here, the class of transformations seen at Chapter 2 is applied and a family of distribution is studied. At first, a general approach is considered in order to establish the theory and prepare the ground for the concrete distributions, that is to say, when considering the baselines at hand. Based on the ideas of the last chapter, a special case of the proposed transformation will be used, from now on, M_p-transform given by (2.9).

The idea is to present a family of distributions as well as to emphasize the *root* character of the transformation that, in particular, can be a source for the well known, although little used in the field of new distributions, Marshall-Olkin transformation, which emerged from M_p.

The junction of the latter with (LIMA et al., 2019) will result on a new family with a higher degree of flexibility, in terms of the failure rate function, as one will see later.

Additionally, the resulting cumulative distribution function and probability density function have their simple forms, that is to say, they do not involve complicated mathematical functions, as in the families given by beta-G (EUGENE; LEE; FAMOYE, 2002) and gamma-G (ZOGRAFOS K.; BALAKRISHNAN, 2009), for example.

The Marshall-Olkin transformation can be used, among other things, as mechanism of skewing as disposed in (RUBIO; STEEL, 2012). On this case its use is for modelling data presenting departures from symmetry, which is ordinary in data analysis. As the application of the transformation takes place, a number of parameter is introduced as seen at Chapter 2, whose mathematical meaning is to allow the fractioning for the values assuming in the global parameter $\theta = (1 - p_1) \cdot (1 - p_2) \cdots (1 - p_k)$, $k \in \mathbb{N}$, as structured in last chapter. However, when this is done, it dawns that, for different values of p_i, p_k, $i \neq j \in \mathbb{N}$, the same scenario emerges. This is why one is using a global parameter θ, but related to the k's, in order to avoid ambiguity for the image of the distribution. Finally, given the current distribution, after transformation, general expressions are derived conceiving the ordinary functions figuring in statistical theory, such the probability density function, hazard function, quantile functions and so on.

3.2 CONSTRUCTING THE FAMILIES

Here, one is addressed to a particular case where the combinations of the parameter vector (a, b, c, d), of ϖ, leads to Marshall-Olkin transformation. The distribution function and probability density function are given, along with some ordinary properties associated to them, such as the shapes these functions can exhibit through the hazard function, as well as the quantile function developed to be applied in the simulations later performed. The moment generating function is introduced and a series expansion is addressed intended to give an alternative method when exact solutions cannot be calculated. The process of estimation is presented through maximum likelihood.

3.2.1 M-Transform and the Marshall-Olkin Transformation

As was described in Chapter 2, a class of transformations was presented in terms of the *M*-transform, for different values of his intrinsic parameters, i.e., a, b, c and d. There, it was pointed out that for the particular values of those parameters, say, $a = 1$, $b = 0$, $c = p$ and $d = 1 - p$, the Marshall-Olkin transformation was derived. In this text, a natural extension of Odd Log-Logistic Geometric family, (OLLG-G for short), (LIMA et al., 2019), is proposed by using that transformation, as well as the ones corresponding to changes in the vector parameter set, according to properties inherited by the transformation. As was seen, it is defined by

$$M(y; p) = \frac{y}{1 - p\,(1 - y)}, \tag{3.1}$$

with $y \in \mathbb{R}|_{(0,1)}$ and $p \in (0, 1)$ is an additional tuning parameter. Henceforth,

$$\boldsymbol{\xi} = \ (\alpha, m, p) = (\alpha, \theta), \quad \text{if} \quad F \quad \text{holds}, \tag{3.2}$$

will represent the general parameter vector sets for the model and $\boldsymbol{\tau}$ will designate the vector parameter set for the baselines for the given F. Here, one should keep in mind that the notation given at (3.2) was that way structured in order to address the identifiability problem discussed in the former chapter. Note that, since $y \in \mathbb{R}|_{(0,1)}$, one may choose a cumulative distribution function (cdf) from some random variables, or family of distributions, and substitute them in (3.1). Here it is chosen the family of distribution known as *OLLG-G Family* (LIMA et al., 2019) which has the probability density function (pdf) expressed by

$$f\left(x;\alpha,m,\boldsymbol{\tau}\right)=\frac{\alpha(1-m)g(x;\boldsymbol{\tau})G(x;\boldsymbol{\tau})[1-G(x;\boldsymbol{\tau})]^{\alpha-1}}{\left\{G^{\alpha}(x;\boldsymbol{\tau})+(1-m)[1-G(x;\boldsymbol{\tau})]^{\alpha}\right\}^{2}},\tag{3.3}$$

where $G(x;\boldsymbol{\tau})$ and $g(x;\boldsymbol{\tau})$ are the cumulative distribution function and probability density function, respectively.

Consequently, the associated cdf is given by

$$F\left(x;\alpha,m,\boldsymbol{\tau}\right)=\frac{G^{\alpha}(x;\boldsymbol{\tau})}{G^{\alpha}(x;\boldsymbol{\tau})+(1-m)\left[1-G(x;\boldsymbol{\tau})\right]^{\alpha}},\tag{3.4}$$

where the parameter α represents the quotient of the log odds ration for the generated and baseline distributions, given by,

$$\alpha=\frac{\log\left[\frac{F(x;\boldsymbol{\xi},\boldsymbol{\tau})}{\overline{F}(x;\boldsymbol{\xi},\boldsymbol{\tau})}\right]}{\log\left[\frac{G(x;\boldsymbol{\tau})}{\overline{G}(x;\boldsymbol{\tau})}\right]},$$

as can be seen in the last reference above. With respect to the parameter m, let T be a geometric random variable with probability mass function given by $P(T=t)=(1-m)m^{t-1}$ for $t\in\mathbb{N}$ and $m\in(0,1)$. Thus, if Y has density given by (3.3), we write $Y\sim$OLLG-G$(\alpha,m,\boldsymbol{\tau})$,

This family is very flexible and depends on the baseline chosen. Besides that, when $\alpha=1$, we obtain the geometric-G family with $(k+n)$ parameters (m,τ), where n stands for the dimension of the parameter vector τ and k the number of parameters carried out by the model. Note that, by the very concept of dimension, these numbers must be positive ones.

By applying (3.4) in (3.1), one finds, after some algebra, the following proposition.

Proposition 7 *Let F be defined in such a way that (3.4) is satisfied. Then one has,*

$$F\left(x;\boldsymbol{\xi},\boldsymbol{\tau}\right)=\frac{G^{\alpha}(x;\boldsymbol{\tau})}{G^{\alpha}(x;\boldsymbol{\tau})+\theta\left[1-G(x;\boldsymbol{\tau})\right]^{\alpha}},\tag{3.5}$$

where $\theta\equiv(1-p)\,(1-m)$ and $\xi=(\alpha,\theta,\boldsymbol{\tau})$ is the parameter vector for this model. Here, the details are the same as one sees on Remark (3).

As was observed in (3.2), the parameter vector $\boldsymbol{\xi}$ has dimension 2. Note, indeed that, since the baseline parameter range depends on the general $G(x;\boldsymbol{\tau})$, previously chosen, the nature and proper range of it will depend only on the concrete G.

Corollary 4 *As direct consequence of (3.5), the pdf reads*

$$f(x;\boldsymbol{\xi}),\boldsymbol{\tau})=\frac{\alpha\theta g(x;\boldsymbol{\tau})G^{\alpha-1}\left(x;\boldsymbol{\tau}\right)\left[1-G\left(x;\boldsymbol{\tau}\right)\right]^{\alpha-1}}{\left\{G^{\alpha}\left(x;\boldsymbol{\tau}\right)+\theta\left[1-G\left(x;\boldsymbol{\tau}\right)\right]^{\alpha}\right\}^{2}}.\tag{3.6}$$

Hence, if X has density given by (3.6), one says that it follows the Transformed Marshall-Olkin G family, (TMO-G, for short), with additional parameters α and θ. It is important to emphasise that θ does involve a combination of parameters. m for the probability of a geometric random variable- described right after (3.4)-, and p, which is the parameter of the transformation given in (3.1).

Remark 5 *Note that, when $\alpha = \theta = 1$, the new model devolves on the baseline.*

Remark 6 *It is allowed for the parameter θ to vary into $\mathbb{R}$. The response to this choice could leads to lack of probability significance to what concerns to variability of P in $(0, 1)$ but, which can be rescued by the process of normalization, in the case of right extrapolation of the later interval, or suitability in the case of negative probability. The later can be addressed to phase space formulation of quantum mechanics, quantum correlations, wave-particle dualism, among others, (BREUER, 2002), (BLASS; GUREVICH, 2020). Inasmuch as one desire to provide a meaning of proportion to θ, it is advised to let them vary inside $(0, 1)$ interval. Here is worth of saying that there exist an essential difference between proportion and probability. While the former is well defined and known- the results of realizations are known-, the latter, besides being, yet, well defined, their results are unknown until the total exhaustion of the event.*

3.2.2 The Shapes of Distributions

When discussing probability distributions one is often lead to the question on what the shapes of the curves, at hand, have to do to statistical meaning.

The question that could arise is, are there relations between central tendency measures and the aforementioned shapes of distributions? The answer is a 'yes'. Once a distribution may be described by a number of maximum points it exhibits, known as its *modality*, it is possible to visualize an association with the *mode*, for example. If the density assumes the greatest value at some point, then the value is the mode. Nevertheless, it is not hard to find a distribution described as *bimodal* or *multimodal* whenever there are more than one pronounced humps in the curves corresponding to their distributions, even though there is only one distinct mode (HAYS; WINKLER, 1970).

Summarizing, as the distributions are described by functional relations, it is expected that the former may have no modes, as can be seen at the first figure in 2, and unimodal, as pictured out in the second one, according to $TMOE$ model detailed in Chapter 4.

Figure 2 – The first graph shows no mode. The second one a graph of an unimodal distribution. The graph do represent univariate distributions plotted for different continuous values of their parameters, for example.

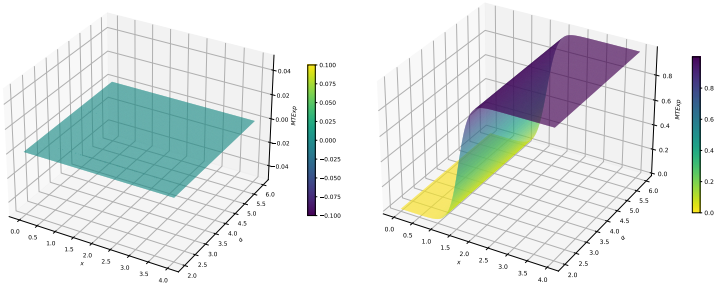

Source: the own author.

This is important when the geometric properties of new distributions are analysed, whether by shape methods developed by Qian, (QIAN, 2012), or by direct plot visualization. By this last condition, once a probability distribution function indicates the likelihood of an event or an outcome, if X is a random variable, then the x-axis does represent the possible outcomes of the experiment, while the y-axis does the probability of each outcome. The way each other do relate is addressed to the *law*, or distribution function the random variable follow. In this sense, the shape of this function gives mathematical meaning to measure likelihood in a visual way, giving rise, quite instantaneously, to useful interpretations.

3.2.3 Hazard Function

In terms of applications for the developed theory here presented, there is a branch of applied statistics, known as Survival Analysis, that these tools can be addressed to. The uses of the method is, by no mean, exhausted in this area, as will be verified in the examples and applications that follows the text. In survival analysis, the outcome variable of interest is the *time* until the occurrence of an event. The physical entity, *time*, has its natural meaning as understood in Physics and corresponding dimension, say, years, month, seconds. By the term *event*, one understands some phenomenon, or experiment, that takes place at some location in space and time, to what some control and knowledge is desirable. Inside this theory, survival analysis, *s.a.* for short, some concepts and properties are developed leading to results that can provide useful tools for the understanding of several branches of knowledge, (GAO; HE, 2020), (SHEN, 2021), (SINGH; MUKHOPADHYAY, 2011). The main characteristic of *s.a.* is embedded in a mathematical expression, known as hazard function, $h(x; \boldsymbol{\xi}, \boldsymbol{\tau})$, or hazard rate function

(hrf) whose mathematical meaning is to give the instantaneous potential, per unit time, for the aforementioned *event* to occur, given that the phenomenon has last, up to time x. If, for example, the phenomenon is the clinical condition of an individual, one think of the individual has survived up to time x, (KLEINBAUM, 2005). Here, without loss of generality, it is used the general independent variable x for denoting *time*, contrary almost all literature that uses t, for time. It's just a notational question. In some occasion the t-notation, for time, is indeed recovered.

Then, given the distribution function $F(x;\boldsymbol{\xi},\boldsymbol{\tau})$, the general expression for the hrf family model, is

$$h(x;\boldsymbol{\xi},\boldsymbol{\tau}) = \frac{\alpha g(x;\boldsymbol{\tau})G^{\alpha-1}(x,\boldsymbol{\tau})}{\left\{G^{\alpha}\left(x;\boldsymbol{\tau}\right)+\theta\left[1-G\left(x;\boldsymbol{\tau}\right)\right]^{\alpha}\right\}\left[1-G\left(x;\boldsymbol{\tau}\right)\right]}, \tag{3.7}$$

with the functions and symbols well understood from text above.

3.2.4 Some properties of the hazard function

As was conceived in (QIAN, 2012), the quotient between f and $1-F$, termed hazard function, allows one to have insight about the nature of distribution through the shape it exhibits. Meanwhile, (MUDHOLKAR; SRIVASTAVA; FREIMER, 1995) suggests the dependence, out of the natural logarithmic one by construction itself for the hazard function, on the monotonicity induced by the parameters of the generating distribution. In the cited case, giving rise to regions of interest from where qualitative analysis may be performed to establish domain on the parameters and their influence on the nature of distributions. Then, consider the following proposition,

Proposition 8 *Let $T(z)$ be defined by*

$$\begin{aligned} T(z) &= (1-z)\left[z^{\alpha}+\theta(1-z)^{\alpha}\right]\left[zg'(z;\boldsymbol{\tau})(1-z)+(\alpha-1)g(x;\boldsymbol{\tau})(1-z)-zg(z;\boldsymbol{\tau})\right] \\ &- g(z;\boldsymbol{\tau})(1-z)\left[z^{\alpha}(1-z)+\theta z(1-z)^{\alpha}\right]. \end{aligned}$$

It follows that the sign of the variation of the hazard function $h(x)$ is the same as that of T.

Dem. 6 *Let z be the restriction of a convex function to its interval, where it is strictly increasing. This is important for, if $z=a^x$, it would be strictly increasing only if $a>1$. Then, without loss of generality let $G(x;\boldsymbol{\tau})=e^x=z$. In that case, such a restriction implies $z>1$,*

if $x > 0$. *It follows that,* $x = \log z$ *and,*

$$r(z) = \frac{\alpha g(x;\boldsymbol{\tau}) z^{\alpha-1}}{\left[z^{\alpha} + \theta(1-z)^{\alpha}\right](1-z)}.$$

By taking logarithm on both sides of the equation and deriving it, one obtains, after some algebra,

$$\frac{r'(z)}{r(z)} = \frac{T(z)}{zg(\boldsymbol{\tau})(1-z)^2\left[z^{\alpha} + \theta(1-z)^{\alpha}\right]}. \tag{3.8}$$

Here, $T(z)$ as given by proposition (8). Once, $g(z, \boldsymbol{\tau}) \geq 0$, $z > 1$, by hypothesis, the denominator is a positive function. It follows that the sign of $r'(z)$ and $T(z)$ are the same under variation. Note that in the figure, (3), there is signal preservation.

Figure 3 – Graph showing the variation of T to enforce the same sign preservation property, as compared to $r'(z)$. The red curve is the denominator of Equation (3.8).

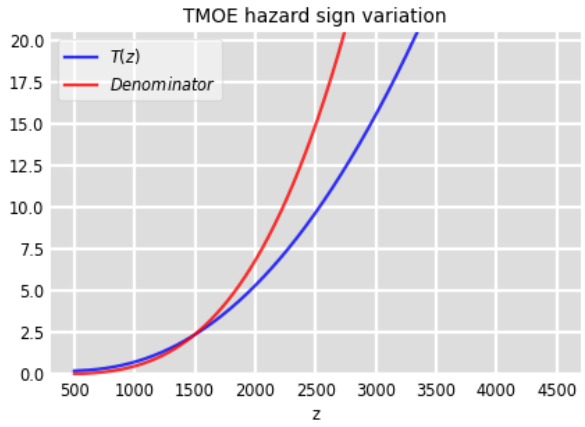

Source: the own author.

When dealing with the baseline at hand, the Factor function T will play an interesting role in terms of the shape inherited by the hazard function and, according to this, it will be defined regions on which a parameter domain will take place to characterize the theory.

3.2.5 Limiting Cases

It is interesting to investigate to where Equation (3.5) tends to converge when the parameter, θ, is bound to approximate to some limit values. Then we have,

$$\begin{aligned} \lim_{\theta \to 0^+} F(x;\boldsymbol{\xi};\boldsymbol{\tau}) &= \lim_{\theta \to 0^+} \frac{1}{1 + \theta\left[\frac{1-G(x;\boldsymbol{\tau})}{G(x;\boldsymbol{\tau})}\right]^{\alpha}} \\ &= 1 \end{aligned}$$

and

$$\begin{aligned}\lim_{\theta\to 1} F\left(x;\boldsymbol{\xi};\boldsymbol{\tau}\right) &= \lim_{\theta\to 1}\frac{G^{\alpha}\left(x;\boldsymbol{\tau}\right)}{G^{\alpha}\left(x;\boldsymbol{\tau}\right)+\theta\left[1-G\left(x;\boldsymbol{\tau}\right)\right]^{\alpha}}\\ &= \frac{G^{\alpha}\left(x;\boldsymbol{\tau}\right)}{G^{\alpha}\left(x;\boldsymbol{\tau}\right)+\left[1-G\left(x;\boldsymbol{\tau}\right)\right]^{\alpha}}\end{aligned}$$

which is the family given by (3.4) proposed by (LIMA et al., 2019), if θ assumes values such that $\theta = (1-p)$, with $p \in (0,1)$. Note, however, that the former equation, above, shows that the parameter range for θ does not need to be constrained to the interval $(0,1)$ since there are no essential singularities presented inside or outside these interval, including the boundaries of it, while the later is just a formality for addressing the nested nature of the model and the one that this was generated from, if one chose to decompose θ in a granular form, such as,

$$\theta = (1-p_1)(1-p_2)\cdots(1-p_n) \in \mathbb{N}$$

as was pointed out in chapter one. It is yet, worth of saying that, on selecting this decomposition for θ, it is possible to have equal values received for F, for different values of the p_i, $i = 1,\cdots,n$, leading to inconsistency, known as incompatibility conditions. Meanwhile, as one is allowed to select values for θ outside the $(0,1)$ interval, it is possible to encounter troubles while defining the quantile function. Inasmuch as the later is charged with probabilistic meaning, in selecting values leading to violations of the probability rules, one is incurring in future errors.

3.3 QUANTILE FUNCTION

Given a probability distribution function. The quantile function has many uses in theory and applications of Probability because, once the later is known, it may be used to construct a random variable X that satisfies the former. The practical importance of the knowledge of it is based on the fact that it can provide a method of simulating samplings from arbitrary distribution, given a generator, (PARZEN, 1979), (ALJARRAH; LEE; FAMOYE, 2014). Then, one has the following

Definition 5 *Let X be a random variable and $F_X(x)$ the associated cumulative distribution function. The quantile function, $Q_X(u) : (0,1) \longrightarrow \mathbb{R}$ is the inverse of the cdf, when the inverse does exist.*

It follows from the definition that

$$Q(u) = inf\left\{x : F(x) \geq u\right\}, \forall u \in (0,1), \tag{3.9}$$

that is to say, the quantile function Q(u), for a given quantile $u \in (0,1)$ returns the smallest x for which $F_X(x) = u$.

Proposition 9 *Since the distribution function given, by (3.5), is a strictly monotonically increasing function of the continuous random variable X, the quantile function is given by the inverse of* $F_X(x) \equiv F(x;\boldsymbol{\xi})$ *and reads*

$$Q(u) = Q_G\left(\frac{1}{1+\left[\frac{1-u}{\theta u}\right]^{1/\alpha}}\right), \tag{3.10}$$

where Q_G *is a reference that* $Q(u)$ *does depend on* $G(x;\boldsymbol{\tau})$*. Furthermore,* $u = F^{-1}(x,\boldsymbol{\xi},\boldsymbol{\tau})$*, the pre-image of* x *by* F*. Calculational details can be seen at (3.3.1).*

3.3.1 Quantile Function Details

First of all it is desirable to show that F is a monotonically increasing function of x. Indeed, starting from the definition (3.5), we must show that the derivative

$$\frac{\partial F(x;\boldsymbol{\xi};\boldsymbol{\tau})}{\partial x} > 0.$$

Operating on the derivative it follows that, after some algebra,

$$\frac{\partial F(x;\boldsymbol{\xi};\boldsymbol{\tau})}{\partial x} = \delta G^{\alpha-1}(x;\boldsymbol{\tau})\frac{\partial G(x;\boldsymbol{\tau})}{\partial x}\left\{[1-F(x;\boldsymbol{\xi};\boldsymbol{\tau})]^{\alpha} + \frac{[1-F(x;\boldsymbol{\xi};\boldsymbol{\tau})]^{\alpha}}{[1-F(x;\boldsymbol{\xi};\boldsymbol{\tau})]}\right\}$$

where $\delta = \alpha\theta > 0$, by hypothesis. Since $0 \leq G(x;\boldsymbol{\tau}) \leq 1$ it verifies that

$$\frac{\partial F(x;\boldsymbol{\xi};\boldsymbol{\tau})}{\partial x} > 0$$

which shows that F is a strictly increasing function of x. Keep in mind that $F : \mathbb{R} \longrightarrow [0,1]$ and the $inf\,(F = 0)$. It is worth of saying that, once F was generated by the transformation (3.1), the proof could be done on it. It is important to do it since neither all transformations preserve structure, as can be seen from Jensen Inequality (BILLINGSLEY, 1995).

3.4 MOMENT GENERATING FUNCTION AND MOMENTS

Here, some special functions are defined with the role of generating moments and probability functions. Their primary role is to simplify calculational tasks of the induced distributions under investigation. When one has the closed form of this function, say, the integrand is integrable, it is possible to calculate moments from it, if $\mathcal{M}_X(s)$ is smooth.

3.4.1 Moment Generating Function

Let X be a random variable of the continuous type with density function $f(x;\boldsymbol{\xi},\boldsymbol{\tau})$ such that $E(e^{sx}) \equiv \mathcal{M}_X(s)$. Thus, if $X \sim$TMO-G$(\boldsymbol{\xi},\boldsymbol{\tau})$, one has

$$\begin{aligned}\mathcal{M}_X(s) &= \int_{-\infty}^{+\infty} e^{sx} f(x;\boldsymbol{\xi},\boldsymbol{\tau})dx \\ &= \alpha\theta \int_{-\infty}^{+\infty} e^{sx} \frac{g(x;\boldsymbol{\tau})G^{\alpha-1}(x;\boldsymbol{\tau})\left[1-G(x;\boldsymbol{\tau})\right]^{\alpha-1}}{\left\{G^{\alpha}(x;\boldsymbol{\tau})+\theta\left[1-G(x;\boldsymbol{\tau})\right]^{\alpha}\right\}^2}dx.\end{aligned} \tag{3.11}$$

For the case where the baseline is the exponential distribution, for example, one has,

$$\mathcal{M}_X(s) = \alpha\theta\lambda \int_0^{+\infty} \frac{e^{(s-\alpha\lambda)x}\left(1-e^{-\lambda x}\right)^{\alpha-1}}{\left\{(1-e^{-\lambda x})^{\alpha}+\theta e^{-\alpha\lambda x}\right\}^2}dx,$$

which already, is not straightforward to solve. Hence, in most cases the improper integrals of the type given by (3.11) are not easy to solve, or even, expressed in terms of a finite number of elementary known functions, reason by which, another technique must be applied, when possible. Sometimes, even this approach seems to be inefficient.

To contour this problem, some power series techniques are applied, when minimal conditions are fulfilled by the involved functions. When this is the case, one may have the following theorem.

Theorem 4 *The cdf given by (3.5) has power series expansion,*

$$F(x;\boldsymbol{\xi};\boldsymbol{\tau}) = \sum_{r=0}^{\infty} d_r H_r(x;\boldsymbol{\xi};\boldsymbol{\tau}), \tag{3.12}$$

where,

$$\begin{aligned} d_0 &= \frac{s_0}{c_0} \quad \textit{and,} \\ d_r &= c_0^{-1}\left(s_r - \sum_{t=1}^{r} c_t s_{r-t}\right), \end{aligned}$$

for $r \geq 1$. Furthermore, $H_r(.)$ denotes the exponentiated-G distribution, with additional parameter r.

Dem. 7 *By using the Ansatz,*

$$(1-z)^b = \sum_{k=0}^{\infty} (-1)^k \binom{b}{k} z^k$$

for $b > 0$ and $|z| < 1$. Therefore, from (3.5), it follows that

$$F(x;\boldsymbol{\xi},\boldsymbol{\tau}) = \frac{G^{\alpha}(x;\boldsymbol{\xi},\boldsymbol{\tau})}{G^{\alpha}(x;\boldsymbol{\xi},\boldsymbol{\tau}) + \sum_{k=0}^{\infty} b_k G^{\alpha}(x;\boldsymbol{\xi},\boldsymbol{\tau})}, \tag{3.13}$$

where

$$b_k \;=\; b_k(\alpha,\theta) \equiv (-1)^k \theta \binom{b}{k}.$$

Furthermore, for $z \in (0,1)$ and $0 \leq \alpha \leq \infty$, consider the series,

$$z^{\alpha} = \sum_{r=0}^{\infty} S_r(\alpha) z^r, \tag{3.14}$$

where,

$$S_r(\alpha) = S_r = \sum_{l=r}^{\infty} (-1)^{l+r} \binom{\alpha}{l} \binom{l}{r}.$$

Therefore, by using (3.14) and (3.13), it follows that,

$$\begin{aligned} F(x;\boldsymbol{\xi},\boldsymbol{\tau}) &= \frac{\sum_{r=0}^{\infty} S_r(\alpha) G^r(x;\boldsymbol{\xi},\boldsymbol{\tau})}{\sum_{i=0}^{\infty} S_i(\alpha) G^i(x;\boldsymbol{\xi},\boldsymbol{\tau}) + \sum_{k=0}^{\infty} b_k G^k(x;\boldsymbol{\xi},\boldsymbol{\tau})} \\ &= \frac{\sum_{r=0}^{\infty} S_r(\alpha) G^r(x;\boldsymbol{\xi},\boldsymbol{\tau})}{\sum_{i=0}^{\infty} c_i(\alpha,\theta) G^i(x;\boldsymbol{\xi},\boldsymbol{\tau})}, \end{aligned}$$

where,

$$c_i(\alpha,\theta) = S_i(\alpha) + b_i(\alpha,\theta).$$

Finally, using a known result concerning the quotient of two power series, Fikhtengol'Ts (1970), one has the result of the theorem. □

Corollary 5 *As a consequence of the theorem above it follows that*

$$f\left(x;\boldsymbol{\xi};\boldsymbol{\tau}\right) = \sum_{r=0}^{\infty} d_{r+1} h_{r+1}\left(x;\boldsymbol{\xi};\boldsymbol{\tau}\right) \tag{3.15}$$

where $h_{r+1}\left(x;\boldsymbol{\xi};\boldsymbol{\tau}\right)$ is the pdf of Exp-G family with additional parameter $r+1$

However, the theory developed in Chapter 2, seems to be promising in the sense that, offering an alternative way to calculate moments without having to calculate integrals, turn the procedures more attractive, because of the avoiding such integration processes and infinity series approaches.

Remark 7 *A functional series is intimately related to its coefficients which, in counterparts, may be real or complex numbers. An ordinary example comes from the geometric series, or*

ideas derived from it, which, in the domain of its radius of convergence, endowed with some more additional hypothesis, can be integrated term-to-term, (FIKHTENGOL'TS, 1970).

The integrated series guards some relations to the former by the similitude, albeit unequal, coefficients, even if the final functions differ significantly: $\frac{1}{1+x}$ *and* $\log(1+x)$*, for example. Additionally, the results obtained in Theorem 4 and, consequently, in the Corollary 5, are similar to those found in the work of Lima et. al (2019), but worth of noting that the weights therein are different.*

3.4.2 Moments

Given a distribution function, there are numerical characteristics, say it classical for, they appears as mandatory for the distribution theory, such as the *expected values* and *variance*, central tools for the inference process. A physical way to understand the meaning of the expected values, seen as the mean of a given distribution is the occasion you must sustain a long rod. If you are an adult, the experience tells you to choose the center of gravity of the rod. If you are a child in process of learning, you'll use trial and error to find that point that will be the experience firstly spoken.

If it is desired to construct a method where one uses the concept of *moment generating function*, just described above, a hierarchical tool arises, with the mean and variance as the first and second *moments*, respectively. The term hierarchical, here, refers to the fact that the process is a concatenated one, with the mean, seen as an expected value, in the kernel of the process. Thus, if a random variable X has absolutely continuous distribution, such as the conditions exposed just above, with a $pdf\ f(x)$, then the moments about zero and the central moments, have the following expressions:

$$\begin{aligned}\mu_n &= EX^n \equiv E(X^n) = \int_{-\infty}^{\infty} x^n f(x)dx \\ \tilde{\mu}_n &= E\left(X - E(X)\right)^n = \int_{-\infty}^{\infty} \left(x - E(X)\right)^n f(x)dx\end{aligned}$$

Again, one says that the moments do exist if,

$$\int_{-\infty}^{\infty} |x|^n f(x)dx < \infty.$$

It's not hard to see that for all classes of functions, this is not an easy task, once the total process involves an improper integration procedure. One should be convinced by choosing, at

(3.11), $\alpha = 1$, leading to exact solution, but in terms of special function, and $\alpha = 2$, an open problem in this text.

In the spirit of the Chapter 2, the expected value and variance are given by:

$$E(X) \;=\; \sqrt{-\frac{1}{2\{M,x\}}} \text{ and } Var(X) = -\frac{1}{2\{M,x\}}, \tag{3.16}$$

where the notation $\{\cdot\}$ indicates the derivative of the operator M in relation to x.

3.5 ESTIMATION

Once the distributions are known, the natural path to proceed is the process of statistical inference and decision. The purpose of dealing with sample statistics is to produce information, here seen as worked data, or better saying, noncrude data. However, the process of generalizing from the sample to population is the duty of statistical inference, the ultimate tool through which the information, as a decision-making process, is applied. In the next chapters some datasets are given. Some, like the one related to COVID-19, are real-time data acquired in official government channels, due to the exception period the world is living in. Other are simulated data generated by physical model, in particular, for hydrodynamical systems.

During the process of statistical model construction, the problem of knowing the values of parameters that enter into the functions, that best fit the data under analysis, comes. In what follows, the method of Maximum Likelihood is used, as a criterion, to solve estimation problems in direction of existence of that best estimate.

Suppose that $\mathbf{X}$ is a vector whose coordinates are real random variables, i.e., $\mathbf{X} = \{x_1, \cdots, x_n\}$. Then, with $\boldsymbol{\xi}, \boldsymbol{\tau}$ the parameter vectors (for the family here studied and the baseline, respectively), and $f(x_i; \boldsymbol{\xi}; \boldsymbol{\tau})$ given by 3.6,

$$\begin{aligned} l\left(x_i; \boldsymbol{\xi}, \boldsymbol{\tau}\right) \;&=\; n\log\left[\alpha\theta\right] + \sum_{i=1}^{n}\log\left[g\left(x_i;\boldsymbol{\tau}\right)\right] + (\alpha-1)\sum_{i=1}^{n}\log\left[G\left(x_i;\boldsymbol{\tau}\right)\right] \\ &+\; (\alpha-1)\sum_{i=1}^{n}\log\left[1-G(x_i;\boldsymbol{\tau})\right] \\ &-\; 2\sum_{i=1}^{n}\log\left\{G^{\alpha}\left(x_i;\boldsymbol{\tau}\right) + \theta\left[1-G(x_i;\boldsymbol{\tau})\right]^{\alpha}\right\}. \end{aligned} \tag{3.17}$$

Once it is established the likelihood function, the next step is proceeding to calculate the score functions and their consequent meaning. For the general expression (3.17) it reads

$$\partial_{\{\boldsymbol{\xi},\boldsymbol{\tau}\}} l\left(x_i; \boldsymbol{\xi}, \boldsymbol{\tau}\right),$$

which is an additive function. Of course when one is dealing with the baselines this vector set is allowed to increase. Meanwhile,

$$\partial_{\{\boldsymbol{\xi},\boldsymbol{\tau}\}} l\left(x_i;\boldsymbol{\xi},\boldsymbol{\tau}\right)=\left[\frac{\partial l\left(x;\boldsymbol{\xi};\boldsymbol{\tau}\right)}{\partial\alpha},\frac{\partial l\left(x;\boldsymbol{\xi};\boldsymbol{\tau}\right)}{\partial\theta},\frac{\partial l\left(x;\boldsymbol{\xi};\boldsymbol{\tau}\right)}{\partial\tau_k}\right]^T, \tag{3.18}$$

where, τ_k is the k^{th} component of parameter vector $\boldsymbol{\tau}$. Once the baseline depends on the $\boldsymbol{\tau}$ that, in its turn, does not depends on α and θ, the derivatives read,

$$\begin{aligned}\frac{\partial l\left(x;\boldsymbol{\xi},\boldsymbol{\tau}\right)}{\partial\alpha} &= \frac{n}{\alpha}+\sum_{i=1}^{n}\log\left\{G(x_i;\boldsymbol{\tau})\left[1-G(x_i;\boldsymbol{\tau})\right]\right\}\\ &- 2\sum_{i=1}^{n}\frac{\left\{G(x_i,\boldsymbol{\tau})\log G(x_i,\boldsymbol{\tau})+\theta\left[1-G(x_i,\boldsymbol{\tau})\right]^{\alpha}\log\left[1-G(x_i,\boldsymbol{\tau})\right]\right\}}{G^{\alpha}(x_i,\boldsymbol{\tau})+\theta\left[1-G(x_i,\boldsymbol{\tau})\right]},\end{aligned}$$

$$\frac{\partial l\left(x;\boldsymbol{\xi},\boldsymbol{\tau}\right)}{\partial\theta} = \frac{n}{\theta}-2\sum_{i=1}^{n}\frac{1-G^{\alpha}(x_i;\boldsymbol{\tau})}{G^{\alpha}(x_i;\boldsymbol{\tau})+\theta\left[1-G(x_i;\boldsymbol{\tau})\right]^{\alpha}}.$$

if $G(x_i;\boldsymbol{\tau})$ does not depend on θ.

For the derivative in relation to parameter vector $\boldsymbol{\tau}$, the componentwise relation reads,

$$\begin{aligned}\frac{\partial l(x;\boldsymbol{\xi},\boldsymbol{\tau})}{\partial\tau_k} &= \sum_{i=1}^{n}\frac{1}{g(x_i;\tau_k)}\frac{\partial g(x_i;\tau_k)}{\partial\tau_k}+(\alpha-1)\sum_{i=1}^{n}\left\{\frac{1-2G\left(x_i;\tau_k\right)}{G\left(x_i;\tau_k\right)\overline{G}(x_i;\tau_k)}\right\}\partial_{x_i,\tau_k}\\ &- 2\alpha\sum_{i=1}^{n}\left\{\frac{G^{\alpha-1}(x_i;\tau_k)-\theta\overline{G}(x_i;\tau_k)^{\alpha-1}}{G^{\alpha}(x_i;\tau_k)+\theta\overline{G}(x_i;\tau_k)^{\alpha}}\right\}\partial_{x_i,\tau_k}.\end{aligned}$$

where

$$\begin{aligned}\overline{G}(x_i;\tau_k) &= \left[1-G\left(x_i;\tau_k\right)\right]\\ \partial_{x_i,\tau_k} &= \frac{\partial G\left(x_i;\tau_k\right)}{\partial\tau_k}\end{aligned}$$

Now, for calculation of estimators, the vector given by (3.18) is set to zero, that is to say,

$$\partial_{\{\boldsymbol{\xi},\boldsymbol{\tau}\}} l\left(x_i;\boldsymbol{\xi},\boldsymbol{\tau}\right)=\left[0,0,0,0\right]^T, \tag{3.19}$$

leading to the system of nonlinear equations whose simultaneous solution leads to the set of estimator

$$\hat{l}\left(x_i;\hat{\boldsymbol{\xi}},\hat{\boldsymbol{\tau}}\right)=\left(\hat{\alpha},\hat{\theta},\hat{\tau}_k\right)$$

$$\begin{cases}0 &= \frac{n}{\hat{\alpha}}+\sum_{i=1}^{n}\log\left\{G(x_i;\boldsymbol{\tau})\left[1-G(x_i;\boldsymbol{\tau})\right]\right\}\\ &- 2\sum_{i=1}^{n}\frac{\left\{G(x_i,\boldsymbol{\tau})\log G(x_i,\boldsymbol{\tau})+\hat{\theta}[1-G(x_i,\boldsymbol{\tau})]^{\hat{\alpha}}\log\left[1-G(x_i,\boldsymbol{\tau})\right]\right\}}{G^{\hat{\alpha}}(x_i,\boldsymbol{\tau})+\hat{\theta}[1-G(x_i,\boldsymbol{\tau})]},\\ 0 &= \frac{n}{\hat{\theta}}-2\sum_{i=1}^{n}\frac{1-G^{\alpha}(x_i;\boldsymbol{\tau})}{G^{\hat{\alpha}}(x_i;\hat{\boldsymbol{\tau}})+\hat{\theta}[1-G(x_i;\hat{\boldsymbol{\tau}})]^{\hat{\alpha}}},\\ 0 &= \sum_{i=1}^{n}\frac{1}{g(x_i;\hat{\tau}_k)}\frac{\partial g(x_i;\hat{\tau}_k)}{\partial\hat{\tau}_k}+(\hat{\alpha}-1)\sum_{i=1}^{n}\left\{\frac{1-2G(x_i;\hat{\tau}_k)}{G(x_i;\hat{\tau}_k)[1-G(x_i;\hat{\tau}_k)]}\right\}\frac{\partial G(x_i;\hat{\tau}_k)}{\partial\hat{\tau}_k}\\ &- 2\hat{\alpha}\sum_{i=1}^{n}\left\{\frac{G^{\hat{\alpha}-1}(x_i;\hat{\tau}_k)-\hat{\theta}[1-G(x_i;\hat{\tau}_k)]^{\hat{\alpha}-1}}{G^{\hat{\alpha}}(x_i;\hat{\tau}_k)+\hat{\theta}[1-G(x_i;\hat{\tau}_k)]^{\hat{\alpha}}}\right\}\frac{\partial G(x_i;\hat{\tau}_k)}{\partial\hat{\tau}_k}.\end{cases}$$

The asymptotic distribution of $(\hat{\boldsymbol{\xi}} - \boldsymbol{\xi})$ is $N_{k+2}(0, J(\hat{\boldsymbol{\xi}})^{-1})$ under standard regularity conditions, where $J(\boldsymbol{\xi})$ is total observed information matrix. Based on this family, one can construct approximate confidence intervals for the individual parameters. Additionally, one can compute the maximum values of the unrestricted and restricted log-likelihoods to obtain likelihood ratio (LR) statistics for testing some sub-models of the TMO-G distribution. Considering $\theta \in (0, 1)$, it is adopted the following reparametrization for $\theta = \frac{\exp(\theta^*}{1+exp(\theta^*)}$, where $\theta^* \in \mathbb{R}$. This procedure is about to be used in all simulations encountered on next chapters of this work.

It is desired to know the exact value of the parameter vectors, $\{\boldsymbol{\xi}, \boldsymbol{\tau}\} \in \mathbb{R}^n$, when dealing with the observed data. However it is not possible once, in practice, the information is not available. The general way to escape from this trap is to infer the parameter values from data.

Since it is given the random variable X, the functional law, f, that relates the vector parameter and the potential outcomes x of X, allows one to establish a positive semi-definite symmetric matrix of dimension in accordance with the dimension of the vector parameters, whose entrances depend on the score function given above. The second derivatives expressed as $\dot{l}$ gives rise to

$$I_X\left(\{\boldsymbol{\xi}, \boldsymbol{\tau}\}\right) = \begin{bmatrix} \frac{\partial^2 l(x;\boldsymbol{\xi};\boldsymbol{\tau})}{\partial \alpha^2} & \frac{\partial^2 l(x;\boldsymbol{\xi};\boldsymbol{\tau})}{\partial \alpha \partial \theta} & \cdots & \frac{\partial^2 l(x;\boldsymbol{\xi};\boldsymbol{\tau})}{\partial \alpha \tau_k} \\ \frac{\partial^2 l(x;\boldsymbol{\xi};\boldsymbol{\tau})}{\partial \theta \partial \alpha} & \frac{\partial^2 l(x;\boldsymbol{\xi};\boldsymbol{\tau})}{\partial \theta^2} & \cdots & \frac{\partial^2 l(x;\boldsymbol{\xi};\boldsymbol{\tau})}{\partial p \partial \tau_k} \\ \vdots & \vdots & \vdots & \vdots \\ \frac{\partial^2 l(x;\boldsymbol{\xi};\boldsymbol{\tau})}{\partial \tau_k \partial \alpha} & \frac{\partial^2 l(x;\boldsymbol{\xi};\boldsymbol{\tau})}{\partial \tau_k \partial \theta} & \cdots & \frac{\partial^2 l(x;\boldsymbol{\xi};\boldsymbol{\tau})}{\partial \tau_k^2} \end{bmatrix} \tag{3.20}$$

whose expressions are given below at (3.6)

3.5.1 Optimization

As described on starting this section, the process of model construction as well as the seek for the parameter values best fitting the data are canonical procedure in a statistical analysis.

Once one is dealing with functions, in general, of several variables, as seen of having several parameters, as multiparameter distributions, Jacobians and Hessians, the operationality is frequently unamenable, due to the proper nature of the functions and relevant procedure. For example, at Chapter 4, the particle approximation is of second order nature. This implies numerical consequences for the results on the simulations performed during the analysis. Do remember that, first-order optimization algorithms use only gradients and, the information

about curvature, that one is probably encountering through the process, turn the later to a state where loss of information takes place, leading to erroneous results.

The solution for this apparent problem is to consider second-order optimization methods. This is, indeed, a requirement when dealing with Hessians for example so, constituting no novelty. The second-order method, in contrast to the former do consider the curvature of descent process and improve the velocity of convergence, (MURPHY, 2021).

The classic second-order method is Newton's method. This consists of updates of the form,

$$\boldsymbol{\theta}_{t+1} = \boldsymbol{\theta}_t - \eta_t \mathbf{H}^{-1}\mathbf{g}_t$$

where,

$$\mathbf{H}^{-1} \triangleq \nabla^2 \mathcal{L}(\boldsymbol{\theta})|_{\boldsymbol{\theta}_t} = \nabla^2 \mathcal{L}(\boldsymbol{\theta}_t) = \boldsymbol{H}(\boldsymbol{\theta}_t)$$

is assumed to be positive-definite ensuring the update process well-defined. Along the applications some methods are used, $BFGS$ being such a one. There are methods known as quasi-Newton sometimes called variable metric methods, iteratively build up an approximation to the Hessian using information gleaned from the gradient vector at each step, (MURPHY, 2021). The most common being **BFGS**. For more details one is addressed to the last reference as well as (NOCEDAL, 2006). Other methods are indeed available among which, the Nelder-Mead who is a numerical method used to find the minimum or maximum of an objective function in a multidimensional space. It is a derivative-free optimization method based on coordinate and pattern-search algorithm that, at any stage of that algorithmic process, only track of $n+1$ points of interest, say, in $\mathbf{R}^n$, are kept, whose convex hull forms a simplex, (NOCEDAL, 2006).

Setting the derivatives of the log-likelihood function for all parameters to zero, the respective MLEs are obtained by numerical method. The approximate variances and the Confidence Intervals(CIs) of the parameters are obtained by inverting the observed Fisher matrix.

The $100(1-\gamma)\%$ symmetric approximate normal CIs of parameters are constructed by

$$\hat{\theta} - z_{\gamma/2}\sqrt{\mathsf{Var}(\hat{\theta})}, \hat{\theta} + z_{\gamma/2}\sqrt{\mathsf{Var}(\hat{\theta})},$$

where $z_{\gamma/2}$ is the upper $\gamma/2$ point of standard normal distribution, and θ can be any parameters.

3.6 GENERAL RESULTS FOR ESTIMATION

As posted above, the derivative of $l(\boldsymbol{\xi};\boldsymbol{\tau};x_i)$ in relation to the parameter vector components, reads

$$\partial_{\{\boldsymbol{\xi},\boldsymbol{\tau}\}} l\left(x_i;\boldsymbol{\xi},\boldsymbol{\tau}\right)=\left[\frac{\partial l\left(x_i;\boldsymbol{\xi},\boldsymbol{\tau}\right)}{\partial\alpha},\frac{\partial l\left(x_i;\boldsymbol{\xi},\boldsymbol{\tau}\right)}{\partial\theta},\frac{\partial l\left(x_i;\boldsymbol{\xi},\boldsymbol{\tau}\right)}{\partial\tau_k}\right]^T, \tag{3.21}$$

where, τ_k is the kth component of parameter vector $\boldsymbol{\tau}$. Then, the score functions read,

$$\begin{aligned}\frac{\partial l\left(x_i;\boldsymbol{\xi},\boldsymbol{\tau}\right)}{\partial\alpha} &= \frac{n}{\alpha}+\sum_{i=1}^{n}\frac{1}{g(x_i;\boldsymbol{\tau})}\frac{\partial g(x_i;\boldsymbol{\tau})}{\partial\alpha}+\sum_{i=1}^{n}\log\left\{G(x_i;\boldsymbol{\tau})\left[1-G(x_i;\boldsymbol{\tau})\right]\right\}\\ &+ (\alpha-1)\sum_{i=1}^{n}\left[\frac{1-2G(x_i;\boldsymbol{\tau})}{G(x_i;\boldsymbol{\tau})\left[1-G(x_i;\boldsymbol{\tau})\right]}\right]\frac{\partial G(x_i;\boldsymbol{\tau})}{\partial\alpha}\\ &- 2\alpha\sum_{i=1}^{n}\frac{G^{\alpha-1}(x_i;\boldsymbol{\tau})-\theta\left[1-G(x_i;\boldsymbol{\tau})\right]^{\alpha-1}}{G^{\alpha}(x_i;\boldsymbol{\tau})+\theta\left[1-G(x_i;\boldsymbol{\tau})\right]^{\alpha}}\frac{\partial G(x_i;\boldsymbol{\tau})}{\partial\alpha},\end{aligned}$$

$$\begin{aligned}\frac{\partial l(x_i;\boldsymbol{\xi},\boldsymbol{\tau})}{\partial\theta} &= \frac{n}{\theta}-2\alpha\sum_{i=1}^{n}\frac{G^{\alpha-1}(x_i;\boldsymbol{\tau})+\theta\left[1-G(x_i;\boldsymbol{\tau})\right]^{\alpha-1}}{G^{\alpha}(x_i;\boldsymbol{\tau})+\theta\left[1-G(x_i;\boldsymbol{\tau})\right]^{\alpha}}\frac{\partial G(x_i;\boldsymbol{\tau})}{\partial\theta}\\ &- 2\sum_{i=1}^{n}\frac{1-G^{\alpha}(x_i;\boldsymbol{\tau})}{G^{\alpha}(x_i;\boldsymbol{\tau})+\theta\left(1-G(x_i;\boldsymbol{\tau})\right)^{\alpha}}.\end{aligned}$$

For the derivative in relation to parameter vector $\boldsymbol{\tau}$, the componentwise relation reads,

$$\begin{aligned}\frac{\partial l(x_i;\boldsymbol{\xi},\boldsymbol{\tau})}{\partial\tau_k} &= \sum_{i=1}^{n}\frac{1}{g(x_i;\tau_k)}\frac{\partial g(x_i;\tau_k)}{\partial\tau_k}+(\alpha-1)\sum_{i=1}^{n}\left\{\frac{1-2G\left(x_i;\tau_k\right)}{G\left(x_i;\tau_k\right)\overline{G}(x_i;\tau_k)}\right\}\frac{\partial G\left(x_i;\tau_k\right)}{\partial\tau_k}\\ &- 2\alpha\sum_{i=1}^{n}\left\{\frac{G^{\alpha-1}(x_i;\tau_k)-\theta\overline{G}(x_i;\tau_k)^{\alpha-1}}{G^{\alpha}(x_i;\tau_k)+\theta\overline{G}(x_i;\tau_k)^{\alpha}}\right\}\frac{\partial G\left(x_i;\tau_k\right)}{\partial\tau_k},\end{aligned}$$

where

$$\overline{G(x_i;\tau_k)}=\left[1-G\left(x_i;\tau_k\right)\right].$$

The Hessian elements are given by

$$\begin{aligned}
\frac{\partial^2 l\left(x_i;\boldsymbol{\xi},\boldsymbol{\tau}\right)}{\partial\alpha^2} &= -\frac{n}{\alpha^2}-\sum_{i=1}^{n}\left\{\frac{1}{g(x_i;\boldsymbol{\tau})^2}\left[\frac{\partial g(x_i;\boldsymbol{\tau})}{\partial\alpha}\right]+\frac{1}{g(x_i;\boldsymbol{\tau})}\frac{\partial^2 g(x_i;\boldsymbol{\tau})}{\partial\alpha}\right\}\\
&+ \sum_{i=1}^{n}\frac{1-2G(x_i;\boldsymbol{\tau})}{G(x_i;\boldsymbol{\tau})\overline{G}(x_i;\boldsymbol{\tau})}\frac{\partial G(x_i;\boldsymbol{\tau})}{\partial\alpha}+\sum_{i=1}^{n}\frac{1}{G(x_i;\boldsymbol{\tau})}\frac{\partial G(x_i;\boldsymbol{\tau})}{\partial\alpha}\\
&+ (\alpha-1)\sum_{i=1}^{n}\left\{\frac{1}{G(x_i;\boldsymbol{\tau})}\frac{\partial^2 G(x_i;\boldsymbol{\tau})}{\partial\alpha^2}-\frac{1}{G^2(x_i;\boldsymbol{\tau})}\left(\frac{\partial G(x_i;\boldsymbol{\tau})}{\partial\alpha}\right)^2\right\}\\
&+ (1-\alpha)\sum_{i=1}^{n}\frac{1}{1-G^2(x_i;\boldsymbol{\tau})}\left(\frac{\partial G(x_i;\boldsymbol{\tau})}{\partial\alpha}\right)^2\\
&- \sum_{i=1}^{n}\frac{1}{1-G(x_i;\boldsymbol{\tau})}\frac{\partial G(x_i;\tau)}{\partial\alpha}\\
&+ (2-\alpha)\sum_{i=1}^{n}\frac{1}{1-G(x_i;\boldsymbol{\tau})}\frac{\partial^2 G(x_i;\boldsymbol{\tau})}{\partial\alpha^2}\\
&- 2\sum_{i=1}^{n}\frac{1}{L^2}\left\{\left(\frac{\partial G(x_i;\boldsymbol{\tau})}{\partial\alpha}\right)\frac{L''L}{\alpha}-\frac{L'^2}{\alpha^2}\right\}\\
&+ \left\{\frac{1}{\alpha}\left(\frac{L'}{L}\right)\left(\frac{\partial G(x_i;\boldsymbol{\tau})}{\partial\alpha}\right)^{-1}\right\}\frac{\partial^2 G(x_i;\boldsymbol{\tau})}{\partial\alpha^2},
\end{aligned}$$

$$\frac{\partial^2 l\left(x_i;\boldsymbol{\xi},\boldsymbol{\tau}\right)}{\partial\theta^2} = -\frac{n}{\theta^2}+2\alpha\sum_{i=1}^{n}\frac{\overline{G}^{\alpha}(x;\tau_k)L'}{L^2}\frac{\partial G(x_i;\boldsymbol{\tau})}{\partial\alpha},$$

$$
\begin{aligned}
\frac{\partial^2 l\left(x_i;\boldsymbol{\xi},\boldsymbol{\tau}\right)}{\partial\tau_k^2} &= \sum_{i=1}^{n}\left\{\frac{1}{g(x_i;\tau_k)}\frac{\partial^2 g(x_i;\tau_k)}{\partial\tau_k^2}-\left[\frac{1}{g}\frac{\partial g(x_i;\tau_k)}{\partial\tau_k}\right]^2\right\}\\
&- \overline{\alpha}_1\sum_{i=1}^{n}\left\{\frac{A}{G^2(x_i;\tau_k)\overline{G}(x;\tau_k)}\left(\frac{\partial G(x_i;\tau_k)}{\partial\tau_k}\right)^2\right\}\\
&- \overline{\alpha}_1\sum_{i=1}^{n}\left\{\frac{1-2G(x_i;\tau)}{G(x_i;\tau_k)\overline{G}(x;\tau_k)}\frac{\partial^2 G(x_i;\tau_k)}{\partial\tau_k^2}\right\}\\
&- \overline{\alpha}_2\sum_{i=1}^{n}\frac{Q_1}{Q_2}\left(\frac{\partial G(x_i;\tau_k)}{\partial\tau_k}\right)^2\\
&+ 2\alpha^2\sum_{i=1}^{n}\frac{G^{\alpha-1}(x_i;\tau_k)-\theta\overline{G}(x;\tau_k)^{\alpha-1}}{\left\{G^{\alpha}(x_i;\tau_k)+\theta\overline{G}(x;\tau_k)^{\alpha}\right\}^2}\left(\frac{\partial G(x_i;\tau_k)}{\partial\tau_k}\right)^2\\
&- 2\alpha\sum_{i=1}^{n}\frac{G^{\alpha-1}(x_i;\tau_k)-\theta\overline{G}(x;\tau_k)^{\alpha-1}}{G^{\alpha}(x_i;\tau_k)+\theta\overline{G}(x;\tau_k)^{\alpha}}\frac{\partial^2 G(x_i;\tau_k)}{\partial\tau_k^2},\\
\frac{\partial^2 l\left(x_i;\boldsymbol{\xi},\boldsymbol{\tau}\right)}{\partial\alpha\partial\theta} &= -\sum_{i=1}^{n}\frac{\overline{G}^{\alpha}(x_i;\boldsymbol{\tau})}{L}\left\{\frac{1}{\overline{G}(x_i;\boldsymbol{\tau})}+\frac{L'}{L}\right\}\frac{\partial G(x_i;\boldsymbol{\tau})}{\partial\alpha}=\frac{\partial^2 l\left(x_i;\boldsymbol{\xi},\boldsymbol{\tau}\right)}{\partial\theta\partial\alpha},\\
\frac{\partial^2 l\left(x_i;\boldsymbol{\xi},\boldsymbol{\tau}\right)}{\partial\theta\partial\tau_k} &= 2\alpha\sum_{i=1}^{n}\frac{\overline{G}^{\alpha}(x_i;\tau_k)}{L}\left\{\frac{1}{\overline{G}(x_i;\boldsymbol{\tau})}+\frac{L'}{L^2}\right\}\frac{\partial G(x_i;\tau_k)}{\partial\tau_k}=\frac{\partial^2 l\left(x;\boldsymbol{\xi};\boldsymbol{\tau}\right)}{\partial\tau_k\partial\theta},\\
\frac{\partial^2 l\left(x_i;\boldsymbol{\xi},\boldsymbol{\tau}\right)}{\partial\tau_k\partial\alpha} &= \sum_{i=1}^{n}\left\{\frac{1}{g(x_i;\boldsymbol{\tau})}\frac{\partial^2 g(x_i;\boldsymbol{\tau})}{\partial\tau_k\partial\alpha}-\frac{\partial g(x_i;\boldsymbol{\tau})}{\partial\tau_k}\frac{\partial g(x_i;\boldsymbol{\tau})}{\partial\alpha}\right\}\\
&+ \sum_{i=1}^{n}\frac{1}{G(x_i;\boldsymbol{\tau})}\frac{\partial G(x_i;\boldsymbol{\tau})}{\partial\tau_k}-\sum_{i=1}^{n}\frac{1}{\overline{G}(x_i;\boldsymbol{\tau})}\frac{\partial G(x_i;\boldsymbol{\tau})}{\partial\tau_k}\\
&- 2(\alpha-1)\sum_{i=1}^{n}\frac{1}{G(x_i;\boldsymbol{\tau})\overline{G}(x_i;\tau)}\frac{\partial G(x_i;\tau_k)}{\partial\tau_k}\frac{\partial G(x_i;\tau_k)}{\partial\alpha}\\
&- (\alpha-1)\sum_{i=1}^{n}\frac{1}{G^2(x_i;\boldsymbol{\tau})}\frac{\partial G(x_i;\tau_k)}{\partial\tau_k}\frac{\partial G(x_i;\tau_k)}{\partial\alpha}\\
&+ (\alpha-1)\sum_{i=1}^{n}\left[\frac{1-2G(x_i;\boldsymbol{\tau})}{G(x_i;\boldsymbol{\tau})\overline{G}(x_i;\boldsymbol{\tau})}\right]\frac{\partial^2 G(x_i;\boldsymbol{\tau})}{\partial\tau_k\partial\alpha}\\
&- -2\alpha\sum_{i=1}^{n}\left\{\left[\frac{L''}{L}-\alpha\frac{L'^2}{L^2}\right]\frac{\partial G(x_i;\tau_k)}{\partial\tau_k}\frac{\partial G(x_i;\tau_k)}{\partial\alpha}-\frac{L'}{L}\frac{\partial^2 G(x_i;\boldsymbol{\tau})}{\partial\tau_k\partial\alpha}\right\}\\
&= \frac{\partial^2 G(x_i;\boldsymbol{\tau})}{\partial\alpha\partial\tau_k},
\end{aligned}
$$

where,

$$
\begin{aligned}
\overline{G}(x;\tau_k) &= [1 - G(x_i;\boldsymbol{\tau})]\,, \\
A(x_i;\tau_k) &= 4G^2(x_i;\tau_k) - 2G(x_i;\tau_k) + 1, \\
\overline{\alpha}_1 &= (\alpha - 1), \\
\overline{\alpha}_2 &= 2\alpha(\alpha - 1), \\
L &= G^{\alpha} + \theta\,[1 - G(x_i;\boldsymbol{\tau})]^{\alpha}\,, \\
L' &= G^{\alpha-1}(x_i;\boldsymbol{\tau}) - \theta\,[1 - G(x_i;\boldsymbol{\tau})]^{\alpha-1}\,, \\
L'' &= G^{\alpha-2}(x_i;\boldsymbol{\tau}) + \theta\,[1 - G(x_i;\boldsymbol{\tau})]^{\alpha-2}\,, \\
Q_1 &= G^{2(\alpha-1)}(x_i;\tau_k) + \theta G^{\alpha-2}(x_i;\tau_k)\overline{G}^{\alpha}(x;\tau_k) + \theta^2\overline{G}^{2(\alpha-1)}(x;\tau_k), \\
Q_2 &= G^{2\alpha}(x_i;\tau_k) + 2\theta G^{\alpha}(x_i;\tau_k)\overline{G}^{\alpha}(x;\tau_k) + \theta^2\overline{G}^{2\alpha}(x;\tau_k).
\end{aligned}
$$

Once the components above are determined, the Fisher Information Matrix can be defined.

3.7 CONCLUSIONS

In this chapter, the Marshall-Olkin G family of distributions was seen to emerge from the class of transformations, by this time, seen as a generator, as depicted in early chapters. It was enough to select particular values, as shown at 2.2.1. Despite the majority of distributions and applications one encounter along this text do refer to the specific aforementioned distribution, there exist a wide number of possible distributions one can acquire.

Furthermore, along the chapter was developed properties of the studied family in the direction of construction of a general approach, such as: cumulative distribution functions, density functions and hazard rate functions, as well as a deeper study of the latter one concerning its shape. As was observed, a closed-form expression was developed for the quantile function and some methods applied to the study of moments was presented. In this sense, moments and moment generating functions was discussed by using an expansion of the density function in power series, once general properties involving, simple functions, such exponential as baseline, cannot be expressed in closed forms for the majority of cases one encounters, due to complexity of functional relationship. Finally, the estimations of parameters was developed by using the method of maximum likelihood. It is hoped, however, that this family come to further contribute to the range of families already existing in the theory of new distributions and its wide field of applications.

4 TRANSFORMED MARSHALL-OLKIN G FAMILY WITH EXPONENTIAL AND WEIBULL DISTRIBUTIONS AS BASELINE

4.1 INTRODUCTION

The general form developed on the last chapter is the fundamental arena where the proposed models, hereafter, will play their roles by realizing themselves in terms of the chosen baselines, which are, in this chapter, exponential and Weibull distributions.

As was mentioned before, the use of exponential distributions is vast, once, many phenomena in nature suggest that the behavior of their events, or dynamics, is particularly well described by this kind of relation. One example is that they characterize the probability distribution for waiting times between consecutive Poisson processes. To be more convincing in the mathematical point of view, the exponential function is a special function with interesting properties arising from the fact that it is an analytic function. From the property of being a convex function, several constructions and applications can arise in many branches of mathematics, (BREZIS, 2010), physics where, for example, Boltzmann-Gibbs distribution is defined as a statistical model in Mechanics, (NAUDTS, 2010), (DRAGULESCU A.; YAKOVENKO, 2001), and other areas of knowledge, such as Economics, (SAMPATH; LALITHA, 2016), (AFIFY; GEMEAY; IBRAHIM, 2020). It occurs, however, that function composition of distributions is allowed, giving rise to new classes of distributions which may model several kinds of phenomena, (NADARAJAH; JAYAKUMAR; RISTIć, 2013). However, in the words of Deming, (DEMING, 1964), all the developed constructions should be seen as a "*figure that can be used for a given purpose, for action*".

During the last few decades, many extensions of exponential scattering have been proposed. We can name a few: Beta Exponential (KOTZ, 2006), Exponentiated Exponential (NADARAJAH, 2011), Transmuted Exponential (OWOLOKO; OGUNTUNDE; ADEJUMO, 2015), Exponentiated Transmuted Exponential (AL-KADIM; MAHDI, 2018), Topp–Leone odd log-logistic exponential distribution, (AFIFY; AL-MOFLEH; DEY, 2021). The applications used in the contexts of the works mentioned above vary a lot, among which ones can cite data on: fatigue, survival time and reliability. The second distribution used as baseline, the Weibull, was detailed by the author, although Fréchet who first identified it, (FRÉCHET, 1927).

Applications go through size particles distribution, to interdisciplinary lifetime distributions, say, in engineering and medical sciences, (LAI, 2014), (ROSIN P. ;RAMMLER, 1934), (VESILIND,

1980), (HALLINAN, 1993). The amount of models that was generated through Weibull distributions and his generalizations advice one to keep focus on new applications, through new families proposition having the former as baseline, in attempt to describe vast classes of natural phenomena.

4.2 TRANSFORMED MARSHALL-OLKIN EXPONENTIAL DISTRIBUTION

In the first chapter, the M-transform was defined and some particular cases was explicitly described. Among them, the case where the well known transformation carried by Marshall and Olkin was derived. In this chapter, a special case of the Transmuted Marshall-Olkin G family is developed. Here, the exponential model is chosen, just for the simplicity and wide application already existing in the literature of extended exponentials.

Let X be a random variable following the exponential distribution, i.e,

$$\begin{aligned} g(x) &= \begin{cases} \lambda \mathrm{e}^{-\lambda x} & , x \geq 0, \\ 0 & , x < 0 \end{cases} \quad \text{and} \\ G(x) &= \begin{cases} 1 - \mathrm{e}^{-\lambda x} & , x \geq 0, \\ 0 & , x < 0. \end{cases} \end{aligned} \tag{4.1}$$

In Figure 4 the plot of exponential distribution and his corresponding probability density function are shown. As can be seen, the exponential pdf is a strictly decreasing function with unique mode at $y = 0$, where f assumes the value λ. As an analytical function the consequent structures derived from it are tractable and well defined, as can be seen, for example, in the quantile function determination.

Thus, considering the exponential model and the TMOG family, presented in last chapter, one obtains the Transformed Marshall-Olkin Exponential distribution (TMOE, for short). So, by inserting the expressions given in (4.1) in the equations of the cdf and pdf of the proposed family, one reads, respectively,

$$F(x; \alpha, \theta, \lambda) = \frac{\left(1 - \mathrm{e}^{-\lambda x}\right)^{\alpha}}{(1 - \mathrm{e}^{-\lambda x})^{\alpha} + \theta \mathrm{e}^{-\alpha \lambda x}}, \tag{4.2}$$

and

$$f(x; \alpha, \theta, \lambda) = \frac{\lambda \alpha \theta \left(1 - \mathrm{e}^{-\lambda x}\right)^{\alpha - 1} \mathrm{e}^{-\alpha \lambda x}}{\left\{(1 - \mathrm{e}^{-\lambda x})^{\alpha} + \theta \mathrm{e}^{-\alpha \lambda x}\right\}^{2}}. \tag{4.3}$$

Figure 4 – Cumulative distribution function and probability density function for exponential distribution, with $\lambda = 1.5$. The analytical properties of that distribution allows one to treat mathematical manipulations in a relatively ease way, including transformations.

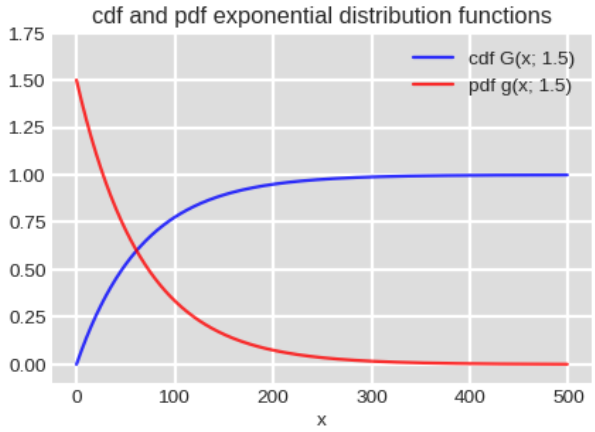

Source: the own author.

Thus, $X \sim$TMOE$(\alpha, \theta, \lambda)$, where α and θ are the additional parameters and λ is the one brought by the baseline.

Note that, as long as the parameter α increases, as seen at the description frame of the figure, the shape of the cumulative distribution function and its correspondent pdf varies, as can be easily observed from the curves in the Figure 5. It is well known that distribution functions, unless their canonical properties, are nondecreasing functions. However, the way of F increases is of particular interest, once the processes of modeling tend to account the diversity of natural phenomena and their forms of variations. In this sense, as wider the the way a function varies, better will be the fidedignity of the model in approximate the reality one is proposed to explain. When observing the right Figure on 5, one can see different properties which characterize and differentiate the model while the parameter brought by the distribution, changes. While varying the α parameter, one tends to recognize a change in the shape of the curve while, changing the parameter θ, one observes a change in the function similar the one obtains when varying the argument of a function. Then, theses parameters can be characterized as *shape* and *scale* parameters, respectively.

Despite the fact that the TMOE model is modified by the induction of parameters inherited from the transformation, it can be seen that the images of the functions given by the distributions have their shapes modified by weight of their tails. Of course this analysis just make sense only for the same scenery where the same set of parameters figures. It follows that, comparing the blue curve with the red one, it is possible to observe that, from the way that

the processes take place, ones are extremely fast in the first case, and slowly in the second one. This leads to conclusions that relates to the fat nature of the tails influenced by the induced parameters.

As the random variable varies the distribution function given by (4.3), gives rise to the surface generated while varying α, which can be seen in the Figure 6.

Figure 5 – Cumulative distribution function and probability density function for the model (4.2) and 4.3 and exponential distribution as baseline.

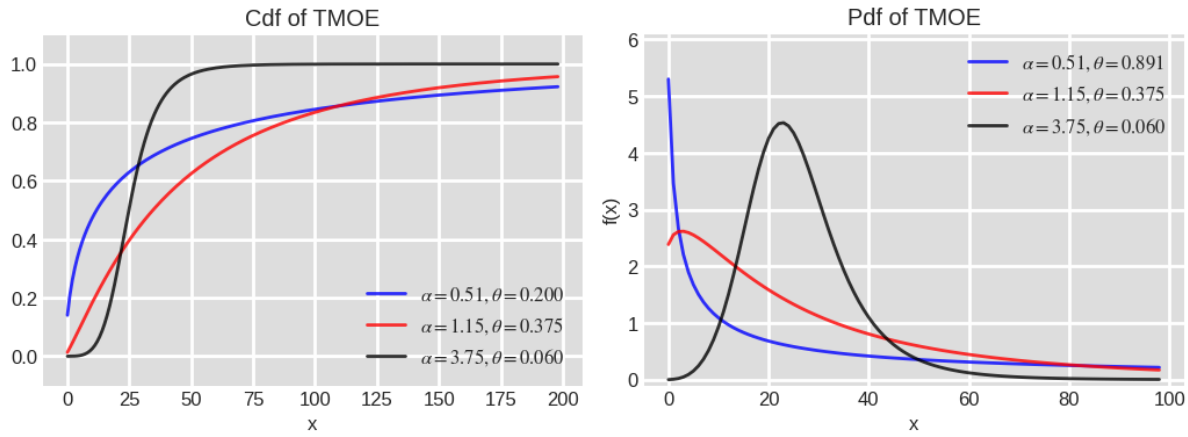

Source: the own author.

Figure 6 – Surface generated while varying α.

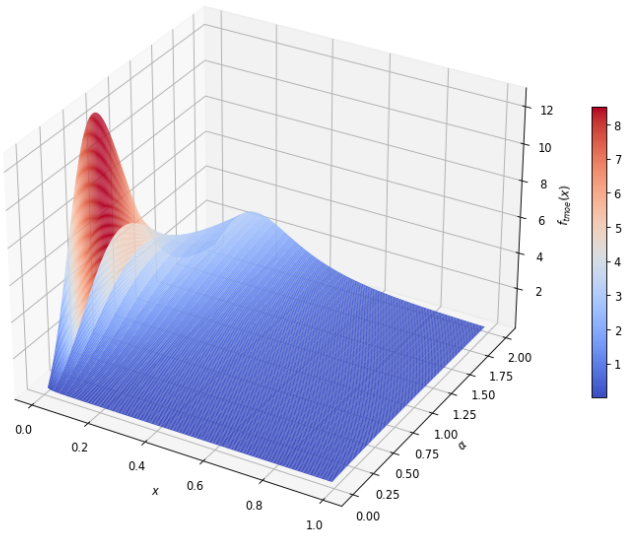

Source: the own author.

4.3 PROPERTIES

In this section, some properties of the TMOE model, such as mean, variance, hazard function and quantile function, are developed. The log-likelihood function is defined and some of its consequences are developed.

4.3.1 TMOE Hazard rate function

A brief commentary concerning the concept of hazard function was made in Chapter 3. However, some essential properties and mathematical meaning behind this construction depends on the concrete functions one is dealing with, not general expressions as seen in the general construction of that chapter. There, was mentioned a shape variation property, coming from the monotonicity of the hazard function which is, in counterpart, subjected to the parameter figuring in the function, itself, (MUDHOLKAR; SRIVASTAVA; FREIMER, 1995). The hazard function for the TMOE model is given and the log-derivative, as well as the function factor $T(x)$, is defined. The importance of the latter will turn clearer below and the former is a mean for the construction of T. The hazard function (hrf) for the new family distribution, according to 3.7, is

$$h_{exp}(x;\alpha,\theta,\lambda) = \frac{\alpha\lambda\left(1-\mathrm{e}^{-\lambda x}\right)^{\alpha-1}}{(1-\mathrm{e}^{-\lambda x})^{\alpha}+\theta\mathrm{e}^{-\alpha\lambda x}}. \tag{4.4}$$

One can see that, due to the increasing character of parameter setting, the hrf, $h(x;\boldsymbol{\xi},\boldsymbol{\tau})$, changes his variation from smooth to fast increments, that is to say, the shape of variation accompanies in the same fashion. This is not a general result, once, there are several practical situations wherein these functions exhibit non-monotone behaviour, (NAIR; SANKARAN; BALAKRISHNAN, 2018), (DAVIS, 1952). As examples, systems with bathtub distributions and periodical character are sources of data with such a property, (PARANJPE; RAJARSHI, 1986). Now, some procedures are made in order to derive a formal attempt to describe the relation between the density at hand and the shape exhibited by the hrf, $h(x;\boldsymbol{\xi},\boldsymbol{\tau})$. If $g(x;\boldsymbol{\tau})$ and $G(x;\boldsymbol{\tau})$ are the pdf and cdf of exponential distribution, respectively, it follows that, according to Proposition (8) in Chapter 3,

$$T(z) = \theta(2z-1) + (2z-1)(z-1)^{\alpha} - \alpha(z-1)^{\alpha}, \tag{4.5}$$

such that

$$\frac{r'(z)}{r(z)} = \frac{T(z)}{z(z-1)\left[\theta + (z-1)^{\alpha}\right]}. \tag{4.6}$$

.

Figure 7 – On the left frame, the hazard function shapes is shown. On the right, the graph shows the variation of T to enforce the same sign preservation property, as compared to $r'(z)$. The red curve is the denominator of the right side of (4.6).

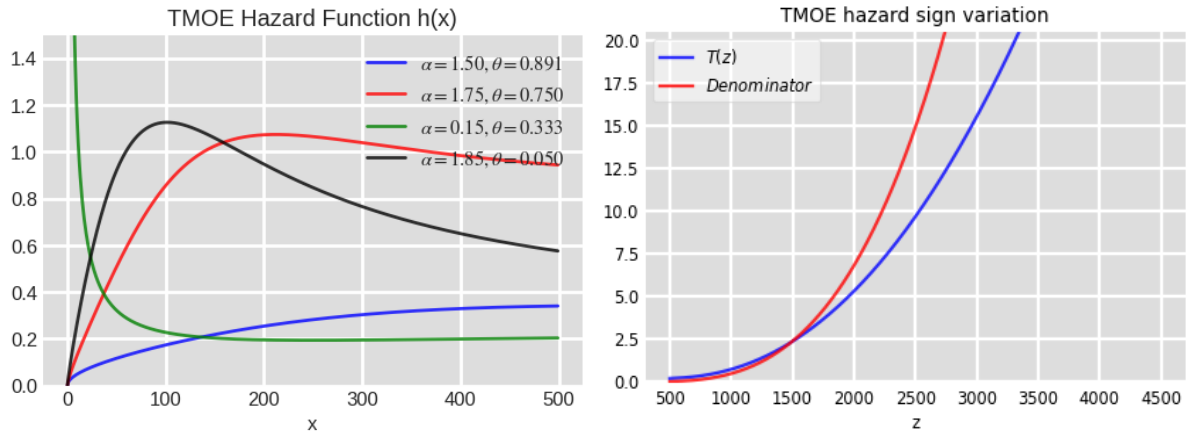

Source: the own author.

On the left of the Figure 7, the hazard function $h(x)$ is shown for fixed value of the baseline parameter λ, while the parameter set (α, θ) varies as shown in figures. Note that it is possible to obtain different forms for the failure rate function: increasing, decreasing, unimodal and inverted bathtub (restricting the parametric space).

The reason of the log-derivative of the hazard function was turned clear on Chapter 1. What should be clarified is the importance of the definition of the T factor function.

In both cases of Figure 8, one represents the factor function T for some different values of the parameter α, with θ and λ kept fixed. The first Figure on 8 expresses the curves for $0 < \alpha < 2$. It is seen on the figures that one can define a separation region, say, Region I, whose curves defined by $T(z)$ take positive values implying that the hazard function is monotonically increasing. Here there's a point worth of mention. By nearer looking the function T , one observes that, as α assumes the value 1, the term containing the factor $(\alpha - 1)$ vanishes, resulting in a balance among positive and negative values, leading to portions of the graph where the function is monotonically decreasing.

However, it constitutes no problem for what is studied here, once it is possible to define restriction of the function to the desired interval of interest, without loss of generality for

Figure 8 – Factor $T(z)$ for the separation regions.

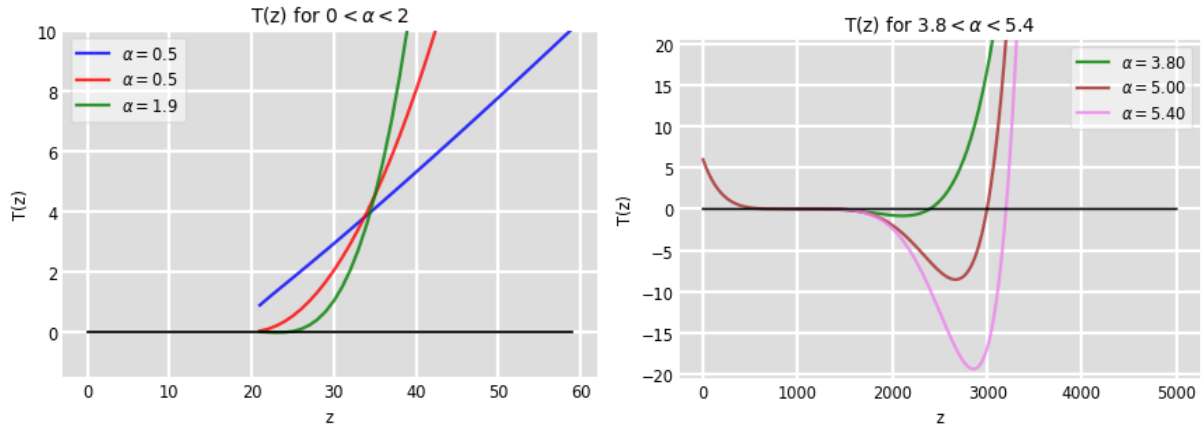

Source: the own author.

practical purposes. The red curve of the first figure, on 8, shows this restriction. Of course that, depending on the problem at hand, some additional hypothesis must be included in order to gain stronger results, where it fits. By observing the right figure, one notes that, for $3.8 < \alpha < 5.5$, there's a restriction of T where the portions of the curves are entirely on the negative branch of the plane. It implies a separation region, Region II, leading to monotone decreasing character of the hazard function. In a nonrestrictive sense, it is possible to define more two regions, say, Region III and Region IV, for where the behavior of the curves are more flexible. For example, in interval where $T(z)$ takes initially positive values, then changing for negative ones, indicates an unimodal character of the hazard function. For the fourth region, $T(z)$ takes initially negative values, then positive ones. This is indicative of bathtube shaped hazard function.

These results have interesting mathematical meaning, with important statistical interpretations. In the mathematical point of view there exist a separation in regions, according to parameter values, in consequence of the monotonicity property of the hazard function and its convexity. On the other hand, this *separation region* gives rise to suppositions on the class of shapes for the given distribution function under analysis. For example, shapes such as unimodal, bathtub and strictly increasing or decreasing behavior, for the distributions, can occur. As was pointed out in (QIAN, 2012), the hazard function and the T factor function share the same sign variation.

4.3.2 TMOE Quantile Function

Once the definition of quantile function was introduced on (3.7), the concept is applied to the exponential cdf, leading to

$$Q_{exp}(u) = \begin{cases} -\infty & \text{if} \quad u = 0 \\ -\frac{1}{\lambda}\log(1-u) & \text{if} \quad u > 0 \end{cases}$$

corroborating, when applied to the current model, to

$$Q_{tmoe}(u) = \begin{cases} -\infty & \text{if} \quad u = 0 \\ -\frac{1}{\lambda}\log\left(\frac{\left[\frac{1}{\theta}\frac{(1-u)}{u}\right]^{\frac{1}{\alpha}}}{1+\left[\frac{1}{\theta}\frac{(1-u)}{u}\right]^{\frac{1}{\alpha}}}\right) & \text{if} \quad u > 0. \end{cases} \tag{4.7}$$

It is important to provide the quantile function of a distribution, since one of the most commonly used methods in the simulation study involves the use of this function. Such a method is known as the inverse method, since the quantile function is the inverse function of the cdf. Figure 9 shows that, for this combination of parameters, the value of the quantile function grows.

Figure 9 – Quantile function for the TMOE model.

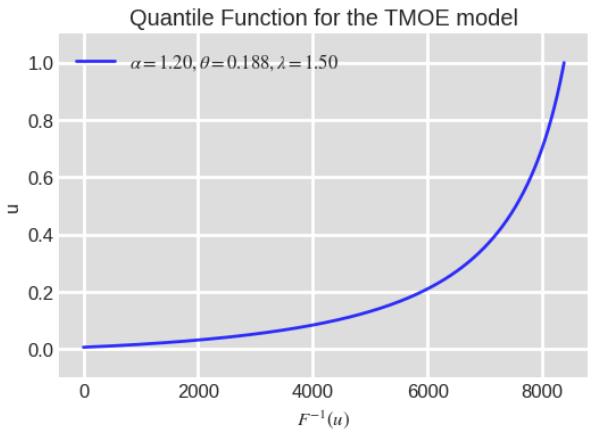

Source: the own author.

4.3.3 Moments

It is known that a proper mathematical treatment of probability distributions must introduce not only the concept of mean and variance, but also some others summary characteristics.

These characteristics, including mean and variance, are called moments of a given distribution whose meaning refers to the expectations of different powers of the given random variables.

It is also known the mathematical meaning of first and second moment, describing the *location* of the distribution on the X-axis and its dispersion, respectively. Following this reasoning the higher order process, or higher moments reflect other features of the distribution one are dealing with. For example, the third moment about the mean is used in certain measures of degree of *skewness* leading to a symmetric distribution in the case of vanishing that third moment. It will be negative for skewness to the left, positive for skewness to the right. The fourth moment indicates the degree of *peakedness*, or *kurtosis*, and so on.

As is known in elementary courses of probability theory, that the calculational framework concerning expectation values is given in terms of sums, discrete or continuous, or in terms of the so called moment generating functions. Among the tools at hand, one is allowed to consider the theory of infinite series or the set of techniques related to integration theory. If it was possible to include all the integrals in a bag and take, at random, one of them, the probability of it to be analytically calculated would tends to zero. This, indeed, constitutes a problem when dealing with expectation values, once one is treating with integrals, frequently improper, describing some classes of random variables. One could say that the problem is solved thanks to numerical recipes perpetrated by powerful computers. But this is not always the case once there exist functions whose the integrals under analysis do not converge.

In what follows some techniques are presented in order to express the moments of some distributions under consideration. Let consider the following Theorem.

Theorem 5 *Let $\alpha = 1$ and consider (3.4.1), in Chapter 3, with*

$$\begin{aligned} G(x;\boldsymbol{\tau}) &= 1 - e^{-\lambda x} \\ g(x;\boldsymbol{\tau}) &= \lambda e^{-\lambda x}. \end{aligned}$$

Then, the moment generating function is given by

$$\mathcal{M}_X(s)|_{\alpha=1} = \theta\lambda\ f(s;\lambda,\theta) \tag{4.8}$$

if, and only if, $\exists\ \mathcal{T}(x,s,\lambda,\theta) \equiv 0$, where

$$f(s;\lambda,\theta) = \frac{\lambda}{\lambda - s} - (1-\lambda)\ln\theta - \frac{1}{\theta} + 1. \tag{4.9}$$

Dem. 8 *Applying the fgm given in the mentioned chapter, one finds,*

$$\mathcal{M}_X(s;\theta,\lambda)|_{\alpha=1} = \theta\lambda\int_0^\infty \frac{e^{-(\lambda-s)x}}{(\theta-\lambda x)^2}dx$$

Integration by parts leads to

$$\begin{aligned}\mathcal{M}_X(s;\theta,\lambda)|_{\alpha=1} &= \theta\lambda f(s;\lambda,\theta)+\theta\lambda g(s;\lambda)\cdot\mathcal{T}(x,s;\lambda,\theta),\\ &\textit{where},\\ f(s;\lambda,\theta) &= \frac{\lambda}{\lambda-s}-(1-\lambda)\ln\theta+\frac{1}{\theta}+1,\\ g(s;\lambda) &= \frac{(\lambda-s)^2}{\lambda}-(\lambda-s),\\ \mathcal{T}(x,s,\lambda,\theta) &= \int_0^\infty e^{-(\lambda-s)x}\ln\left[1-(1-\theta)e^{-\lambda x}\right]dx\end{aligned}$$

Note, however, if $\mathcal{T}(x,s;\lambda,\theta)\equiv 0$, the requirement is, indeed, satisfied. Now, it must be shown that $\mathcal{T}(x,s;\lambda,\theta)$, indeed, vanishes. In effect, integration by parts, again, leads to

$$\begin{aligned}\mathcal{T}(x,s;\lambda,a) &= \frac{e^{-(\lambda-s)x}}{\lambda}\int\frac{\ln w}{1-w}dw|_0^\infty+\frac{\lambda-s}{\lambda}\int_0^\infty e^{-(\lambda-s)x}\left(\int\frac{\ln w}{1-w}dw\right)dx\\ &= \frac{1}{\lambda}Li_2(0)-\frac{(\lambda-s)}{\lambda}\int_0^\infty e^{-(\lambda-s)}Li_2(x)dx,\end{aligned}$$

where $Li_k(x)$ is identified as the Spence' special function, (CARTIER et al., 2007). It is not hard to show that the last integral vanishes and $Li_2(0)\equiv 0$, so that $\mathcal{T}(x,s;\lambda,a)=0$. □

By using Theorem 5, above, one finds,

$$\frac{\partial\mathcal{M}_X(s)}{\partial s}|_{s=0;\alpha=1} = \theta\lambda\frac{\partial f(s;\lambda,a)}{\partial s}=\theta \quad \text{and} \tag{4.10}$$

$$\frac{\partial^2\mathcal{M}_X(s)}{\partial s^2}|_{s=0;\alpha=1} = \theta\lambda\frac{\partial^2 f(s;\lambda,a)}{\partial s^2}=\frac{2\theta}{\lambda}. \tag{4.11}$$

Whose numerical values are, for $\theta=0.1875$ and $\lambda=1.500$,

$$E(X)_{fgm} = 0.1875 \quad \text{and} \tag{4.12}$$

$$Var(X)_{fgm} = 0.2500. \tag{4.13}$$

The integral numerical solutions, for (3.4.1) in the same conditions, are,

$$E(X)_{num} = 0.2575 \quad \text{and} \tag{4.14}$$

$$Var(X)_{num} = 0.2257. \tag{4.15}$$

One is referred to the proximities of values encountered in 4.12 through 4.14, showing the effectiveness of the method which, in principle, can be enhanced by introducing some corrector functions, as is proposed in future works. The same is applied to the values encountered in 4.16 through 4.18.

Following the general theory developed on both Chapters 2 and 3, one is addressed to two canonical procedures, that is to say, integration and M-transform method. The former may not have analytical developments, leading to numerical implementations, to reach the solutions. The later is a new method, still under formal development, but with *ad hoc* applications whose results are interesting.

For the first and second moments, with $(\alpha, \theta, \lambda) = (1.200, 1.188, 1.500)$ in both cases, one finds,

$$E(X)_{num} = 0.2616 \quad \text{and} \tag{4.16}$$

$$Var(X)_{num} = 0.1838, \tag{4.17}$$

and

$$E(X)_{\mathcal{M}} = 0.2713 \quad \text{and} \tag{4.18}$$

$$Var(X)_{\mathcal{M}} = 0.1529, \tag{4.19}$$

where the subscripts *num* and $\mathcal{M}$ do refer to numerical and M-transform, respectively. The definition leads to the curve described in Figure 10.

Figure 10 – The mean is expressed as a limit process as indicated on chapter 2.

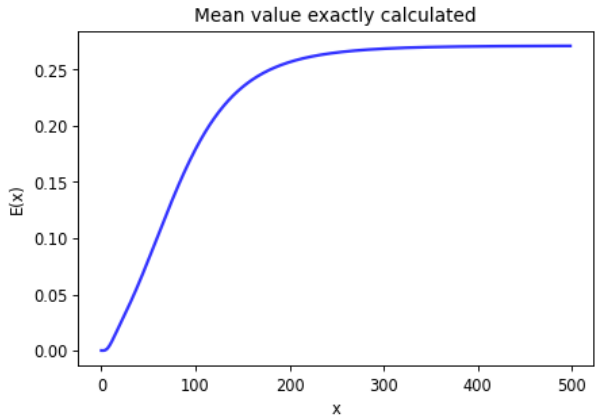

Source: the own author.

4.3.4 Estimation

As was done in (3.17), for the general case where the log-likelihood function $l(x;\boldsymbol{\xi},\boldsymbol{\tau})$ was established, one may check that, in the case of the TMOE, the general expression leads to the function $l_{exp}(x;\boldsymbol{\xi},\boldsymbol{\tau})$, where $\boldsymbol{\xi}=(\alpha,\theta)$ and, in this case, $\boldsymbol{\tau}=\lambda$. So, let x_i, $i=1,\cdots,n$, be an n-size random sample, of the TMOE distribution. Then one has,

$$\begin{aligned} l_{exp}(x_i;\boldsymbol{\xi},\boldsymbol{\tau}) &= n\log(\alpha\lambda\theta)+(\alpha-1)\sum_{i=1}^{n}\log\left(1-\mathrm{e}^{-\lambda x_i}\right) \\ &- \alpha\lambda\sum_{i=1}^{n}x_i-2\sum_{i=1}^{n}\log\left\{\left(1-\mathrm{e}^{-\lambda x_i}\right)^{\alpha}+\theta\mathrm{e}^{-\alpha\lambda x_i}\right\}. \end{aligned}$$

In this way, the elements of the corresponding score vector are given as follows

$$\begin{aligned} \frac{\partial l_{exp}\left(x_i;\boldsymbol{\xi},\boldsymbol{\tau}\right)}{\partial\lambda} &= \frac{n}{\lambda}+(\alpha-1)\sum_{i=1}^{n}\frac{x_i\mathrm{e}^{-\lambda x_i}}{1-\mathrm{e}^{-\lambda x_i}}-\alpha\sum_{i=1}^{n}x_i \\ &- 2\alpha\sum_{i=1}^{n}\left[\frac{\mathrm{e}^{-\lambda x_i}\left(1-\mathrm{e}^{-\lambda x_i}\right)^{\alpha-1}-\theta\mathrm{e}^{-\alpha\lambda x_i}}{(1-\mathrm{e}^{-\lambda x_i})^{\alpha}+\theta\mathrm{e}^{-\alpha\lambda x_i}}x_i\right]. \end{aligned}$$

So, it has

$$\begin{aligned} \frac{\partial l_{exp}\left(x_i;\boldsymbol{\xi},\boldsymbol{\tau}\right)}{\partial\alpha} &= \frac{n}{\alpha}+\sum_{i=1}^{n}\log\left[1-\mathrm{e}^{-\lambda x_i}\right]-\lambda\sum_{i=1}^{n}x_i \\ &- 2\lambda\theta\sum_{i=0}^{n}\left[\frac{x_i\mathrm{e}^{-\alpha\lambda x_i}}{(1-\mathrm{e}^{-\lambda x_i})^{\alpha}+\theta\mathrm{e}^{-\alpha\lambda x_i}}\right] \\ &- 2\sum_{i=1}^{n}\frac{\left(1-\mathrm{e}^{-\lambda x_i}\right)^{\alpha}\log\left(1-\mathrm{e}^{-\lambda x_i}\right)}{(1-\mathrm{e}^{-\lambda x_i})^{\alpha}+\theta\mathrm{e}^{-\alpha\lambda x_i}}, \end{aligned}$$

,

$$\frac{\partial l_{exp}\left(x_i;\boldsymbol{\xi},\boldsymbol{\tau}\right)}{\partial\theta}=\frac{n}{\theta}-2\sum_{i=1}^{n}\left[\frac{\mathrm{e}^{-\alpha\lambda x_i}}{(1-\mathrm{e}^{-\lambda x_i})^{\alpha}+\theta\mathrm{e}^{-\alpha\lambda x_i}}\right].$$

The second derivatives read as the entrance of the symmetric positive-definite information matrix,

$$I_X^{exp}\left(\{\boldsymbol{\xi},\boldsymbol{\tau}\}\right)=-E\left(\frac{\partial^2 l(x;\boldsymbol{\theta})}{\partial\theta_r\partial\theta_s}\right)=-\left(\frac{\partial^2 l(x;\boldsymbol{\theta})}{\partial\theta_r\partial\theta_s}\right), \tag{4.20}$$

where $\boldsymbol{\theta}$ stands for the vector class $(\boldsymbol{\xi},\boldsymbol{\tau})$. Note that the left hand side of (4.20) is evolved to an expression on which the expected value is avoided for the calculation (GOVAERTS M. NORBERT HOUNKONNOU, 2006). For the components of the Hessian see appendix A.

4.4 TRANSFORMED MARSHALL-OLKIN WEIBULL DISTRIBUTION

In this section, we provide a distribution that generalizes the TMOE model. Here, this proposed distribution is called Transformed Marshakk-olkin Weibull (TMOW, for short).

If $X \sim Weibull(x; a, b)$ it follows that the cdf and pdf of TMOW distribution is given, respectively, by

$$F(x; \alpha, \theta, a, b) = \frac{\left[1 - \mathrm{e}^{-\left(\frac{x}{b}\right)^a}\right]^\alpha}{\left[1 - \mathrm{e}^{-\left(\frac{x}{b}\right)^a}\right]^\alpha + \theta \mathrm{e}^{-\alpha\left(\frac{x}{b}\right)^a}} \quad \text{and}$$

$$f(x; \alpha, \theta, a, b) = \frac{\alpha a \theta \left(\frac{x}{b}\right)^{a-1} \mathrm{e}^{-\alpha\left(\frac{x}{b}\right)^a} \left[1 - \mathrm{e}^{-\left(\frac{x}{b}\right)^a}\right]^{\alpha-1}}{b\left\{\left[1 - \mathrm{e}^{-\left(\frac{x}{b}\right)^a}\right]^\alpha + \theta \mathrm{e}^{-\alpha\left(\frac{x}{b}\right)^a}\right\}^2}.$$

Figure 12 plots the cdf and pdf, respectively, for the TMOW, under different parameter settings.

Figure 11 – Cumulative and probability distribution functions for the Weibull distribution.

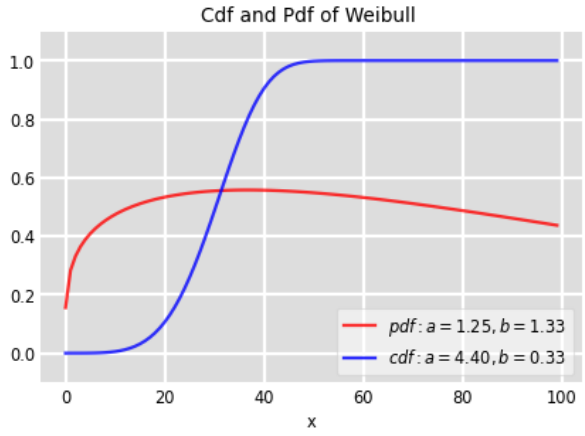

Source: the own author.

Note that there exist certain flexibility of the proposed model, when compared to the baseline, once the Weibull distribution only shows unimodal shape for the density.

Figure 12 – Cumulative and probability distribution functions for the model and Weibull distribution as baseline. The parameter set is shown in the frame of the current figures.

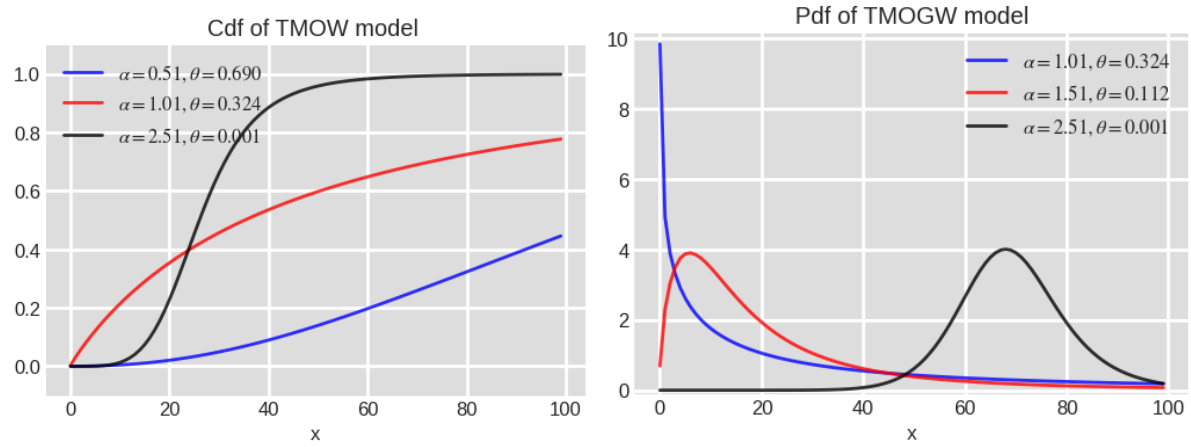

Source: the own author.

4.5 SOME PROPERTIES

4.5.1 TMOW Hazard Rate Function

Following the results for the TMOE, the hazard rate function for the TMOW model reads,

$$h(x;\boldsymbol{\xi},\boldsymbol{\tau}) = \frac{\alpha a}{b}\left(\frac{x}{b}\right)^{a-1}\left\{\frac{\left[1-\mathrm{e}^{-\left(\frac{x}{b}\right)^{a}}\right]^{\alpha-1}}{\left[1-\mathrm{e}^{-\left(\frac{x}{b}\right)^{a}}\right]^{\alpha}+\theta\mathrm{e}^{-\alpha\left(\frac{x}{b}\right)^{a}}}\right\}.$$

Figure 13 – Hazard function $h_w(x;\boldsymbol{\xi};\boldsymbol{\tau})$ for the $TMOW$ Model.

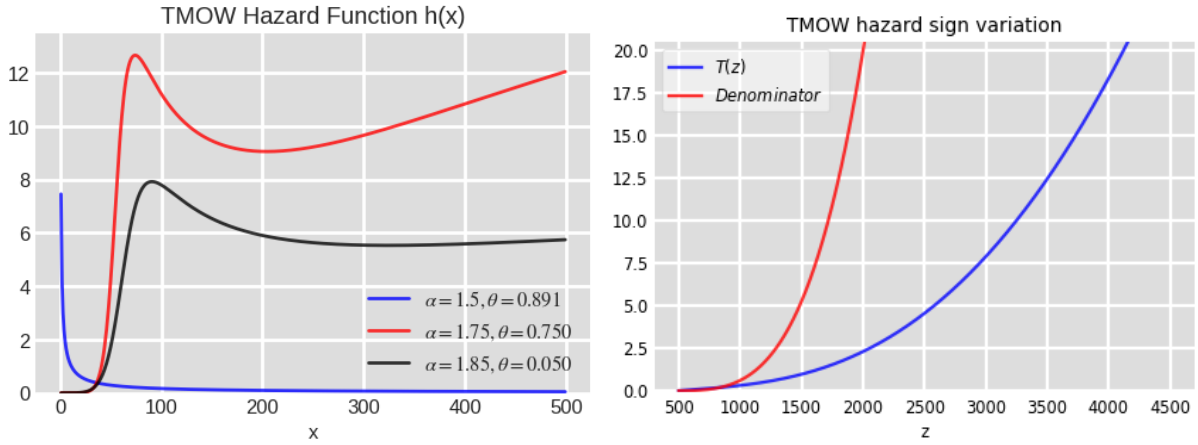

Source: the own author.

The $T(z)$ factor function , according to (8) in Chapter 3, is given by

$$\begin{aligned} T(z) &= [(z-1)^{\alpha}+\theta]\,[(a-1)(z-1)+a(z-1)+a(z-1)\log z - az\log z] \\ &+ a\alpha\theta\log z \end{aligned} \tag{4.21}$$

such that

$$\frac{r'(z)}{r(z)} = \frac{T(z)}{az(z-1)\,[(z-1)^{\alpha}+\theta]\log z}.$$

Figure 14 – Factor function $T(x;\boldsymbol{\xi};\boldsymbol{\tau})$ for the Model.

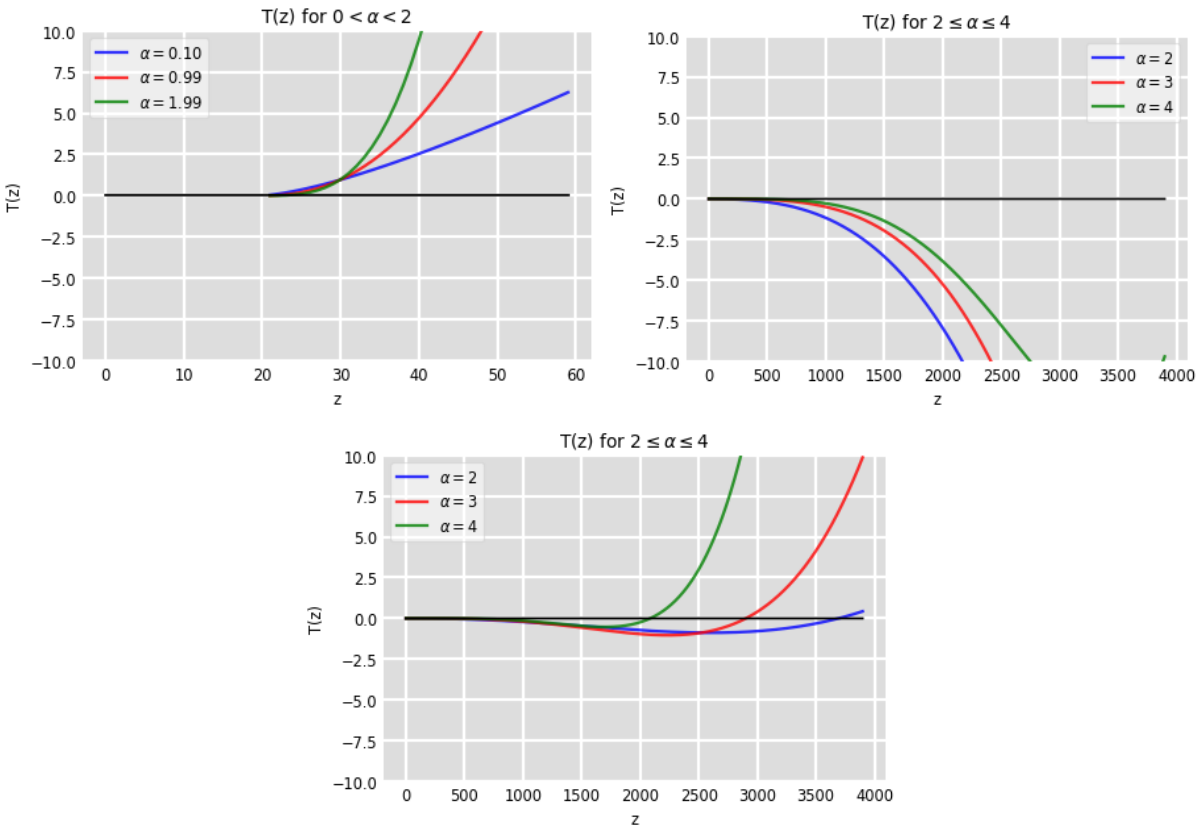

Source: the own author.

The graphs on Figure 14 are plotted for different values of the TMOW model parameter set. The first graph on the left, the α parameter varies inside the range indicated on the frame of the figure, while θ and α are kept fixed with values, 0.0094 and 1.5, respectively. For the second graph on the right, the parameter α is taken inside the interval described but, now, the parameter $\theta = 0.0075$ and $0.10 \leq a < 0.63$. Last, the third graph is such that α takes the same values as before but, a takes values in the interval $0.63 \leq a < 0.74$. The a values used to plot the graph being $0.63, 0.65$ and 0.68. Each range exhibited defines a separation region for which statistical meaning are addressed. For example, in the case where $T(z)$ takes

purely positive values, the region in question is termed *region I*, leading to monotone increasing hazard function. When this is not the case and $T(z)$ takes, instead, purely negative values, the hazard function exhibit a monotone decreasing character and the *region II* is established. When it first takes positive values, then dropping to negative ones, the separation region, *region III*, is considered leading to unimodal characterized hazard function. The counterpart, that is to say, when negative values figures first, followed by positive ones, the hazard function does exhibit bathtube characteristics. When this is the case, the region is termed *region IV*.

4.5.2 Weibull Quantile Function

Analogously to the development for the exponential case, the Weibull quantile function is given by

$$Q_w(u) = \begin{cases} +\infty & \text{if} \quad u = 0 \\ b\left[\log\left(\frac{1}{1-u}\right)\right]^{\frac{1}{\alpha}} & \text{if} \quad u > 0 \end{cases}$$

so that the quantile function for the TMOW model reads

$$Q_{tmow}(u) = -b\left\{\log\frac{\left[\frac{1}{\theta}\frac{(1-u)}{u}\right]^{\frac{1}{\alpha}}}{1+\left[\frac{1}{\theta}\frac{(1-u)}{u}\right]^{\frac{1}{\alpha}}}\right\}^{\frac{1}{a}}$$

Figure 15 – Quantile function for the $TMOW$ model for values of parameter set as described in the frame of figure.

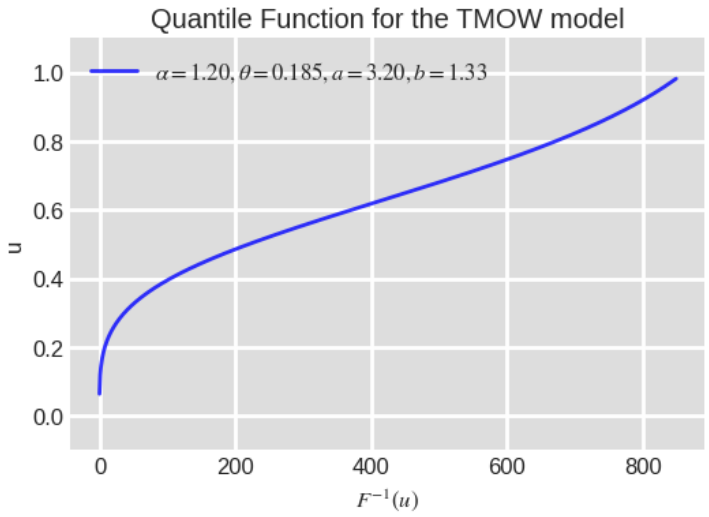

Source: the own author.

4.5.3 Estimation

Again, from the general expression (3.17), if x_i, $i = 1, \cdots, n$, is a sequence of an n-size random sample, the log-likelihood function $l_w(x, \boldsymbol{\xi}; \boldsymbol{\tau})$ reads,

$$\begin{aligned} l_w(x_i, \boldsymbol{\xi}, \boldsymbol{\tau}) &= n \log a\alpha\theta + (a-1)\sum_{i=1}^{n} \log x_i - a\sum_{i=1}^{n} \log b - \alpha \sum_{i=1}^{n} \left(\frac{x_i}{b}\right) \\ &+ (\alpha - 1)\sum_{i=1}^{n} \log\left[1 - \mathrm{e}^{-\left(\frac{x_i}{b}\right)^a}\right] - 2\sum_{i=1}^{n} \log\left\{\left[1 - \mathrm{e}^{-\left(\frac{x_i}{b}\right)^a}\right]^{\alpha} + \theta \mathrm{e}^{-\alpha\left(\frac{x_i}{b}\right)^a}\right\}, \end{aligned}$$

whose derivatives read,

$$\begin{aligned} \frac{\partial l_w(x_i; \boldsymbol{\xi}, \boldsymbol{\tau})}{\partial \alpha} &= \frac{n}{\alpha} + \sum_{i=1}^{n} \log\left[1 - \mathrm{e}^{-\left(\frac{x_i}{b}\right)^a}\right] - \sum_{i=1}^{n} \left(\frac{x_i}{b}\right)^a \\ &+ 2\theta \sum_{i=1}^{n} \frac{\left(\frac{x_i}{b}\right)^a \mathrm{e}^{-\alpha\left(\frac{x_i}{b}\right)^a}}{\left[1 - \mathrm{e}^{-\left(\frac{x_i}{b}\right)^a}\right]^{\alpha} + \theta \mathrm{e}^{-\alpha\left(\frac{x_i}{b}\right)^a}} \\ &- 2\sum_{i=1}^{n} \frac{\left[1 - \mathrm{e}^{-\left(\frac{x_i}{b}\right)^a}\right]^{\alpha} \log\left[1 - \mathrm{e}^{-\left(\frac{x_i}{b}\right)^a}\right]}{\left[1 - \mathrm{e}^{-\left(\frac{x_i}{b}\right)^a}\right]^{\alpha} + \theta \mathrm{e}^{-\alpha\left(\frac{x_i}{b}\right)^a}}, \end{aligned}$$

$$\frac{\partial l_w(x_i; \boldsymbol{\xi}, \boldsymbol{\tau})}{\partial \theta} = \frac{n}{\theta} - 2\sum_{i=1}^{n} \frac{\mathrm{e}^{-\alpha\left(\frac{x_i}{b}\right)^a}}{\left[1 - \mathrm{e}^{-\left(\frac{x_i}{b}\right)^a}\right]^{\alpha} + \theta \mathrm{e}^{-\alpha\left(\frac{x_1}{b}\right)^a}},$$

$$\begin{aligned} \frac{\partial l_w(x_i; \boldsymbol{\xi}, \boldsymbol{\tau})}{\partial a} &= \frac{n}{a} + \sum_{i=1}^{n} \log\left(\frac{x_i}{b}\right) - \alpha \sum_{i=1}^{n} \left(\frac{x_i}{b}\right)^a \log\left(\frac{x_i}{b}\right) \\ &+ (\alpha - 1)\sum_{i=1}^{n} \frac{\left(\frac{x_i}{b}\right)^a \mathrm{e}^{-\left(\frac{x_i}{b}\right)^a} \log\left(\frac{x_i}{b}\right)}{1 - \mathrm{e}^{-\left(\frac{x_i}{b}\right)^a}} \\ &- 2\alpha \sum_{i=1}^{n} \frac{\left(\frac{x_i}{b}\right)^a \mathrm{e}^{-\left(\frac{x_i}{b}\right)^a} \log\left(\frac{x_i}{b}\right) \left[1 - \mathrm{e}^{-\left(\frac{x_i}{b}\right)^a}\right]^{\alpha - 1}}{\left[1 - \mathrm{e}^{-\left(\frac{x_i}{b}\right)^a}\right]^{\alpha} + \theta \mathrm{e}^{-\alpha\left(\frac{x_i}{b}\right)^a}} \\ &+ 2\alpha\theta \sum_{i=1}^{n} \frac{\left(\frac{x_i}{b}\right)^a \mathrm{e}^{-\alpha\left(\frac{x_i}{b}\right)^a \log\left(\frac{x_i}{b}\right)^a}}{\left[1 - \mathrm{e}^{-\left(\frac{x_i}{b}\right)^a}\right]^{\alpha} + \theta \mathrm{e}^{-\alpha\left(\frac{x_i}{b}\right)^a}}, \end{aligned}$$

$$\begin{aligned}\frac{\partial l_w\left(x_i;\boldsymbol{\xi},\boldsymbol{\tau}\right)}{\partial b} &= -\frac{a}{b}+\left(\frac{\alpha a}{b}\right)\sum_{i=1}^{n}\left(\frac{x_i}{b}\right)^a-\frac{a\left(\alpha-1\right)}{b}\sum_{i=1}^{n}\frac{\left(\frac{x_i}{b}\right)^a\mathrm{e}^{-\left(\frac{x_i}{b}\right)^a}}{1-\mathrm{e}^{-\left(\frac{x_i}{b}\right)^a}}\\ &+ \frac{2\alpha a}{b}\sum_{i=1]}^{n}\frac{\left(\frac{x_i}{b}\right)^a\mathrm{e}^{-\left(\frac{x_i}{b}\right)^a}\left[1-\mathrm{e}^{-\left(\frac{x_i}{b}\right)^a}\right]^{\alpha-1}}{\left[1-\mathrm{e}^{-\left(\frac{x_i}{b}\right)^a}\right]^{\alpha}+\theta\mathrm{e}^{-\alpha\left(\frac{x_i}{b}\right)^a}}\\ &- \frac{2a\alpha\theta}{b}\sum_{i=1}^{n}\frac{\left(\frac{x_i}{b}\right)^a\mathrm{e}^{-\alpha\left(\frac{x_i}{b}\right)^a}}{\left[1-\mathrm{e}^{-\left(\frac{x_i}{b}\right)^a}\right]^{\alpha}+\theta\mathrm{e}^{-\alpha\left(\frac{x_i}{b}\right)^a}}.\end{aligned}$$

Following the the results of (3.5), the second derivatives, as expressed thereof, give rise to

$$I_X^{wei}\left(\{\boldsymbol{\xi},\boldsymbol{\tau}\}\right)=-E\left(\frac{\partial^2 l(x_i;\boldsymbol{\theta})}{\partial\theta_r\partial\theta_s}\right)=-\left(\frac{\partial^2 l(x_i;\boldsymbol{\theta})}{\partial\theta_r\partial\theta_s}\right),$$

whose expressions are explicitly given at Appendix B. The same remarks concerning in the TMOE case, for the expectation in the information matrix, sets, indeed, here.

4.6 SIMULATION STUDY

According to the Quantile function given by 4.7, when it is running through the data set, as seen as a function in parameter space, the results are shown at tables below.

Throughout this section a number of simulations are carried out in order to test the quality of adjusting of the parameter inference process in comparison to the real ones, i.e., the set of parameters given at the beginning of the process. For such a task, a number of Monte Carlo replications are constructed, given the dimension of the sample space, and the deviation is given as a measure through mean squared error as well as the biases of the corresponding processes.

Here, a simulation for the TMOE model is considered. The task, as was said above, is to compare the values found through simulation and how they differ from the true values at hand. The analysis of the process will be of great value for the understanding of the underlying behavior of data as seen of manifestation through the model in appreciation.

The measurement of error for an estimate T, for the parameter vector $\boldsymbol{\xi}$ and the process under analysis, is given in terms of mean square error, denoted by MSE($\boldsymbol{\xi}$). Smaller MSE($\boldsymbol{\xi}$) means greater precision, such that, in comparing two estimate, say, T_1 and T_2 of $\boldsymbol{\xi}$, the one with smaller measure is the chosen one.

Table 1 – AEs, Bias, MSE and lower and upper bounds of 95% (HPD) CIs of the parameter - first scenario

n	True	AE	Bias	MSE	Lower	Upp
50	0.5	0.5037	0.0037	0.0053	0.3594	0.6480
	0.3	0.3468	0.0468	0.0266	0.1082	0.6544
	0.8	0.9667	0.1667	0.2606	0.1371	1.7964
100	0.5	0.5011	0.0011	0.0026	0.4000	0.6022
	0.3	0.3239	0.0239	0.0118	0.1536	0.5486
	0.8	0.8794	0.0794	0.0897	0.3248	1.4339
150	0.5	0.4999	-0.00005	0.0018	0.4178	0.5820
	0.3	0.3153	0.0153	0.0070	0.1745	0.4972
	0.8	0.8607	0.0607	0.0580	0.4144	1.3071
300	0.5	0.5002	0.0002	0.0008	0.4422	0.5582
	0.3	0.3069	0.0069	0.0032	0.2041	0.4324
	0.8	0.8288	0.0288	0.0261	0.5210	1.1366

Table 2 – AEs, Bias, MSE and lower and upper bounds of 95% (HPD) CIs of the parameter - second scenario

n	True	AE	Bias	MSE	Lower	Upp
50	0.8	0.8334	0.0334	0.0196	0.5598	1.1071
	0.7	0.7011	0.0011	0.0800	0.0225	0.9522
	1.5	1.5083	0.0083	0.2714	0.3814	2.6352
100	0.8	0.8133	0.0133	0.0097	0.6170	1.0095
	0.7	0.7083	0.0083	0.0530	0.0670	0.9356
	1.5	1.5190	0.0190	0.1645	0.6541	2.3840
150	0.8	0.8049	0.0049	0.0067	0.6430	0.9669
	0.7	0.7186	0.0186	0.0425	0.1067	0.9276
	1.5	1.5421	0.0421	0.1285	0.8002	2.2840
300	0.8	0.8014	0.0014	0.0032	0.6845	0.9183
	0.7	0.7162	0.0162	0.0265	0.2143	0.9063
	1.5	1.5303	0.0303	0.0732	0.9804	2.0801

To do this, Monte Carlo realizations with 1000 replicas and sample length n in $\{50, 100, 150, 300\}$ was considered. To be more emphatic, a test for the α is carried out. For the first scenario, the parameter vector $(\alpha, \theta, \lambda) = (0.5, 0.3, 0.8)$ is considered and, for the second one, $(\alpha, \theta, \lambda) = (0.8, 0.7, 1.5)$.

By looking the Tables 1 and 2 one sees that, as long as the sample length increases, the associated values for the MSEs and bias decrease, as expected. Besides that, mean estimates for the configurations considered are within their respective confidence intervals.

4.7 APPLICATIONS

In this section, the main goal is to provide the potential of the TMO-G family of distributions, in the context of applications to real data. To do this, we choose some models to compare the TMOE and TMOW distributions to them:

- Exponential distribution (EXP), (KONSUK; AKTAS, 2013);
- Exponentiated Exponential distribution (EXP-EXP), (NADARAJAH, 2011);
- Kumaraswamy Exponential distribution (KW-EXP), (MOHAN RAKHI; CHACKO, 2020);
- Lindley Exponential distribution (L-EXP), (BHATI; MALIK; VAMAN, 2015);
- Weibull distribution (W), (DASH; NANDI; SETT, 2016);
- Exponentiated Weibull distribution (EXP-W), (MUDHOLKAR; SRIVASTAVA; FREIMER, 1995);
- Kumaraswamy Weibull distribution (KW-W), (NADARAJAH, 2010);
- Beta Weibull distribution (B-W), (NEKOUKHOU; BIDRAM; ROOZEGAR, 2017);
- Gamma distribution (Ga), (RADICE, 2022);
- Gamma Frechet distribution (Ga-FE), (SILVA et al., 2013).

Here, two data sets are studied in order to evaluate the flexibility of the proposed model. Their descriptions and developments are as follow.

4.7.1 Epidemiology

The first data set (Cov-SC) - It is referred to the amount of confirmed COVID-19 cases in Santa Catarina, a south Brazilian State, as was publicized by the state government, on December, 31/2020. The data can be found at (SAúDE..., 2021). For the current study, the observations was taken as the number of cases in each 1000 inhabitants. In addition, only the 80 first listed municipalities, namely: Abdon Batista, Abelardo Luz, Agrolândia, Agronômica, Água Doce, Águas de Chapecó, Águas Frias, Águas Mornas, Alfredo Wagner, Alto Bela Vista, Anchieta, Angelina, Anita Garibaldi, Anitápolis, Antônio Carlos, Apiúna, Arabutã, Araquari, Araranguá, Armazém, Arroio Trinta, Arvoredo, Ascurra, Atalanta, Aurora, Balneário Arroio

do Silva, Balneário Barra do Sul, Balneário Camboriú, Balneário Gaivota, Balneário Piçarras, Balneário Rincão, Bandeirante, Barra Bonita, Barra Velha, Bela Vista do Toldo, Belmonte, Benedito Novo, Biguaçu, Blumenau, Bocaina do Sul, Bom Jardim da Serra, Bom Jesus, Bom Jesus do Oeste, Bom Retiro, Bombinhas, Botuverá, Braço do Norte, Braço do Trombudo, Brunópolis, Brusque, Caçador, Caibi, Calmon, Camboriú, Campo Alegre, Campo Belo do Sul, Campo Erê, Campos Novos, Canelinha, Canoinhas, Capão Alto, Capinzal, Capivari de Baixo, Catanduvas, Caxambu do Sul, Celso Ramos, Cerro Negro, Chapadão do Lageado, Chapecó, Cocal do Sul, Concórdia, Cordilheira Alta, Coronel Freitas, Coronel Martins, Correia Pinto, Corupá, Criciúma, Cunha Porã, Cunhataí e Curitibanos, was performed in the process of analysis.

4.7.2 Taylor-Green Numerical Instability

The second data set is referred to a hydrodynamic problem where a process of numerical instability, in fluids, dawning from the sph numerical method, is studied. Below some theoretical rudiments on the theme are presented in order to clarify the ideas.

First of all, it is described the physical process by which the instability of the numerical solution for the Taylor-Green vortices arises, from the smoothed particle hydrodynamics approach.

4.7.3 Smoothing Operators

Here and in Chapter 6, one is addressed to hydrodynamical systems from which data are generated. It is briefly described the mathematical process involved in treating the governing equations for the process. The simulations are coded in Python, (ROSSUM; DRAKE, 2009), through Anaconda environment, (ANACONDA..., 2022).

4.7.4 Formulation

The formulation of smoothing process, or sph formulation, (LIU, 2003) can be introduced by two steps. The first one is introduced by using an integral representation, or kernel approximation for the field functions one is handling. The second step is referred to an idea,

came from physics, that approximate a value of a given operator by particles. Indeed, the integral approximation of the operator, or function, can be made by summing up the values of the nearest neighbor particles, leading to the desired approximation of the operator, at a discrete point, or, as the system under analysis is a hydrodynamical one, a particle. Let f be a continuous function of the three dimensional position vector $\boldsymbol{x}$. Then, one has

$$f(\boldsymbol{x}) = \int_{\Omega} f(\boldsymbol{x}')\delta(\boldsymbol{x} - \boldsymbol{x}')d\boldsymbol{x}' \tag{4.22}$$

where $\delta(\boldsymbol{x} - \boldsymbol{x}')$ is the Dirac delta function, given by,

$$\delta(\boldsymbol{x} - \boldsymbol{x}') = \begin{cases} 1 & \text{if} \quad \boldsymbol{x} = \boldsymbol{x}' \\ 0 & \text{if} \quad \boldsymbol{x} \neq \boldsymbol{x}' \end{cases}$$

where, Ω appearing in (4.22) is the volume of the integral containing $\boldsymbol{x}$. The mathematical meaning of (4.22) establishes that a given function can be represented in integral form, with some hypothesis such as the requirement that $f(x)$ is defined and continuous in Ω.

If the delta function $\delta(\boldsymbol{x} - \boldsymbol{x}')$ is replaced by a smoothing function given by $W(\boldsymbol{x} - \boldsymbol{x}', h)$, the integral in (4.22) is rewritten as

$$f(\boldsymbol{x}) = \int_{\Omega} f(\boldsymbol{x}')W(\boldsymbol{x} - \boldsymbol{x}', h)d\boldsymbol{x}', \tag{4.23}$$

where $W(\boldsymbol{x} - \boldsymbol{x}', h)$ is termed *kernel* of the integral equation. The function h is the smoothing function related to length and defines the influence region of the smoothing function W.

Through this process, once W differs significantly from the delta function, the integral representation figuring in (4.23) is an approximation called, approximation operator, and is defined by the function under angle brackets,

$$< f(\boldsymbol{x}) >= \int_{\Omega} f(\boldsymbol{x}')W(\boldsymbol{x} - \boldsymbol{x}', h)d\boldsymbol{x}'. \tag{4.24}$$

The smoothing function W is usually chosen to be an *even function*, satisfying some conditions, say,

1. Resolution of identity. Over its support domain,

$$\int_{\Omega} W(\boldsymbol{x} - \boldsymbol{x}', h)d\boldsymbol{x}' = 1;$$

2. W must have compact support, i.e.,

$$\begin{aligned} W(\boldsymbol{x}-\boldsymbol{x}',h) &= 0 \quad \text{for} \\ |\boldsymbol{x}-\boldsymbol{x}'| &> \kappa h, \end{aligned} \tag{4.25}$$

where κ is a control parameter for adjusting the smoothing length h;

3. Positivity, i.e.,

$$W(\boldsymbol{x}-\boldsymbol{x}',h) \geq 0 \quad \forall \boldsymbol{x}' \in \Omega;$$

4. Decaying property. The value of the smoothing function must be monotonically decreasing as the distance from a given interest particle increases;

5. W must satisfy the Dirac delta function condition as the smoothing length approaches to zero, i.e.,

$$\lim_{h\to 0} W(\boldsymbol{x}-\boldsymbol{x}',h) = \delta(\boldsymbol{x}-\boldsymbol{x}');$$

6. W should be an even function. This property is related to symmetry;

7. W must be sufficiently smooth.

In (4.25), κ determines the spread of the specified smoothing function. Examples of such smoothing functions are

$$\begin{aligned} W_1(\boldsymbol{x}-\boldsymbol{x}',h) &= W_1(R,h) = \alpha_d \begin{cases} (1+3R)(1-R)^3 & \text{if} \quad R \leq 1 \\ 0 & \text{if} \quad R > 1 \end{cases} \quad \text{and} \\ W_2 &= W_2(R,h) = \alpha_d \mathrm{e}^{-R^2}, \end{aligned}$$

where α_d is a constant that depends on the underlying dimension where the systems is immersed in. Of course that the resolution to identity leads to a specific value of that constant. For example, in the W_1 case, one finds $\alpha_d = 5/4h, 5/\pi h^2$ and $105/16\pi h^3$, for one, two and three

dimensional problems, respectively. In the equations above, R is the relative distance between two point-particles at points $\boldsymbol{x}$ and $\boldsymbol{x}'$,

$$R = \frac{r}{h} = \frac{|\boldsymbol{x} - \boldsymbol{x}'|}{h}$$

r being the distance between the two points.

Figure 16 – Smoothing functions for W_1 and W_2, respectively, as well as their derivatives.

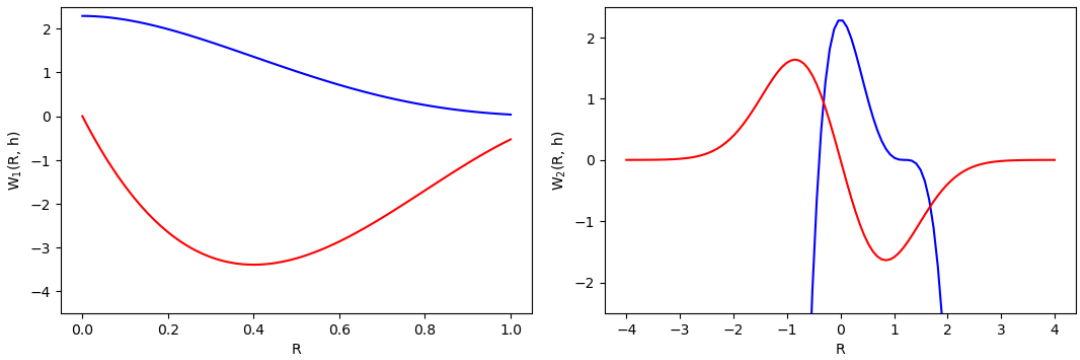

Source: the own author.

Using the compactness condition, the integration over the whole region where the problem is defined is seen as integration over the support domain of the smoothing function. The kernel approximation has, when some conditions are fulfilled, second order accuracy, as can be verified with a little algebra, by using Taylor' series expansion. However, this is not the case when the smoothing function is not, indeed, an even function. Following the same path, it is possible to express the spatial derivative of the function, represented by $\nabla \cdot f(x)$, and given by,

$$< \nabla \cdot f(\boldsymbol{x}) >= -\int_{\Omega} f(\boldsymbol{x}') \cdot \nabla W\left(\boldsymbol{x} - \boldsymbol{x}', h\right) d\boldsymbol{x}'. \tag{4.26}$$

One should note that, once the derivative sign acts on the function $f(x)$, it induces the derivative on the kernel W. This is a very important property because it leads the operation in a smooth, by hypothesis, function, which is known a priory. The negative sign under the integration is due to the fact that the differential operator acts on $\boldsymbol{x}'$.

4.7.5 Point-Particle Approximation

In the method just described above, the whole system is represented by a finite number of point-particles, (LIU, 2003), each one carrying an individual mass and occupying an individual

space. Hence, the integral appearing at (4.24) and (4.26) can be converted to discretized forms of summation over all the particles on the supported domain, as shown in figure (17)

Figure 17 – Point-particle approximations in terms of particles within the support domain of W, for particle i. The support domain is circular with a radius κh.

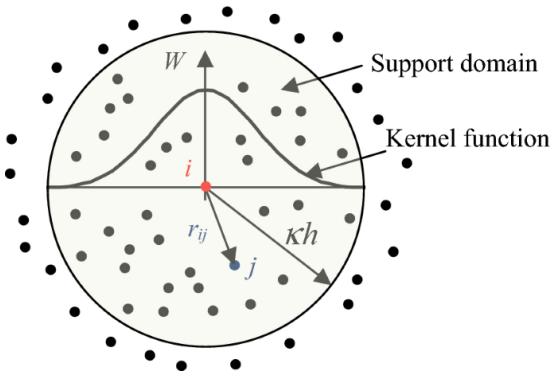

Source: (PENG et al., 2019), and (LIU, 2003).

The approximations are given by,

$$\begin{aligned} < f(x_i) > &= \sum_{j=1}^{N} \frac{m_j}{\rho_j} f(x_j) W_{ij} \\ < \nabla f(x_i) > &= \sum_{j=1}^{N} \frac{m_j}{\rho_j} f(x_j) \nabla_i W_{ij} \\ W_{ij} &= W\left(x_i - x_j.h\right) \\ \nabla_i W_{ij} &= \frac{x_i - x_j}{r_{ij}} \frac{\partial W_{ij}}{\partial r_{ij}} \end{aligned}$$

These are the essential tools to be used in the hydrodynamic simulations used in Taylor-Green problem, below, and in Chapter 6, from where the data are extracted for posterior statistical analysis.

In that approach the extension of fluid is described by particles on which values of positions, velocities, forces and pressures are addressed by means of a process of smoothing through convolution with a given kernel function, (LIU, 2003), obeying the governing equations. The Navier Stokes equations, for a two dimensional time-dependent system of incompressible fluid, is solved. The process is done by using the *stream function* ψ and *vorticity*, ω, having the physical plane as arena. Then, one has,

$$\begin{aligned} \frac{\partial^2 \psi}{\partial x^2} + \frac{\partial^2 \psi}{\partial y^2} &= -\omega, \\ \frac{\partial \omega}{\partial t} + u\frac{\partial \omega}{\partial x} + v\frac{\partial \omega}{\partial y} &= \frac{1}{Re}\left(\frac{\partial^2 \omega}{\partial x^2} + \frac{\partial^2 \omega}{\partial y^2}\right) \end{aligned}$$

From Hydrodynamics theory, it is known that the stream function and the velocity are related by

$$\boldsymbol{v} = \boldsymbol{\nabla} \times \boldsymbol{\psi}$$

with $\boldsymbol{\psi} = (0, 0, \psi)^t$, while the equation for the vorticity $|\boldsymbol{\omega}| = \omega$ is such that,

$$\boldsymbol{\omega} = \boldsymbol{\nabla} \times \boldsymbol{v}$$

The velocity vector components, in terms of the stream function, are given by

$$\begin{aligned} u &= \frac{\partial \psi}{\partial y} \\ v &= -\frac{\partial \psi}{\partial x} \end{aligned}$$

As a partial differential equation, boundary conditions must be given in order to establish solutions. For the 2D problem in question, it is solved in a periodic domain such that,

$$0 \leq x \leq 1$$

$$0 \leq y \leq 1$$

with initial conditions,

$$\begin{aligned} \psi(x, y, 0) &= \frac{1}{2\pi} \cos 2\pi x \cos 2\pi y \\ \omega(x, y, 0) &= 4\pi \cos 2\pi x \cos 2\pi y \end{aligned}$$

giving rise to the solutions,

$$\begin{aligned} \psi(x, y, t) &= \frac{\mathrm{e}^{-\frac{8\pi^2}{Re}t}}{2\pi} \cos 2\pi x \cos 2\pi y \\ \omega(x, y, t) &= 4\pi \mathrm{e}^{-\frac{8\pi^2}{Re}t} \cos 2\pi x \cos 2\pi y \end{aligned} \tag{4.27}$$

which is the analytical solution for the problem. It is well known that, in spite of the apparent equilibrium solution given by 4.27, it is not the case, once that it is not numerically stable due to disturbance referred to numerical reasons. The figure 18 shows this assertive, as reflecting on the decay of the maximum velocity, in time, of the process. The discrepancy is due to the approach used, that is to say, traditional sph, without improvements on boundary conditions, for example. This problem is considerably enhanced by using other strategies like, (RAMACHANDRAN; PURI, 2019).

Figure 18 – Here, exact and numerical solutions, for decay of the maximum velocity in time.

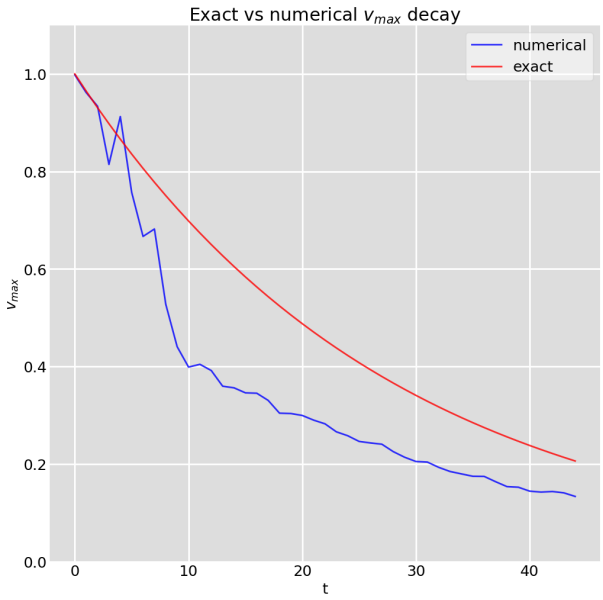

Source: the own author.

4.7.6 Computational Platform

In this section, we will describe some of the functions, packages and estimation methods that have been used on the simulations and graphing processes. The software used to create the graphs, obtain the estimators and verify the flexibility of the model, in terms of fit, was R, (R Core Team, 2013) through RStudio environment, (RStudio Team, 2020).

Regarding the estimation method, the maximum likelihood method was used to obtain the estimators for the parameters of each given model. Here, the CG method is considered and was chosen once the results on using this method were better than those obtained on using the BFGS method.

Most of the initial guesses were obtained through heuristic method by using the GenSA and MASS R packages. When the initial guesses from this method provided unsatisfactory results, or when there was a problem of convergence, the guesses were chosen randomly.

Furthermore, the statistics of Anderson Darling (A^*) and Cramer Von Mises (W^*) were used to verify the performance of the proposed models when compared to those mentioned above.

4.7.7 Descriptive Statistics

Here, the data set presented will be analyzed from a descriptive perspective, in order to improve the visualization potentialized in the data. As far as the first data is concerned, that is to say, COVID-19 in SC, the descriptive measures can be seen at Table 22, below. The lowest values are related to the municipalities of Calmon, Cunhataí and Balneário Piçarras. (Abelardo Luz, Antônio Carlos e Balneário Piçarras), with the minimum value addressed to the Municipality of Calmon, 14 occurrences.

In order to understand the possible causes for these numbers, some investigation must be done. Issues like political ideology, option for preventive treatment, overall sanitation, observation to social distancing, mask mandates, as well as, influx of tourists in early days of the virus spreading, are key points to the understanding of those numbers. For example, Blumenal was the municipality with the major number of confirmed cases: 26324. What are the particularities involved of considering this number, in comparison to places around, with similar characteristics? What happens if compared to Capitals in all the Brazilian country, sharing similar characteristics? These analysis can be brought to surface by a method called *Spatial Autocorrelation*, which is related to the similarity, in values, occurring in observations of a data set when compared to locations of such observations as well as their surroundings. Unfortunately this method won't be applied here and is left for future works. However, some issues can be discussed while considering features, crossing with the data, in order to create a bridge for understanding, or at least questioning, the causes behind the results.

The plots in Figure 19 are addressed for the lowest and largest number of cases, as seen at the data set, respectively, occurring in the state of Santa Catarina, for the unique day of 31/12/2020. As one notes, the data are taken from a more general data set but, as a snapshot of the day just spoken, for a question of economy of time while simulating. In statistics it is known as *cross-section*, (HAYS; WINKLER, 1970). What indeed happens here is that one is representing, only for the simulation, the cases in all state of Santa Catarina, as the punctual occurrence of cases spread along the municipalities of that state, in that very given day.

In trying to understand the roots of such behavior, some simple features was included as a possible candidate for explanation, always keeping in mind that correlation does not implies cause, in principle. The data set was endowed with the features,

- altitude;

Figure 19 – Evolution of the case numbers in municipalities with the lowest and highest incidence of infections. Despite the principal data used in the applications do refer to a specific day, the evolutions of these particular occasions on both municipalities is of interest to gain insight over the dynamics of the process of virus spreading.

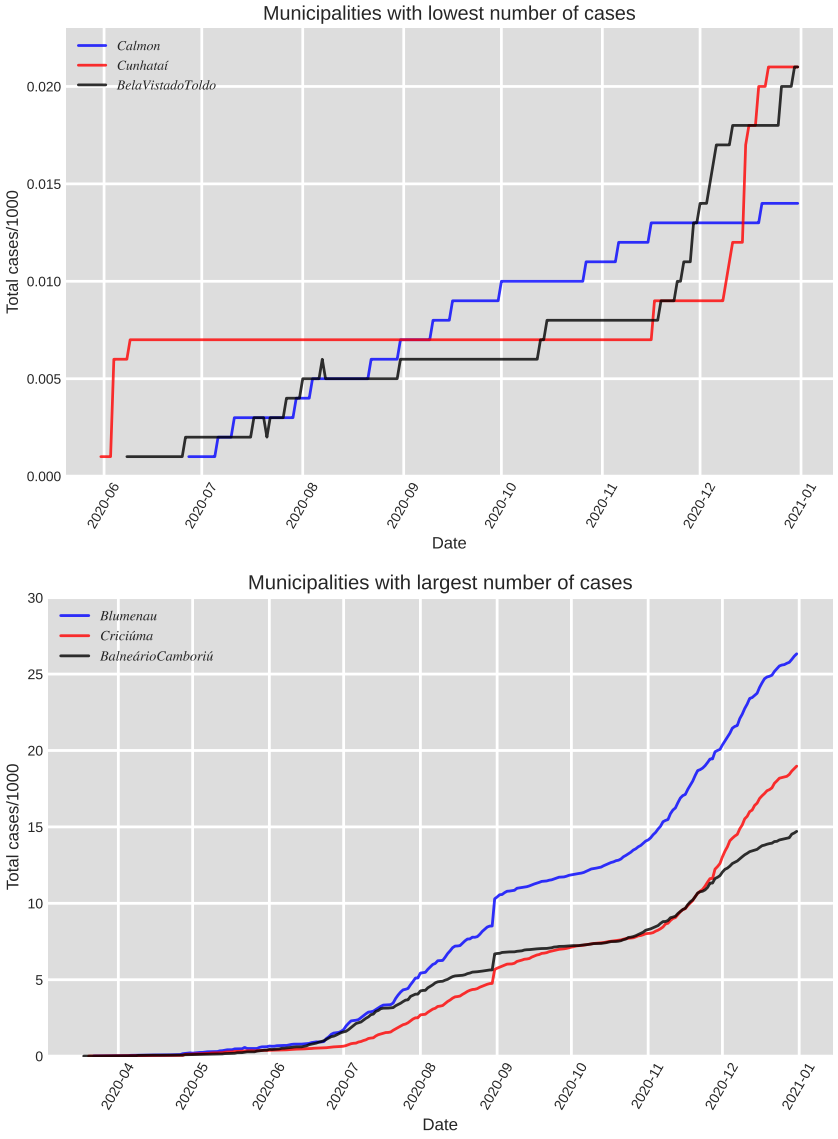

Source: the own author.

- density pkm2;
- idh municipality ;
- mean temp;
- mean hum;
- mean press;
- gov;

Figure 20 – Autocorrelation lag graphic for the data under analysis, on the bottom, followed by the correlations with selected features, on the top. In the former, the observation is correlated with n time steps apart while, the latter, the influence of the selected attribute is subjected to analysis.

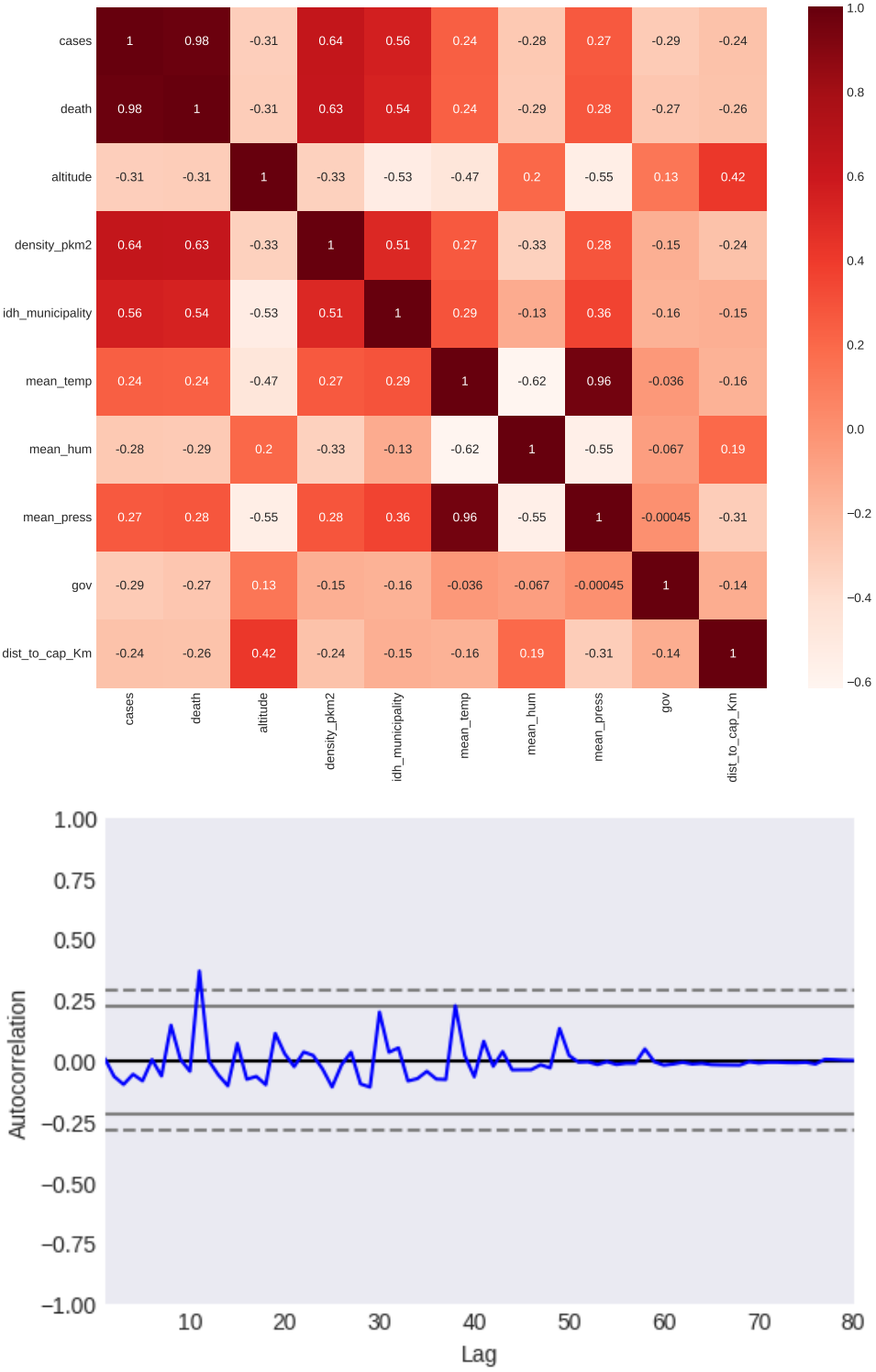

Source: the own author.

- dist to cap km;
- neighbors.

Figure 21 – Evolution of new cases for the three municipalities with the lowest number of cases, during the period of the first semester of 2022.

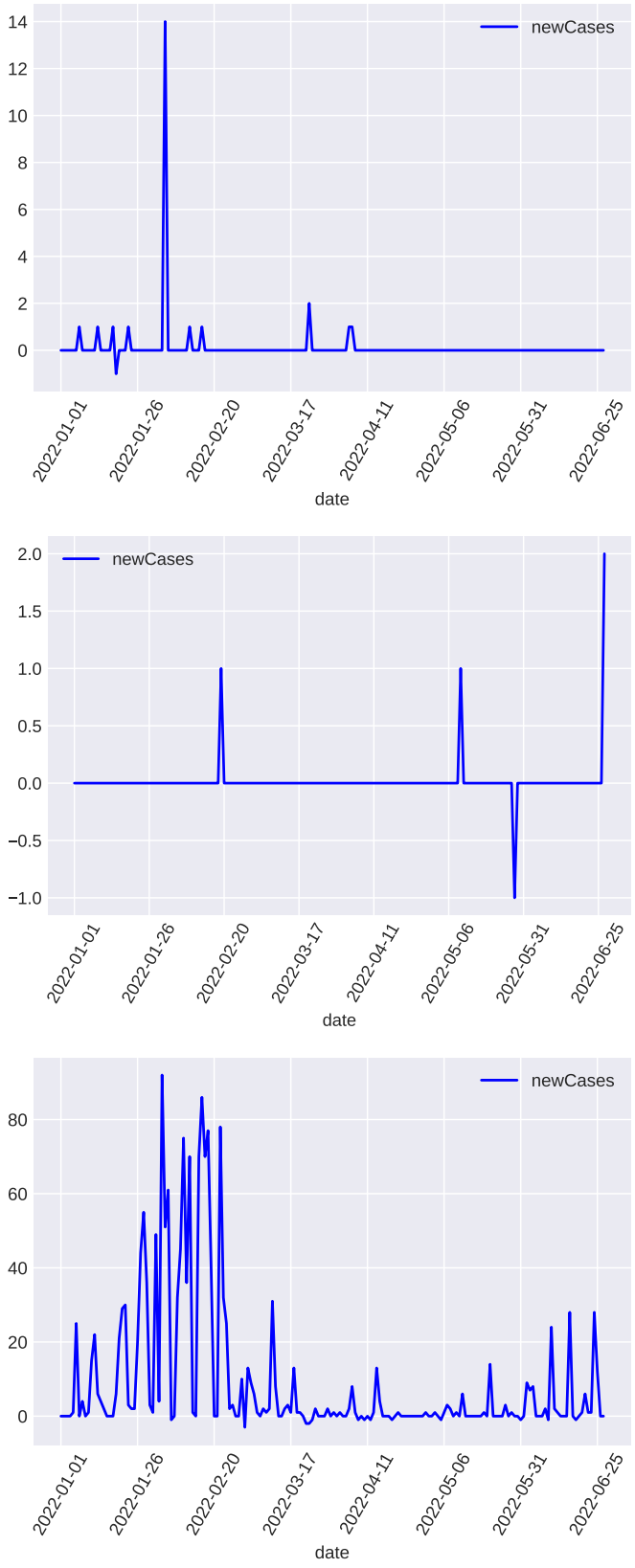

Source: the own author.

Figure 22 – Evolution of new cases for the three municipalities with the highest number of cases, during the period of the first semester of 2022.

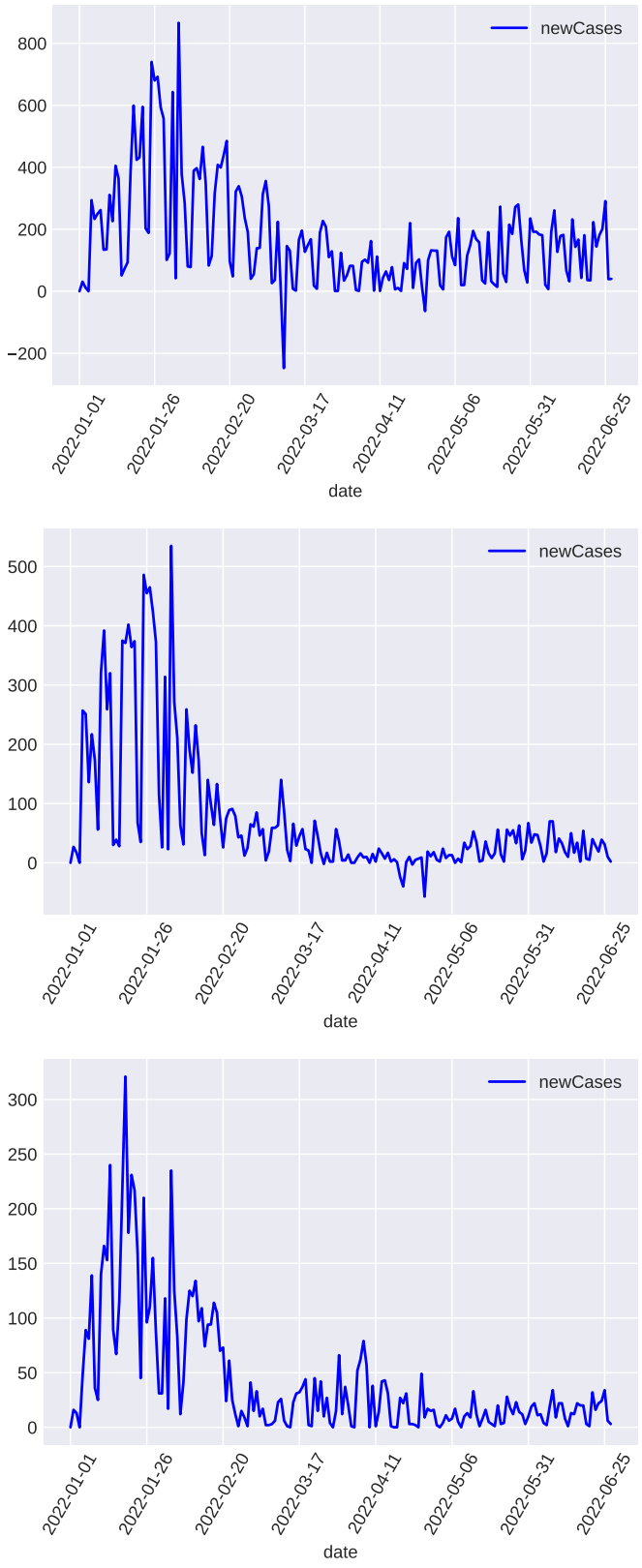

Source: the own author.

The idea of bringing features like altitude, mean temperature and humidity, was based on the factors under which the viruses systems diffuse themselves through environment, directly influenced by the physical properties of the mean surrounding the phenomenon, (S. PRETTNER K., 2021), (BOUVIER, 2012). Of course these are only parts to be taken as plausibles, once the spreading itself, depends on another factors, like contact with vectors and infective rate, properly. Yet, in the case of gov attribute, related to the government, the idea is associated with data acquisition, as well as, management of them. This is a very important information to be put on the table, once the intelligence through which data can dispose, will serve to decision making that will impact all the society, as was seen in the period of lockdown and his drastic break of constitutional order, by nonsense impositions, and anti-scientific measures. In this sense, the acquisition and treatment of data are crucial, as can be seen at (ROHATGI; ROHATGI; BOWONDER, 1979), when it says "$[\cdots]$ using them could do more damage than using no forecasts at all $[\cdots]$".

The attribute related to geometry, that is to say, distances and neighbors are interesting. In spite of the absence of much details and results on this direction, the mention is worth of saying. However the question that arises, and is important to know is, what factors do contribute to the results for the low and large cases, as described above. The Figure 20 represents two kinds of graphs. The first one on the left, is related to the concept of Lag. When modeling time series one can assume a relationship between an observation and the previous one. The latter, in a time series, is called lag. With this in mind, one can quantify the strength and type of relationship between observations and the corresponding lags. In statistical point of view, the process is called *correlation* and, while calculated against lag values of the series at hand, it is called *autocorrelation*, (HAYS; WINKLER, 1970).

The second one plots the Pearson correlation heatmap frequently used to see correlation of independent variable with the proposed output variable, *cases*. It serves as a selection filtering for features that have considerable influence on the interest variable, say, *cases* feature. As its value varies between -1 to 1, a value in the neighborhood of zero implies a weaker correlation while, being exactly zero, implying no correlation. In that sense, a value close to 1 implies stronger positive correlation and, close to -1, the contrary. Addressing the values on the heatmap, one sees that the attributes referred to population density and mean humidity are worth of analysis, being the former, the one intuitively acceptable once the density of population measures how near are the inhabitants of a given municipality. Starting from the hypothesis that the interaction between individuals is a necessary- but not sufficient-, condition

to virus transmission, the larger the density, larger will be the transmission in large scale, leading to high number of cases.

However, when considering city like Cerro Negro, for example, with 55 cases and a population density of 7.5 people in Km^2, plausible values to indicate lower number of cases, if compared to Cunhataí, it does not exhibit the expected tendency. This shows, or at least could show, that the essence of these results are not available in these state of granular data, that is to say, one would need to refine, to increment the data set with more information, avoiding discontinuities, gaps of information. Note further, that the distance between minimum and maximum is quite significant. It is interesting how municipalities inside the same state are capable to present such a huge difference. The cause of these discrepancies, in data, is not properly easy to qualify because of issues described above. Consider, for example, the Municipality of Antônio Carlos. It is possible to consider, when compared to the whole state, to be in the vicinity of Florianópolis. When the former adds 734 cases, the later does 42079. Can one speculate that is just because of the population density? tourist qualifications? The three plots on Figure 21 show the number of cases along the year of 2022, since July, for the municipalities with relatively few cases. On the plots in Figure 22 the same situation but, now, for the municipalities with a relatively high number of cases. In both situations, the evolution of case numbers follows the trend, as expected, if compared to the early values of 2020.

Table 3 – Descriptive statistics for the first data set.

Min.	1st Qu.	Median	Mean	3rd Qu.	Max.
0.0140	0.1475	0.4325	1.9217	1.3137	26.3240

From Figure 23 it is possible to note the existence of several *outliers*. The outliers observations are: 5.571, 14.706, 5.980, 26.324, 4.337, 12.992, 6.563, 13.657, 5.288 e 18.976. Each one of them, referring itself to the municipalities of Araranguá, Bauneário Camboriú, Biguaçu, Blumenau, Braço do Norte, Brusque, Camboriú, Chapecó, Concórdia and Criciúma, respectively. Besides that, it can be seen that this data is right-skewed.

The Table 4 shows the statistical descriptions referring to the second data set.

Table 4 – Descriptive statistics for the second data set.

Min.	1st Qu.	Median	Mean	3rd Qu.	Max.
0.01930	0.05178	0.13891	0.25079	0.37277	1.00000

Figure 23 – Box-plot for the first data

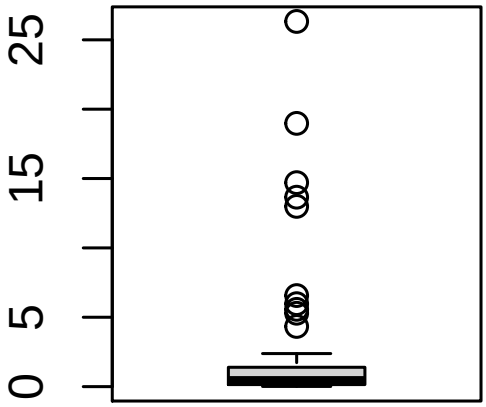

Source: the own author.

Figure 24 shows the Box-plot for the second data. It is possible to see the existence of 5 atypical observations, namely: 1, 0.9647469, 0.9307366, 0.8979253 e 0.8662707. Such observations do represent outliers figuring in the data. It would be interesting to know its sources in order to gain a better explanatory capacity for the data. For example, did rain in the specific day? How were the temperature? Besides that, it can be seen that this data is right-skewed.

As one can see, some distributions was chosen in order to make comparisons with the proposed models, i.e., TMOE and TMOW. One important feature, besides the ones addressed before, when discussing the exponential distribution, was the fact of it be a one parameter distribution. This works as an initial condition on the study. A natural idea to enhance the model is to introduce, as the competitors, sets of distribution functions with two or more parameters, (GEMEAY et al., 2023).

After a wide revision on the literature, the set of distributions given at 4.7 was selected due to their applicability on the case studies, and generalities they present, if not directly, or, by the use as baselines in other models. Examples follow, (ELBATAL, 2021), (ALMAZAH et al., 2022), among others. For the gamma distribution one can see, for example, (DUCHESNE;

Figure 24 – Box-plot for the second data

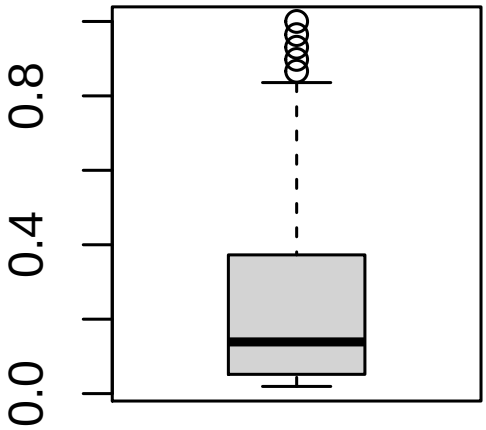

Source: the own author.

COUBARD, 2022), which makes a study considering the first wave pandemic process.

For the second data set, by considering the nature of the processes, better saying, the decaying nature of the physical process at hand, distributions whose nucleus are decreasing exponentials, were chosen. Here, the term nucleus must be understood as essential part, characterizing rapid decreasing nature. Of course the gamma function was marked for a diverse reason, that is to say, for his wide applicability.

Table 5 – Estimation results for the first data set

Model	$\hat{\alpha}$	$\hat{\theta}$	$\hat{p}$	$\hat{\lambda}$	$\hat{\beta}$	W^*	A^*
TMOE	0.7920	0.1388	-	0.1813	-	0.1288	0.8565
	(0.0004)	(0.0004)	(-)	(0.0004)	(-)		
TMOW	14.3479	544.7290	-	8196.8400	0.0066	0.0584	0.4048
	(<0.0001)	(<0.0001)	(-)	(<0.0001)	(<0.0001)		
EXP	-	-	-	0.5203	-	0.5811	3.4804
	(-)	(-)	(-)	(0.0581)	(-)		
EXP-EXP	0.6601	-	-	0.7679	-	0.7476	4.3922
	(0.0797)	(-)	(-)	(0.0740)	(-)		
KW-EXP	-	0.5285	6.1727	0.0214	-	0.3715	2.2945
	(-)	(0.0493)	(1.6926)	(0.0092)	(-)		
L-EXP	0.3370	-	-	0.3929	-	0.8637	5.0016
	(0.0459)	(-)	(-)	(0.0625)	(-)		
W	-	-	0.3370	0.3929	-	0.8637	5.0016
	(-)	(-)	(0.0459)	(0.0625)	(-)		
EXP-W	6.0491	0.2824	-	0.0270	-	0.1660	1.0761
	(0.7336)	(0.0139)	(-)	(0.0001)	(-)		
KW-W	18.8518	0.2820	0.3143	0.0019	-	0.1483	0.9664
	(0.9201)	(0.3230)	(0.0783)	(0.0599)	(-)		
B-W	454.7197	360.2270	0.0284	31.3816	-	0.4433	2.7220
	(0.0093)	(0.00006)	(0.0011)	(0.1118)	(-)		
Ga	0.4381	-	-	0.2280	-	0.5543	3.3311
	(0.0565)	(-)	(-)	(0.0484)	(-)		
Ga-FE	0.1405	0.2654	3926.2150	120.0207	-	0.2038	1.2853
	(0.0154)	(0.0000001)	(16.6785)	(0.00067)	(-)		

Table 6 – Estimation results for the second data set

Model	$\hat{\alpha}$	$\hat{\theta}$	$\hat{p}$	$\hat{\lambda}$	$\hat{\beta}$	W^*	A^*
TMOE(α, θ, λ)	0.0103	23.9233	1.0427	1.5061	-	0.1488	1.0959
	(4×10^{-7})	(5×10^{-7})	(3×10^{-7})	(5×10^{-7})	(-)		
TMOW($\alpha, \theta, \lambda, \beta$)	0.0043	0.9842	-	0.4191	1.9492	0.1586	1.1430
	(0.0001)	(0.0004)	(-)	(0.0004)	(0.0005)		
EXP(λ)	-	-	-	3.9873	-	0.2649	1.7986
	(-)	(-)	(-)	(0.3784)	(-)		
EXP-EXP(α, λ)	1.4860	-	-	7.0735	-	0.2703	1.8325
	(0.1665)	(-)	(-)	(0.5443)	(-)		
KW-EXP(m, p, λ)	-	1.2634	0.1931	21.4660	-	0.3837	2.4052
	(-)	(0.0046)	(0.0183)	(0.0042)	(-)		
L-EXP(α, λ)	0.9603	-	-	4.5795	-	0.2731	1.8451
	(0.1208)	(-)	(-)	(0.5091)	(-)		
W(p, λ)	-	-	0.9591	4.5725	-	0.2730	1.8449
	(-)	(-)	(0.0459)	(0.0625)	(-)		
EXP-W(α, p, λ)	18.2965	-	0.2990	0.0025	-	0.2410	1.6609
	(2.5294)	(0.0120)	(-)	(0.0002)	(-)		
KW-W(α, m, p, λ)	16.3539	518307.9	0.0799	167.7748	-	0.2440	1.6774
	(0.0005)	(0.1369)	(0.0013)	(5.4165)	(-)		
B-W(α, m, p, λ)	0.3369	165342.6	2.0759	201.3981	-	0.2754	2.0125
	(0.0301)	(23.7266)	(0.0001)	(0.0004)	(-)		
Ga(α, λ)	0.9794	-	-	3.9052	-	0.2648	1.7978
	(0.1155)	(-)	(-)	(0.5937)	(-)		

4.8 CONCLUSIONS

This is, effectively, the first application developed in the thesis due to the constructions made in the last chapters. Strategically, the first baseline used for $G(x;\boldsymbol{\xi},\boldsymbol{\tau})$, in the new models, is the exponential distribution, followed by the Weibull distribution, which, indeed, is an extension of the former.

Here, two data sets are used as source for applications of the distributions under analysis and comparisons are made with the models firstly chosen. The first one does refer to data collected, in the pandemic, in virtue of the COVID-19 virus spreading. As one could see above the data were collected in the state of Santa Catarina, Brazil and were subjected to descriptive statistical analysis. The second one are artificial data generated by a physical model with specific approach, which leads to instabilities on the dynamics under investigation. In the first case, some conclusions were achieved when evaluated according to the results encountered on Table 5. It is worth of saying that the model proposed is submitted to techniques, such as Anderson-Darling (A^*), Cramer Mises (W^*) and Kolmogorov-Smirnov (KS^*), as well as TTPlot, in order to select the best models, when compared to canonical ones in the literature.

For a method of selection, the lower the values of these indicators, more specified will be the model. By observing the table 5, one sees that the two proposed models have superior performance, if comparable to those of its competitors. Specially, the TMOW model have the highest performance. The same as before happens for the second data set, as observed in Table 6.

5 TRANSFORMED MARSHALL-OLKIN BIRNBAUM-SAUNDERS DISTRIBUTION

5.1 INTRODUCTION

As was pointed out at the general introduction of this text, the problem of stress concentration must be seriously considered in order to avoid losses in practical everyday systems, as well as dangerous fails leading to crack propagation, reasons for accidents and their harmful consequences. As it is obtained through a monotonic transformation on the standard normal, it is not hard to think of the wide range of applicability of the latter (BALAKRISHNAN N.; KUNDU, 2018), in a variate class of systems which exhibit a large number of entities, like, particles, for example, or Big data systems. As seen at (BIRNBAUM; SAUNDERS, 1969), Birnbaum and Saunders have brought to the surface these properties in a more clearer way, in the statistical point of view, through application into fatigue modeling with certain conditions, say, periodic stress.

However, this is not exhaustive. Its field of application is beyond fatigue problems in materials and reliability analysis. The Birnbaum-Saunders distribution can model tension concentration in systems where quantifiable characteristics are about to exceed a critical threshold leading to yield process.

Some examples, in many branches of knowledge are

- Migration of metallic flaws in nano-circuits due to heat in a computer chip.
- Accumulation of deleterious substances in the lungs from air pollution.
- Ingestion by humans of toxic chemicals from industrial waste.
- Occurrence of chronic cardiac diseases and different types of cancer due to cumulative damage caused by several risk factors, which produce degradation and conduct to a fatigue process.
- Air quality due to an accumulation of pollutants in the atmosphere over time.
- Generation of action potentials in neural activity.
- Late human mortality due to how the risk of death occurs at a late stage of human life.
- Occurrence of natural disasters such as earthquakes and tsunamis.

as described in (LEIVA, 2016). As was pointed out in the very last reference, the empirical fitting property is a reasonable argument for justifying the modeling process of the data under analysis through Birnbaum-Saunders distribution.

Let X be a random variable and (λ, β) be nonvanishing positive vector parameter. Let Φ represents the cdf of the canonical Normal distribution with $(\mu, \sigma) \equiv (0, 1)$. The transformation performed by Birnbaum and Saunders, over the normal distribution, is given by,

$$G(x; \lambda, \beta) = \Phi\left[\frac{1}{\lambda}\left\{\left(\frac{x}{\beta}\right)^{\frac{1}{2}} - \left(\frac{\beta}{x}\right)^{\frac{1}{2}}\right\}\right]$$

and the corresponding density,

$$g(x; \lambda, \beta) = \frac{1}{2\lambda\beta\sqrt{2\pi}}\left[\left(\frac{\beta}{x}\right)^{\frac{1}{2}} + \left(\frac{\beta}{x}\right)^{\frac{3}{2}}\right]\exp\left\{-\frac{1}{2\lambda^2}\left(\frac{x}{\beta} + \frac{\beta}{x} - 2\right)\right\}.$$

Along the chapter this canonical form of the Birnbaum-Saunders distribution will be used to be the baseline of the enquired family, as will be clear in the next sections.

5.2 TRANSFORMED MARSHALL-OLKIN BIRNBAUM-SAUNDERS DISTRIBUTION

Again, inserting Equation (5.1) into (3.5), by considering (3.6), it leads to

$$F(x; \alpha, \theta, \lambda, \beta) = \frac{\Phi\left[\frac{1}{\lambda}\left\{\left(\frac{x}{\beta}\right)^{\frac{1}{2}} - \left(\frac{\beta}{x}\right)^{\frac{1}{2}}\right\}\right]^{\alpha}}{\Phi\left[\frac{1}{\lambda}\left\{\left(\frac{x}{\beta}\right)^{\frac{1}{2}} - \left(\frac{\beta}{x}\right)^{\frac{1}{2}}\right\}\right]^{\alpha} + \theta\left\{1 - \Phi\left[\frac{1}{\lambda}\left\{\left(\frac{x}{\beta}\right)^{\frac{1}{2}} - \left(\frac{\beta}{x}\right)^{\frac{1}{2}}\right\}\right]\right\}^{\alpha}},$$

or, after a few algebra,

$$F(x; \alpha, \theta, \lambda, \beta) = \frac{\mathrm{e}^{-\alpha A(x,\beta)}}{\mathrm{e}^{-\alpha A(x,\beta)} + \theta\left[\sqrt{2\pi} - \mathrm{e}^{-A(x,\beta)}\right]^{\alpha}}, \tag{5.1}$$

where,

$$A(x, \beta) = \frac{1}{2\lambda^2}\left(\frac{x}{\beta} + \frac{\beta}{x} - 2\right)$$

and

$$f(x; \boldsymbol{\xi}; \boldsymbol{\tau}) = \frac{\alpha\theta\nu^{\alpha}}{2\beta\lambda^2}\left[\left(\frac{\beta}{x}\right)^2 - 1\right]\frac{\left[1 - \nu\mathrm{e}^{-\omega(x;\lambda,\beta)}\right]^{\alpha-1}\mathrm{e}^{-\alpha\omega(x;\lambda,\beta)}}{\left\{\nu^{\alpha}\mathrm{e}^{-\alpha\omega(x;\lambda,\beta)} + \theta\left[1 - \nu\mathrm{e}^{-\omega(z;\lambda,\beta)}\right]^{\alpha}\right\}^2},$$

with,

$$\omega(x; \lambda, \beta) = \frac{1}{2\lambda^2}\left[\left(\frac{x}{\beta}\right)^{\frac{1}{2}} - \left(\frac{\beta}{x}\right)^{\frac{1}{2}}\right]^2 \text{ and } \nu = \frac{1}{\sqrt{2\pi}}.$$

Figure 25 – Distribution Function and Probability Density Function for the Transformed Marshall-Okin Birnbaum-Saunders Model.

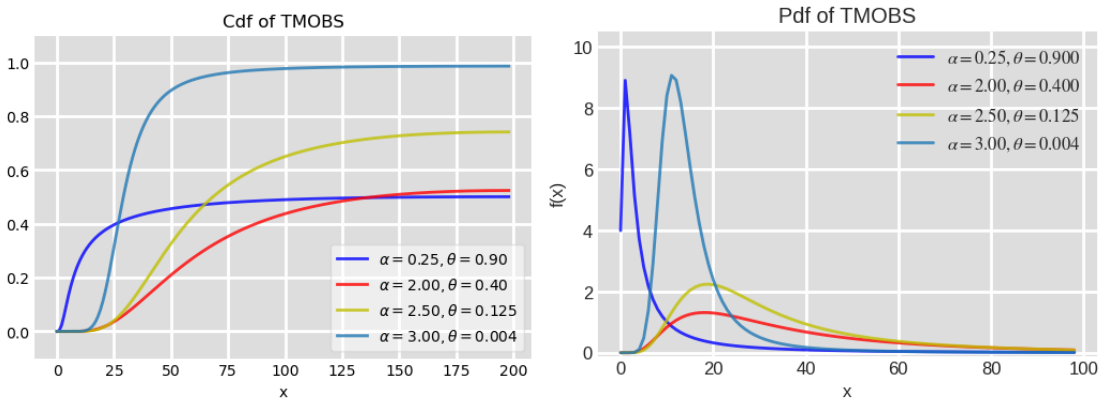

Source: the own author.

In Figure 25, the parameter set $\boldsymbol{\xi} = (\alpha, \theta)$ is allowed to vary while the baseline parameter set $\boldsymbol{\tau} = (\lambda, \beta)$ is kept constant.

Figure 26 – Surface parameter defined by the parameter variation α and θ.

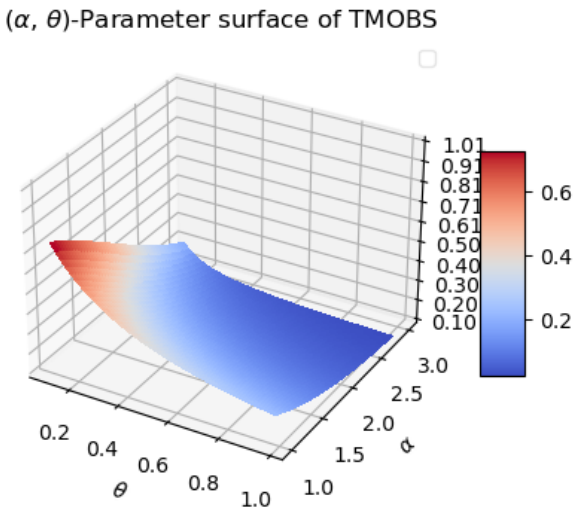

Source: the own author.

As long as the parameter α ranges in the interval $1 < \alpha < 3$ and θ is kept fixed, the surface for the distribution function for different values of x is graphed at figure 35. This figure together with the left graph on figure 25 describe how the variations on the values of α change the forms of the distribution. These variations allows one to see how the model can be applied to a variety of real data, due to his flexibility subjecting the model to a wide range of parameter values, in a given interval.

5.2.1 TMOBS Hazard Rate Function

By following (3.7), the hazard function for the TMOBS model reads,

$$h\left(x;\alpha,\theta,\lambda,\beta\right)=\alpha\left(\frac{\beta}{x^2}-\frac{1}{\beta}\right)\left\{\frac{\mathrm{e}^{-A(x;\beta)}}{\varrho}+\frac{\theta\mathrm{e}^{-A(x;\beta)}\varrho^{\alpha-1}-\mathrm{e}^{\alpha A(x;\beta)}}{\mathrm{e}^{-\alpha A(x;\beta)}+\theta\varrho}\right\}, \tag{5.2}$$

where,

$$\begin{aligned} A(x;\beta) &= \frac{1}{2\lambda^2}\left(\frac{x}{\beta}+\frac{\beta}{x}-2\right) \quad \text{and} \\ \varrho &= \sqrt{2\pi}-\mathrm{e}^{-A(x;\beta)}. \end{aligned}$$

Then, for the T factor function, one reads,

$$\begin{aligned} T_+(z) &= \Phi'_+(z)\left(2\Phi_+(z)-1\right)\left(2\theta\eta^{\alpha-1}(z)-1\right)\left(\theta\eta^{\alpha}(z)+1\right)+ \\ &+ \sqrt{2\pi}\theta\Phi_+(z)(1-\Phi_+(z))\left[\mathcal{P}_2(z,\alpha)+\mathcal{P}_1(z,\alpha)\right], \end{aligned} \tag{5.3}$$

where,

$$\begin{aligned} \Phi_+(z) &= \lambda^2\log z+\left(1+\lambda^2\log z\right)^2+2\lambda\sqrt{\log z}\left(1+\lambda^2\log z\right), \\ \Phi'_+(z) &= \frac{\lambda^2}{z}\left[1+2\left(1+\lambda^2\log z\right)+\frac{(1+\lambda^2\log z)}{\lambda\sqrt{\log z}}+2\lambda\sqrt{\log z}\right], \end{aligned}$$

and the polynomials, $\mathcal{P}_2$ and $\mathcal{P}_1$ are given by

$$\begin{aligned} \mathcal{P}_2(z;\alpha,\theta) &= -2\theta\eta^{2(\alpha-1)}(z) \text{ and} \\ \mathcal{P}_1(z;\alpha,\eta) &= 2(\alpha-1)\eta^{\alpha-2}(z)+\alpha\eta^{\alpha-1}(z), \end{aligned}$$

where $\eta(z)=\sqrt{2\pi}z-1$. According to the last lines, one reads,

$$\frac{r'_+(z)}{r_+(z)}=\frac{T_+(z)}{\Phi_+(z)\left[1-\Phi_+(z)\right]\left[2\theta\eta^{\alpha-1}(z)-1\right]\left[\theta\eta^{\alpha}(z)+1\right]}. \tag{5.4}$$

For the second case, where one defines the $T_-(z)$, one has

$$\begin{aligned} T_-(z) &= \Phi'_-(z)\left(2\Phi_-(z)-1\right)\left(2\theta\eta^{\alpha-1}(z)-1\right)\left(\theta\eta^{\alpha}(z)+1\right)+ \\ &+ \sqrt{2\pi}\theta\Phi_-(z)(1-\Phi_-(z))\left[\mathcal{P}_2(z,\alpha)+\mathcal{P}_1(z,\alpha)\right], \end{aligned} \tag{5.5}$$

where,

$$\begin{aligned} \Phi_-(z) &= \lambda^2\log z+\left(1+\lambda^2\log z\right)^2-2\lambda\sqrt{\log z}\left(1+\lambda^2\log z\right), \\ \Phi'_-(z) &= \frac{\lambda^2}{z}\left[1+2\left(1+\lambda^2\log z\right)-\frac{(1+\lambda^2\log z)}{\lambda\sqrt{\log z}}+2\lambda\sqrt{\log z}\right]. \end{aligned}$$

Figure 27 – Sign variation of $T_+(z)$ and $T_-(z)$, as compared to the denominator of (5.4), or (5.6).

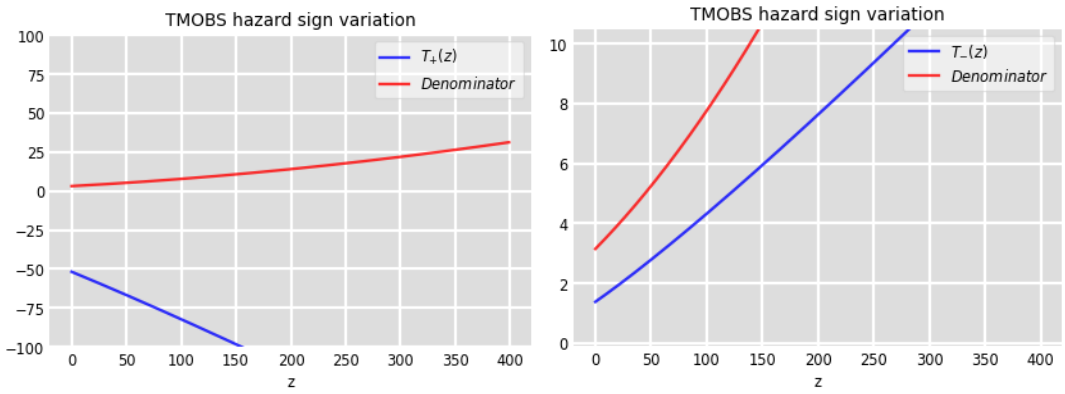

Source: the own author.

Figure 28 – $T_-(z)$ according to the regions they are immersed.

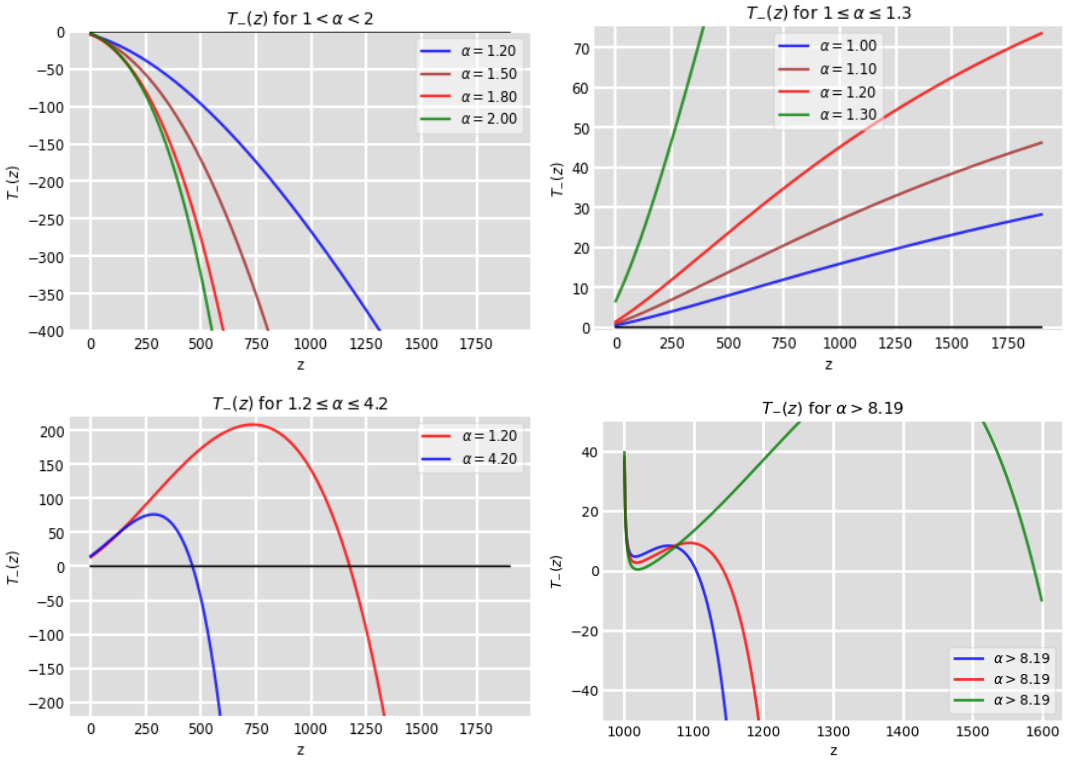

Source: the own author.

and

$$\frac{r'_-(z)}{r_-(z)} = \frac{T_-(z)}{\Phi_-(z)\left[1-\Phi_-(z)\right]\left[2\theta\eta^{\alpha-1}(z)-1\right]\left[\theta\eta^{\alpha}(z)+1\right]}, \tag{5.6}$$

$\mathcal{P}_i$, $i = 1, 2$ and $\eta(z)$ as given above.

Proposition 10 *If the hazard rate function is given by (5.2), there exist two classes of separation regions, $T_+(z)$ and $T_-(z)$, one of which preserving probabilistic meaning, that is to say,*

the hazard rate function associated is a nondecreasing function of z.

Dem. 9 *As was shown in 5.3 and 5.5, theses two functions was derived from 5.2. Each of them are given in terms of* $\left\{\Phi_+(z), \Phi'_+(z)\right\}$ *and* $\left\{\Phi_-(z), \Phi'_-(z)\right\}$*:*

$$\begin{aligned} T_+(z) &= T_+\left(\Phi_+, \Phi'_+\right), \\ T_-(z) &= T_-\left(\Phi_-, \Phi'_-\right). \end{aligned} \tag{5.7}$$

Given $\lambda > 0$, $z_1, z_2 \in \mathbb{R}$, $z_1, z_2 > 1$ *and* $z_2 > z_1$. *Then one has,*

$$\begin{aligned} T_+(z_2) &= \lambda^2 \log z_2 + \left(1 + \lambda^2 \log z_2\right)\left[\left(1 + \lambda^2 \log z_2\right) + 2\lambda\sqrt{\log z_2}\right] + \zeta(\Phi'_+(z_2)), \\ T_+(z_1) &= \lambda^2 \log z_1 + \left(1 + \lambda^2 \log z_1\right)\left[\left(1 + \lambda^2 \log z_1\right) + 2\lambda\sqrt{\log z_1}\right] + \zeta(\Phi'_+(z_1)), \end{aligned}$$

where $\zeta(\Phi'_+(z_i)), i = 1, 2$ *are functions of* Φ'_+*, in order to justify (5.7), above. However, by hypothesis,*

$$z_2 > z_1 \rightarrow \begin{cases} z_2 - z_1 > 0, \\ \frac{z_2}{z_1} > 1 > 0. \end{cases} \tag{5.8}$$

It follows that,

$$\begin{aligned} T_+(z_2) - T_+(z_1) &= 3\lambda^2 \log \frac{z_2}{z_1} + \lambda^4\left(\log^2 z_2 - \log^2 z_1\right) + 2\lambda\left[\delta_1 + \lambda^2\delta_2\right] \\ &+ \left(\zeta(\Phi'_+(z_2)) - \zeta(\Phi'_+(z_1))\right); \\ \delta_1 &= \sqrt{\log z_2} - \sqrt{\log z_1}; \\ \delta_2 &= \log z_2\sqrt{\log z_2} - \log z_1\sqrt{\log z_1}. \end{aligned}$$

Algebraic analysis considering (5.8) leads to

$$T_+(z_2) - T_+(z_1) < 0 \quad \Rightarrow T_+(z_2) < T_+(z_1), \tag{5.9}$$

which shows the decreasing nature of T_+*, in particular, showing the break of structure-preserving for the hazard rate function characteristics.*

For the second case, one has,

$$\begin{aligned} T_-(z_2) - T_-(z_1) &= 3\lambda^2 \log \frac{z_2}{z_1} + \lambda^4\left(\log^2 z_2 - \log^2 z_1\right) - 2\lambda\left[\delta_1 + \lambda^2\delta_2\right] \\ &+ \left(\zeta(\Phi'_-(z_2)) - \zeta(\Phi'_-(z_1))\right), \end{aligned}$$

where $\zeta(\Phi'_-(z_i)), i = 1, 2$ *are functions of* Φ'_-*, in order to justify (5.7), above, and* δ_1 *and* δ_2 *as given above. Again, algebraic analysis considering (5.8) leads to,*

$$T_-(z_2) - T_-(z_1) > 0 \quad \Rightarrow T_-(z_2) > T_-(z_1), \tag{5.10}$$

which shows the non-decreasing nature of T_{-}. In particular, it shows the structure-preserving for the hazard rate function characteristics corroborating what one sees in the Figure 27, on the left. □

Note, however that, for values of α greater than 2.20, the shape of the last figure in 28 addresses the meaning of the one which precedes it, that is to say, the separation region is induced by the process of crossing axis, changing sign. As was pointed out at corresponding Chapter 3, it indicates that the hazard function exhibits unimodal property.

5.2.2 TMOBS Quantile Function

In this section, a closed form expression is developed for the TMOBS quantile function. Then, let consider the following Proposition.

Proposition 11 *Let $p : \mathbb{R}|_{(0,1)} \to \mathbb{R}|_{\Xi}$ where $u \mapsto p(u)$ is such that*

$$p(u) = 1 - \lambda^2 \log\left(\frac{\sqrt{2\pi}}{1 + \left[\frac{1}{\theta}\left(\frac{1-u}{u}\right)\right]^{\frac{1}{\alpha}}}\right)$$

and Ξ is the interval where the restriction of F^{-1}, for the $TMOBS$ model, has image in $(0,1)$ in accordance with 3.9.

$$Q_{TMOBS}(u) = \beta\left(p(u) - \sqrt{p(u)^2 - 1}\right) \tag{5.11}$$

Figure 29 – Quantile function for the Transformed Marshall-Okin Birnbaum-Saunders Model.

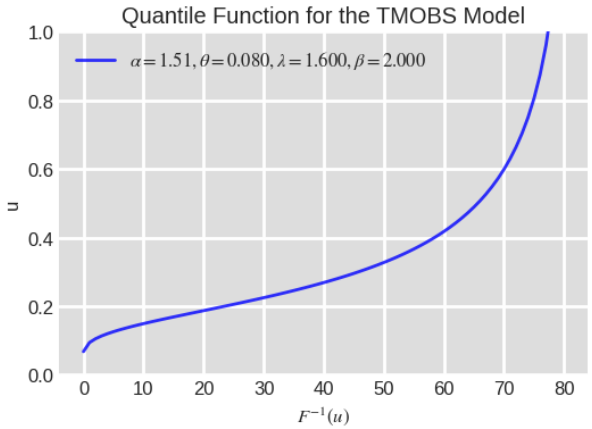

Source: the own author.

α	θ	λ	β	$Q(u = 1/2)$
1.00	0.90	1.10	0.10	0.2486
2.00	0.40	1.50	0.50	1.9737
2.50	0.125	1.70	1.00	5.5808
3.00	0.004	2.00	1.50	17.9529

Table 7 – Quantile function for $u = 1/2$ and increasing different values of α, λ and β and decreasing the θ value.

Note that, in Table 7 the values of $Q(u = 1/2)$ are increasing ones, as the parameter θ increases. This is a direct consequence of the nature of the considered functions in terms of the variable in question.

Figure 30 – Graph of $Q(u = 1/2)$ and continuous values of α and θ, for the Transformed Marshall-Olkin Birnbaum-Saunders Model.

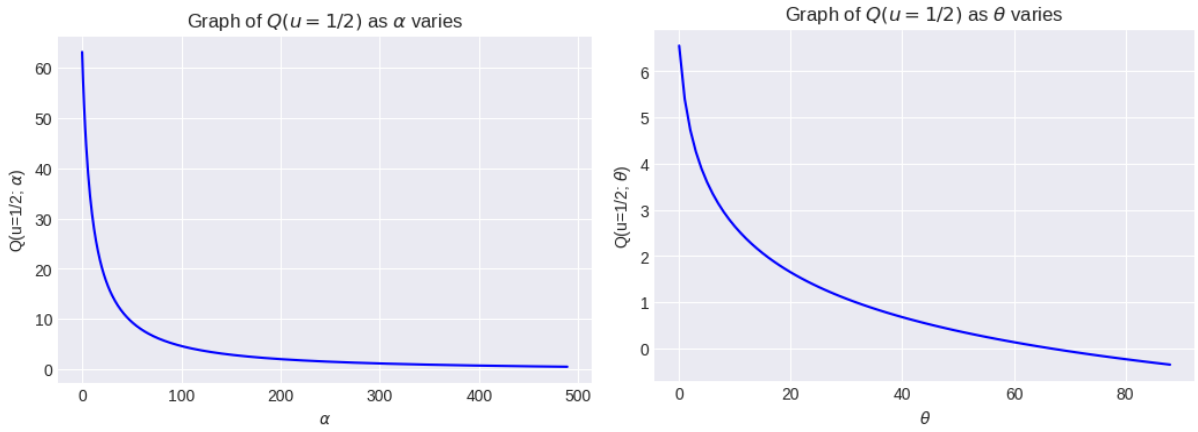

Source: the own author.

The plots in Figures 30 and 31 express the values of the median as the α and β parameters vary, respectively, in the former case, and jointly with θ, λ and β, in the latter case. The figures show the velocity of the decreasing character in each case.

Figure 31 – Graph of $Q(u = 1/2)$ and continuous values of m, λ and β for the Transformed Marshall-Olkin Birnbaum-Saunders Model.

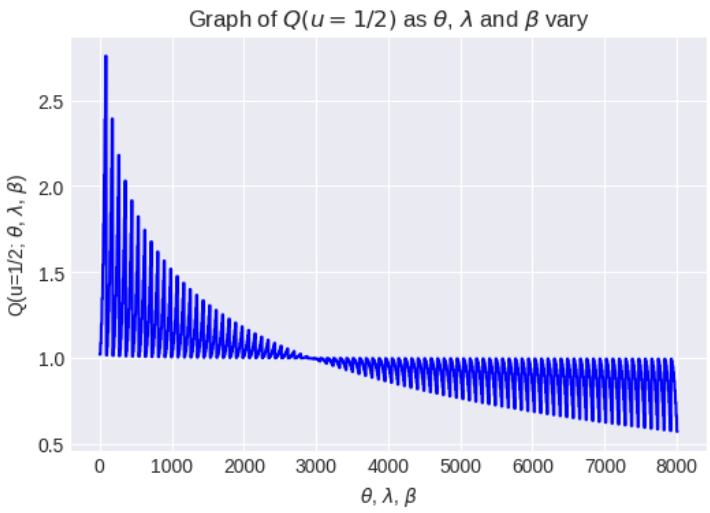

Source: the own author.

5.3 ESTIMATION

Here, again, one makes the use of (3.18) in order to express the log-likelihood function, l, for the TMOBS model which reads, if x_i, $i = 1, \cdots, n$, is a sequence of an n-size random sample,

$$\begin{aligned} l_{tmobs}(\boldsymbol{\xi}, \boldsymbol{\eta}; x) &= n \log\left(\frac{\alpha\theta\nu^{\alpha}}{2\beta\lambda^2}\right) + \sum_{i=1}^{n} \log\left[\left(\frac{\beta}{x_i}\right)^2 - 1\right] \\ &+ (\alpha - 1)\sum_{i=1}^{n} \log\left[1 - \nu \mathrm{e}^{-\omega(x_i,\lambda,\beta)}\right] - \alpha\sum_{i=1}^{n} \omega(x_i, \lambda, \beta) \\ &- 2\sum_{i=1}^{n} \log\left\{\nu^{\alpha}\mathrm{e}^{-\alpha\omega(x_i,\lambda,\beta)} + \theta\left[1 - \nu\mathrm{e}^{-\omega(x_i,\lambda,\beta)}\right]^{\alpha}\right\}. \end{aligned}$$

In order to proceed for the determination of the score vectors, the following derivatives are

calculated,

$$\begin{aligned}
\frac{\partial l_{bs}(\boldsymbol{\xi},\boldsymbol{\tau};x_i)}{\partial\alpha} &= \frac{n\left(\alpha\log\nu+1\right)}{\alpha}-\sum_{i=1}^{n}\omega(x_i\lambda,\beta)+\sum_{i=1}^{n}\log\left[1-\nu\mathrm{e}^{-\omega(x_i,\lambda,\beta)}\right]\\
&- \frac{1}{\lambda^2}\sum_{i=1}^{n}\frac{\nu^{\alpha}\mathrm{e}^{-\alpha\omega(x_i,\lambda,\beta)}\left\{2\lambda^2\log\nu-\tilde{\Upsilon}^2(x_i,\beta)\right\}}{\nu^{\alpha}\mathrm{e}^{-\alpha\omega(x_i,\lambda,\beta)}+\theta\left[1-\nu\mathrm{e}^{-\omega(x_i,\lambda,\beta)}\right]^{\alpha}}\\
&- 2\theta\sum_{i=1}^{n}\frac{\left[1-\nu\mathrm{e}^{-\omega(x_i,\lambda,\beta)}\right]^{\alpha}\log\left[1-\nu\mathrm{e}^{-\omega(x_i,\lambda,\beta)}\right]}{\nu^{\alpha}\mathrm{e}^{-\alpha\omega(x_i,\lambda,\beta)}+\theta\left[1-\nu\mathrm{e}^{-\omega(x_i,\lambda,\beta)}\right]^{\alpha}},\\
\frac{\partial l_{bs}(\boldsymbol{\xi},\boldsymbol{\tau};x)}{\partial\theta} &= \frac{n}{\theta}-2\sum_{i=1}^{n}\frac{\left[1-\nu\mathrm{e}^{-\omega(x_i,\lambda,\beta)}\right]^{\alpha}}{\nu^{\alpha}\mathrm{e}^{-\alpha\omega(x_i,\lambda,\beta)}+\theta\left[1-\nu\mathrm{e}^{-\omega(x_i,\lambda,\beta)}\right]^{\alpha}},\\
\frac{\partial l_{bs}(\boldsymbol{\xi},\boldsymbol{\tau};x)}{\partial\lambda} &= \frac{\alpha}{\lambda^3}\sum_{i=1}^{n}\tilde{\Upsilon}^2(x_i,\beta)-\frac{2n}{\lambda}-\frac{\alpha}{\nu\lambda^3}\sum_{i=1}^{n}\frac{\mathrm{e}^{-\omega(x_i,\lambda,\beta)}\tilde{\Upsilon}^2(x_i,\beta)}{\left[1-\nu\mathrm{e}^{-\omega(x_i,\lambda,\beta)}\right]}\\
&- \frac{2\alpha}{\nu\lambda^3}\frac{\mathrm{e}^{-\omega(x_i,\lambda,\beta)}\left\{\nu^{\alpha+1}\mathrm{e}^{-\alpha\omega(x_i,\lambda,\beta)}-\theta\left[1-\nu\mathrm{e}^{-\omega(x_i,\lambda,\beta)}\right]^{\alpha-1}\right\}\tilde{\Upsilon}^2(x_i,\beta)}{\nu\mathrm{e}^{-\alpha\omega(x_i,\lambda,\beta)}+\theta\left[1-\nu\mathrm{e}^{-\omega(x_i,\lambda,\beta)}\right]^{\alpha}},\\
\frac{\partial l_{bs}(\boldsymbol{\xi},\boldsymbol{\tau};x)}{\partial\beta} &= 2\beta\sum_{i=1}^{n}\frac{1}{x_i^2\Upsilon(x_i,\beta)}+\frac{\alpha}{2\lambda^2}\sum_{i=1}^{n}\frac{\Upsilon(x_i,\beta)}{x_i}-\frac{(\alpha-1)\nu}{2}\frac{\Upsilon(x_i,\beta)}{x_i\left[1-\nu\mathrm{e}^{-\omega(x_i,\lambda,\beta)}\right]}\\
&+ \frac{\alpha}{\lambda^2}\sum_{i=1}^{n}\frac{\Upsilon(x_i,\beta)}{x_i}\frac{\nu^{\alpha}\mathrm{e}^{-\alpha\omega(x_i,\lambda,\beta)}+\theta\nu\left[1-\nu\mathrm{e}^{-\omega(x_i,\lambda,\beta)}\right]^{\alpha-1}\mathrm{e}^{-\omega(x_i,\lambda,\beta)}}{\nu^{\alpha}\mathrm{e}^{-\alpha\omega(x_i,\lambda,\beta)}+\theta\left[1-\nu\mathrm{e}^{-\omega(x_i,\lambda,\beta)}\right]^{\alpha}}-\frac{n}{\beta},
\end{aligned}$$

where

$$\begin{aligned}
\Upsilon(x_i,\beta) &= \left[\left(\frac{x_i}{\beta}\right)^2-1\right],\\
\tilde{\Upsilon}(x_i,\beta) &= \left[\left(\frac{x_i}{\beta}\right)^{\frac{1}{2}}-\left(\frac{\beta}{x_i}\right)^{\frac{1}{2}}\right].
\end{aligned}$$

Given the log likelihood, above, and the Hessian, as given in Chapter 3, the information matrix reads

$$I_X^{bs}\left(\{\boldsymbol{\xi},\boldsymbol{\tau}\}\right)=-E\left(\frac{\partial^2 l(x;\boldsymbol{\theta})}{\partial\theta_r\partial\theta_s}\right)=-\left(\frac{\partial^2 l(x;\boldsymbol{\theta})}{\partial\theta_r\partial\theta_s}\right),$$

where the elements of the Hessian is on the Appendix C.

5.3.1 MLEs

Setting the derivatives of the log-likelihood function for (α, θ, λ, β) to zero, the MLEs ($\hat{\alpha}$, $\hat{\theta}$, $\hat{\lambda}$ $\hat{\beta}$) are obtained by numerical method. The approximate variances and the CIs of the parameters are obtained by inverting the observed Fisher matrix.

The $100 \cdot (1-\gamma)\%$ symmetric approximate normal CIs of (α, θ, λ, β) are constructed by

$$\left(\hat{\phi} - z_{\gamma/2}\sqrt{\mathrm{Var}(\hat{\phi})}, \hat{\phi} + z_{\gamma/2}\sqrt{\mathrm{Var}(\hat{\phi})}\right)$$

where $z_{\gamma/2}$ is the upper $\gamma/2$ point of standard normal distribution and ϕ can be α, θ, λ and β.

5.4 SIMULATIONS

In this section a simulation study is provided in order to verify the asymptotic properties of the parameters. To do this, an inverse method is considered and, thus, Equation (5.11) is used. The simulation algorithm below was used:

- Generate values from a distribution X$\sim$U$(0,1)$, where U refers to Uniform distribution;
- The inverse method is used and, therefore, the quantile function given in (5.11);
- Simulated TMOBS distributed data of $n \in \{50, 100, 150, 300\}$ are obtained by means of the above two items and 1,000 replicas of Monte Carlo were considered;
- Two scenarios are considered:
  1. $(\alpha, \theta, \lambda, \beta) = (0.5, 0.5, 0.8, 0.8)$,
  2. $(\alpha, \theta, \lambda, \beta) = (0.8, 0.5, 0.8, 0.8)$.
- Generated data is submitted to maximum likelihood estimation to obtain MSE's.

Tables 8 and 9 gives the MSEs for $(\alpha, \theta, \lambda, \beta)$ for both scenarios. Bias and MSE values decrease as the sample size increases as expected. Further, smaller values of the MSE at a specified pair are associated to the smaller parameter values. Besides that, mean estimates for the configurations considered are within their respective confidence intervals.

It can also be noted that the increase in the value of α causes an increase in the value of the bias in $n = 100$, but soon after the expected behavior occurs. The same oscillation occurs in the λ parameter for the same sample size value. This may indicate a certain influence of the α parameter on the λ parameter.

Table 8 – AEs, Bias and lower and upper bounds of 95% (HPD) CIs of the parameter - first scenario

n	True	AE	Bias	MSE	Lower	Upp
50	0.5	0.5240	0.0240	0.3797	-0.5328	1.5810
	0.5	0.5536	0.0536	0.0415	0.1459	0.8296
	0.8	0.8083	0.0083	0.5770	-0.4549	2.0716
	0.8	0.8038	0.0038	0.0376	0.4406	1.1670
100	0.5	0.5110	0.0110	0.0633	0.0094	1.0126
	0.5	0.5313	0.0313	0.0226	0.2357	0.7665
	0.8	0.8024	0.0024	0.0847	0.2171	1.3877
	0.8	0.7981	-0.0018	0.0170	0.5406	1.0556
150	0.5	0.4962	-0.0037	0.0360	0.1172	0.8753
	0.5	0.5186	0.0186	0.0132	0.2891	0.7237
	0.8	0.7876	-0.0123	0.0529	0.3462	1.2290
	0.8	0.7955	-0.0044	0.0106	0.5898	1.0012
300	0.5	0.4997	-0.0002	0.0171	0.2361	0.7633
	0.5	0.5092	0.0092	0.0060	0.3504	0.6626
	0.8	0.7960	-0.0039	0.0236	0.4895	1.1026
	0.8	0.7974	-0.0025	0.0051	0.6522	0.9426

Table 9 – AEs, Bias and lower and upper bounds of 95% (HPD) CIs of the parameter - second scenario

n	True	AE	Bias	MSE	Lower	Upp
50	0.8	0.7743	-0.0256	0.9044	-1.3025	2.8513
	0.5	0.5917	0.0917	0.0697	0.0822	0.8835
	0.8	0.7632	-0.0367	0.5513	-0.9230	2.4495
	0.8	0.8054	0.0054	0.0512	0.3638	1.2470
100	0.8	0.8437	0.0437	0.4865	-0.7319	2.4195
	0.5	0.5565	0.0565	0.0450	0.1429	0.8360
	0.8	0.8313	0.0313	0.3404	-0.4843	2.1471
	0.8	0.8032	0.0032	0.0284	0.4660	1.1403
150	0.8	0.7872	-0.0127	0.1717	-0.0069	1.5814
	0.5	0.5396	0.0396	0.0285	0.1994	0.7983
	0.8	0.7841	-0.0158	0.1238	0.1331	1.4351
	0.8	0.7971	-0.0028	0.0173	0.5337	1.0606
300	0.8	0.7789	-0.0210	0.0960	0.2895	1.2683
	0.5	0.5205	0.0205	0.0135	0.2855	0.7300
	0.8	0.7754	-0.0245	0.0791	0.3768	1.1740
	0.8	0.7975	-0.0024	0.0080	0.6141	0.9808

5.5 APPLICATIONS

In this section, we provide applications to real data set in order to provide the overfit of the TMOBS model. To do this, some well-known models are considered as a comparative models:

- Birnbaum-Saunders (BS), (REYES et al., 2021);
- Marshall-Olkin Birnbaum-Saunders (MOBS), (BIRNBAUM; SAUNDERS, 1969);
- Odd Log-Logistic Birnbaum-Saunders (OLLBS), (CORDEIRO et al., 2018);
- Odd Log-Logistic Birnbaum-Saunders Poisson (OLLBSP), (CORDEIRO et al., 2018);
- Kumaraswamy Birnbaum-Saunders (KWBS), (SAULO; LEãO; BOURGUIGNON, 2012);
- Gamma Birnbaum-Saunders (GBS), (CORDEIRO et al., 2016);

Based on the fact that applications in the area of sunspots were not found in the literature of New Distributions Theory, it was selected such competing models because they are extensions of the baseline and the baseline itself. The aim here is, therefore, to investigate the behavior of the family, in terms of goodness of fit, when compared with other families with the same baseline.

5.5.1 Sunspots

"Galileo was the first to study dark spots on the Sun which we call "sunspots". They typically measure about 10,000 kilometers across, which makes them on the order of the size of the Earth. They often occur in groups, and come and go. At some times the Sun has hundreds of sunspots, while at other times it may have almost none. Individual spots may last from 1 to 100 days. A large group of spots typically lasts 50 days," (SUNSPOT..., 2022a).

Recently, the information that the Earth is being under exposition of strong solar flare, as part of a natural cycle of events, has come to dawn, (SOLAR..., 2022). Despite this is not a new discovery, once the phenomena is studied yet a long time, the natural process interests the scientific community and the humanity, in general.

Here, two random sample parts of the dataset are presented and analysed for the statistical point of view. The proposed distributions are employed and some simulations are carried out. The two sets are shown at Tables 10 and 11 and have their significance explained below.

Month	Sunspot	Month	Sunspot	Month	Sunspot
1	8.2	1	7.5	1	4.7
2	10.7	2	5.3	2	5.1
3	8.6	3	4.8	3	4.9
4	6.9	4	8.2	4	3.5
5	7.5	5	8.6	5	4.7
6	7.7	6	6.3	6	2.0
7	7.4	7	5.7	7	3.8
8	7.6	8	5.2	8	4.5
9	8.7	9	6.4	9	3.8
10	6.9	10	5.4	10	3.1
11	8.5	11	5.2	11	2.6
12	7.4	12	5.4	12	2.4

Table 10 – Sample for the first dataset. It begins on December, 2013 and ends on April 2022. The complete data set is hosted at, (SUNSPOT..., 2022b), under source project: WDC-SILSO, Royal Observatory of Belgium, Brussels.

Month	Sunspot	Month	Sunspot	Month	Sunspot
1	96.70	1	122.2	1	116.7
2	104.3	2	126.5	2	72.50
3	116.7	3	148.7	3	75.50
4	92.80	4	147.2	4	94.00
5	141.7	5	150.0	5	101.2
6	139.2	6	166.7	6	84.50
7	158.0	7	142.3	7	110.5
8	110.5	8	171.7	8	99.70
9	126.5	9	152.0	9	39.20
10	125.8	10	109.5	10	38.70
11	264.3	11	105.5	11	47.50
12	142.0	12	125.7	12	73.30

Table 11 – Sample for the second data set. It begins on January, 1749 and ends on October 2022, in the complete dataset, (SUNSPOT..., 2022b), under source project: WDC-SILSO, Royal Observatory of Belgium, Brussels.

For the first data set, the sequence of data are disposed, since 2013 to 2022, as a monthly sequence of events, i.e, sunspots. These values are monthly mean standard deviation of the input sunspot numbers as given at the reference above. The purpose of this sequence of data is to test the flexibility of the proposed model, as the parameter set changes, as well as the best fitting property, as compared with canonical and other distributions available for analysis.

The second set of data is a small modification of the original one. It relates the time to the first maximum of sunspot, for each year, since 1749 to nowadays. It must be understood as follow: for the first year, that is to say, 1749, the highest spot happens to be on November with value 264.3; for the second year, 1750, the highest spot happens to be on August with value 171.7, and so on.

However, the *time* in question must be read such that, in the first time, that is, November, which is equivalent to the fraction 11/12 of a year, or better, 0,916666667 year, is the used format. Thus, the time sequence for consideration is the one obtained by this process under the column on months appearing at Table 11, from the original dataset, 0.916666667, 0.666666667, 0.083333333, 0.583333333, and so on.

The importance of knowing this phenomenon is beyond the mere passion for explaining things. In spite of *emergence point of view*, that is to say, the point of view that *an emergent phenomenon, as life, thought, or computation about which there are comprehensible facts or explanations that are not simply deducible from lower-level theories, but which may be explicable or predictable by higher-level theories referring directly to that phenomenon*, there exist the *instrumentalist* point of view, from where *the purpose of scientific theory is to predict outcomes of experiments*, (DEUTSCH, 1997). This is, in some sense, the practical of statistics.

Again, in this sense, the comprehension of the phenomena may be useful, in this specific case of sunspot, to predicting various interference processes that happen on the ionosphere, (JAIN et al., 2022), for example, when the interaction of the ejected particles and electromagnetic waves, coming from the Sun, reach the ionosphere causing destructive interference in the communication systems, since the occurrence of solar flares, which is burst of light, occurring in the chromosphere near a sunspot, (DAVIES, 1961), (MCINTOSH et al., 2020).

This fact, indeed, is a worrying one once almost all technological systems and processes of the present-day are linked by communication systems like mobile networks, satellites and all paraphernalia that depends on that.

"Why should not a gosling say thus: All the parts of the Universe regard me; the earth serves me for walking, the sun to give me light, the stars to inspire one with their influences. I have this use of the winds, that of the waters; there is nothing which this vault so favourably regards as me; I am the darling of nature. Does not man look after, lodge, and serve me? It is for me he sows and grinds: if he eat me, so does he his fellow-man as well; and so do I the worms that kill and eat him...", (WHEELER, 1986)

5.5.2 Computational Platform

In this section, we will describe some of the functions, packages and estimation methods that have been used on the simulations and graphing processes. The software used to create the graphs, obtain the estimators and verify the flexibility of the model, in terms of fit, was R, (R Core Team, 2013) through RStudio environment, (RStudio Team, 2020).

Regarding the estimation method, the maximum likelihood method was used to obtain the estimators for the parameters of each given model. Here, the BFGS method is considered for the first data and, for the second one, the SANN method was chosen. Both methods, however, being selected in virtue of the best results obtained by them.

Most of the initial guesses were obtained through heuristic method by using the GenSA and MASS R packages. When the initial guesses from this method provided unsatisfactory results, or when there was a problem of convergence, the guesses were chosen randomly.

Furthermore, the statistics of Anderson Darling (A^*) and Cramer Von Mises (W^*) were used to verify the performance of the proposed models when compared to those mentioned above.

5.5.3 Descriptive statistics and results

In this section, we provide a brief comments about some descriptive statistics for both data. Besides that, an analysis will be made about the flexibility of the proposed model, in terms of goodness of fit, when compared to the chosen competing models.

Table 12 shows some descriptive statistics of the first data.

Table 12 – Descriptive statistics for the first data set.

Min.	1st Qu.	Median	Mean	3rd Qu.	Max.
0.100	1.000	4.100	4.463	7.000	15.600

Figures 32 and 33 represent the Box-plot for both data. Note that they have no outliers.

Tables 12 and 14 show descriptive statistics for the first and second data sets. In the former, the measures summarize the data and give insights for understanding the whole behavior of the underlying phenomenon, in particular, the object of analysis concerning the maximum sunspot reached out by the event and its consequences. For the latter, beyond the facts discussed

Figure 32 – Box-plot for the first data

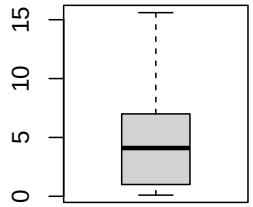

Source: the own author.

Table 13 – Estimation results for the first data set

Model	$\hat{\alpha}$	$\hat{\theta}$	$\hat{p}$	$\hat{\lambda}$	$\hat{\beta}$	W^*	A^*
TMOBS	1.8084	1.6364	-	19.2597	0.4174	0.2375	1.4092
	(0.0005)	(0.0005)	(-)	(0.0008)	(0.0005)		
MOBS	0.2619	-	-	12.9569	215.7538	2.1034	12.1990
	(0.0459)	(-)	(-)	(0.8949)	(8.9888)		
BS	-	-	-	1.6483	1.7137	0.5884	3.8312
	(-)	(-)	(-)	(0.1173)	(0.2073)		
OLLBS	537.3262	-	-	76.9884	2.6746	0.6302	3.8952
	(4×10^{-7})	(-)	(-)	(0.00002)	(2×10^{-6})		
OLLBSP	536.4979	0.8640	-	76.1452	3.0846	0.5233	3.0724
	(8×10^{-8})	(2×10^{-6})	(-)	(0.00004)	(7×10^{-6})		
BBS	74.7289	88.2912	-	85.4821	123.3944	1.8757	11.0707
	(1.9321)	(0.000005)	(-)	(0.00001)	(5.9795)		
GBS	0.3867	-	-	2.7438	19.0941	1.3151	8.0507
	(0.0358)	(-)	(-)	(0.000003)	(0.0479)		

above, the description does refer to the time such event takes to happen, as discussed in this section.

Table 14 – Descriptive statistics for the second data set.

Min.	1st Qu.	Median	Mean	3rd Qu.	Max.
0.08333	0.2500	0.5000	0.53133	0.81250	1.00000

As can be seen in the Tables 13 and 15, the proposed model produced a better fit to the data sets considered when compared to the shrunken competitors in each case.

Figure 33 – Box-plot for the second data

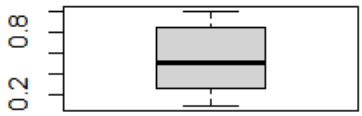

Source: the own author.

Table 15 – Estimation results for the second data set

Model	$\hat{\alpha}$	$\hat{\theta}$	$\hat{p}$	$\hat{\lambda}$	$\hat{\beta}$	W^*	A^*
TMOBS	4.3295	0.0315	-	57.8971	738.3755	2.0235	13.2512
	(0.00009)	(0.00007)	(-)	(0.0001)	(0.0005)		
MOBS	11.9860	-	-	134.0471	0.0649	3.28125	20.3993
	(0.0029)	(-)	(-)	(0.0005)	(0.0026)		
OLLBS	0.2669	-	-	0.3295	0.2056	4.2891	25.9210
	(0.00000009)	(-)	(-)	(0.0010)	(0.000005)		
OLLBSP	320.0840	0.0014	-	41.4460	5.7016	2.6542	16.7972
	(1.8167)	(0.0003)	(-)	(5.3956)	(0.3571)		
BBS	80.1466	112.2476	-	68.7853	97.7474	2.9601	18.8079
	(0.0147)	(0.9854)	(-)	(0.6413)	(0.000001)		
GBS	13.4080	-	-	997.8837	0.0887	2.5279	16.3726
	(0.0004)	(-)	(-)	(0.0004)	(0.0053)		

For the first data considered, the OLLBSP model presented the second best fit. Note that this is a model with three parameters and, depending on the chosen ones, presents bimodality. So, this result was expected. For more details, see (CORDEIRO et al., 2018).

About the second data, we can observe that the model that obtained the second best fit was the GBS. Despite presenting some complexity in computational terms and being very robust in mathematical terms, the models derived from the G-gamma family have some flexibility, as shown in the work of (CORDEIRO et al., 2016), among others.

Thus, we can state that the proposed model proved to be quite competitive with other

existing in the literature, considering the analyzed data.

5.6 CONCLUSIONS

In this chapter the model Transformed Marshall-Olkin Birnbaum-Saunders was proposed and some of its mathematical properties was stablished. A deeper enquiring of the hazard rate function was made such that a particular study, in the field of survival analysis, can be performed. Once the Birnbaum-Saunders model has wide applications in several fields of knowledge, with emphasis on fatigue data, it was decided to extrapolate the range of applicability of the model to more general phenomena, such as that of the sunspot, in astrophysics, here dealt with. The results have shown that the model under study exhibited higher performance when compared to other models disposed in the literature which, in turn, are extensions of the Birnbaum-Saunders.

Two real data sets are under analysis. For the first one the tables 8 and 9 give the MSE errors for the distribution, TMOB. The values were obtained by the BFGS method, from Monte Carlo simulation which shows a systematic decreasing on its values, for each parametric estimate made for the proposed model. The importance of inquiry like this one is on the necessity to know the sunspots occurrence distribution and the successive times of each of them. As was pointed out on the text, always next to sunspot there exist solar blasts ejecting interfering agents. From the information about these time distributions, once the best models have been chosen, forecasts can be done in order to mitigate possible damages to the systems guided by communication signals. An analysis on table 13, one sees that the TMOBS model has best performance. Furthermore, for the flexibility tests on the proposed models, the second data set treats the distribution of the modified data, as said above. The results can be read on table 15, which shows a better performance of the proposed model.

6 TRANSFORMED MARSHALL-OLKIN BURR XII DISTRIBUTION

6.1 INTRODUCTION

Along the years the seek for flexible distributions, as seen as having ability of fitting real data, has been getting intense and intense, particularly in the Big Data age, as said earlier. Hence, some distributions have been earned prominence in the branch of the theory of new distributions, for exhibiting great flexibility on adjusting a wide number of different kinds of datasets. One example of such distributions is the Burr-XII, also known as Singh-Maddala distribution. It has several distributions as particular cases: normal, log-normal, gamma, logistic, type-one extreme value, among others. These are some of the reasons why such a model well suits to different types of sets.

During the last decades, therefore, many other distributions have been proposed, in the literature, heading the Burr-II as baseline. The Beta Burr-II and Kumaraswamy Burr-XII, for example, were introduced in the thesis of Paranaíba (2012). These distributions were build by using the Beta-G generators (proposed by Eugene, Famoye and Lee, 2009) and Kumaraswamy-G, (CORDEIRO GAUSS M.; DE CASTRO, 2011).

Another distributions have been proposed through other methods. The geometric Burr-XII model, for example, was obtained by the mixing method between, geometric and Burr-XII, distributions. Such a model was proposed in the PhD thesis of Lanjoni, (LANJONI, 2013) and, in this work, the author has presented some mathematical properties, proposed the regression models, geometric type-one log-Burr-XII and geometric type-two log-Burr-XII.

Some interesting studies also have been used the Burr-XII as a candidate for modeling. Peralta, (MAZUCHELI et al., 2018), (PERALTA et al., 2017), have used, among other distributions, the Burr-XII to verify its adequacy to describe the behavior of the age, as measured in days, to the first quail posture (event) from yellow, blue and red lineage and subjected to two levels of feeding diet. After some analysis, the authors verified that the Burr-XII distribution turned out to be the most indicated in the majority of studied groups.

Another Burr-XII interesting application was presented for Oliveira et. al (2017). In the work the authors mention the importance of the probability density function in the parametric Monte Carlo technique to model the percentage relative frequency profile, of a real given bones samples, (OLIVEIRA et al., 2017). It was observed that the density function has shown right asymmetry and, therefore, one proposes the utilization of the three-parameter Burr-XII, for

the manufacturing of trabecular synthetic bones.

6.2 TRANSFORMED MARSHALL-OLKIN BURR XII DISTRIBUTION

In this section it is introduced the proposed model, named Transformed Marshall-Olkin Burr-XII. It is said that a random variable follows the Burr-XII distribution, if its probability density function is expressed by

$$g(x) = \rho\kappa \left(\frac{x}{\sigma}\right)^{\rho-1} \left[1 + \left(\frac{x}{\sigma}\right)^{\rho}\right]^{-\kappa-1}, \tag{6.1}$$

where the parameters $\rho, \sigma, \kappa > 0$ and $x > 0$. Consequently, its cumulative distribution function is given by

$$G(x) = 1 - \left[1 + \left(\frac{x}{\sigma}\right)^{\rho}\right]^{-\kappa}. \tag{6.2}$$

Following the trends of the last sections, the transformed Marshall-Olkin Burr XII distribution, and the corresponding density, are given, respectively, by

$$F\left(x;\boldsymbol{\xi},\boldsymbol{\tau}\right) = \frac{\left\{1 - \left[1 + \left(\frac{x}{\sigma}\right)^{\rho}\right]^{-\kappa}\right\}^{\alpha}}{\left\{1 - \left[1 + \left(\frac{x}{\sigma}\right)^{\rho}\right]^{-\kappa}\right\}^{\alpha} + \theta\left[1 + \left(\frac{x}{\sigma}\right)^{\rho}\right]^{-\alpha\kappa}},$$

and

$$f\left(x;\boldsymbol{\xi},\boldsymbol{\tau}\right) = \left(\frac{\alpha\kappa\rho\theta}{\sigma^{\rho}}\right) \frac{x^{\rho-1}\left\{\left[1 - \left(\frac{x}{\sigma}\right)^{\rho}\right]^{-\kappa} - 1\right\}^{\alpha-1}\left[1 + \left(\frac{x}{\sigma}\right)^{\rho}\right]^{\kappa-1}}{\left\{\theta + \left\{\left[1 + \left(\frac{x}{\sigma}\right)^{\rho}\right]^{\kappa} - 1\right\}^{\alpha}\right\}^{2}}.$$

As shown in Figure 34, for the graphs of the distribution function and his corresponding density function.

The Figure 35 describe the surface generated when the vector parameter $\boldsymbol{\xi} = (\alpha, \theta)$ varies. For different interval of variations of these parameters, different classes of shapes can occur which, in counterpart, may be useful to select properties of data tied by these conditions.

6.2.1 TMOBXII Hazard Rate Function

By following (3.7), the hazard function for the TMOBXII model reads,

$$h(x;\boldsymbol{\xi},\boldsymbol{\tau}) = \left(\frac{\alpha\kappa\rho}{\sigma^{\rho}}\right) \frac{x^{\rho-1}\zeta^{\kappa(\alpha+1)-1}}{\zeta^{\alpha} - 1}\left[\frac{(1-\zeta^{-\kappa})^{\alpha}}{\theta + \zeta^{\alpha\kappa}(1-\zeta^{-\kappa})^{\alpha}}\right],$$

Figure 34 – Cumulative distribution function and probability density function for Burr XII. The parameter set not explicitly occurring in figure frame is $\{\alpha = (0.25, 0.75, 1.00), \theta = (0.900, 0.675, 0.225)\}$, respectively for the blue, red and black curves.

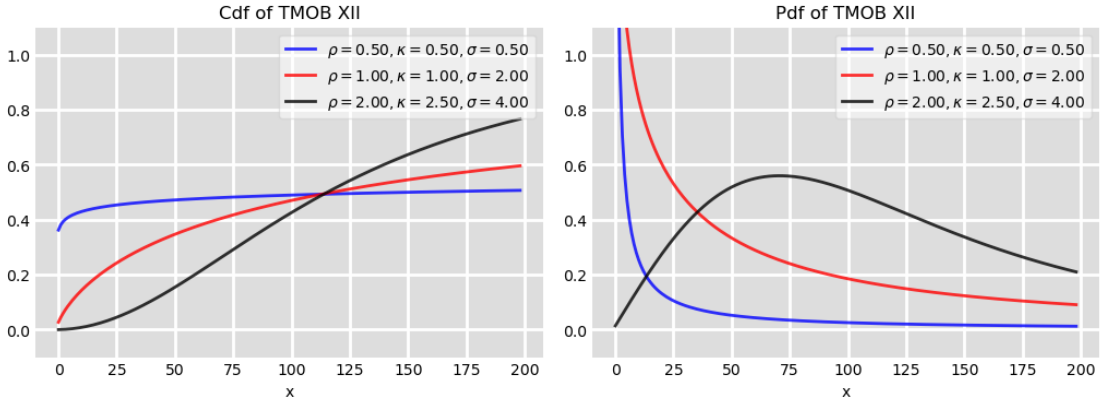

Source: the own author.

Figure 35 – Surface parameter defined by the parameter variation α and θ, for the model.

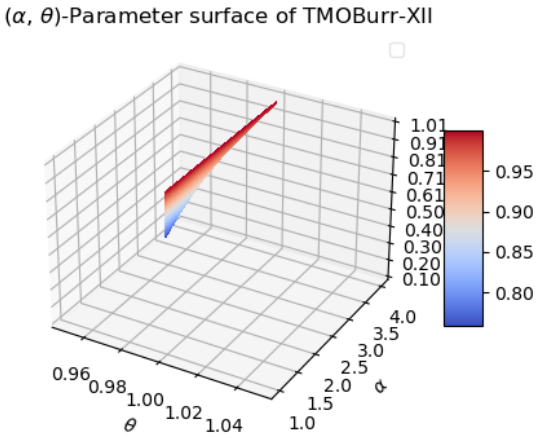

Source: the own author.

where $\zeta = \left[1 + \left(\frac{x}{\sigma}\right)^{\rho}\right]$.

With the parameter set given by, $\boldsymbol{\xi} = (\alpha, \theta)$ and $\boldsymbol{\tau} = (\rho, \kappa, \sigma)$, the graph of the hazard rate function is given by Figure 36.

Then, for the T factor function, one reads,

$$\begin{aligned} T(z) &= (\kappa-1)(z-1)(z^{\kappa}-1)\left[(z^{\kappa}-1)^{\alpha}+\theta\right] + z(z^{\kappa}-1)\left[(z^{\kappa}-1)^{\alpha}+\theta\right] \\ &+ (\alpha-1)\kappa z^{\kappa-1} z(z-1)\left[(z^{\kappa}-1)^{\alpha}+\theta\right] \\ &- \alpha\kappa z^{\kappa-1}(z^{\kappa}-1)^{\alpha-1} z(z-1)(z^{\kappa}-1), \end{aligned}$$

and, for $z \equiv 1 + \left(\frac{x}{\sigma}\right) > 1$, $x > 0$,

$$\frac{r'(z)}{r(z)} = \frac{T(z)}{z(z-1)(z^{\kappa}-1)\left[(z^{\kappa}-1)^{\alpha}+\theta\right]}.$$

Figure 36 – The parameter set not explicitly occurring in figure frame is $\alpha = (0.50, 1.00, 1.20)$ and $\theta = (0.038, 0.125, 0.900)$, respectively for the blue, red and black curves.

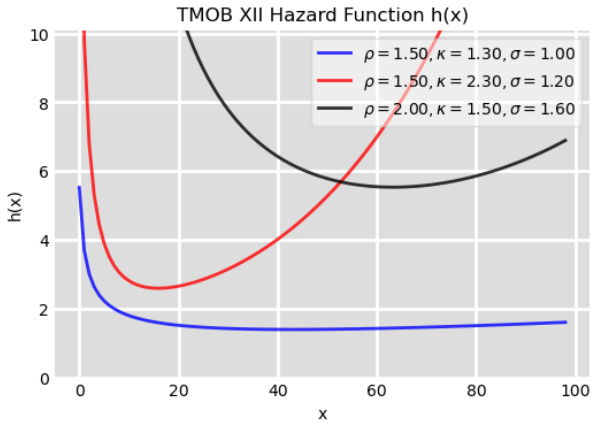

Source: the own author.

Now, as customary, one will proceed to the designation of the separation regions induced by the T factor function, as addressed by the graphs below.

Figure 37 – The parameter θ is kept fixed at 0.047. The bottom right graph returns the values near the ones next above, even for different values of α. The κ parameter receives values 0.5, 1.0 and 1.5, for all situations.

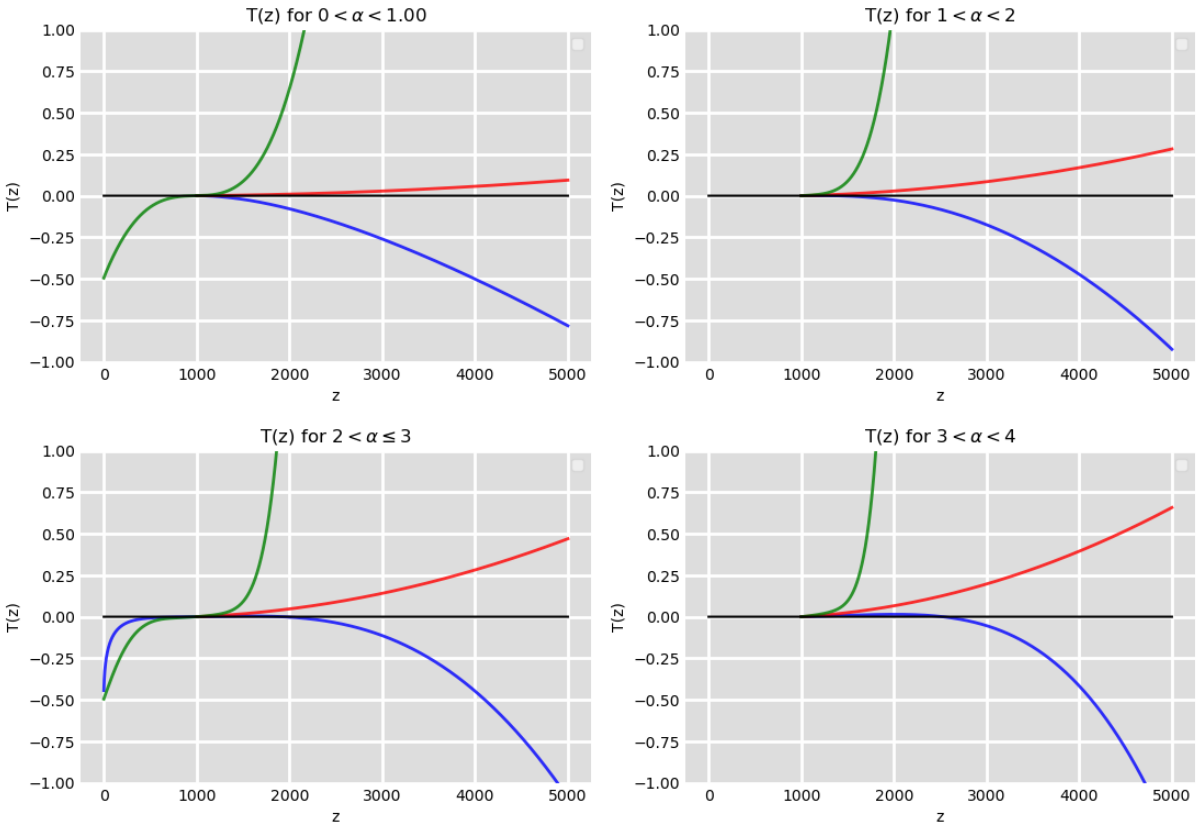

Source: the own author.

As was pointed out in last chapters, the shape of the distribution, through hazard function, can be pictured by mean of Qian technique (QIAN, 2012). This is what is observed in Figure 37 and similar commentaries made above, in corresponding chapters.

6.2.2 TMOBXII Quantile Function

Let X a random variable following TMOBXII distribution. Then, the quantile function of $x \in X$ is given by

$$Q_{\text{TMOBXII}}(u) = \sigma \left\{ \left[\frac{1 + \left(\frac{1-u}{\theta u} \right)^{\frac{1}{\alpha}}}{\left(\frac{1-u}{\theta u} \right)^{\frac{1}{\alpha}}} \right]^{\frac{1}{\kappa}} - 1 \right\}^{\frac{1}{\rho}}, \tag{6.3}$$

where $u = F^{-1}(x, \boldsymbol{\xi}, \boldsymbol{\tau})$, the pre-image of x by F.

6.2.3 Moments

As was developed in the last chapters the expressions and values of the mean and variance is allowable to be calculated with the methods described on the proper section of the referred chapters. It happens that, as the natural complexity of the functions describing the distributions tends to increase, as is seen on the long expressions read in the text, some operational calculus may be hard to implement, even if numerical approaches are in use, due to problems of convergence, or nonintegrability, as was pointed out earlier.

6.2.4 Estimation

Let x_i, $i = 1, \cdots, n$, be a sequence of an n-size random sample. The log-likelihood for the TMOBXII reads,

$$\begin{aligned} l(x_i, \boldsymbol{\xi}, \boldsymbol{\tau}) &= n \log \frac{\alpha\kappa\rho\theta}{\sigma^{\rho}} + (\rho - 1) \sum_{i=1}^{n} \log x_i + (\alpha - 1) \sum_{i=1}^{n} \log \left(\zeta^{\kappa} - 1 \right) \\ &+ (\kappa - 1) \sum_{i=1}^{n} \log \zeta - 2 \sum_{i=1}^{n} \log \left\{ \theta + \left(\zeta^{\kappa} - 1 \right)^{\alpha} \right\}, \end{aligned}$$

where,

$$\zeta_i = 1 + \left(\frac{x_i}{\sigma} \right)^{\rho}. \tag{6.4}$$

Following the ideas developed in the chapters above, one calculates the derivatives of $l(x_i, \boldsymbol{\xi}, \boldsymbol{\tau})$ in order to proceed in deriving the MLEs, through score vectors and consequent Hessian. They read,

$$\begin{aligned}
\frac{\partial l(x_i,\boldsymbol{\xi},\boldsymbol{\tau})}{\partial \alpha} &= \frac{n}{\alpha}+\sum_{i=1}^{n}\log\left(\zeta^{\kappa}-1\right)-2\sum_{i=1}^{n}\frac{\left(\zeta^{\kappa}-1\right)^{\alpha}\log\left(\zeta^{\kappa}-1\right)}{\theta+\left(\zeta^{\kappa}-1\right)^{\alpha}},\\
\frac{\partial l(x_i,\boldsymbol{\xi},\boldsymbol{\tau})}{\partial \theta} &= \frac{n}{\theta}+2\sum_{i=1}^{n}\frac{1}{\theta+\left(\zeta^{\kappa}-1\right)^{\alpha}},\\
\frac{\partial l(x_i,\boldsymbol{\xi},\boldsymbol{\tau})}{\partial \rho} &= \sum_{i=1}^{n}\log x_i+(\kappa-1)\sum_{i=1}^{n}\frac{\left(\frac{x_i}{\sigma}\right)^{\rho}\log\frac{x_i}{\sigma}}{\zeta}+\kappa\left(\alpha-1\right)\sum_{i=1}^{n}\frac{\left(\frac{x_i}{\sigma}\right)^{\rho}\zeta^{\kappa}\log\frac{x_i}{\sigma}}{\zeta\left(\zeta^{\kappa}-1\right)}\\
&+ \frac{n}{\rho}\left(1-\rho\log\sigma\right)-2\alpha\kappa\sum_{i=1}^{n}\frac{\left(\frac{x_i}{\sigma}\right)^{\rho}\zeta^{\kappa-1}\left(\zeta^{\kappa}-1\right)^{\alpha}\log\frac{x_i}{\sigma}}{\left[\theta+\left(\zeta^{\kappa}-1\right)^{\alpha-1}\right]},\\
\frac{\partial l(x_i,\boldsymbol{\xi},\boldsymbol{\tau})}{\partial \kappa} &= \frac{n}{\kappa}+\sum_{i=1}^{n}\log\zeta+(\alpha-1)\sum_{i=1}^{n}\frac{\zeta^{\kappa}\log\zeta}{\zeta^{\kappa}-1}-2\alpha\sum_{i=1}^{n}\frac{\zeta^{\kappa}\left(\zeta^{\kappa}-1\right)^{\alpha-1}\log\zeta}{\theta+\left(\zeta^{\kappa}-1\right)^{\alpha}},\\
\frac{\partial l(x_i,\boldsymbol{\xi},\boldsymbol{\tau})}{\partial \sigma} &= -\frac{n\rho}{\sigma}-\frac{\rho\left(\kappa-1\right)}{\sigma}\sum_{i=1}^{n}\frac{\left(\frac{x_i}{\sigma}\right)^{\rho}}{\zeta}-\frac{\kappa\rho(\alpha-1)}{\sigma}\sum_{i=1}^{n}\frac{\left(\frac{x_i}{\sigma}\right)^{\rho}\zeta^{\kappa-1}}{\zeta^{\kappa}-1}\\
&+ \frac{2\alpha\kappa\rho}{\sigma}\sum_{i=1}^{n}\frac{\left(\frac{x_i}{\sigma}\right)^{\rho}\zeta^{\kappa-1}\left(\zeta^{\kappa}-1\right)^{\alpha-1}}{\theta+\left(\zeta^{\kappa}-1\right)^{\alpha}}.
\end{aligned}$$

6.2.5 MLEs

Setting the derivatives of the log-likelihood function for (α, θ, ρ, κ, σ) to zero, the MLEs ($\hat{\alpha}$, $\hat{\theta}$, $\hat{\rho}$, $\hat{\kappa}$, $\hat{\sigma}$) are obtained by numerical method. The approximate variances and the CIs of the parameters are obtained by inverting the observed Fisher matrix.

The $100\cdot(1-\gamma)\%$ symmetric approximate normal CIs of (α, θ, ρ, κ, σ) are constructed by

$$\left(\hat{\phi}-z_{\gamma/2}\sqrt{\mathrm{Var}(\hat{\phi})},\hat{\phi}+z_{\gamma/2}\sqrt{\mathrm{Var}(\hat{\phi})}\right)$$

where $z_{\gamma/2}$ is the upper $\gamma/2$ point of standard normal distribution and ϕ can be α, θ, ρ, κ and σ.

6.3 SIMULATIONS

In this section a simulation study is provided in order to verify the asymptotic properties for the maximum likelihood estimators. To do this, an inverse method is considered and, thus,

Equation (6.3) is used. The simulation algorithm below was used:

- Generate values from a distribution X$\sim$U$(0,1)$, where U is the uniform distribution in $(0,1)$;
- The inverse method is used and, therefore, the quantile function given in Equation (6.3);
- Simulated TMOBXII distributed data of $n \in \{50, 100, 150, 300\}$ are obtained by means of the above two items and 1000 replicas of Monte Carlo were considered;
- Two scenarios are considered:
  1. $(\alpha, \theta, \rho, k, \sigma) = (0.5, .0.2, 1.6, 0.7, 1.4)$.
- Generated data is submitted to ML estimation to obtain MSE's.

Table 16 gives the means, bias and MSEs for $(\alpha, \theta, \rho, \kappa, \sigma)$. The MSE values decrease as the sample size increases as expected. Further, smaller values of the MSE at a specified pair are associated to the smaller parameter values.

Table 16 – AEs, Bias and lower and upper bounds of 95% (HPD) CIs of the parameter - first scenario

n	True	AE	Bias	MSE	95%	Lower	Upp
50	0.5	0.5514	0.0514	1.4197	46.7	-2.6741	3.777
	0.2	0.5909	0.3909	0.2656	88.4	0.04439	0.8325
	1.6	1.1817	-0.4182	9.2492	14.9	-1.1906	3.5541
	0.7	1.1826	0.4826	2.5314	67.4	-0.3101	2.6754
	1.4	1.3651	-0.0348	5.9228	38.7	-0.5532	3.2836
100	0.5	1.0378	0.5378	1.2918	54.1	-2.4381	4.5139
	0.2	0.5228	0.3228	0.2121	82.9	0.0555	0.7978
	1.6	1.2580	-0.3419	6.0797	21.8	-2.4687	4.9848
	0.7	0.6908	-0.0091	0.3075	75.9	-0.0282	1.4100
	1.4	1.8656	0.4656	2.1534	36.9	0.3070	3.4243
150	0.5	0.4959	-0.0040	1.0587	43.6	-1.8131	2.8049
	0.2	0.4868	0.2868	0.1998	76.5	0.0718	0.7289
	1.6	1.5717	-0.0282	10.5427	22.2	-1.4356	4.5790
	0.7	0.9272	0.2272	0.5000	72.1	0.2112	1.6432
	1.4	1.2510	-0.1489	3.5165	28.9	-0.2179	2.7201
300	0.5	1.0856	0.5856	1.4327	67.4	-2.5475	4.7188
	0.2	0.4102	0.2102	0.1382	83.4	0.0585	0.7808
	1.6	1.2007	-0.3992	3.7037	35.8	-2.3525	4.7540
	0.7	0.6462	-0.0537	0.0666	88.6	0.0733	1.2191
	1.4	1.2740	-0.1259	1.3649	45.6	-0.4279	2.9760

6.4 APPLICATIONS

In this section, one is provided with applications considering a real data set and a simulated one in order to provide the overfit of the TMOBXII model, as well as to show the flexibility of the new model. To do this, some well-known models are considered as a comparative models:

- Weibull distribution (W), (DASH; NANDI; SETT, 2016);
- EXP-W, (BEL GOLAN; ASHKENAZY, 2013);
- KW-W, (NADARAJAH, 2010);
- Gumbel, (LIU; LIU, 2018);
- Logistic, (ZANG et al., 2019);
- BXII, (SáNCHEZ, 2019);

- EXP-BXII, (TSAI et al., 2021);
- KW-BXII, (AFIFY; MEAD, 2017);
- B-BXII, (PARANAÍBA et al., 2011).

As was done in the cases before, a wide search was performed in order to select the above distributions, always keeping in mind the nucleus of of the baseline distribution, i.e., the Burr XII, its characteristics and performance while adjusting different types of data, for several kinds of phenomena.

6.4.1 Computational Platform

In this section, we will describe some of the functions, packages and estimation methods that have been used on the simulations and graphing processes. The software used to create the graphs, obtain the estimators and verify the flexibility of the model, in terms of fit, was R, (R Core Team, 2013) through RStudio environment, (RStudio Team, 2020).

Regarding the estimation method, the maximum likelihood method was used to obtain the estimators for the parameters of each given model. Here, the CG method is considered for the first application and, for the second one, the SANN method was chosen. These choices were made because their respective results were more satisfactory, in terms of goodness of fit, when compared to those obtained using another method.

Most of the initial guesses were obtained through heuristic method by using the GenSA and MASS R packages. When the initial guesses from this method provided unsatisfactory results, or when there was a problem of convergence, the guesses were chosen randomly.

Furthermore, the statistics of Anderson Darling (A^*) and Cramer Von Mises (W^*) were used to verify the performance of the proposed models when compared to those mentioned above.

6.4.2 Maternal mortality

The first data set does refer to death of women at fertile age (10 to 49 years) divided by 1.000 in the five brazilian regions, along the years 2016 to 2020, summing up 25 observations. They represent maternal mortality and late maternal mortality and have its origins in Sistema de Informações sobre Mortalidade (SIM)- System of Information about Mortality-. The data

set is described below and is post in decreasing order, with the year, and according to the five brazilian regions, that is to say, counted with periodicity 5. The order of regions is as follows: North, Northeast, Southwest, South and Midwest, (WOMEN, 2020). The original data are:

6844, 21002, 31333, 9109, 5777, 5741, 17963, 27082, 8520, 4952, 5762, 17968, 26430, 8508, 5025, 5679, 18394, 26658, 8762, 4873, 5502, 18917, 28218, 9216, 5294.

The data, as seen in set above, leads to the following descriptive statistics (see Table 17). Note that the amplitude here is reasonably large, showing a sharp discrepancy among regions. The minimum refers to the number of deaths in the Midwest in 2017, while the maximum does the Southeast in 2020. Note, however, that both regions suffered a significant increasing in deaths of women, when one compares the years 2017 and 2020.

Table 17 – Descriptive statistics for the first data set.

Min.	1st Qu.	Median	Mean	3rd Qu.	Max.
4.873	5.741	8.762	13.341	18.917	31.333

The Table 18 shows the results of the parameters estimation process, through maximum likelihood. Additionally, it also show statistical results concerned by W^* and A^*. Note that the smallest values were obtained by the TMOBXII, followed by EXP-W.

Table 18 – Estimation results for the first data set

Model	$\hat{\alpha}$	$\hat{\theta}$	$\hat{\sigma}$	$\hat{\rho}$	$\hat{\kappa}$	W^*	A^*
TMOBXII	0.0020	0.9946	86.000	1.1000	0.0156	0.2118	1.3156
	(0.00008)	(0.0001)	(0.0002)	(0.0002)	(0.0001)		
W	-	-	12.0946	1.4248	-	0.2686	1.5645
	(-)	(-)	(1.7387)	(0.2361)	(-)		
EXP-W	91.4869	-	0.3667	0.1352	-	0.2416	1.4421
	(18.3693)	(-)	(0.0006)	(0.0012)	(-)		
KW-W	0.0478	1.0000	19.7906	30.7049	-	0.2816	1.6220
	(0.0120)	(0.2526)	(0.0030)	(0.0030)	(-)		
Gumbel	9.30108	6.3021	-	-	-	0.2812	1.6362
	(1.3199)	(1.0915)	(-)	(-)	(-)		
Logistic	12.3012	5.2949	-	-	-	0.3286	1.8891
	(1.9015)	(0.8643)	(-)	(-)	(-)		

6.5 RAYLEIGH-TAYLOR

A second application is addressed to time, when a Rayleigh-Taylor hydrodynamic system is allowed to evolve and a particular situation is studied: the time for the system to achieve a given state of turbulence. The Rayleigh-Taylor problem is briefly describe below. However, the Table 21, whose columns are the referred times, noise and noisy smooth length, for the simulation, one can study the series of times in order to gain statistical insight about the problem of evolution of turbulence.

6.5.1 A Few Notes on Turbulence

The word *turbulence*, from Late Latin *turbulentia* "trouble, disquiet". At not too late times, it is a reference to atmospheric eddies that affect airplanes, by 1918, (SCHMITT, 2017). Nowadays, in technical terms, it is referred to as an important branch of physics called Hydrodynamics, with interfaces on condensed matter physics and nonlinear dynamics, for example, (SAGDEEV D. A. USIKOV, 1992), (BENISTON, 1998). As direct references one includes negative temperatures, anomalous diffusion and the concept of power-law scaling in many-body problems. In general, the turbulence is related to no-unique solutions or that depend sensitively on initial conditions, leading to the problem of predictability and his study. With wide applications on Engineering, geophysics, biology, astrophysics, cosmology and, recently, on financial markets, (MANTEGNA ROSARIO N.; STANLEY, 1996), (FALKOVICH GREGORY; SREENIVASAN, 2006a), (UTHAMACUMARAN, 2020), (BARDINA; COAKLEY; MARVIN, 1992).

6.5.2 Waves and Instabilities: Rayleigh-Taylor

Before entering the Rayleigh-Taylor phenomenon, (RAYLEIGH; STRUTT, 2011), properly, some elements of the explanation for the roots of instability are provided. The common sense is allowed to believe that the intuitive knowledge of instability is just related to the concept of waves. But waves are a very general feature of fluids. Several types of waves occur in incompressible fluids, indeed, almost always taking place at surfaces. But not always. The presence of an interface between two dissimilar fluids allows vorticity to be generated across the surface layer, leading to wave propagation along the given interface. That one then forming a tangential discontinuity allowing only the normal component of the velocity to be continuous.

In some cases, the amplitude of the wave fades due to damping but, when this is not the case, it is possible for the amplitude of the wave to grow up exponentially. For more details on the theme, the reader is addressed to several good textbooks on hydrodynamics, with emphasis on statistical mechanics, such as (MONIN A. M. YAGLOM, 2007).

Backing to the interface phenomena consider two liquids exhibiting different values for their respective density. Under the influence of gravity a heavy fluid with density ρ_+ is supported by a lighter one, say, with ρ_-, leading to an unstable situation, known as *Rayleigh-Taylor* instability.

Figure 38 – . As the difference in density leads to instability, the heavier fluid interpenetrates the lighter one, as if the former was pushed by the later in a battle for occupying spaces.

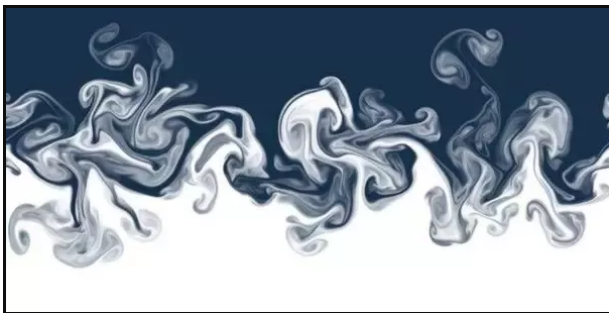

Fonte: Chiel van Heerwaarden. http://github.com/microhh

It is possible for the interfacial perturbations to be composed of one wavelength, say λ, or to be made of a spectrum, that is to say, comprised of a superposition of many waves. In the first case, the wavelength will grow exponentially with time before saturating to a constant terminal velocity, *at late time*. When the lighter fluid penetrates the heavy one, the phenomenon is called *bubbles* while the emerging *fingers* generated by the later is termed *spikes*.

When dealing with a spectrum of waves, the interaction of the resulting modes, with each other, is the cause of turbulent flow, who is characterized by a high degree of mixing between the fluids under analysis. For the simulation one is treating here, two fluids with different densities are concerned and with a specified initial condition such that, at $t = t_0$, the system undergoes a process in accordance with the Law of Nature. The Figure 39 below shows this condition. The process is modeled in stages. In first stage a small amplitude perturbation is observed, if compared to the initial wavelength of the process. By this hypothesis, the equations of motion can be linearized such that an exponential instability growth is deduced, as pointed out above. At early times, in the vicinity of $t = t_0$, the sinusoidal pattern, given by Figure 39,

Figure 39 – Initial condition for the Rayleigh-Taylor process physical simulation. The red as blue fluids are of different densities and are contained in a rectangular region.

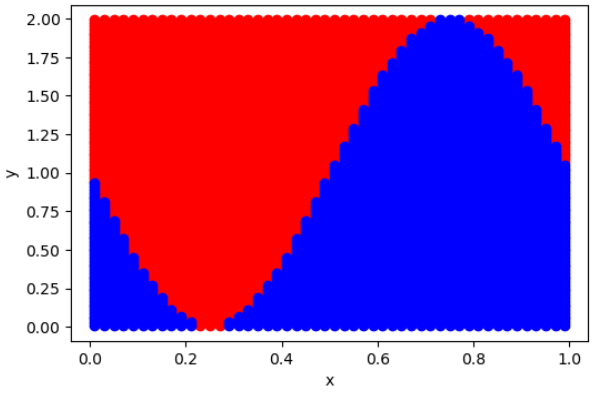

Source: the own author.

is preserved until the time that the system enters into another stage, when nonlinear effects come to light, leading to spikes and bubbles.

In a second stage, the structures of pattern that emerge can be modeled by equations describing buoyancy drag of the portions appearing in the mixing processes, leading to an approximately constant growth rate, in time.

6.5.3 Physical Simulation

In this section a brief description about the method and simulation process is presented, as well as the statistical procedure with the acquired data.

Back in the Section 4.7.5 from Chapter 4, the Figure 17 shows how particles enter into account in the process of suavization through smoothing length h. There, the general process keeps this function constant along the simulation. However, here, a random initial condition is established by allowing the aforementioned smoothing length to receive values according to uniformly distributed random numbers, $\epsilon(z)$, inside the interval $(0, 1)$, namely,

$$h(z; \eta_0) = 1 + \eta_0 \epsilon(z)|_{(0,1)}$$

where $\eta_0 = 1.2$.

The immediate consequence of this choice for the initial condition is the effect of, observed and expected, process of evolution of turbulence. This is of wide practical applications in control theory of engineering processes, (HIGH-SPEED..., 2019), (YIBO et al., 2022).

Some domain and reference values for the physical model is given in the Table 19, below.

Table 19 – Domain and reference values for the simulation process.

L_x	L_y	ρ_+	ρ_-	Re	t_s
1.0 m	2.0 m	1.8Kg/m^3	1.0 Kg/m^3	4200	100.0 s

where L_x, L_y stand for the simulated physical environment where the fluids evolve its dynamics, as seen at Figure 40; $\rho_\pm$ refer to heavier and lighter densities of involved fluids and, Re, is the nondimensional Reynolds number. The process lasts t_s time units. For each random initial condition on the smoothing length, the time for the computer simulation was about 3 to 5 hours, as was described in Table, 20.

Order	Time	Order	Time	Order	Time
1	11198.33	21	10627.03	41	10939.56
2	10251.22	22	12037.93	42	14444.74
3	13284.47	23	10226.31	43	11875.98
4	13284.47	24	13351.18	44	12467.77
5	13401.75	25	10969.26	45	13110.37
6	13117.33	26	13135.60	46	13221.97
7	10982.38	27	14857.80	47	15055.44
8	13899.09	28	11894.26	48	13254.20
9	11650.80	29	13189.25	49	15299.19
10	12041.82	30	11558.30	50	15102.00
11	10544.57	31	12665.61	51	14575.16
12	10219.57	32	12307.52	52	14378.32
13	9958.000	33	10662.70	53	9940.42
14	13501.97	34	10766.21	54	13611.19
15	13230.37	35	11555.70	55	12224.28
16	11658.38	36	14066.94	56	14128.68
17	13227.27	37	10300.74	57	9962.76
18	12473.52	38	13155.11	58	14597.73
19	10922.39	39	13869.11	59	15023.49
20	13505.65	40	10485.89	60	13185.11

Table 20 – Computer time for the simulation, since the beginning, for each random initial condition in the smoothing length, in seconds.

On generating the plots in Figure 40, the simulation was carried out by pysph python modulo with modified stochastic initial conditions.

At Table 22, the Min and Max times do refer to the minimum and maximum times that

Figure 40 – Snapshots of the Rayleigh-Taylor process as evolved in smoothed particle approach.

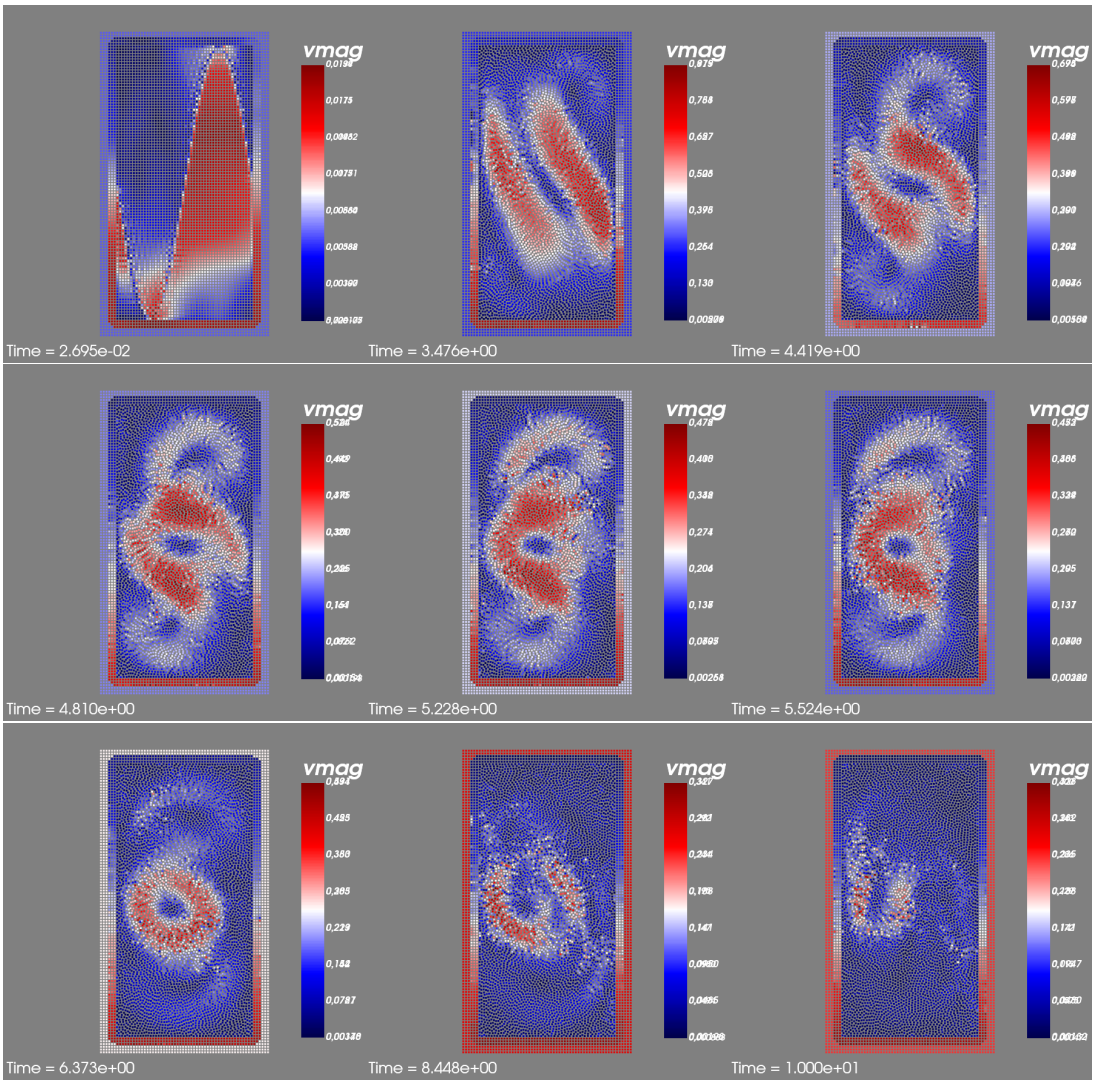

Source: the own author.

the system access a given state of turbulence. As is shown in the same table, the mean time is an important result in order to gain insight and propose models for controlling turbulence, if possible, or its effects.

The Table 23 shows the results for the parameter estimation in concern. Furthermore, the results exhibited by the statistics described reinforce the claim of satisfactory results.

Observation	Time	Noise	Noisy hdx	Observation	Time	Noise	Noisy hdx
1	9.99728	0.0446	1.0535	31	9.99201	0.1517	1.1820
2	9.98711	0.6569	1.7883	32	9.98598	0.1511	1.1813
3	9.98141	0.3124	1.3749	33	9.99501	0.3749	1.4499
4	9.98800	0.7463	1.8956	34	9.98260	0.8429	2.0115
5	9.99422	0.7226	1.8671	35	9.99362	0.0760	1.0912
6	9.98038	0.7259	1.8711	36	9.97962	0.7440	1.8928
7	9.98437	0.2688	1.3226	37	9.98241	0.8141	1.9769
8	9.98124	0.8261	1.9913	38	9.99802	0.1122	1.1346
9	9.99584	0.3860	1.4632	39	9.98891	0.2622	1.3146
10	9.99333	0.4291	1.5149	40	9.97624	0.9297	2.1156
11	9.99388	0.0110	1.0132	41	9.98472	0.4003	1.4804
12	9.98654	0.0061	1.0073	42	9.98940	0.5310	1.6372
13	9.99795	0.6303	1.7564	43	9.99627	0.6999	1.8399
14	9.99874	0.6489	1.7787	44	9.99574	0.6172	1.7406
15	9.99424	0.3597	1.4316	45	9.97441	0.9434	2.1321
16	9.99311	0.7126	1.8551	46	9.98390	0.5701	1.6841
17	9.98746	0.5860	1.7032	47	9.99007	0.9426	2.1311
18	9.99151	0.2435	1.2922	48	9.99145	0.9278	2.1134
19	9.99569	0.7410	1.8892	49	9.98014	0.9587	2.1504
20	9.98375	0.1923	1.2308	50	9.98695	0.8953	2.0744
21	9.99255	0.4697	1.5636	51	9.99472	0.0441	1.0529
22	9.98530	0.0739	1.0887	52	9.99358	0.6822	1.8186
23	9.99698	0.6297	1.7556	53	9.98304	0.4821	1.5785
24	9.98556	0.2390	1.2868	54	9.99199	0.8036	1.9643
25	9.99963	0.7289	1.8747	55	9.98986	0.0346	1.0415
26	9.97339	0.9866	2.1839	56	9.98392	0.8557	2.0268
27	9.99570	0.4371	1.5245	57	9.98385	0.9884	2.1861
28	9.99208	0.3811	1.4573	58	9.97660	0.9773	2.1728
29	9.99874	0.5295	1.6354	59	0.98705	0.6005	1.7206
30	9.99545	0.4786	1.5743	60	9.99519	0.7806	1.9367

Table 21 – The sequence of times to a given state of the system of Rayleigh-Taylor process with initial noise condition and corresponding noisy random smooth length.

Table 22 – Descriptive statistics for the Rayleigh-Taylor time data set.

Min.	1st Qu.	Median	Mean	3rd Qu.	Max.
9.97339	9.98392	9.98963	9.98898	9.99436	9.99963

Table 23 – Estimation results for the second data set

Model	$\hat{\alpha}$	$\hat{\theta}$	$\hat{\sigma}$	$\hat{\rho}$	$\hat{\kappa}$	W^*	A^*
TMOBXII	0.2995	316.7073	11.8366	32.7800	3.4107	0.1137	0.6944
	(0.0004)	(0.0135)	(0.0004)	(0.0004)	(0.0007)		
BXII	-	-	-	21.4266	0.0202	0.1170	0.7241
	(-)	(-)	(-)	(3.9633)	(0.0015)		
EXP-BXII	5273.4310	-	-	140.1278	269.5379	0.1171	0.7247
	(1020.5350)	(-)	(-)	(3.8121)	(0.0001)		
KW-BXII	2508.6100	2070.3900	-	9.1557	0.2744	0.1168	0.7221
	(0.0001)	(0.0016)	(-)	(0.0001)	(0.0001)		
B-BXII	39.6149	9.3204	-	6.3603	0.1155	0.1179	0.7310
	(<0.0001)	(<0.0001)	(-)	(1.3210)	(0.0132)		
B-W	205.8366	1037.3340	107.4710	-	10.1493	0.1183	0.7345
	(0.0014)	(1.8759)	(0.1216)	(-)	(0.0009)		
EXP-W	21.8136	-	484.7488	9.9633	-	0.1475	0.9673
	(4.0464)	(-)	(22.8358)	(<0.00001)	(-)		
KW-W	59.4386	146.0447	133.4699	9.9227	-	0.1170	0.7237
	(0× 1042)	(16.6398)	(13.0851)	(0.0067)	(-)		

6.6 CONCLUSIONS

In this chapter a new model, called Transformed Marshall-Olkin Burr-XII was developed and studied. Some inherent mathematical properties in the model were studied through the text. Furthermore, a simulation study was performed in order to confirm the asymptotic properties of the parameters of the model. Finally, two sets of real data were worked with the aim to show the performance of the proposed distribution. It was verified that the model at hand has shown higher performance when compared with others considered in both data set.

The first one gives the amount of women deaths at fertile age. It is a real data set and, as so, has important consequences in the attempts of implementing countermeasures in order to reduce these numbers. The second data set was obtained by simulating a physical system in such a way that the times of occurrence of a desired scenery, was reached. The importance of understanding processes like that had its importance discussed on the text.

7 GENERAL CONCLUSIONS AND FUTURE WORKS

7.1 METHODS

In this work a class of transformation was proposed in order to generate new probability distributions. Along the development, new techniques was provided to overcome the natural difficulties arising as the process develops. As was indicated in the text, inasmuch as proposition of new distributions increases, indeed do the complexity of functional relations describing them. Properties like moments calculation turns out to be hard or even resulting in divergence. Hence, even though the tools provided by computers and techniques of approximations, it is possible to one find results which is not satisfactory or even ill estimated, whatever the causes and, in reference to the latter, due to failing in express qualitative hypotheses in quantitative form, (GOOD, 2008).

A new method was presented that avoid the use of integrals for calculating moments, as was pointed out in Chapter 2. For example, the integral for the expected value of the $TMOE$ model, even for $\alpha = 1$, as given by Equation (3.11), is not as ease to calculate as its source baseline.

Instead of the traditional

$$\int_{\Omega} xf(x)dx,$$

where Ω stands for the domain under consideration, one can use $T\,(M_X \circ \mathcal{F})$, T the differential operator given by Equation (2.15). Of course, for $F, \mathcal{F}, \mathcal{G}, \cdots$, sufficiently smooth, differentiable, the task reduces to algebraic calculations. For the TMOE case, one obtains the table,

Model	Mean $(\alpha = 1.2)$	Var $(\alpha = 1.2)$	Mean $(\alpha = 1.0)$	Var $(\alpha = 1.0)$
Num_TMOE	0.2616	0.1838	0.2575	0.2257
MT_TMOE	0.2713	0.1529	0.2778	0.1543
fgm_TMOE	-	-	0.1875	0.2500

The scheme above illustrates, for the TMOE model, the results for mean and variance through the methods developed and applied along the text. As was emphasized there, as long as the mathematical expressions increase in its forms, so do the complexity of solving them and express simple results derived from them. One source of this behavior is the use of integrals

which, in the generality, are not even solvable. This must be understood in the sense that, if one could put all functions into a bag and select one from within, the probability of it being analytically integrable, or even numerically integrable, is indeed short. Our propose suggest a process that is not integral-directed, instead, algebraic inspired. The resources required being differentiation of algebraic continuous and differentiable functions. The formal mathematics are under construction and must be worked hardly for generalizations. As one can see in the scheme above, the results differ according to the methods used, but are better related with the increasing of the value of the parameter α. A correcting expression is on the way in order to better correct theses values. Basically, it is given by,

$$\tilde{f}_{corr} = \left(\frac{c+d}{a+b}\right) \frac{\det(M) G^{\alpha}(x;\boldsymbol{\xi},\boldsymbol{\tau})}{\det(M) + G^{\alpha}(x;\boldsymbol{\xi},\boldsymbol{\tau})\left[1 - G(x;\boldsymbol{\xi},\boldsymbol{\tau})\right]^{\alpha}}$$

where $\det(M)$ is the determinant of M, given at Chapter 2. The final expression, then, reads,

$$M \circ \mathcal{F}(x) = \tilde{f}_{corr} F(x,\boldsymbol{\xi},\boldsymbol{\tau}).$$

On the table, above, the trace $-$ refers to lack of result following the approach of analytical integration due to the complexity of the integrand. This, however, does not imply absence of this kind of solution.

7.2 SIMULATIONS

The parameters of the worked distributions was estimated by means of the *maximum likelihood* method. In this sense, x_i, $i = 1, \cdots, n$, was a random n-sample size of the TMO-model distribution, with vector parameters $(\boldsymbol{\xi},\boldsymbol{\tau})$, as explained in Chapter 3. There, the log-likelihood function, as seen at Equation 3.17, lead to the calculation of the score vector by means of the Equation 3.18. These, together with the Hessian 3.20, was the ingredients for the process of estimation.

As was emphasized along the text some simulations was performed in order to verify the asymptotic character of the estimators. The finite sample performance of the MLEs is assessed for the given distributions appearing along the text.

The processes was done by varying the true parameters and the samples size, n, at hand, as well as by employing a Monte Carlo simulation with a 1000 replications. The procedure was performed in order to quantify some asymptotic properties of the MLEs for the model parameters. In these realizations the R software was used.

7.3 APPLICATIONS

Once the distributions has been set, some applications- general and physical ones-, was performed in order to gain insight of the underlying processes while described by those:

1. Epidemiology. Data related to COVID-19 cases;
2. Hydrodynamics. Data of Taylor-Green process, for a given approach, leading to instability in the numerical solutions;
3. Astrophysics. Sunspots;
4. Women death at fertile age;
5. Hydrodynamics. Rayleigh-Taylor process.

At (1), as was depicted in Chapter 4, some data was collected doing reference to the number of cases, at a given day, of COVID-19 incidence in the whole State of Santa Catarina. The idea, among others, was to gain insight of the virus spreading while considering the proposed models as well as the potential influences driving the diffusion among the population. Features like mean temperature, humidity, population density, was enquired as forces increasing the diffusibility, among others. As can be seen at Figure 20, the number of cases correlates with population density, as one expect. However, a stronger correlation was expected once the spreading of virus is intuitively proportional to the number of entities , in this case, the number of individuals porting it, contained in a given compartment, better saying, region, State, Municipality. These measure results, we believe, is so in virtue of the choice of data acquisition, i.e., the snapshot of a day, performed for the data analysis. As a future work, it is possible to include, besides a wide range of data taken with intervals as instantaneously as it can be produced, for a wider period of time, an approach of dynamic probabilistic systems. (HOWARD, 1971), in which is constructed a master equation, (BREUER, 2002), from the best model developed, among the ones above. On this approach it is possible to include fields in order to measure the effectiveness of mask mandates as well as social distancing, for example.

At (3), the sunspots data are used in Chapter 5 as source in the application for the model developed there. As a developing work, some probabilities are being calculated in order to forecast some scenarios involving the Earth magnetic field as well as the consequences of interactions of that with the ejecting coronal mass coming from the sun in its maximal

activity. The importance of the application was briefly discussed in the referred chapter, as well as consequences for the environment in general. It is worth of saying that the data under analysis are disposed under CC BY-NC 4.0 licence terms, which can be accessed at <https://www.sidc.be/silso/infossntotmonthly>, whose data police is managed by (SILSO data/image, Royal Observatory of Belgium, Brussels) such that images and data can be freely downloaded as public data.

Additionally is under construction, for the near future, an application following (5.5.1), and considering the data as seen at Table 24, below. taking into account the Sun-Earth system,

Month	Max sunspot
11	264.3
8	171.7
1	116.7
7	130.7
3	76.2
6	44.5
10	39.5
11	28.3
4	120.5
9	128.7
8	126
5	178.7

Table 24 – Sample for maximum sunspots dataset. Similar to what was done above and referred in the same sources over there considered.

as well as the interaction with the magnetic field anomalies that are being observed recently, as one can verify, for example, at (HARTMANN; PACCA, 2009), (PAVÓN-CARRASCO; SANTIS, 2016), (AMIT et al., 2021), (MARTUCCI et al., 2022). The idea is to select the models proposed on the thesis to promote forecasts and produce results for decision-making, when appropriate.

At (5), the second hydrodynamic applications, the emphasis was given to time to state of turbulence. This knowledge is very important in science and technology and, specially, in new developments and control of hypersonic flights objects, be them air-air or hybrid, water-air, air-water systems. As the world enters in age of hypersonic dynamics, the stability of the underlying processes depends on the sensitive knowledge of that phenomenon. Through *Control Theory*, a branch of engineering, the enquire of the time to turbulence, in a given process, is crucial for the stability of the initial condition in the interface of both media, during

the evolution of motion. As the number of entities, better saying, particles is sufficiently high, the better the statistical description is, the best will be the results concerning control.

REFERENCES

AFIFY, A. Z.; AL-MOFLEH, H.; DEY, S. Topp–leone odd log-logistic exponential distribution: Its improved estimators and applications. *Anais da Academia Brasileira de Ciências*, SciELO Brasil, v. 93, 2021.

AFIFY, A. Z.; GEMEAY, A. M.; IBRAHIM, N. A. The heavy-tailed exponential distribution: Risk measures, estimation, and application to actuarial data. *Mathematics*, v. 8, n. 8, 2020. ISSN 2227-7390. Disponível em: <https://www.mdpi.com/2227-7390/8/8/1276>.

AFIFY, A. Z.; MEAD, M. On five-parameter burr xii distribution: properties and applications. *South African Statistical Journal*, South African Statistical Association (SASA), v. 51, n. 1, p. 67–80, 2017.

AL-KADIM, K. A.; MAHDI, A. A. Exponentiated transmuted exponential distribution. *Journal of University of Babylon for Pure and Applied Sciences*, v. 26, n. 2, p. 78–90, 2018.

ALJARRAH, M. A.; LEE, C.; FAMOYE, F. On generating t-x family of distributions using quantile functions. *Journal of Statistical Distributions and Applications vol. 1 iss. 1*, v. 1, jun 2014.

ALMAZAH, M.; ULLAH, K.; HUSSAM, E.; HOSSAIN, M.; ALDALLAL, R.; RIAD, F. H. et al. New statistical approaches for modeling the covid-19 data set: A case study in the medical sector. *Complexity*, Hindawi, v. 2022, 2022.

ALZAATREH CARL LEE, F. F. A. A new method for generating families of continuous distributions. *METRON vol. 71 iss. 1*, v. 71, apr 2013.

AMIT, H.; TERRA-NOVA, F.; LÉZIN, M.; TRINDADE, R. I. Non-monotonic growth and motion of the south atlantic anomaly. *Earth, Planets and Space*, SpringerOpen, v. 73, n. 1, p. 1–10, 2021.

ANACONDA Software Distribution. Anaconda Inc., 2022. Disponível em: <https://docs.anaconda.com/>.

Are you up for the TrackML challenge? (Ed.). *Can machine learning assist high-energy physics in discovering and characterising new particles?* 2018. Disponível em: <https://home.cern/news/news/knowledge-sharing/are-you-trackml-challenge>.

ARMSTRONG, M. A. *Groups and symmetry*. [S.l.]: Springer, 1988. (Undergraduate Texts in Mathematics). ISBN 0387966757; 9780387966755.

BALAKRISHNAN N.; KUNDU, D. Birnbaum-Saunders distribution: A review of models, analysis, and applications. *Applied Stochastic Models in Business and Industry vol. 35 iss. 1*, v. 35, jul 2018.

BARDINA, J.; COAKLEY, T.; MARVIN, J. [american institute of aeronautics and astronautics 4th symposium on multidisciplinary analysis and optimization - cleveland,oh,u.s.a. (21 september 1992 - 23 september 1992)] 4th symposium on multidisciplinary analysis and optimization - two-equation turbulence modeling for 3-d hypersonic flows. American Institute of Aeronautics and Astronautics, sep 1992.

BECK, C. Recent developments in superstatistics. *Brazilian Journal of Physics*, v. 39,2A, Sept 2009. Disponível em: <https://doi.org/10.1590/S0103-97332009000400003>.

BEL GOLAN; ASHKENAZY, Y. The relationship between the statistics of open ocean currents and the temporal correlations of the wind stress. *New Journal of Physics 2013-may 15 vol. 15 iss. 5*, v. 15, may 2013.

BENISTON, M. *From turbulence to climate: numerical investigations of the atmosphere with a hierarchy of models*. [S.l.]: Springer Science & Business Media, 1998.

BHATI, D.; MALIK, M. A.; VAMAN, H. J. Lindley–exponential distribution: properties and applications. *METRON 2015-feb 06 vol. 73 iss. 3*, v. 73, feb 2015.

BILLINGSLEY, P. *Probability and measure*. 3rd ed. ed. [S.l.]: Wiley, 1995. (Wiley series in probability and mathematical statistics). ISBN 9780471007104.

BIRNBAUM, Z. W.; SAUNDERS, S. C. A new family of life distributions. *Journal of Applied Probability vol. 6 iss. 2*, v. 6, aug 1969.

BLASS, A.; GUREVICH, Y. Negative probabilities: What they are and what they are for. *arXiv preprint arXiv:2009.10552*, 2020.

BOUVIER, N. P. N. M. Environmental factors affecting the transmission of respiratory viruses. *Current Opinion in Virology 2012-feb vol. 2 iss. 1*, v. 2, feb 2012.

BREUER, F. P. H.-P. *The theory of open quantum systems*. [S.l.]: Oxford University Press, 2002. ISBN 0198520638; 9780198520634.

BREZIS, H. *Functional Analysis, Sobolev Spaces and Partial Differential Equations*. 1. ed. [S.l.]: Springer-Verlag New York, 2010. (Universitext). ISBN 0387709134,978-0-387-70913-0.

CARTIER, P. E.; JULIA, B.; MOUSSA, P.; VANHOVE, P. *Frontiers in number theory, physics, and geometry II*. 1. ed. [S.l.]: Springer, 2007. ISBN 3540303073; 9783540303077; 9783540303084; 3540303081.

CHALLENGE, T. P. T. (Ed.). *High Energy Physics particle tracking in CERN detectors*. 2018. Disponível em: <https://www.kaggle.com/competitions/trackml-particle-identification>.

COHEN, C. B. E. Superstatistics. *Physica A: Statistical Mechanics and its Applications vol. 322 iss. none*, v. 322, may 2003.

CORDEIRO, G. M.; LIMA, M. D. C. S.; CYSNEIROS, A. H.; PASCOA, M. A. R.; PESCIM, R. R.; ORTEGA, E. M. M. An extended birnbaum–saunders distribution: Theory, estimation, and applications. *Communication in Statistics- Theory and Methods 2016-mar 30 vol. 45 iss. 8*, v. 45, mar 2016.

CORDEIRO, G. M.; LIMA, M. D. C. S. D.; ORTEGA, E. M. M.; SUZUKI, A. K. A new extended birnbaum–saunders model: Properties, regression and applications. *Stats*, v. 1, n. 1, p. 32–47, 2018. ISSN 2571-905X. Disponível em: <https://www.mdpi.com/2571-905X/1/1/4>.

CORDEIRO, G. M.; ORTEGA, E. M.; CUNHA, D. C. da. The exponentiated generalized class of distributions. *Journal of data science*, v. 11, n. 1, p. 1–27, 2013.

CORDEIRO GAUSS M.; DE CASTRO, M. A new family of generalized distributions. *Journal of Statistical Computation and Simulation 2011-jul vol. 81 iss. 7*, v. 81, jul 2011.

COXETER, H. S. *The Lorentz group and the group of homographies*. [S.l.]: na, 1967.

COZMAN, F. G. Sets of probability distributions, independence, and convexity. *Synthese*, Springer, v. 186, n. 2, p. 577–600, 2012. ISSN 00397857, 15730964. Disponível em: <http://www.jstor.org/stable/41494902>.

DASH, S.; NANDI, B. K.; SETT, P. Multiplicity distributions in e^+e^- collisions using weibull distribution. *Phys. Rev. D*, American Physical Society, v. 94, p. 074044, Oct 2016. Disponível em: <https://link.aps.org/doi/10.1103/PhysRevD.94.074044>.

DAVIES, K. *Ionospheric radio Propagation*. [S.l.]: National Bureau of Standards Monograph 80, 1961. ISBN 64-60061.

DAVIES, P. J. B. R. *De Havilland Comet. The Worlds First Jet Airliner*. [S.l.]: Paladwr Press, 1999. ISBN 1888962143; 9781888962147.

DAVIS, D. J. An analysis of some failure data. *Journal of the American Statistical Association*, American Statistical Association, v. 47, p. 113–150, 1952. ISSN 0162-1459,1537-274X. Disponível em: <http://doi.org/10.2307/2280740>.

DEMING, W. E. *Statistical adjustment of data*. 1. ed. [S.l.]: Dover, 1964.

DEUTSCH, D. *The fabric of reality: the science of parallel universes– and its implications*. 1. ed. [S.l.]: Allen Lane, 1997. (Allen Lane Science). ISBN 9780713990614; 0713990619.

DEVI, R. Application of survival analysis model on drug addiction dataset. *International Journal of computer science trends and technology*, v. 3, 05 2015.

DRAGULESCU A.; YAKOVENKO, V. Evidence for the exponential distribution of income in the USA. *The European Physical Journal B- Condensed Matter and Complex Systems.*, v. 20, n. 4, 2001.

DUCHESNE, J.; COUBARD, O. A. First-wave covid-19 daily cases obey gamma law. *Infectious Disease Modelling*, Elsevier, v. 7, n. 2, p. 64–74, 2022.

ELBATAL, I. A new lifetime family of distributions: Theoretical developments and analysis of covid 19 data. *Results in Physics*, Elsevier, v. 31, p. 104979, 2021.

EUGENE, N.; LEE, C.; FAMOYE, F. Beta-normal distribution and its applications. *Communications in Statistics - Theory and Methods*, Taylor Francis, v. 31, n. 4, p. 497–512, 2002. Disponível em: <https://doi.org/10.1081/STA-120003130>.

FALKOVICH GREGORY; SREENIVASAN, K. R. Averaging operators in turbulence. *Physics Today vol. 59 iss. 11*, v. 59, nov 2006.

FALKOVICH GREGORY; SREENIVASAN, K. R. Lessons from hydrodynamic turbulence. *Physics Today 2006-apr vol. 59 iss. 4*, v. 59, apr 2006.

FERMI, E.; PASTA, P.; ULAM, S.; TSINGOU, M. *Studies of the nonlinear problems*. [S.l.], 1955.

FIKHTENGOL'TS, G. *Functional Series, by G.M. Fichtenholz. Translated and Freely Adapted by Richard A. Silverman*. [S.l.: s.n.], 1970. (Gordon and Breach, Science Publishers).

FRANCO, C. M. R.; DUTRA, R. F. Sir model for propagation of covid-19 in the paraíba's state (brazil). *INTERMATHS*, v. 2, n. 2, p. 39–48, 2021.

FRANK, S. A. The common patterns of nature. *Journal of Evolutionary Biology vol. 22 iss. 8*, v. 22, jul 2009.

FRÉCHET, M. Sur la loi de probabilité de l'écart maximum. *Ann. Soc. Math. Polon.*, v. 6, p. 93–116, 1927.

GAO, F.; HE, X. Survival analysis: Theory and application in finance. *Handbook of Financial Econometrics, Mathematics, Statistics, and Machine Learning*, 2020. Disponível em: <https://www.worldscientific.com/doi/abs/10.1142/9789811202391_0120>.

GEMEAY, A. M.; HALIM, Z.; EL-RAOUF, M. M. A.; HUSSAM, E.; ABDULRAHMAN, A. T.; MASHAQBAH, N. K.; ALSHAMMARI, N.; MAKUMI, N. General two-parameter distribution: Statistical properties, estimation, and application on covid-19. *PLOS ONE*, Public Library of Science, v. 18, n. 2, p. 1–20, 02 2023. Disponível em: <https://doi.org/10.1371/journal.pone.0281474>.

GOOD, J. W. H. P. I. *Common Errors in Statistics [and how to avoid them]*. 2nd. ed. [S.l.]: Wiley-Interscience, 2008. ISBN 9780470388105; 0470388102.

GOVAERTS M. NORBERT HOUNKONNOU, A. Z. M. J. *Contemporary Problems in Mathematical Physics*. [S.l.]: World Scientific Publishing Company, 2006. ISBN 9789812568533; 9812568530.

GUPTA, R. C.; GUPTA, P. L.; GUPTA, R. D. Modeling failure time data by Lehman alternatives. *Communications in Statistics - Theory and Methods*, Taylor Francis, v. 27, n. 4, p. 887–904, 1998. Disponível em: <https://doi.org/10.1080/03610929808832134>.

GZYL, H. Integration of the linear filtering problem by means of canonical transformations. *Systems Control Letters vol. 3 iss. 4*, v. 3, sep 1983.

HALLINAN, A. J. A review of the Weibull distribution. *Journal of Quality Technology vol. 25 iss. 2*, v. 25, apr 1993.

HARTMANN, G. A.; PACCA, I. G. Time evolution of the south atlantic magnetic anomaly. *Anais da Academia Brasileira de Ciências*, SciELO Brasil, v. 81, p. 243–255, 2009.

HAWRYLUK, I. M. T. A. H. H. M. S. S. R. P. W. C. Z. H. G. A. D. C. A. F. S. B. S. Inference of covid-19 epidemiological distributions from brazilian hospital data. *Journal of The Royal Society Interface 2020-nov 25 vol. 17 iss. 172*, v. 17, nov 2020.

HAYS, W. L.; WINKLER, R. L. *Statistics: Probability, Inference and Decision*. 1. ed. [S.l.]: Holt, Rinehart and Winston, Inc., 1970. (International Series in Decision Processes). ISBN 03-084429-0.

HIGH-SPEED experiments enhance hypersonic missile design by predicting sources of turbulence. 2019. Disponível em: <https://www.militaryaerospace.com/computers/article/16711550/highspeed-experiments-enhance-hypersonic-missile-design-by-predicting-sources-of-turbulence>.

HOWARD, R. A. *Dynamic Probabilistic Systems Volume 1 & 2*. 1. ed. [S.l.]: John Wiley & Sons Inc, 1971. ISBN 9780486458700.

HUNTSVILLE., U. of Alabama in. Transformations of random variables. *https://stats.libretexts.org/@go/page/10147*, 2021.

JAIN, S.; PODLADCHIKOVA, T.; VERONIG, A. M.; SUTYRINA, O.; DUMBOVIĆ, M.; CLETTE, F.; PÖTZI, W. *Predicting the solar cycle amplitude with the new catalogue of hemispheric sunspot numbers*. [S.l.], 2022.

JIZBA, P.; KLEINERT, H. Superpositions of probability distributions. *Physical review. E, Statistical, nonlinear, and soft matter physics*, v. 78, p. 031122, 10 2008.

JOLLIFFE, I. *Principal Component Analysis*. 2nd ed.. ed. Springer, 2010. (Springer Series in Statistics). ISBN 9781441929990; 1441929991. Disponível em: <libgen.li/file.php?md5=81f9d1d3248d78026b68f27c2107f162>.

KIMMOUN, O. e. a. Modulation instability and phase-shifted Fermi-Pasta-Ulam recurrence. *Scientific Reports vol. 6 iss. 1*, v. 6, jul 2016.

KLEINBAUM, M. K. a. D. G. Survival analysis: A self-learning text. *Statistics for Biology and Health*, Springer New York, 2005.

KONSUK, H.; AKTAS, S. Estimating the recurrence periods of earthquake data in turkey. Scientific Research Publishing, 2013.

KOTZ, S. N. S. The beta exponential distribution. *Reliability Engineering System Safety 2006-jun vol. 91 iss. 6*, v. 91, jun 2006.

KOUKOULOPOULOS, D. *The Distribution of Prime Numbers*. [S.l.]: American Mathematical Society, 2020. (Graduate Studies in Mathematics 203). ISBN 1470447541; 9781470447540.

KUMAR, N.; QI, S. ang; KUAN, L.-H.; SUN, W.; ZHANG, J.; GREINER, R. Learning accurate personalized survival models for predicting hospital discharge and mortality of covid-19 patients. *Scientific Reports*, v. 12, 2022.

KUNDU, R. D. G. D. Exponentiated exponential family: An alternative to gamma and Weibull distributions. *Biometrical Journal vol. 43 iss. 1*, v. 43, feb 2001.

LAI, C.-D. *Generalized Weibull Distributions*. 1. ed. [S.l.]: Springer, 2014. (SpringerBriefs in Statistics). ISBN 9783642391057; 3642391052; 9783642391064; 3642391060.

LANJONI, B. R. *O modelo Burr XII geométrico: propriedades e aplicações*. Tese (Doutorado) — Master's Dissertation, Escola Superior de Agricultura Luiz de Queiroz . . . , 2013.

LEHMANN, J. P. R. E. *Testing Statistical Hypotheses (Springer Texts in Statistics)*. 3rd. ed. [S.l.]: Springer, 2005. ISBN 0387988645; 9780387988641.

LEIVA, V. *The Birnbaum-Saunders Distribution*. 1. ed. [S.l.]: Elsevier, Academic Press, 2016. ISBN 0128037695; 9780128037690; 9780128038277; 0128038276.

LIMA, M. do C. S.; PRATAVIERA, F.; ORTEGA, E. M. M.; CORDEIRO, G. M. The odd log-logistic geometric family with applications in regression models with varying dispersion. *Journal of Statistical Theory and Applications*, v. 18, p. 278–294, 2019. ISSN 2214-1766. Disponível em: <https://doi.org/10.2991/jsta.d.190818.003>.

LIU, M. B. L. G. R. *Smoothed particle hydrodynamics: a meshfree particle method*. World Scientific Publishing Company, 2003. ISBN 9789812384560; 9812384561. Disponível em: <libgen.li/file.php?md5=ff1cbf3440b33e27308b1d2c889e3e35>.

LIU, W.-C.; LIU, H.-M. Integrating monte carlo and the hydrodynamic model for predicting extreme water levels in river systems. Preprints, 2018.

LORENZ, E. N. Deterministic nonperiodic flow. *Journal of Atmospheric Sciences*, American Meteorological Society, Boston MA, USA, v. 20, n. 2, p. 130 – 141, 1963. Disponível em: <https://journals.ametsoc.org/view/journals/atsc/20/2/1520-0469_1963_020_0130_dnf_2_0_co_2.xml>.

MANTEGNA ROSARIO N.; STANLEY, H. E. Turbulence and financial markets. *Nature 1996-oct vol. 383 iss. 6601*, v. 383, oct 1996.

MARSHALL, A. W.; OLKIN, I. A new method for adding a parameter to a family of distributions with application to the exponential and Weibull families. *Biometrika*, Oxford University Press, v. 84, n. 3, p. 641–652, 1997.

MARTUCCI, M.; BARTOCCI, S.; BATTISTON, R.; CAMPANA, D.; CARFORA, L.; CONTI, L.; CONTIN, A.; DONATO, C. D.; SANTIS, C. D.; FOLLEGA, F. M. et al. New results on protons inside the south atlantic anomaly, at energies between 40–250 mev in the period 2018-2020, from the cses-01 satellite mission. *Physical Review D*, APS, v. 105, n. 6, p. 062001, 2022.

MAZUCHELI, J.; OLIVEIRA, R. P.; PERALTA, D.; EMANUELLI, I. P. Application of discrete burr xii distribution in the analysis of animal production data. *Ciência e Natura*, v. 40, p. e25, Mar. 2018. Disponível em: <https://periodicos.ufsm.br/cienciaenatura/article/view/28307>.

MCCONNELL, A. J. *Applications of tensor analysis*. [S.l.]: Dover Publications, 1957. ISBN 0486603733.

MCINTOSH; W., S.; CHAPMAN, S.; LEAMON, R. J.; EGELAND, R.; WATKINS, N. W. Overlapping magnetic activity cycles and the sunspot number: Forecasting sunspot cycle 25 amplitude. *Solar Physics 2020-nov 24 vol. 295 iss. 12*, v. 295, nov 2020.

MITTELSTAEDT, P. A. W. P. *Laws of Nature.* 2005.

MOEIN, S.; NICKAEEN, N.; ROOINTAN, A.; BORHANI, N.; HEIDARY, Z.; JAVANMARD, S. H.; GHAISARI, J.; GHEISARI, Y. Inefficiency of sir models in forecasting covid-19 epidemic: a case study of isfahan. *Scientific reports*, Nature Publishing Group UK London, v. 11, n. 1, p. 4725, 2021.

MOHAN RAKHI; CHACKO, M. Estimation of parameters of kumaraswamy-exponential distribution based on adaptive type-ii progressive censored schemes. *Journal of Statistical Computation and Simulation 2020-sep 01 vol. 91 iss. 1*, v. 91, sep 2020.

MONIN A. M. YAGLOM, J. L. L. A. S. *Statistical Fluid Mechanics: Mechanics of Turbulence, Vols. 1 and 2*. First english ed. [S.l.]: Dover, 2007. ISBN 0486458830; 978-0486458830; 0486458911, 978-0486458915.

MUDHOLKAR, G. S.; SRIVASTAVA, D. K.; FREIMER, M. The exponentiated weibull family: A reanalysis of the bus-motor-failure data. *Technometrics vol. 37 iss. 4*, v. 37, nov 1995.

MURPHY, K. P. *Probabilistic Machine Learning: An Introduction*. Illustrated. [S.l.]: The MIT Press, 2021.

NADARAJAH, G. M. C. E. M. O. S. The kumaraswamy weibull distribution with application to failure data. *Journal of the Franklin Institute 2010-oct vol. 347 iss. 8*, v. 347, oct 2010.

NADARAJAH, S. The exponentiated exponential distribution: a survey. *AStA Advances in Statistical Analysis 2011-feb 11 vol. 95 iss. 3*, v. 95, feb 2011.

NADARAJAH, S.; JAYAKUMAR, K.; RISTIć, M. M. A new family of lifetime models. *Journal of Statistical Computation and Simulation*, Taylor Francis, v. 83, n. 8, p. 1389–1404, 2013. Disponível em: <https://doi.org/10.1080/00949655.2012.660488>.

NAIR, N. U.; SANKARAN, P.; BALAKRISHNAN, N. Chapter 5 - bathtub distributions. In: NAIR, N. U.; SANKARAN, P.; BALAKRISHNAN, N. (Ed.). *Reliability Modelling and Analysis in Discrete Time*. Boston: Academic Press, 2018. p. 247–279. ISBN 978-0-12-801913-9. Disponível em: <https://www.sciencedirect.com/science/article/pii/B9780128019139000051>.

NAUDTS, J. The q-exponential family in statistical physics. *Journal of Physics: Conference Series*, IOP Publishing, v. 201, p. 012003, feb 2010. Disponível em: <https://doi.org/10.1088/1742-6596/201/1/012003>.

NEKOUKHOU, V.; BIDRAM, H.; ROOZEGAR, R. The beta-weibull distribution on the lattice of integers. *Ciência e Natura*, v. 39, n. 1, p. 40–58, 2017.

NEUENSCHWANDER, D. E. *Emmy Noether's Wonderful Theorem*. First. [S.l.]: Johns Hopkins U. P., 2011. ISBN 9780801896934; 0801896932; 9780801896941; 0801896940.

NOCEDAL, S. W. J. *Numerical Optimization*. 2nd ed. ed. [S.l.]: Springer, 2006. (Springer series in operations research). ISBN 9780387303031; 0387303030.

NOETHER, E. Invariant variation problems. *Transport Theory and Statistical Physics vol. 1 iss. 3*, v. 1, jan 1971.

OLIVEIRA, F. G.; ANDRADE, A. F. de; VIEIRA, J. W.; OLIVEIRA, A. C. de; FILHO, J. d. M. L.; LIMA, F. R. Aplicacao da distribuicao Burr xii para construcao de ossos trabeculares sinteticos por metodo monte carlo parametrico. *Proceeding Series of the Brazilian Society of Computational and Applied Mathematics*, v. 5, n. 1, 2017.

OSBORNE, J. Notes on the use of data transformations. *Practical assessment, research and evaluation*, v. 9, n. 1, p. 42–50, 2005.

OWOLOKO, E. A.; OGUNTUNDE, P. E.; ADEJUMO, A. O. Performance rating of the transmuted exponential distribution: an analytical approach. *SpringerPlus 2015-dec 24 vol. 4 iss. 1*, v. 4, dec 2015.

PARANAÍBA, P. F.; ORTEGA, E. M.; CORDEIRO, G. M.; PESCIM, R. R. The beta burr xii distribution with application to lifetime data. *Computational statistics & data analysis*, Elsevier, v. 55, n. 2, p. 1118–1136, 2011.

PARANJPE, S.; RAJARSHI, M. Modelling non-monotonic survivorship data with bathtub distributions. *Ecology*, JSTOR, v. 67, n. 6, p. 1693–1695, 1986.

PARZEN, E. Nonparametric statistical data modeling. *Journal of the American Statistical Association vol. 74 iss. 365*, v. 74, mar 1979.

PAVÓN-CARRASCO, F. J.; SANTIS, A. D. The south atlantic anomaly: The key for a possible geomagnetic reversal. *Frontiers in Earth Science*, Frontiers Media SA, v. 4, p. 40, 2016.

PENG, X.; YU, P.; CHEN, G.; XIA, M.; ZHANG, Y. Development of a coupled dda–sph method and its application to dynamic simulation of landslides involving solid–fluid interaction. *Rock Mechanics and Rock Engineering 2019-jul 09 vol. 53 iss. 1*, v. 53, jul 2019. Disponível em: <https://doi.org/10.1007/s00603-019-01900-x>.

PERALTA, D.; MAZUCHELI, J.; EMANUELLI, I. P.; ROSSI, R. M. AplicaÇÃo da distribuiÇÃo burr xii na anÁlise do tempo atÉ a primeira postura de codornas. *Brazilian Journal of Biometrics*, v. 35, n. 1, p. 1–16, Mar. 2017. Disponível em: <https://biometria.ufla.br/index.php/BBJ/article/view/291>.

QIAN, L. The Fisher information matrix for a three-parameter exponentiated Weibull distribution under type ii censoring. *Statistical Methodology vol. 9 iss. 3*, v. 9, may 2012.

R Core Team. *R: A Language and Environment for Statistical Computing*. Vienna, Austria, 2013. Disponível em: <http://www.R-project.org/>.

R Core Team. *R: A Language and Environment for Statistical Computing*. Vienna, Austria, 2020. Disponível em: <https://www.R-project.org/>.

R., M. J. A. *Foundations of Mechanics*. 2 revised, enlarged, and reset. ed. [S.l.: s.n.], 1987.

RADICE, M. Diffusion processes with gamma-distributed resetting and non-instantaneous returns. *Journal of Physics A: Mathematical and Theoretical*, IOP Publishing, v. 55, n. 22, p. 224002, 2022.

RAMACHANDRAN, P.; BHOSALE, A.; PURI, K.; NEGI, P.; MUTA, A.; DINESH, A.; MENON, D.; GOVIND, R.; SANKA, S.; SEBASTIAN, A. S.; SEN, A.; KAUSHIK, R.; KUMAR, A.; KURAPATI, V.; PATIL, M.; TAVKER, D.; PANDEY, P.; KAUSHIK, C.; DUTT, A.; AGARWAL, A. PySPH: A Python-based Framework for Smoothed Particle Hydrodynamics. *ACM Transactions on Mathematical Software*, v. 47, n. 4, p. 1–38, dez. 2021. ISSN 0098-3500, 1557-7295.

RAMACHANDRAN, P.; PURI, K. Entropically damped artificial compressibility for sph. *Computers Fluids*, v. 179, p. 579–594, 2019. ISSN 0045-7930. Disponível em: <https://www.sciencedirect.com/science/article/pii/S0045793018309046>.

RAYBAUT, P. Spyder-documentation. *Available online at: pythonhosted. org*, 2009.

RAYLEIGH; STRUTT, J. W. *Investigation of the Character of the Equilibrium of an Incompressible Heavy Fluid of Variable Density*. Zenodo, 2011. Disponível em: <https://doi.org/10.1017/cbo9780511703973.023>.

REIS, L. D. R.; CORDEIRO, G. M.; LIMA, M. d. C. S. The stacy-g class: A new family of distributions with regression modeling and applications to survival real data. *Stats*, v. 5, n. 1, p. 215–257, 2022. ISSN 2571-905X. Disponível em: <https://www.mdpi.com/2571-905X/5/1/15>.

REYES, J.; ARRUé, J.; LEIVA, V.; MARTIN-BARREIRO, C. A new birnbaum–saunders distribution and its mathematical features applied to bimodal real-world data from environment and medicine. *Mathematics*, v. 9, n. 16, 2021. ISSN 2227-7390. Disponível em: <https://www.mdpi.com/2227-7390/9/16/1891>.

RICHARD, S. A. M. R. D. *Estadística Biométrica y Sanitaria*. 1. ed. [S.l.]: Prentice Hall International, 1974. ISBN 0-13-289298-7.

ROHATGI, P. K.; ROHATGI, K.; BOWONDER, B. *Technological Forecasting*. 1. ed. [S.l.]: TATA McGraw-Hill- New Delhi, 1979.

ROHATGI, V. K. *Statistical Inference*. [S.l.]: Dover Publications, 2003. (Dover Books on Mathematics). ISBN 0486428125; 9780486428123.

ROSIN P. ;RAMMLER, E. Die kornzusammensetzung des mahlgutes im lichte der wahrscheinlichkeitslehre. *Kolloid Zeitschrift vol. 67 iss. 1*, v. 67, apr 1934.

ROSSUM, G. V.; DRAKE, F. L. *Python 3 Reference Manual*. Scotts Valley, CA: CreateSpace, 2009. ISBN 1441412697.

RStudio Team. *RStudio: Integrated Development Environment for R*. Boston, MA, 2020. Disponível em: <http://www.rstudio.com/>.

RUBIO, F.; STEEL, M. On the Marshall–Olkin transformation as a skewing mechanism. *Computational Statistics Data Analysis*, v. 56, n. 7, p. 2251–2257, 2012. ISSN 0167-9473. Disponível em: <https://www.sciencedirect.com/science/article/pii/S0167947312000059>.

S. PRETTNER K., K. M. e. a. C. Climate and the spread of covid-19. *Sci Rep.*, v. 11, April 2021. Disponível em: <https://rdcu.be/cQu9c>.

SAGDEEV D. A. USIKOV, G. M. Z. R. Z. *Nonlinear Physics. From pendulum to turbulence and chaos*. [S.l.]: Harwood Academic Publishes, 1992. ISBN 3718648296.

SAMPATH, S.; LALITHA, S. Economic reliability test plan under hybrid exponential distribution. *International Journal of Computational and Theoretical Statistics*, University of Bahrain, v. 3, n. 01, 2016.

SAULO, H.; LEãO, J.; BOURGUIGNON, M. The kumaraswamy birnbaum–saunders distribution. *Journal of Statistical Theory and Practice*, Taylor Francis, v. 6, n. 4, p. 745–759, 2012. Disponível em: <https://doi.org/10.1080/15598608.2012.719814>.

SAúDE SC. 2021. Disponível em: <https://saude.sc.gov.br/index.php/noticias-geral/todas-as-noticias/1652-noticias-2020/11925>.

SCHMITT, F. G. Turbulence from 1870 to 1920: The birth of a noun and of a concept. *Comptes Rendus Mécanique 2017-sep vol. 345 iss. 9*, v. 345, sep 2017. Disponível em: <libgen.li/file.php?md5=0a592ed5b46bfd0a940a5b3ee95ad3c7>.

SHEN, M. B. Y. Z. Y. Gradient boosting survival tree with applications in credit scoring. *arxiv*, April 2021. Disponível em: <https://arxiv.org/pdf/1908.03385.pdf>.

SILVA, R. V. da; ANDRADE, T. A. de; MACIEL, D. B.; CAMPOS, R. P.; CORDEIRO, G. M. A new lifetime model: The gamma extended fréchet distribution. *J. Stat. Theory Appl.*, v. 12, n. 1, p. 39–54, 2013.

SINGH, R.; MUKHOPADHYAY, K. Survival analysis in clinical trials: Basics and must know areas. *Perspectives in Clinical Research*, v. 2, n. 4, p. 145–148, 2011.

SOLAR Flare. 2022. Disponível em: <https://blogs.nasa.gov/solarcycle25/2022/10/03/sun-releases-strong-solar-flare-2/#:~:text=The20Sun20emitted20a20strong,an20image20of20the20event.&text=Solar20flares20are20powerful20bursts20of20energy.>

SPENCE, W. *An Essay on the Theory of the Various Orders of Logarithmic Transcendents: With an Inquiry Into Their Applications to the Integral Calculus and the Summation of Series*. John Murray and Archibald Constable and Company, 1809. Disponível em: <https://books.google.com.br/books?id=o0xDAQAAMAAJ>.

SUNSPOT and Solar Storms. 2022. Disponível em: <http://hyperphysics.phy-astr.gsu.edu/hbase/Solar/sunspot.html>.

SUNSPOT Number. 2022. Disponível em: <https://www.sidc.be/silso/datafiles>.

SáNCHEZ, E. Some physical features of the burr type-xii distribution. *Physical Review E*, v. 99, 01 2019.

TSAI, T.-R.; LIO, Y.; XIN, H.; PHAM, H. Parameter estimation for composite dynamical systems based on sequential order statistics from burr type xii mixture distribution. *Mathematics*, v. 9, n. 8, 2021. ISSN 2227-7390. Disponível em: <https://www.mdpi.com/2227-7390/9/8/810>.

UTHAMACUMARAN, A. Cancer: A turbulence problem. *Neoplasia 2020-dec vol. 22 iss. 12*, v. 22, dec 2020.

VASSILOPOULOS, A.; KELLER, T. Statistical analysis of fatigue data. *Eng Mater Process*, 07 2011.

VESILIND, P. The rosin-rammler particle size distribution. *Resource Recovery and Conservation vol. 5 iss. 3*, v. 5, sep 1980.

WEINBERG C. N. YANG, E. G. E. S. *The Oskar Klein memorial lectures Volume 1*. [S.l.]: World Scientific, 1991. ISBN 9810203527.

WESTRöM, D. J. S. D. M. Canonical transformations in quantum mechanics. *Annalen der Physik vol. 481 iss. 1*, v. 481, 1971.

WHEELER, J. D. B. F. J. T. J. A. *The Anthropic Cosmological Principle*. First. [S.l.]: Oxford University Press, 1986. ISBN 0198519494; 9780198519492.

WOMEN. 2020. Disponível em: <http://tabnet.datasus.gov.br/cgi/tabcgi.exe?sim/cnv/mat10uf.def>.

YIBO, D.; XIAOKUI, Y.; GUANGSHAN, C.; JIASHUN, S. Review of control and guidance technology on hypersonic vehicle. *Chinese Journal of Aeronautics*, Elsevier, v. 35, n. 7, p. 1–18, 2022.

ZANG, C.; CUI, P.; ZHU, W.; WANG, F. Dynamical origins of distribution functions. Association for Computing Machinery, New York, NY, USA, p. 469–478, 2019. Disponível em: <https://doi.org/10.1145/3292500.3330842>.

ZOGRAFOS K.; BALAKRISHNAN, N. On families of beta- and generalized gamma-generated distributions and associated inference. *Statistical Methodology 2009-jul vol. 6 iss. 4*, v. 6, jul 2009.

APPENDIX A – HESSIAN FOR THE TMOE MODEL

Let $\Theta_{x\lambda} = 1 - \mathrm{e}^{-\lambda x_i}$. One reads,

$$\begin{aligned}\frac{\partial^2 l_{exp}(x_i;\boldsymbol{\xi};\boldsymbol{\tau})}{\partial\alpha^2} &= -\frac{n}{\alpha^2} - 2\lambda^2\theta\sum_{i=1}^{n}\frac{x_i^2\mathrm{e}^{-\alpha\lambda x_i}}{\Theta_{x\lambda}^{\alpha}+\theta\mathrm{e}^{-\alpha\lambda x_i}} \\ &- 2\sum_{i=1}^{n}\frac{\Theta_{x\lambda}^{\alpha}\log\Theta_{x\lambda}^{2}}{\Theta_{x\lambda}^{\alpha}+\theta\mathrm{e}^{-\alpha\lambda x_i}} \\ &+ 2\sum_{i=1}^{n}\frac{\left[\lambda\theta x_i\mathrm{e}^{-\alpha\lambda x_i}-\Theta_{x\lambda}^{\alpha}\log\Theta_{x\lambda}\right]\left[\Theta_{x\lambda}^{\alpha}\log\Theta_{x\lambda}-\lambda\theta x_i\mathrm{e}^{-\alpha\lambda x_i}\right]}{\left\{\Theta_{x\lambda}^{\alpha}+\theta\mathrm{e}^{-\alpha\lambda x_i}\right\}^2},\end{aligned}$$

$$\frac{\partial^2 l_{exp}(x_i;\boldsymbol{\xi};\boldsymbol{\tau})}{\partial\theta^2} = -\frac{n}{\theta^2} + 2\sum_{i=1}^{n}\frac{\mathrm{e}^{-2\alpha\lambda x_i}}{\left\{\Theta_{x\lambda}^{\alpha}+\theta\mathrm{e}^{-\alpha\lambda x_i}\right\}^2}$$

,

$$\begin{aligned}\frac{\partial^2 l_{exp}(x_i;\boldsymbol{\xi};\boldsymbol{\tau})}{\partial\lambda^2} &= -\frac{n}{\lambda^2} - (\alpha-1)\sum_{i=1}^{n}\frac{x_i^2\mathrm{e}^{-\lambda x_1}}{\Theta_{x\lambda}} - (\alpha-1)\sum_{i=1}^{n}\frac{x_i^2\mathrm{e}^{-2\lambda x_i}}{\Theta_{x\lambda}^2} \\ &- 2\alpha^2\theta\sum_{i=1}^{n}\frac{x_i^2\mathrm{e}^{-\alpha\lambda x_i}}{\Theta_{x\lambda}^{\alpha}+\theta\mathrm{e}^{-\alpha\lambda x_i}} - 2\alpha^2\sum_{i=1}^{n}\frac{x_i^2\Theta_{x\lambda}^{\alpha-2}\mathrm{e}^{-2\lambda x_i}}{\Theta_{x\lambda}^{\alpha}+\theta\mathrm{e}^{-\alpha\lambda x_i}} \\ &+ 2\alpha\sum_{i=1}^{n}\frac{x_i^2\Theta_{x\lambda}^{\alpha-1}\mathrm{e}^{-\lambda x_i}}{\Theta_{x\lambda}^{\alpha}+\theta\mathrm{e}^{-\alpha\lambda x_i}} + 2\alpha\sum_{i=1}^{n}\frac{x_i^2\Theta_{x\lambda}^{\alpha-2}\mathrm{e}^{-2\lambda x_i}}{\Theta_{x\lambda}^{\alpha}+\theta\mathrm{e}^{-\alpha\lambda x_i}} \\ &- 2\alpha\sum_{i=1}^{n}\frac{\left[x_i\Theta_{x\lambda}^{\alpha-1}\mathrm{e}^{-\lambda x_i}-\theta x_i\mathrm{e}^{-\alpha\lambda x_i}\right]\left[\theta x_i\mathrm{e}^{-\alpha\lambda x_i}-x_i\Theta_{x\lambda}^{\alpha-1}\mathrm{e}^{-\lambda x_i}\right]}{\left\{\Theta_{x\lambda}^{\alpha}+\theta\mathrm{e}^{-\alpha\lambda x_i}\right\}^2}\end{aligned}$$

,

$$\begin{aligned}\frac{\partial^2 l_{exp}(x_i,\boldsymbol{\xi};\boldsymbol{\tau})}{\partial\alpha\partial\lambda} &= -\sum_{x_i}^{n}x_i + \sum_{i=1}^{n}\frac{x_i\mathrm{e}^{-\lambda x_i}}{\Theta_{x\lambda}} - 2\sum_{i=1}^{n}\frac{x_i\mathrm{e}^{-\lambda x_i}\Theta_{x\lambda}^{\alpha-1}}{\Theta_{x\lambda}^{\alpha}+\theta\mathrm{e}^{-\alpha\lambda x_i}} \\ &- 2\alpha\lambda\theta\sum_{i=1}^{n}\frac{x_i^2\mathrm{e}^{-\alpha\lambda x_i}}{\Theta_{x\lambda}^{\alpha}+\theta\mathrm{e}^{-\alpha\lambda x_i}} + 2\theta\sum_{i=1}^{n}\frac{x_i\mathrm{e}^{-\alpha\lambda x_i}}{\Theta_{x\lambda}^{\alpha}+\theta\mathrm{e}^{-\alpha\lambda x_i}} \\ &- 2\sum_{i=1}^{n}\frac{\left[\alpha x_i\mathrm{e}^{-\lambda x_i}\Theta_{x\lambda}^{\alpha-1}-\alpha\theta x_i\mathrm{e}^{-\alpha\lambda x_i}\right]\left[\lambda\theta x_i\mathrm{e}^{-\alpha\lambda x_i}-\Theta_{x\lambda}^{\alpha}\log\Theta_{x\lambda}\right]}{\left\{\Theta_{x\lambda}^{\alpha}+\theta\mathrm{e}^{-\alpha\lambda x_i}\right\}^2} \\ &- 2\alpha\sum_{i=1}^{n}\frac{x_i\mathrm{e}^{-\lambda x_i}\Theta_{x\lambda}^{\alpha-1}\log\Theta_{x\lambda}}{\Theta_{x\lambda}^{\alpha}+\theta\mathrm{e}^{-\alpha\lambda x_i}} = \frac{\partial^2 l_{exp}(x_i,\boldsymbol{\xi};\boldsymbol{\tau})}{\partial\lambda\partial\alpha},\end{aligned}$$

$$\begin{aligned}\frac{\partial^2 \mathrm{l}_{exp}(x_i,\boldsymbol{\xi};\boldsymbol{\tau})}{\partial\alpha\partial\theta} &= 2\lambda\sum_{i=1}^{n}\frac{x_i\mathrm{e}^{-\alpha\lambda x_i}}{\Theta_{x\lambda}^{\alpha}+\theta\mathrm{e}^{-\alpha\lambda x_i}} - 2\lambda\theta\sum_{i=1}^{n}\frac{x_i\mathrm{e}^{-2\alpha\lambda x_i}}{\left\{\Theta_{x\lambda}^{\alpha}+\theta\mathrm{e}^{-\alpha\lambda x_i}\right\}^2} \\ &+ 2\sum_{i=1}^{n}\frac{\Theta_{x\lambda}\mathrm{e}^{-\alpha\lambda x_i}\log\Theta_{x\lambda}}{\left\{\Theta_{x\lambda}^{\alpha}+\theta\mathrm{e}^{-\alpha\lambda x_i}\right\}^2} = \frac{\partial^2 l_{exp}(x_i,\boldsymbol{\xi};\boldsymbol{\tau})}{\partial\theta\partial\alpha}\end{aligned}$$

$$\begin{aligned}\frac{\partial^2 l_{exp}(x_i,\boldsymbol{\xi};\boldsymbol{\tau})}{\partial\lambda\partial\theta} &= -2\alpha\sum_{i=1}^{n}\frac{x_i \mathrm{e}^{-\alpha\lambda x_i}}{\Theta_{x\lambda}^{\alpha}+\theta\mathrm{e}^{-\alpha\lambda x_i}} - 2\alpha\theta\sum_{i=1}^{n}\frac{x_i \mathrm{e}^{-2\alpha\lambda x_i}}{\left\{\Theta_{x\lambda}^{\alpha}+\theta\mathrm{e}^{-\alpha\lambda x_i}\right\}^2} \\ &+ 2\alpha\sum_{i=1}^{n}\frac{x_i \mathrm{e}^{-\lambda x_i}\Theta_{x\lambda}^{\alpha-1}\mathrm{e}^{-\alpha\lambda x_i}}{\left\{\Theta_{x\lambda}^{\alpha}+\theta\mathrm{e}^{-\alpha\lambda x_i}\right\}^2} = \frac{\partial^2 l_{exp}(x_i,\boldsymbol{\xi};\boldsymbol{\tau})}{\partial\theta\partial\lambda}.\end{aligned}$$

APPENDIX B – HESSIAN FOR THE TMOW MODEL

Let $\Phi_{xab} = 1 - \mathrm{e}^{-\left(\frac{x_i}{b}\right)^a}$. So, one has

$$
\begin{aligned}
\frac{\partial^2 l_w\left(x;\boldsymbol{\xi};\boldsymbol{\tau}\right)}{\partial\alpha^2} &= -\frac{n}{\alpha^2} - 2\theta\sum_{i=1}^{n}\frac{\left(\frac{x_i}{b}\right)^{2a}\mathrm{e}^{-\alpha\left(\frac{x_i}{b}\right)^a}}{\Phi_{xab}^{\alpha}+\theta\mathrm{e}^{-\alpha\left(\frac{x_i}{b}\right)^a}} \\
&- 2\sum_{i=1}^{n}\frac{\Phi_{xab}^{\alpha}\log\Phi_{xab}^{2}}{\Phi_{xab}^{\alpha}+\theta\mathrm{e}^{-\alpha\left(\frac{x_i}{b}\right)^a}} \\
&- 2\left\{\sum_{i=1}^{n}\frac{\Phi_{xab}^{\alpha}\log\Phi_{xab}-\theta\left(\frac{x_i}{b}\right)^a\mathrm{e}^{-\alpha\left(\frac{x_i}{b}\right)^a}}{\Phi_{xab}^{\alpha}+\theta\mathrm{e}^{-\alpha\left(\frac{x_i}{b}\right)^a}}\right\} \\
&\times \left\{\sum_{i=1}^{n}\frac{\theta\left(\frac{x_i}{b}\right)^a\mathrm{e}^{-\alpha\left(\frac{x_i}{b}\right)^a}-\Phi_{xab}^{\alpha}\log\Phi_{xab}}{\Phi_{xab}^{\alpha}+\theta\mathrm{e}^{-\alpha\left(\frac{x_i}{b}\right)^a}}\right\}, \\
\frac{\partial^2 l_w\left(x;\boldsymbol{\xi};\boldsymbol{\tau}\right)}{\partial\theta^2} &= -\frac{n}{\theta^2} + 2\sum_{i=1}^{n}\frac{\mathrm{e}^{-2\alpha\left(\frac{x_i}{b}\right)^a}}{\left[\Phi_{xab}^{\alpha}+\theta\mathrm{e}^{-\alpha\left(\frac{x_i}{b}\right)}\right]^2}, \\
\frac{\partial^2 l_w\left(x;\boldsymbol{\xi};\boldsymbol{\tau}\right)}{\partial a^2} &= -\frac{n}{a^2} - \alpha\sum_{i=1}^{n}\left(\frac{x_i}{b}\right)^a\log\left(\frac{x_i}{b}\right)^2 - (\alpha-1)\sum_{i=1}^{n}\frac{\left(\frac{x_i}{b}\right)^{2a}\mathrm{e}^{-\left(\frac{x_i}{b}\right)^a}\log\left(\frac{x_i}{b}\right)^2}{\Phi_{xab}} \\
&- (\alpha-1)\sum_{i=1}^{n}\frac{\left(\frac{x_i}{b}\right)^{2a}\mathrm{e}^{-2\left(\frac{x_i}{b}\right)^a}\log\left(\frac{x_i}{b}\right)^2}{\Phi_{xab}^2} + (\alpha-1)\sum_{i=1}^{n}\frac{\left(\frac{x_i}{b}\right)^{a}\mathrm{e}^{-\left(\frac{x_i}{b}\right)^a}\log\left(\frac{x_i}{b}\right)^2}{\Phi_{xab}} \\
&- 2\alpha^2\sum_{i=1}^{n}\frac{\left(\frac{x_i}{b}\right)^{2a}\mathrm{e}^{-2\left(\frac{x_i}{b}\right)^a}\log\left(\frac{x_i}{b}\right)^2\Phi_{xab}^{\alpha-2}}{\Phi_{xab}^{\alpha}+\theta\mathrm{e}^{-\alpha\left(\frac{x_i}{b}\right)^a}} \\
&- 2\alpha^2\theta\sum_{i=1}^{n}\frac{\left(\frac{x_i}{b}\right)^{2a}\mathrm{e}^{-\alpha\left(\frac{x_i}{b}\right)^a}\log\left(\frac{x_i}{b}\right)^2}{\Phi_{xab}^{\alpha}+\theta\mathrm{e}^{-\alpha\left(\frac{x_i}{b}\right)^a}} \\
&+ 2\alpha\sum_{i=1}^{n}\frac{\left(\frac{x_i}{b}\right)^{2a}\mathrm{e}^{-\left(\frac{x_i}{b}\right)^a}\log\left(\frac{x_i}{b}\right)^2\Phi_{xab}^{\alpha-1}}{\Phi_{xab}^{\alpha}+\theta\mathrm{e}^{-\alpha\left(\frac{x_i}{b}\right)^a}} \\
&+ 2\alpha\sum_{i=1}^{n}\frac{\left(\frac{x_i}{b}\right)^{2a}\mathrm{e}^{-2\left(\frac{x_i}{b}\right)^a}\log\left(\frac{x_i}{b}\right)^2\Phi_{xab}^{\alpha-2}}{\Phi_{xab}^{\alpha}+\theta\mathrm{e}^{-\alpha\left(\frac{x_i}{b}\right)^a}} \\
&+ 2\alpha\theta\sum_{i=1}^{n}\frac{\left(\frac{x_i}{b}\right)^{a}\mathrm{e}^{-\alpha\left(\frac{x_i}{b}\right)^a}\log\left(\frac{x_i}{b}\right)^2}{\Phi_{xab}^{\alpha}+\theta\mathrm{e}^{-\alpha\left(\frac{x_i}{b}\right)^a}} \\
&- 2\alpha\sum_{i=1}^{n}\frac{\left(\frac{x_i}{b}\right)^{a}\mathrm{e}^{-\left(\frac{x_i}{b}\right)^a}\log\left(\frac{x_i}{b}\right)^2\Phi_{xab}^{\alpha-1}}{\Phi_{xab}^{\alpha}+\theta\mathrm{e}^{-\alpha\left(\frac{x_i}{b}\right)^a}} \\
&+ 2\alpha^2\sum_{i=1}^{n}\frac{\Theta_1^2(\alpha,a,b)-\Theta_2^2(\alpha,a,b)}{\left\{\Phi_{xab}^{\alpha}+\theta\mathrm{e}^{-\alpha\left(\frac{x_i}{b}\right)^a}\right\}^2},
\end{aligned}
$$

$$
\begin{aligned}
\frac{\partial l_w^2(x;\boldsymbol{\xi};\boldsymbol{\tau})}{\partial b^2} &= \frac{na}{b^2} - \frac{a^2\alpha}{b^2}\sum_{i=1}^{n}\left(\frac{x_i}{b}\right)^a - \frac{a^2(\alpha-1)}{b^2}\sum_{i=1}^{n}\frac{\left(\frac{x_i}{b}\right)^a \mathrm{e}^{-\left(\frac{x_i}{b}\right)^a}}{\Phi_{xab}} - \frac{a(\alpha-1)}{b^2}\sum_{i=1}^{n}\left(\frac{x_i}{b}\right)^a \\
&+ \frac{a(\alpha-1)}{b^2}\sum_{i=1}^{n}\frac{\left(\frac{x_i}{b}\right)^a \mathrm{e}^{-\left(\frac{x_i}{b}\right)^a}}{\Phi_{xab}} + \frac{2a^2\alpha}{b^2}\sum_{i=1}^{n}\left(\frac{x_i}{b}\right)^{2a}\Phi_{xab}^{\alpha-1}\mathrm{e}^{-\left(\frac{x_i}{b}\right)^a} \\
&- \frac{a^2(\alpha-1)}{b^2}\sum_{i=1}^{n}\frac{\left(\frac{x_i}{b}\right)^{2a}\mathrm{e}^{-\alpha\left(\frac{x_i}{b}\right)^a}}{\Phi_{xab}^2} - \frac{a\alpha}{b^2}\sum_{i=1}^{n}\left(\frac{x_i}{b}\right)^a \\
&+ \frac{a^2(\alpha-1)}{b^2}\sum_{i=1}^{n}\frac{\left(\frac{x_i}{b}\right)^a \mathrm{e}^{-\left(\frac{x_i}{b}\right)^a}}{\Phi_{xab}} - \frac{2a^2\alpha^2\theta}{b^2}\sum_{i=1}^{n}\frac{\left(\frac{x_i}{b}\right)^{2a}\mathrm{e}^{-\alpha\left(\frac{x_i}{b}\right)^a}}{\Phi_{xab}^{\alpha}+\theta\mathrm{e}^{-\alpha\left(\frac{x_i}{b}\right)^a}} \\
&+ \frac{2a^2\alpha\theta}{b^2}\sum_{i=1}^{n}\frac{\left(\frac{x_i}{b}\right)^a \mathrm{e}^{-\alpha\left(\frac{x_i}{b}\right)^a}}{\Phi_{xab}^{\alpha}+\theta\mathrm{e}^{-\alpha\left(\frac{x_i}{b}\right)^a}} - \frac{2a^2\alpha}{b^2}\sum_{i=1}^{n}\frac{\left(\frac{x_i}{b}\right)^a \mathrm{e}^{-\left(\frac{x_i}{b}\right)^a}\Phi_{xab}^{\alpha-1}}{\Phi_{xab}^{\alpha}+\theta\mathrm{e}^{-\alpha\left(\frac{x_i}{b}\right)^a}} \\
&- \frac{2a^2\alpha^2}{b^2}\sum_{i=1}^{n}\frac{\left(\frac{x_i}{b}\right)^{2a}\mathrm{e}^{-2\left(\frac{x_i}{b}\right)^a}\Phi_{xab}^{\alpha-2}}{\Phi_{xab}^{\alpha}+\theta\mathrm{e}^{-\alpha\left(\frac{x_i}{b}\right)^a}} + \frac{2a\alpha\theta}{b^2}\sum_{i=1}^{n}\frac{\left(\frac{x_i}{b}\right)^a \mathrm{e}^{-\alpha\left(\frac{x_i}{b}\right)^a}}{\Phi_{xab}^{\alpha}+\theta\mathrm{e}^{-\alpha\left(\frac{x_i}{b}\right)^a}} \\
&+ \frac{2a^2\alpha^2}{b^2}\sum_{i=1}^{n}\frac{(\Theta_1-\Theta_2)^2}{\left\{\Phi_{xab}^{\alpha}+\theta\mathrm{e}^{-\alpha\left(\frac{x_i}{b}\right)^a}\right\}^2\log^2\left(\frac{x_i}{b}\right)} \\
&- \frac{2a\alpha}{b^2}\sum_{i=1}^{n}\frac{\left(\frac{x_i}{b}\right)^a \mathrm{e}^{-\left(\frac{x_i}{b}\right)^a}\Phi_{xab}^{\alpha-1}}{\Phi_{xab}^{\alpha}+\theta\mathrm{e}^{-\alpha\left(\frac{x_i}{b}\right)^a}} + \frac{2a^2\alpha}{b^2}\sum_{i=1}^{n}\frac{\left(\frac{x_i}{b}\right)^{2a}\mathrm{e}^{-2\left(\frac{x_i}{b}\right)^a}\Phi_{xab}^{\alpha-2}}{\Phi_{xab}^{\alpha}+\theta\mathrm{e}^{-\alpha\left(\frac{x_i}{b}\right)^a}}
\end{aligned}
$$

where

$$
\begin{aligned}
\Theta_1^2(\alpha,a,b) &= \theta\sum_{i=1}^{n}\left(\frac{x_i}{b}\right)^a \mathrm{e}^{-\left(\frac{x_i}{b}\right)^a}\log\left(\frac{x_i}{b}\right) \\
\Theta_2^2(\alpha,a,b) &= \sum_{i=1}^{n}\left(\frac{x_i}{b}\right)^a \mathrm{e}^{-\left(\frac{x_i}{b}\right)^a}\Phi_{xab}^{\alpha-1}\log\left(\frac{x_i}{b}\right)
\end{aligned}
$$

$$
\begin{aligned}
\frac{\partial^2 l_w\left(x;\boldsymbol{\xi};\boldsymbol{\tau}\right)}{\partial\theta\partial\alpha} &= 2\sum_{i=1}^{n}\frac{\left(\frac{x_i}{b}\right)^a \mathrm{e}^{-\alpha\left(\frac{x_i}{b}\right)^a}}{\Phi_{xab}^{\alpha}+\theta\mathrm{e}^{-\alpha\left(\frac{x_i}{b}\right)^a}} \\
&- 2\theta\sum_{i=1}^{n}\frac{\left(\frac{x_i}{b}\right)^a \mathrm{e}^{-2\alpha\left(\frac{x_i}{b}\right)^a}}{\left[\Phi_{xab}^{\alpha}+\theta\mathrm{e}^{-\alpha\left(\frac{x_i}{b}\right)^a}\right]^2} \\
&+ 2\sum_{i=1}^{n}\frac{\Phi_{xab}^{\alpha}\mathrm{e}^{-\alpha\left(\frac{x_i}{b}\right)^a}\log\Phi_{xab}}{\left[\Phi_{xab}^{\alpha}+\theta\mathrm{e}^{-\alpha\left(\frac{x_i}{b}\right)^a}\right]^2} = \frac{\partial^2 l_w\left(x;\boldsymbol{\xi};\boldsymbol{\tau}\right)}{\partial\alpha\partial\theta},
\end{aligned}
$$

$$
\begin{aligned}
\frac{\partial^2 l_w\left(x_i;\boldsymbol{\xi};\boldsymbol{\tau}\right)}{\partial\alpha\partial a} &= -\sum_{i=1}^{n}\left(\frac{x_i}{b}\right)^a\log\left(\frac{x_i}{b}\right)+\sum_{i=1}^{n}\frac{\left(\frac{x_i}{b}\right)^a \mathrm{e}^{-\left(\frac{x_i}{b}\right)^a}\log\left(\frac{x_i}{b}\right)}{\Phi_{xab}} \\
&- 2\alpha\theta\sum_{i=1}^{n}\frac{\left(\frac{x_i}{b}\right)^{2a} \mathrm{e}^{-\alpha\left(\frac{x_i}{b}\right)^a}\log\left(\frac{x_i}{b}\right)}{\Phi_{xab}^{\alpha}+\theta\mathrm{e}^{-\alpha\left(\frac{x_i}{b}\right)^a}} - 2\theta\sum_{i=1}^{n}\frac{\left(\frac{x_i}{b}\right)^a \mathrm{e}^{-\alpha\left(\frac{x_i}{b}\right)^a}\log\left(\frac{x_i}{b}\right)}{\Phi_{xab}^{\alpha}+\theta\mathrm{e}^{-\alpha\left(\frac{x_i}{b}\right)^a}} \\
&+ 2\alpha\sum_{i=1}^{n}\frac{\left(\frac{x_i}{b}\right)^a \Phi_{xab}^{\alpha-1}\mathrm{e}^{-\left(\frac{x_i}{b}\right)^a}\log\left(\frac{x_i}{b}\right)\log\Phi_{xab}}{\Phi_{xab}^{\alpha}+\theta\mathrm{e}^{-\alpha\left(\frac{x_i}{b}\right)^a}} \\
&+ 2\sum_{i=1}^{n}\frac{\left(\frac{x_i}{b}\right)^a \Phi_{xab}^{\alpha-1}\mathrm{e}^{-\left(\frac{x_i}{b}\right)^a}\log\left(\frac{x_i}{b}\right)}{\Phi_{xab}^{\alpha}+\theta\mathrm{e}^{-\alpha\left(\frac{x_i}{b}\right)^a}} \\
&- 2\alpha\left\{\sum_{i=1}^{n}\frac{\theta\left(\frac{x_i}{b}\right)^a \mathrm{e}^{-\alpha\left(\frac{x_i}{b}\right)^a}-\Phi_{xab}^{\alpha}\log\Phi_{xab}}{\Phi_{xab}^{\alpha}+\theta\mathrm{e}^{-\alpha\left(\frac{x_i}{b}\right)^a}}\right\} \\
&\times \left\{\sum_{i=1}^{n}\frac{\left(\frac{x_i}{b}\right)^a \Phi_{xab}^{\alpha-1}\mathrm{e}^{-\left(\frac{x_i}{b}\right)^a}\log\left(\frac{x_i}{b}\right)^a-\theta\left(\frac{x_i}{b}\right)^a \mathrm{e}^{-\alpha\left(\frac{x_i}{b}\right)^a}\log\left(\frac{x_i}{b}\right)}{\Phi_{xab}^{\alpha}+\theta\mathrm{e}^{-\alpha\left(\frac{x_i}{b}\right)^a}}\right\} \\
&= \frac{\partial^2 l_w\left(x_i;\boldsymbol{\xi};\boldsymbol{\tau}\right)}{\partial a\partial\alpha},
\end{aligned}
$$

$$
\begin{aligned}
\frac{\partial^2 l_w\left(x_i;\boldsymbol{\xi};\boldsymbol{\tau}\right)}{\partial\alpha\partial b} &= \frac{a}{b}\sum_{i=1}^{n}\left(\frac{x_i}{b}\right)^a - \frac{a}{b}\sum_{i=1}^{n}\frac{\left(\frac{x_i}{b}\right)^a \mathrm{e}^{-\left(\frac{x_i}{b}\right)^a}}{\Phi_{xab}} - \frac{2a\theta}{b}\sum_{i=1}^{n}\frac{\left(\frac{x_i}{b}\right)^a \mathrm{e}^{-\alpha\left(\frac{x_i}{b}\right)^a}}{\Phi_{xab}^{\alpha}+\theta\mathrm{e}^{-\alpha\left(\frac{x_i}{b}\right)^b}} \\
&+ \frac{2a\alpha\theta}{b}\sum_{i=1}^{n}\frac{\left(\frac{x_i}{b}\right)^{2a}\mathrm{e}^{-\alpha\left(\frac{x_i}{b}\right)^a}}{\Phi_{xab}^{\alpha}+\theta\mathrm{e}^{-\alpha\left(\frac{x_i}{b}\right)^a}} \\
&+ \frac{2a\alpha}{b}\sum_{i=1}^{n}\frac{\mathrm{e}^{-\left(\frac{x_i}{b}\right)^a}\Phi_{xab}^{\alpha-1}\log\Phi_{xab}}{\Phi_{xab}^{\alpha}+\theta\mathrm{e}^{-\alpha\left(\frac{x_i}{b}\right)^a}} \\
&+ \frac{2a}{b}\sum_{i=1}^{n}\frac{\left(\frac{x_i}{b}\right)^a\mathrm{e}^{-\left(\frac{x_i}{b}\right)^a}\Phi_{xab}^{\alpha-1}}{\Phi_{xab}^{\alpha}+\theta\mathrm{e}^{-\alpha\left(\frac{x_i}{b}\right)^a}} \\
&- \frac{2\alpha a}{b}\left\{\sum_{i=1}^{n}\frac{\theta\left(\frac{x_i}{b}\right)^a\mathrm{e}^{-\alpha\left(\frac{x_i}{b}\right)^a}-\Phi_{xab}^{\alpha}\log\Phi_{xab}}{\Phi_{xab}^{\alpha}+\theta\mathrm{e}^{-\alpha\left(\frac{x_i}{b}\right)^a}}\right\} \\
&\times \left\{\sum_{i=1}^{n}\frac{\theta\left(\frac{x_i}{b}\right)^a\mathrm{e}^{-\alpha\left(\frac{x_i}{b}\right)^a}-\left(\frac{x_i}{b}\right)^a\Phi_{xab}^{\alpha-1}\mathrm{e}^{-\left(\frac{x_i}{b}\right)^a}}{\Phi_{xab}^{\alpha}+\theta\mathrm{e}^{-\alpha\left(\frac{x_i}{b}\right)^a}}\right\} \\
&= \frac{\partial^2 l_w\left(x_i;\boldsymbol{\xi};\boldsymbol{\tau}\right)}{\partial b\partial\alpha},
\end{aligned}
$$

$$
\begin{aligned}
\frac{\partial^2 l_w\left(x_i;\boldsymbol{\xi};\boldsymbol{\tau}\right)}{\partial\theta\partial a} &= -2\alpha\theta\sum_{i=1}^{n}\frac{\left(\frac{x_i}{b}\right)^a\mathrm{e}^{-2\alpha\left(\frac{x_i}{b}\right)^a}\log\left(\frac{x_i}{b}\right)}{\left\{\Phi_{xab}^{\alpha}+\theta\mathrm{e}^{-\alpha\left(\frac{x_i}{b}\right)^a}\right\}^2} \\
&+ 2\alpha\sum_{i=1}^{n}\frac{\left(\frac{x_i}{b}\right)^a\mathrm{e}^{-\alpha\left(\frac{x_i}{b}\right)^a}\log\left(\frac{x_i}{b}\right)}{\Phi_{xab}^{\alpha}+\theta\mathrm{e}^{-\alpha\left(\frac{x_i}{b}\right)^a}} \\
&+ 2\alpha\sum_{i=1}^{n}\frac{\left(\frac{x_i}{b}\right)^a\mathrm{e}^{-\alpha\left(\frac{x_i}{b}\right)^a}\mathrm{e}^{-\left(\frac{x_i}{b}\right)^a}\Phi_{xab}^{\alpha-1}\log\left(\frac{x_i}{b}\right)}{\left\{\Phi_{xab}^{\alpha}+\theta\mathrm{e}^{-\alpha\left(\frac{x_i}{b}\right)^a}\right\}^2} = \frac{\partial^2 l_w\left(x_i;\boldsymbol{\xi};\boldsymbol{\tau}\right)}{\partial a\partial\theta}
\end{aligned}
$$

$$
\begin{aligned}
\frac{\partial^2 l_w\left(x_i;\boldsymbol{\xi};\boldsymbol{\tau}\right)}{\partial\theta\partial b} &= \frac{2a\alpha\theta}{b}\sum_{i=1}^{n}\frac{\left(\frac{x_i}{b}\right)^a\mathrm{e}^{-2\alpha\left(\frac{x_i}{b}\right)^a}}{\left\{\Phi_{xab}^{\alpha}+\theta\mathrm{e}^{-\alpha\left(\frac{x_i}{b}\right)^a}\right\}^2} \\
&- \frac{2a\alpha}{b}\sum_{i=1}^{n}\frac{\left(\frac{x_i}{b}\right)^a\mathrm{e}^{-\alpha\left(\frac{x_i}{b}\right)^a}}{\Phi_{xab}^{\alpha}+\theta\mathrm{e}^{-\alpha\left(\frac{x_i}{b}\right)^a}} \\
&- \frac{2a\alpha}{b}\sum_{i=1}^{n}\frac{\left(\frac{x_i}{b}\right)^a\mathrm{e}^{-\alpha\left(\frac{x_i}{b}\right)^a}\mathrm{e}^{-\left(\frac{x_i}{b}\right)^a}\Phi_{xab}^{\alpha-1}}{\left\{\Phi_{xab}^{\alpha}+\theta\mathrm{e}^{-\alpha\left(\frac{x_i}{b}\right)^a}\right\}^2} = \frac{\partial^2 l_w\left(x_i;\boldsymbol{\xi};\boldsymbol{\tau}\right)}{\partial b\partial\theta}
\end{aligned}
$$

,

$$
\begin{aligned}
\frac{\partial^2 l_w\left(x_i;\boldsymbol{\xi};\boldsymbol{\tau}\right)}{\partial a \partial b} &= -\frac{n}{b}-\frac{(\alpha-1)}{b}\sum_{i=1}^{n}\frac{\left(\frac{x_i}{b}\right)^a \mathrm{e}^{-\left(\frac{x_i}{b}\right)^a}}{\Phi_{xab}}+\frac{a\alpha}{b}\sum_{i=1}^{n}\left(\frac{x_i}{b}\right)^a \log\left(\frac{x_i}{b}\right)\\
&+ \frac{a(\alpha-1)}{b}\sum_{i=1}^{n}\frac{\left(\frac{x_i}{b}\right)^{2a} \mathrm{e}^{-\left(\frac{x_i}{b}\right)^a}\log\left(\frac{x_i}{b}\right)}{\Phi_{xab}}+\frac{a(\alpha-1)}{b}\sum_{i=1}^{n}\frac{\left(\frac{x_i}{b}\right)^{2a} \mathrm{e}^{-2\left(\frac{x_i}{b}\right)^a}\log\left(\frac{x_i}{b}\right)}{\Phi_{xab}^2}\\
&- \frac{a(\alpha-1)}{b}\sum_{i=1}^{n}\frac{\left(\frac{x_i}{b}\right)^{a} \mathrm{e}^{-\left(\frac{x_i}{b}\right)^a}\log\left(\frac{x_i}{b}\right)}{\Phi_{xab}}+\frac{\alpha}{b}\sum_{i=1}^{n}\left(\frac{x_i}{b}\right)^a\\
&+ \frac{2a\alpha^2\theta}{b}\sum_{i=1}^{n}\frac{\left(\frac{x_i}{b}\right)^{2a} \mathrm{e}^{-\alpha\left(\frac{x_i}{b}\right)^a}\log\left(\frac{x_i}{b}\right)}{\Phi_{xab}^{\alpha}+\theta \mathrm{e}^{-\alpha\left(\frac{x_i}{b}\right)^a}}\\
&+ \frac{2a\alpha^2}{b}\sum_{i=1}^{n}\frac{\left(\frac{x_i}{b}\right)^{2a} \Phi_{xab}^{\alpha-2}\mathrm{e}^{-2\left(\frac{x_i}{b}\right)^a}\log\left(\frac{x_i}{b}\right)}{\Phi_{xab}^{\alpha}+\theta \mathrm{e}^{-\alpha\left(\frac{x_i}{b}\right)^a}}\\
&- \frac{2a\alpha}{b}\sum_{i=1}^{n}\frac{\left(\frac{x_i}{b}\right)^{2a} \Phi_{xab}^{\alpha-1}\mathrm{e}^{-\left(\frac{x_i}{b}\right)^a}\log\left(\frac{x_i}{b}\right)}{\Phi_{xab}^{\alpha}+\theta \mathrm{e}^{-\alpha\left(\frac{x_i}{b}\right)^a}}\\
&- \frac{2a\alpha}{b}\sum_{i=1}^{n}\frac{\left(\frac{x_i}{b}\right)^{2a} \Phi_{xab}^{\alpha-2}\mathrm{e}^{-2\left(\frac{x_i}{b}\right)^a}\log\left(\frac{x_i}{b}\right)}{\Phi_{xab}^{\alpha}+\theta \mathrm{e}^{-\alpha\left(\frac{x_i}{b}\right)^a}}\\
&- \frac{2a\alpha\theta}{b}\sum_{i=1}^{n}\frac{\left(\frac{x_i}{b}\right)^{a} \mathrm{e}^{-\alpha\left(\frac{x_i}{b}\right)^a}\log\left(\frac{x_i}{b}\right)}{\Phi_{xab}^{\alpha}+\theta \mathrm{e}^{-\alpha\left(\frac{x_i}{b}\right)^a}}\\
&+ \frac{2a\alpha}{b}\sum_{i=1}^{n}\frac{\left(\frac{x_i}{b}\right)^{a} \Phi_{xab}^{\alpha-1}\mathrm{e}^{-\left(\frac{x_i}{b}\right)^a}\log\left(\frac{x_i}{b}\right)}{\Phi_{xab}^{\alpha}+\theta \mathrm{e}^{-\alpha\left(\frac{x_i}{b}\right)^a}}\\
&- \frac{2\alpha\theta}{b}\sum_{i=1}^{n}\frac{\left(\frac{x_i}{b}\right)^{a} \mathrm{e}^{-\alpha\left(\frac{x_i}{b}\right)^a}}{\Phi_{xab}^{\alpha}+\theta \mathrm{e}^{-\alpha\left(\frac{x_i}{b}\right)^a}}\\
&+ \frac{2\alpha}{b}\sum_{i=1}^{n}\frac{\left(\frac{x_i}{b}\right)^{a} \Phi_{xab}^{\alpha-1}\mathrm{e}^{-\left(\frac{x_i}{b}\right)^a}}{\Phi_{xab}^{\alpha}+\theta \mathrm{e}^{-\alpha\left(\frac{x_i}{b}\right)^a}}\\
&- 2a\alpha^2\sum_{i=1}^{n}\log\left(\frac{x_i}{b}\right)\left\{\sum_{i=1}^{n}\frac{\theta\left(\frac{x_i}{b}\right)^{a} \mathrm{e}^{-\alpha\left(\frac{x_i}{b}\right)^a}-\left(\frac{x_i}{b}\right)^{a} \Phi_{xab}^{\alpha-1}\mathrm{e}^{-\left(\frac{x_i}{b}\right)^a}}{\Phi_{xab}^{\alpha}+\theta \mathrm{e}^{-\alpha\left(\frac{x_i}{b}\right)^a}}\right\}^2\\
&= \frac{\partial^2 l_w\left(x_i;\boldsymbol{\xi};\boldsymbol{\tau}\right)}{\partial b \partial a}
\end{aligned}
$$

APPENDIX C – HESSIAN FOR THE TMOBS MODEL

$$
\begin{aligned}
\frac{\partial^2 l(x_i;\boldsymbol{\xi},\boldsymbol{\tau})}{\partial\alpha^2} &= \frac{n\log\nu}{\alpha} - \frac{n\left(\alpha\log\nu+1\right)}{\alpha^2} \\
&- 2\nu^{\alpha}\sum_{i=1}^{n}\frac{\mathrm{e}^{-\alpha\omega(x_i,\lambda,\beta)}\log\nu^2 + 2\theta\Omega^{\alpha}\log\Omega^2}{\nu^{\alpha}\mathrm{e}^{-\alpha\omega(x_i,\lambda,\beta)}+\theta\Omega^{\alpha}} \\
&+ \frac{2}{\lambda^2}\sum_{i=1}^{n}\frac{\nu^{\alpha}\mathrm{e}^{-\alpha\omega(x_i,\lambda,\beta)}\log\nu\left[\left(\frac{x_i}{\beta}\right)^{\frac{1}{2}}-\left(\frac{\beta}{x_i}\right)^{\frac{1}{2}}\right]^2}{\nu^{\alpha}\mathrm{e}^{-\alpha\omega(x_i,\lambda,\beta)}+\theta\Omega^{\alpha}} \\
&- \frac{1}{2\lambda^2}\sum_{i=1}^{n}\frac{\nu^{\alpha}\mathrm{e}^{-\alpha\omega(x_i,\lambda,\beta)}\left[\left(\frac{x_i}{\beta}\right)^{\frac{1}{2}}-\left(\frac{\beta}{x_i}\right)^{\frac{1}{2}}\right]^4}{\nu^{\alpha}\mathrm{e}^{-\alpha\omega(x_i,\lambda,\beta)}+\theta\Omega^{\alpha}} \\
&+ 2\sum_{i=1}^{n}\frac{\Theta^2_{\alpha\lambda\beta}(x_i)-\Psi^2_{\alpha mp\lambda\beta}(x_i)}{\left\{\nu^{\alpha}\mathrm{e}^{-\alpha\omega(x_i,\lambda,\beta)}+\theta\Omega^{\alpha}\right\}^2},
\end{aligned}
$$

where

$$
\begin{aligned}
\Theta_{\alpha\lambda\beta}(x_i) &= \nu^{\alpha}\mathrm{e}^{-\alpha\omega(x_i,\lambda,\beta)}\log\nu, \\
\Psi_{\alpha mp\lambda\beta}(x_i) &= \theta\left[1-\nu\mathrm{e}^{-\omega(x_i,\lambda,\beta)}\right]^{\alpha}\log\left[1-\nu\mathrm{e}^{-\omega(x_i,\lambda,\beta)}\right] \\
&- \frac{1}{2\lambda^2}\nu^{\alpha}\mathrm{e}^{-\alpha\omega(x_i,\lambda,\beta)}\left[\left(\frac{x_i}{\beta}\right)^{\frac{1}{2}}-\left(\frac{\beta}{x_i}\right)^{\frac{1}{2}}\right]^2 \\
&- \frac{1}{2\lambda^2}\nu^{\alpha}\mathrm{e}^{-\alpha\omega(x_i,\lambda,\beta)}\left[\left(\frac{x_i}{\beta}\right)^{\frac{1}{2}}-\left(\frac{\beta}{x_i}\right)^{\frac{1}{2}}\right]^2.
\end{aligned}
$$

$$
\begin{aligned}
\frac{\partial^2 l(x_i;\boldsymbol{\xi},\boldsymbol{\tau})}{\partial\theta^2} &= -\frac{n}{\theta^2}+2\sum_{i=1}^{n}\frac{\Omega^{2\alpha}}{\left\{\nu^{\alpha}\mathrm{e}^{-\alpha\omega(x_i,\lambda,\beta)}+\theta\Omega^{\alpha}\right\}^2},\\
\frac{\partial^2 l(x_i;\boldsymbol{\xi},\boldsymbol{\tau})}{\partial\lambda^2} &= \frac{6\alpha}{\lambda^4}\sum_{i=1}^{n}\frac{3\nu\varsigma^2(x_i,\beta)\left\{\theta\Omega^{\alpha-1}\mathrm{e}^{-\omega(x_i,\lambda,\beta)}-\nu\mathrm{e}^{-\alpha\omega(x_i,\lambda,\beta)}\right\}}{\nu^{\alpha}\mathrm{e}^{-\alpha\omega(x_i,\lambda,\beta)}+\theta\Omega^{\alpha}}\\
&+ \frac{\alpha}{2\pi\lambda^6}\sum_{i=1}^{n}\frac{\varsigma^4(x_i,\beta)\left\{2\pi\alpha\nu^{\alpha}\mathrm{e}^{-\alpha\omega(x_i,\lambda,\beta)}+\theta\Omega^{\alpha-2}\mathrm{e}^{-\omega(x_i,\lambda,\beta)}\right\}}{\nu^{\alpha}\mathrm{e}^{-\alpha\omega(x_i,\lambda,\beta)}+\theta\Omega^{\alpha}}\\
&- \frac{\alpha\theta}{\lambda^6}\sum_{i=1}^{n}\frac{\mathrm{e}^{-\omega(x_i,\lambda,\beta)}\varsigma^4(x_i,\beta)\left\{\nu\Omega^{\alpha-1}-\Omega^{\alpha-2}\right\}}{\nu^{\alpha}\mathrm{e}^{-\alpha\omega(x_i,\lambda,\beta)}+\theta\Omega^{\alpha}}\\
&+ \frac{2n}{\lambda^2}-\frac{3\alpha}{\lambda^4}\sum_{i=1}^{n}\varsigma^2(x_i,\beta)+\frac{3\nu(\alpha-1)}{\lambda^4}\sum_{i=1}^{n}\frac{\varsigma^2(x_i,\beta)\mathrm{e}^{-\omega(x_i,\lambda,\beta)}}{\Omega}\\
&+ \frac{(\alpha-1)}{2\pi\lambda^6}\frac{\varsigma^4(x_i,\beta)\mathrm{e}^{-\omega(x_i.\lambda,\beta)}\left\{1-2\pi\Omega\right\}}{\Omega^2}\\
&+ \frac{2}{\lambda^6}\frac{\Omega}{\left\{\nu^{\alpha}\mathrm{e}^{-\alpha\omega(x_i,\lambda,\beta)}+\theta\Omega^{\alpha}\right\}^2},\\
\frac{\partial^2 l(x_i;\boldsymbol{\xi},\boldsymbol{\tau})}{\partial\beta^2} &= -2\beta^2\sum_{i=1}^{2}\frac{1}{x_i^4\Upsilon^2(x_i,\beta)}-2\sum_{i=1}^{2}\frac{E(x_i,\alpha,m,p,\lambda,\beta)}{\nu^{\alpha}\mathrm{e}^{-\alpha\omega(x_i,\lambda,\beta)}+\theta\Omega^{\alpha}}\\
&+ \frac{1}{2\lambda^2}\sum_{i=1}^{n}\frac{\varpi_3^2-\varpi_4^2}{\left\{\nu^{\alpha}\mathrm{e}^{-\alpha\omega(x_i,\lambda,\beta)}+\theta\Omega^{\alpha}\right\}^2}+2\sum_{i=1}^{n}\frac{1}{x_i^2\Upsilon(x_i,\beta)}+\frac{n}{\beta^2}\\
&- \frac{\alpha}{2\lambda^2}\sum_{i=1}^{2}\iota(x_i,\beta)\varsigma(x_i,\beta)+\frac{\alpha}{2\lambda^2}\sum_{i=1}^{n}\iota_1(x_i,\beta)\iota_2(x_i,\beta)\\
&+ \frac{(\alpha-1)}{2\lambda^2}\sum_{i=1}^{n}\frac{\iota_3(x_i,\beta)\varsigma(x_i,\beta)\mathrm{e}^{-\omega(x_i,\lambda,\beta)}}{\Omega}\\
&- \frac{(\alpha-1)}{2\lambda^2}\sum_{i=1}^{n}\frac{\iota_1(x_i,\beta)\iota_2(x_i,\beta)\mathrm{e}^{-\omega(x_i,\lambda,\beta)}}{\Omega}\\
&- \frac{(\alpha-1)}{4\lambda^2}\sum_{i=1}^{n}\varsigma^2(x_i,\beta)\mathrm{e}^{-\omega(x_i,\lambda,\beta)}\left\{\frac{\nu\iota_2^2(x_i,\beta)}{\lambda^2\Omega}-\frac{\iota_2^2(x_i,\beta)}{2\Omega^2}\right\},\\
\frac{\partial^2 l(x_i;\boldsymbol{\xi},\boldsymbol{\tau})}{\partial\theta\partial\alpha} &= \frac{\nu^{\alpha}}{2\lambda^2}\sum_{i=1}^{n}\frac{e^{-\alpha\omega(x_i,\lambda,\beta)}\Omega^{\alpha}\left\{2\lambda^2\log\nu-\left[\left(\frac{x_i}{\beta}\right)^{\frac{1}{2}}-\left(\frac{\beta}{x_i}\right)^{\frac{1}{2}}\right]\right\}}{\left\{\nu^{\alpha}\mathrm{e}^{-\alpha\omega(x_i,\lambda,\beta)}+\theta\Omega^{\alpha}\right\}^2}\\
&- 2\sum_{i=1}^{n}\frac{\Omega^{\alpha}\log\Omega}{\nu^{\alpha}\mathrm{e}^{-\alpha\omega(x_i,\lambda,\beta)}+\theta\Omega^{\alpha}}\\
&= \frac{\partial^2 l(x_i;\boldsymbol{\xi},\boldsymbol{\tau})}{\partial\alpha\partial\theta},
\end{aligned}
$$

where

$$
\begin{aligned}
\Omega &= \left[1-\nu \mathrm{e}^{-\omega(x_i,\lambda,\beta)}\right], \\
\varpi_1 &= \alpha\theta\nu \mathrm{e}^{-\omega(x_i,\lambda,\beta)}\varsigma^2(x_i,\beta)\left[1-\nu \mathrm{e}^{-\omega(x_i,\lambda,\beta)}\right], \\
\varpi_2 &= \alpha\nu^{\alpha}\varsigma^2(x_i,\beta)\mathrm{e}^{-\alpha\omega(x_i,\lambda,\beta)}, \\
\varpi_3 &= \alpha\nu\varsigma(x_i,\beta)\iota_2(x_i,\beta)\mathrm{e}^{-\alpha\omega(x_i,\lambda,\beta)}, \\
\varpi_4 &= \alpha\nu\theta\left[1-\nu \mathrm{e}^{-\omega(x_i,\lambda,\beta)}\right]^{\alpha-1}\varsigma(x_i,\beta)\iota(x_i,\beta)\mathrm{e}^{-\omega(x_i,\beta)}, \\
\iota_1 &= \left[\frac{1}{2\beta}\left(\frac{x_i}{\beta}\right)^{\frac{1}{2}}+\frac{1}{2\beta}\left(\frac{\beta}{x_i}\right)^{\frac{1}{2}}\right], \\
\iota_2 &= \left[-\frac{1}{\beta}\left(\frac{x_i}{\beta}\right)^{\frac{1}{2}}-\frac{1}{\beta}\left(\frac{\beta}{x_i}\right)^{\frac{1}{2}}\right], \\
\iota_3 &= \left[\frac{3}{2\beta^2}\left(\frac{x_i}{\beta}\right)^{\frac{1}{2}}+\frac{1}{2\beta^2}\left(\frac{\beta}{x_i}\right)^{\frac{1}{2}}\right], \\
\varsigma(x_i,\beta) &= \left[\left(\frac{x_i}{\beta}\right)^{\frac{1}{2}}-\left(\frac{\beta}{x_i}\right)^{\frac{1}{2}}\right], \\
E(x_i,\alpha,\theta,\lambda,\beta) &= \frac{\alpha\nu}{2\lambda^2}\left\{\frac{\Delta_1\left[\iota_1(x_i,\beta)\iota_2(x_i,\beta)-\varsigma(x_i,\beta)\iota_3(x_i)\right]}{\nu^{\alpha}\mathrm{e}^{-\alpha\omega(x_i,\lambda,\beta)}+\left[1-\nu \mathrm{e}^{-\omega(x_i,\lambda,\beta)}\right]^{\alpha}}\right\} \\
&+ \frac{\nu}{2\lambda^2}\frac{\iota_2(x_i,\beta)\varsigma^3(x_i,\beta)}{\nu^{\alpha}\mathrm{e}^{-\alpha\omega(x_i,\lambda,\beta)}+\left[1-\nu \mathrm{e}^{-\omega(x_i,\lambda,\beta)}\right]^{\alpha}}\times \\
&\times \left\{\frac{1}{2}\mathrm{e}^{-\alpha\omega(x_i,\lambda,\beta)}+\frac{\alpha\theta\left[1-\nu \mathrm{e}^{-\omega(x_i,\lambda,\beta)}\right]^{\alpha-2}\iota(x_i,\beta)\mathrm{e}^{-\omega(x_i,\lambda,\beta)}}{4\pi\lambda^2}-\Delta_2\right\}, \\
\Delta_1 &= \left[\mathrm{e}^{-\alpha\omega(x_i,\lambda,\beta)}-\theta\left[1-\nu \mathrm{e}^{-\omega(x_i,\lambda,\beta)}\right]^{\alpha-1}\mathrm{e}^{-\omega(x_i,\beta)}\right], \\
\Delta_2 &= \frac{\theta\left[1-\nu \mathrm{e}^{-\omega(x_i,\lambda,\beta)}\right]^{\alpha-1}\iota(x_i,\beta)\mathrm{e}^{-\omega(x_i,\lambda,\beta)}}{2\lambda^2},
\end{aligned}
$$

$$\begin{aligned}
\frac{\partial^2 l(x_i;\boldsymbol{\xi},\boldsymbol{\tau})}{\partial\alpha\partial\lambda} &= \frac{2}{\lambda^3}\sum_{i=1}^{n}\frac{\varsigma^2(x_i,\beta)D(x_i;\alpha,m,p,\lambda,\beta)}{\nu^\alpha \mathrm{e}^{-\alpha\omega(x_i,\lambda,\beta)}+\left[1-\nu\mathrm{e}^{-\omega(x_i,\lambda,\beta)}\right]^\alpha} \\
&+ \frac{\alpha\nu}{\lambda^5}\sum_{i=1}^{n}\frac{\varsigma^4(x_i,\beta)\mathrm{e}^{-\alpha\omega(x_i,\lambda,\beta)}}{\nu^\alpha \mathrm{e}^{-\alpha\omega(x_i,\lambda,\beta)}+\left[1-\nu\mathrm{e}^{-\omega(x_i,\lambda,\beta)}\right]^\alpha} \\
&+ \frac{1}{\lambda^3}\sum_{i=1}^{n}\varsigma^2(x_i,\beta)-\frac{\nu}{\lambda^3}\frac{\varsigma^2(x_i,\beta)}{\left[1-\nu\mathrm{e}^{-\omega(x_i,\lambda,\beta)}\right]} \\
&- \frac{\nu}{\lambda^3}\sum_{i=1}^{n}\frac{\mathrm{e}^{-\omega(x_i,\lambda,\beta)}}{\left[1-\nu\mathrm{e}^{-\omega(x_i,\lambda,\beta)}\right]} \\
&- -\frac{2\alpha}{\lambda^3}\sum_{i=1}^{n}\frac{\varsigma^2(x_i,\beta)F(x_i,\boldsymbol{\xi},\boldsymbol{\tau})\left\{\nu\theta\left[1-\nu\mathrm{e}^{-\omega(x_i,\lambda,\beta)}\right]^{\alpha-1}\mathrm{e}^{-\omega(x_i,\lambda,\beta)}\right\}}{\left\{\nu^\alpha \mathrm{e}^{-\alpha\omega(x_i,\lambda,\beta)}+\theta\left[1-\nu\mathrm{e}^{-\omega(x_i,\lambda,\beta)}\right]^\alpha\right\}^2} \\
&= \frac{\partial^2 l(x_i;\boldsymbol{\xi},\boldsymbol{\tau})}{\partial\lambda\partial\alpha},
\end{aligned}$$

where

$$\begin{aligned}
D(x_i;\boldsymbol{\xi},\boldsymbol{\tau}) &= \alpha\theta\nu\left[1-\nu\mathrm{e}^{-\omega(x_i,\lambda,\beta)}\right]^{\alpha-1}\mathrm{e}^{-\omega(x_i,\lambda,\beta)}\log\left[1-\nu\mathrm{e}^{-\omega(x_i,\lambda,\beta)}\right] \\
&- \alpha\nu^\alpha\log\nu\mathrm{e}^{-\alpha\omega(x_i,\lambda,\beta)}-\nu^\alpha\mathrm{e}^{-\alpha\omega(x_i,\lambda,\beta)} \\
&- \theta\nu\left[1-\nu\mathrm{e}^{-\omega(x_i,\lambda,\beta)}\right]^{\alpha-1}\mathrm{e}^{-\omega(x_i,\lambda,\beta)}, \\
F(x_i,\boldsymbol{\xi},\boldsymbol{\tau}) &= \nu^\alpha\mathrm{e}^{-\alpha\omega(x_i,\lambda,\beta)}\left(\log\nu+\frac{\varsigma^2(x_i,\beta)}{2\lambda^2}\right) \\
&+ \theta\left[1-\nu\mathrm{e}^{-\omega(x_i,\lambda,\beta)}\right]^\alpha\log\left[1-\nu\mathrm{e}^{-\omega(x_i,\lambda,\beta)}\right],
\end{aligned}$$

$\varsigma(x_i,\beta)$ and $\omega(x_i,\lambda,\beta)$ as given above.

$$\begin{aligned}
\frac{\partial^2 l(x_i;\boldsymbol{\xi},\boldsymbol{\tau})}{\partial\lambda\partial\theta} &= -2\alpha\nu\sum_{i=1}^{n}\frac{\left[1-\nu\mathrm{e}^{-\omega(x_i,\lambda,\beta)}\right]^{\alpha-1}H_1(x_i,\boldsymbol{\xi},\boldsymbol{\tau})}{\left\{\nu^\alpha\mathrm{e}^{-\alpha\omega(x_i,\lambda,\beta)}+\theta\left[1-\nu\mathrm{e}^{-\omega(x_i,\lambda,\beta)}\right]^\alpha\right\}^2} \\
&- 2\alpha\nu\sum_{i=1}^{n}\frac{\left[1-\nu\mathrm{e}^{-\omega(x_i,\lambda,\beta)}\right]^{\alpha}H_2(x_i,\boldsymbol{\xi},\boldsymbol{\tau})}{\left\{\nu^\alpha\mathrm{e}^{-\alpha\omega(x_i,\lambda,\beta)}+\theta\left[1-\nu\mathrm{e}^{-\omega(x_i,\lambda,\beta)}\right]^\alpha\right\}^2} = \frac{\partial^2 l(x_i;\boldsymbol{\xi},\boldsymbol{\tau})}{\partial\theta\partial\lambda},
\end{aligned}$$

where,

$$\begin{aligned}
H_1(x_i,\boldsymbol{\xi},\boldsymbol{\tau}) &= \mathrm{e}^{-\omega(x_i,\lambda,\beta)}\left[\nu^\alpha\mathrm{e}^{-\alpha\omega(x_i,\lambda,\beta)}+\theta\left(1-\nu\mathrm{e}^{-\omega(x_i,\lambda,\beta)}\right)^\alpha\right]\frac{\partial\omega(x_i;\lambda,\beta)}{\partial\lambda}, \\
H_2(x_i,\boldsymbol{\xi},\boldsymbol{\tau}) &= \mathrm{e}^{-\omega(x_i,\lambda,\beta)}\left[\nu^\alpha\mathrm{e}^{-\alpha\omega(x_i,\lambda,\beta)}-\theta\left(1-\nu\mathrm{e}^{-\omega(x_i,\lambda,\beta)}\right)^{\alpha-1}\right]\frac{\partial\omega(x_i;\lambda,\beta)}{\partial\lambda},
\end{aligned}$$

$$\begin{aligned}\frac{\partial^2 l(x_i;\boldsymbol{\xi},\boldsymbol{\tau})}{\partial\alpha\partial\beta} &= -\frac{1}{\lambda^2}\sum_{i=1}^{n}\frac{\varsigma(x_i,\beta)\iota(x_i,\beta)J_1(x_i,\boldsymbol{\xi},\boldsymbol{\tau})}{\nu^{\alpha}\mathrm{e}^{-\alpha\omega(x_i,\lambda,\beta)}+\theta\left[1-\nu\mathrm{e}^{-\omega(x_i,\lambda,\beta)}\right]^{\alpha}}\\ &- \frac{1}{\lambda^2}\sum_{i=1}^{n}\frac{\varsigma(x_i,\beta)\iota(x_i,\beta)\nu^{\alpha}J_2(x_i,\boldsymbol{\xi},\boldsymbol{\tau})}{\left\{\nu^{\alpha}\mathrm{e}^{-\alpha\omega(x_i,\lambda,\beta)}+\theta\left[1-\nu\mathrm{e}^{-\omega(x_i,\lambda,\beta)}\right]^{\alpha}\right\}^2}\\ &- \frac{1}{2\lambda^2}\sum_{i=1}^{n}\varsigma(x_i,\beta)\iota_1(x_i,\beta)+\frac{\nu}{2\lambda^2}\sum_{i=1}^{n}\frac{\varsigma(x_i,\beta)\iota_2(x_i,\beta)\mathrm{e}^{-\omega(x_i,\lambda,\beta)}}{\left[1-\nu\mathrm{e}^{-\omega(x_i,\lambda,\beta)}\right]}\\ &= \frac{\partial^2 l(x_i;\boldsymbol{\xi},\boldsymbol{\tau})}{\partial\beta\partial\alpha},\end{aligned}$$

where,

$$\begin{aligned}J_1(x_i,\boldsymbol{\xi},\boldsymbol{\tau}) &= \nu^{\alpha}\mathrm{e}^{-\alpha\omega(x_i,\lambda,\beta)}\left(\frac{\alpha\varsigma^2(x_i,\beta)}{2}-\alpha\log\nu-1\right)\\ &+ \nu\theta\Omega^{\alpha-1}\mathrm{e}^{-\omega(x_i,\lambda,\beta)}\left(\alpha\log\Omega+1\right),\\ J_2(x_i,\boldsymbol{\xi},\boldsymbol{\tau}) &= \left[\alpha\nu^{\alpha}\mathrm{e}^{-\alpha\omega(x_i,\lambda,\beta)}-\nu\theta\Omega^{\alpha-1}\mathrm{e}^{-\omega(x_i,\beta)}\right]\times\\ &\times \left[\mathrm{e}^{-\alpha\omega(x_i,\lambda,\beta)}\log\nu+\theta\Omega^{\alpha}\log\Omega-\kappa(x_i,\boldsymbol{\xi},\boldsymbol{\tau})\right],\end{aligned}$$

where,

$$\begin{aligned}\kappa(x_i,\boldsymbol{\xi},\boldsymbol{\tau}) &= \frac{\mathrm{e}^{-\alpha\omega(x_i,\lambda,\beta)}\varsigma^2(x_i,\beta)}{2\lambda^2},\\ \Omega &= \left[1-\nu\mathrm{e}^{-\omega(x_i,\lambda,\beta)}\right].\end{aligned}$$

$$\begin{aligned}\frac{\partial^2 l(x_i;\boldsymbol{\xi},\boldsymbol{\tau})}{\partial\theta\partial\beta} &= \frac{\alpha\nu}{\lambda^2}\sum_{i=1}^{n}\frac{\Upsilon(x_i,\beta)}{x_i}\frac{\mathrm{e}^{-\omega(x_i,\lambda,\beta)}\left[1-\nu\mathrm{e}^{-\omega(x_i,\lambda,\beta)}\right]^{\alpha-1}}{\nu^{\alpha}\mathrm{e}^{-\alpha\omega(x_i,\lambda,\beta)}+\theta\left[1-\nu\mathrm{e}^{-\omega(x_i,\lambda,\beta)}\right]^{\alpha}}\\ &- \frac{\alpha}{\lambda^2}\sum_{i=1}^{n}\frac{\Upsilon(x_i,\beta)}{x_i}\frac{\left[1-\nu\mathrm{e}^{-\omega(x_i,\lambda,\beta)}\right]^{\alpha}M(x_i,\boldsymbol{\xi},\boldsymbol{\tau})}{\left\{\nu^{\alpha}\mathrm{e}^{-\alpha\omega(x_i,\lambda,\beta)}+\theta\left[1-\nu\mathrm{e}^{-\omega(x_i,\lambda,\beta)}\right]^{\alpha}\right\}^2}\\ &= \frac{\partial^2 l(x_i;\boldsymbol{\xi},\boldsymbol{\tau})}{\partial\beta\partial\theta},\end{aligned}$$

where

$$M(x_i,\boldsymbol{\xi},\boldsymbol{\tau})=\left[\nu^{\alpha}\mathrm{e}^{-\alpha\omega(x_i,\lambda,\beta)}+\nu\theta\left(1-\nu\mathrm{e}^{-\omega(x_i,\lambda,\beta)}\right)^{\alpha-1}\right]\mathrm{e}^{-\omega(x_i,\lambda,\beta)},$$

$$\begin{aligned}
\frac{\partial^2 l(x_i;\boldsymbol{\xi},\boldsymbol{\tau})}{\partial\beta\partial\lambda} &= \frac{2}{\lambda^3}\sum_{i=1}^{n}\frac{\varsigma(x_i,\beta)\iota(x_i,\beta)\left[\sum_{k=1}^{3}N_k(x_i,\boldsymbol{\xi},\boldsymbol{\tau})\right]}{\nu^{\alpha}\mathrm{e}^{-\alpha\omega(x_i,\lambda,\beta)}+\theta\left[1-\nu\mathrm{e}^{-\omega(x_i,\lambda,\beta)}\right]^{\alpha}} \\
&- \frac{\alpha^2}{\lambda^5}\sum_{i=1}^{n}\frac{\varsigma^3(x_i,\beta)\iota_2(x_i,\beta)P(x_i,\boldsymbol{\xi},\boldsymbol{\tau})}{\left\{\nu^{\alpha}\mathrm{e}^{-\alpha\omega(x_i,\lambda,\beta)}+\theta\left[1-\nu\mathrm{e}^{-\omega(x_i,\lambda,\beta)}\right]^{\alpha}\right\}^2} \\
&- \frac{\alpha}{\lambda^3}\sum_{i=1}^{n}\varsigma(x_i,\beta)\iota_2(x_i,\beta) \\
&- \frac{\nu(\alpha-1)}{\lambda^3}\frac{\varsigma(x_i,\beta)\iota_2(x_i,\beta)\mathrm{e}^{-\omega(x_i,\lambda,\beta)}}{\left[1-\nu\mathrm{e}^{-\omega(x_i,\lambda,\beta)}\right]} \\
&+ \frac{\nu(\alpha-1)}{2\lambda^3}\frac{\varsigma^3(x_i,\beta)\iota_2(x_i,\beta)\mathrm{e}^{-\omega(x_i,\lambda,\beta)}}{\left[1-\nu\mathrm{e}^{-\omega(x_i,\lambda,\beta)}\right]} \\
&+ \frac{\alpha-1}{4\pi\lambda^5}\frac{\varsigma^3(x_i,\beta)\iota_2(x_i,\beta)\mathrm{e}^{-\omega(x_i,\lambda,\beta)}}{\left[1-\nu\mathrm{e}^{-\omega(x_i,\lambda,\beta)}\right]^2} = \frac{\partial^2 l(x_i;\boldsymbol{\xi},\boldsymbol{\tau})}{\partial\lambda\partial\beta},
\end{aligned}$$

where,

$$\begin{aligned}
N_1(x_i,\boldsymbol{\xi},\boldsymbol{\tau}) &= \alpha^2\nu^{\alpha\varsigma^2(x_i,\beta)}\mathrm{e}^{-\alpha\omega(x_i,\lambda,\beta)}-\alpha^{\nu}\mathrm{e}^{-\alpha\omega(x_i,\lambda,\beta)} \\
&+ \nu\alpha\theta\left[1-\nu\mathrm{e}^{-\omega(x_i,\lambda,\beta)}\right]^{\alpha-1}\mathrm{e}^{-\omega(x_i,\lambda,\beta)}, \\
N_2(x_i,\boldsymbol{\xi},\boldsymbol{\tau}) &= \frac{\alpha^2\theta\left[1-\nu\mathrm{e}^{-\omega(x_i,\lambda,\beta)}\right]^{\alpha-2}\varsigma^2(x_i,\beta)\mathrm{e}^{-\omega(x_i,\lambda,\beta)}}{4\pi\lambda^2} \\
&- \frac{\nu\alpha\theta\left[1-\nu\mathrm{e}^{-\omega(x_i,\lambda,\beta)}\right]^{\alpha-1}\varsigma^2(x_i,\beta)\mathrm{e}^{-\omega(x_i,\lambda,\beta)}}{2\lambda^2}, \\
N_3(x_i,\boldsymbol{\xi},\boldsymbol{\tau}) &= -\frac{\alpha\theta\left[1-\nu\mathrm{e}^{-\omega(x_i,\lambda,\beta)}\right]^{\alpha-2}\varsigma^2(x_i,\beta)\mathrm{e}^{-\omega(x_i,\lambda,\beta)}}{4\pi\lambda^2}, \\
P(x_i,\boldsymbol{\xi},\boldsymbol{\tau}) &= \left\{\nu\theta\left[1-\nu\mathrm{e}^{-\omega(x_i,\lambda,\beta)}\right]^{\alpha-1}\mathrm{e}^{-\omega(x_i,\lambda,\beta)}-\nu^{\alpha}\mathrm{e}^{-\alpha\omega(x_i,\lambda,\beta)}\right\}\times \\
&\times \left\{\nu\theta\left[1-\nu\mathrm{e}^{-\omega(x_i,\lambda,\beta)}\right]\mathrm{e}^{-\omega(x_i,\lambda,\beta)}-\nu^{\alpha}\mathrm{e}^{-\alpha\omega(x_i,\lambda,\beta)}\right\},
\end{aligned}$$

APPENDIX D – HESSIAN FOR THE TMOBXII MODEL

$$
\begin{aligned}
\frac{\partial^2 l(x_i;\boldsymbol{\xi},\boldsymbol{\tau})}{\partial\alpha^2} &= -\frac{n}{\alpha^2} - 2\sum_{i=1}^{n}\frac{(\zeta^\kappa-1)^\alpha \log(\zeta^\kappa-1)^2}{\theta+(\zeta^\kappa-1)^\alpha} + 2\sum_{i=1}^{n}\frac{(\zeta^\kappa-1)^{2\alpha}\log(\zeta^\kappa-1)^2}{[\theta+(\zeta^\kappa-1)^\alpha]^2},\\
\frac{\partial^2 l(x_i;\boldsymbol{\xi},\boldsymbol{\tau})}{\partial\theta^2} &= -\frac{n}{\theta^2} + 2\sum_{i=1}^{n}\frac{1}{[\theta+(\zeta^\kappa-1)^\alpha]^2},\\
\frac{\partial^2 l(x_i;\boldsymbol{\xi},\boldsymbol{\tau})}{\partial\rho^2} &= \frac{\mathcal{H}_1(x_x;\boldsymbol{\xi},\boldsymbol{\tau})}{\rho^2R^2(x_i,\boldsymbol{\xi},\boldsymbol{\eta})\zeta^{15}Q^{10}(x_i,\boldsymbol{\xi},\boldsymbol{\eta})},
\end{aligned}
$$

where,

$$
\begin{aligned}
\mathcal{H}_1(x_i;\boldsymbol{\xi},\boldsymbol{\tau}) &= 2(\alpha\kappa\rho P)^2\zeta^{2\kappa+13}Q^{2\alpha+8}S + 2\alpha(1-\alpha)(\kappa\rho P)^2 R\zeta^{2\kappa+13}Q^{\alpha+8}S\\
&+ 2\alpha\kappa(1-\kappa)\rho^2P^2\zeta^{\kappa+13}Q^{\alpha+9}S - 2\alpha\kappa\rho^2PR\zeta^{\kappa+14}Q^{\alpha+9}S\\
&+ (1-\alpha)(\kappa\rho PR)^2\zeta^{2\kappa+13}Q^8S + \kappa(\alpha-1)(\kappa-1)(\rho PR)^2\zeta^{\kappa+13}Q^9S\\
&+ \kappa(\alpha-1)\rho^2PR^2\zeta^{\kappa+14}Q^9S - n\rho R^2\zeta^{15}Q^{10}\log\sigma + nR^2(\rho\log\sigma-1)\zeta^{15}Q^{10}\\
&+ (1-\kappa)(\rho PR)^2\zeta^{13}Q^{10}S + (\kappa-1)P(\rho R)^2\zeta^{14}Q^{10}S,
\end{aligned}
$$

and

$$
\begin{aligned}
P = P(x_i,\boldsymbol{\xi},\boldsymbol{\eta}) &= \left(\frac{x_i}{\sigma}\right)^\rho,\\
Q = Q(x_i,\boldsymbol{\xi},\boldsymbol{\eta}) &= (\zeta^\kappa-1),\\
R = R(x_i,\boldsymbol{\xi},\boldsymbol{\eta}) &= [\theta+Q^\alpha(x_i,\boldsymbol{\xi},\boldsymbol{\eta})],\\
S = S(x_i,\boldsymbol{\xi},\boldsymbol{\eta}) &= \log\left(\frac{x_i}{\sigma}\right)^2,
\end{aligned}
$$

with,

$$
\begin{aligned}
\zeta &= 1+\left(\frac{x_i}{\sigma}\right)^\rho\\
&= 1+P(x_i,\boldsymbol{\xi},\boldsymbol{\eta}).
\end{aligned}
$$

$$
\begin{aligned}
\frac{\partial^2 l(x_i;\boldsymbol{\xi},\boldsymbol{\tau})}{\partial\kappa^2} &= -\frac{n}{\kappa^2} - 2\alpha^2\sum_{i=1}^{n}\frac{\zeta^{2\kappa}Q^{\alpha-2}\log(\zeta)^2}{R} + 2\alpha^2\sum_{i=1}^{n}\frac{\zeta^{2\kappa}Q^{2(\alpha-1)}\log(\zeta)^2}{R^2}\\
&+ 2\alpha\sum_{i=1}^{n}\frac{\zeta^{2\kappa}Q^{\alpha-2}\log(\zeta^2)}{R} - 2\alpha\sum_{i=1}^{n}\frac{\zeta^\kappa Q^{\alpha-1}\log(\zeta^2)}{R}\\
&- (\alpha-1)\sum_{i=1}^{n}\frac{\zeta^{2\kappa}\log(\zeta^2)}{Q^2} + (\alpha-1)\sum_{i=1}^{n}\frac{\zeta^\kappa\log(\zeta^2)}{Q},\\
\frac{\partial^2 l(x_i;\boldsymbol{\xi},\boldsymbol{\tau})}{\partial\sigma^2} &= \frac{\mathcal{H}_2(x_x;\boldsymbol{\xi},\boldsymbol{\tau})}{\sigma^2R^2(x_i,\boldsymbol{\xi},\boldsymbol{\eta})\zeta^{15}Q^{10}(x_i,\boldsymbol{\xi},\boldsymbol{\eta})},
\end{aligned}
$$

where,

$$
\begin{aligned}
\mathcal{H}_2(x_i;\boldsymbol{\xi},\boldsymbol{\tau}) &= 2\left(\alpha\kappa\rho P\right)^2\zeta^{2\kappa+13}Q^{2\alpha+8}S + 2\alpha(1-\alpha)\left(\kappa\rho P\right)^2 R\zeta^{2\kappa+13}Q^{\alpha+8} \\
&+ 2\alpha\kappa(1-\kappa)\rho^2P^2\zeta^{\kappa+13}Q^{\alpha+9} - 2\alpha\kappa\rho(\rho+1)PR\zeta^{\kappa+14}Q^{\alpha+9} \\
&+ (1-\alpha)\left(\kappa\rho PR\right)^2\zeta^{2\kappa+13}Q^8 + \kappa(\alpha-1)(\kappa-1)\left(\rho PR\right)^2\zeta^{\kappa+13}Q^9 \\
&+ \kappa\rho(\alpha-1)(\rho+1)PR^2\zeta^{\kappa+14}Q^9 + n\rho R^2\zeta^{15}Q^{10} + (1-\kappa)\left(\rho PR\right)^2\zeta^{13}Q^{10} \\
&- \rho(1-\kappa)(\rho+1)PR^2\zeta^{14}Q^{10}.
\end{aligned}
$$

$$
\begin{aligned}
\frac{\partial^2 l(x_i;\boldsymbol{\xi},\boldsymbol{\tau})}{\partial\alpha\partial\theta} &= 2\sum_{i=1}^{n}\frac{Q^\alpha\log Q}{R^2} = \frac{\partial^2 l(x_i;\boldsymbol{\xi},\boldsymbol{\tau})}{\partial\theta\partial\alpha}, \\
\frac{\partial^2 l(x_i;\boldsymbol{\xi},\boldsymbol{\tau})}{\partial\alpha\partial\rho} &= \kappa\sum_{i=1}^{n}\frac{P\zeta^{\kappa-1}}{R^2}\left\{2\alpha Q^{2\alpha-1}\log Q - 2\alpha Q^{\alpha-1}\log\left(Q+1\right)R + R^2Q^{-1}\right\}\sqrt{S} \\
&= \frac{\partial^2 l(x_i;\boldsymbol{\xi},\boldsymbol{\tau})}{\partial\rho\partial\alpha}, \\
\frac{\partial^2 l(x_i;\boldsymbol{\xi},\boldsymbol{\tau})}{\partial\alpha\partial\kappa} &= -2\alpha\sum_{i=1}^{n}\frac{\zeta^\kappa Q^{\alpha-1}\log\zeta\log Q}{R} + 2\alpha\sum_{i=1}^{n}\frac{\zeta^\kappa Q^{2\alpha-1}\log\zeta\log Q}{R^2} \\
&+ \sum_{i=1}^{n}\frac{\zeta^\kappa\log\zeta}{Q} - 2\sum_{i=1}^{n}\frac{\zeta^\kappa Q^{\alpha-1}\log\zeta}{R} = \frac{\partial^2 l(x_i;\boldsymbol{\xi},\boldsymbol{\tau})}{\partial\kappa\partial\alpha}, \\
\frac{\partial^2 l(x_i;\boldsymbol{\xi},\boldsymbol{\tau})}{\partial\alpha\partial\sigma} &= \frac{2\alpha\kappa\rho}{\sigma}\sum_{i=1}^{n}\frac{P\zeta^{\kappa-1}Q^{2\alpha-1}\log Q}{R} - \frac{2\alpha\kappa\rho}{\sigma}\sum_{i=1}^{n}\frac{P\zeta^{\kappa-1}Q^{\alpha-1}\log Q}{R^2} \\
&- \frac{\kappa\rho}{\sigma}\sum_{i=1}^{n}\frac{P\zeta^{\kappa-1}}{Q} + \frac{2\kappa\rho}{\sigma}\sum_{i=1}^{n}\frac{P\zeta^{\kappa-1}Q^{\alpha-1}}{R} = \frac{\partial^2 l(x_i;\boldsymbol{\xi},\boldsymbol{\tau})}{\partial\sigma\partial\alpha}, \\
\frac{\partial^2 l(x_i;\boldsymbol{\xi},\boldsymbol{\tau})}{\partial\theta\partial\rho} &= \frac{2\alpha\kappa}{\rho}\sum_{i=1}^{n}\frac{P\zeta^{\kappa-1}Q^{\alpha-1}\log P}{R^2} = \frac{\partial^2 l(x_i;\boldsymbol{\xi},\boldsymbol{\tau})}{\partial\rho\partial\theta}, \\
\frac{\partial^2 l(x_i;\boldsymbol{\xi},\boldsymbol{\tau})}{\partial\theta\partial\kappa} &= 2\alpha\sum_{i=1}^{n}\frac{\zeta^\kappa Q^{\alpha-1}\log\zeta}{R^2} = \frac{\partial^2 l(x_i;\boldsymbol{\xi},\boldsymbol{\tau})}{\partial\kappa\partial\theta}, \\
\frac{\partial^2 l(x_i;\boldsymbol{\xi},\boldsymbol{\tau})}{\partial\theta\partial\sigma} &= -\frac{2\alpha\kappa\rho}{\sigma}\sum_{i=1}^{n}\frac{P\zeta^{\kappa-1}Q^{\alpha-1}}{R^2} = \frac{\partial^2 l(x_i;\boldsymbol{\xi},\boldsymbol{\tau})}{\partial\sigma\partial\theta}, \\
\frac{\partial^2 l(x_i;\boldsymbol{\xi},\boldsymbol{\tau})}{\partial\rho\partial\kappa} &= \frac{1}{\rho}\sum_{i=1}^{n}\frac{P\log P}{\zeta} - \frac{2\alpha\kappa}{\rho}\sum_{i=1}^{n}\frac{\zeta^{2\kappa-1}Q^{\alpha-2}\log P\log\zeta}{R} + \frac{(\alpha-1)}{\rho}\sum_{i=1}^{n}\frac{P\zeta^{\kappa-1}\log P}{Q} \\
&+ \frac{n}{\kappa}\left(1-\log\sigma\right) + \frac{\kappa(\alpha-1)}{\rho}\sum_{i=1}^{n}P\log P\log\zeta\left[\frac{\zeta^{\kappa-1}}{Q}\left(1-\frac{\zeta^\kappa}{Q}\right)\right] \\
&- \frac{2\alpha}{\rho}\sum_{i=1}^{n}\frac{P\zeta^{\kappa-1}Q^{\alpha-1}\log P}{R} - \frac{2\alpha\kappa}{\rho}\sum_{i=1}^{n}\frac{P\log P\log\zeta\left[\zeta^{\kappa-1}Q^{\alpha-1}\right]}{R} \\
&+ \frac{2\alpha\kappa}{\rho}\sum_{i=1}^{n}\frac{\zeta^{2\kappa-1}Q^{\alpha-2}P\log P\log\zeta}{R} = \frac{\partial^2 l(x_i;\boldsymbol{\xi},\boldsymbol{\tau})}{\partial\kappa\partial\rho},
\end{aligned}
$$

$$
\begin{aligned}
\frac{\partial^2 l(x_i;\boldsymbol{\xi},\boldsymbol{\tau})}{\partial\rho\partial\sigma} &= \frac{2\alpha^2\kappa^2\rho^2}{\sigma}\sum_{i=1}^{n}\frac{\left(P\zeta^{\kappa-1}\right)^2 Q^{\alpha-2}\log P}{R} - \frac{2\alpha^2\kappa^2\rho^2}{\sigma}\sum_{i=1}^{n}\frac{\left[P\zeta^{\kappa-1}Q^{\alpha-1}\right]^2\log P}{R^2} \\
&- \frac{2\alpha\kappa^2\rho^2}{\sigma}\sum_{i=1}^{n}\frac{\left(P\zeta^{\kappa-1}\right)^2 Q^{\alpha-2}\log P}{R} + \frac{2\alpha\kappa^2\rho}{\sigma}\sum_{i=1}^{n}\frac{P^2\zeta^{\kappa-2}Q^{\alpha-1}\log P}{R} \\
&- \frac{2\alpha\kappa\rho}{\sigma}\sum_{i=1}^{n}\frac{P^2\zeta^{\kappa-2}Q^{\alpha-1}\log P}{R} + \frac{2\alpha\kappa\rho^2}{\sigma}\sum_{i=1}^{n}\frac{P\zeta^{\kappa-1}Q^{\alpha-1}\log P}{R} \\
&+ \frac{2\alpha\kappa}{\sigma}\sum_{i=1}^{n}\frac{P\zeta^{\kappa-1}Q^{\alpha-1}}{R} + \frac{\kappa^2\rho^2(\alpha-1)}{\sigma}\sum_{i=1}^{n}\frac{P^2\left(\zeta^{\kappa-1}\right)^2\log P}{Q^2} \\
&- \frac{\kappa^2\rho^2(\alpha-1)}{\sigma}\sum_{i=1}^{n}\frac{P^2\zeta^{\kappa-2}\log P}{Q} + \frac{\kappa\rho^2(\alpha-1)}{\sigma}\sum_{i=1}^{n}\frac{P^2\zeta^{\kappa-2}\log P}{Q} \\
&- \frac{\kappa\rho^2(\alpha-1)}{\sigma}\sum_{i=1}^{n}\frac{P\zeta^{\kappa-1}\log P}{Q} - \frac{\kappa(\alpha-1)}{\sigma}\sum_{i=1}^{n}\frac{P\zeta^{\kappa-1}}{Q} \\
&- \frac{\rho^2(\kappa-1)}{\sigma}\sum_{i=1}^{n}\frac{P}{\zeta}\log P + \frac{n}{\sigma}\sum_{i=1}^{n}(1-\rho\log\sigma) + \frac{n}{\sigma}\sum_{i=1}^{n}(\rho\log\sigma-2) \\
&+ \frac{\kappa-1}{\sigma}\sum_{i=1}^{n}\frac{P}{\zeta} + \frac{\rho^2(\kappa-1)}{\sigma}\sum_{i=1}^{n}\frac{P^2\log P}{\zeta^2} = \frac{\partial^2 l(x_i;\boldsymbol{\xi},\boldsymbol{\tau})}{\partial\sigma\partial\rho}, \\
\frac{\partial^2 l(x_i;\boldsymbol{\xi},\boldsymbol{\tau})}{\partial\kappa\partial\sigma} &= \frac{2\alpha^2\kappa\rho}{\sigma}\sum_{i=1}^{n}\frac{P\zeta^{2\kappa-1}Q^{\alpha-1}\log\zeta}{R^2} - \frac{2\alpha^2\kappa\rho}{\sigma}\sum_{i=1}^{n}\frac{P\zeta^{2\kappa-1}Q^{2\alpha-2}\log\zeta}{R^2} \\
&- \frac{2\alpha\kappa\rho}{\sigma}\sum_{i=1}^{n}\frac{P\zeta^{2\kappa-1}Q^{2\alpha-2}\log\zeta}{R} + \frac{2\alpha\rho}{\sigma}\sum_{i=1}^{n}\frac{P\zeta^{\kappa-1}Q^{\alpha-1}}{R} \\
&+ \frac{\kappa\rho(\alpha-1)}{\sigma}\sum_{i=1}^{n}\frac{P\zeta^{2\kappa-1}\log\zeta}{Q^2} - \frac{\kappa\rho(\alpha-1)}{\sigma}\sum_{i=1}^{n}\frac{P\zeta^{2\kappa-1}\log\zeta}{Q} \\
&- \frac{\rho(\alpha-1)}{\sigma}\sum_{i=1}^{n}\frac{P\zeta^{\kappa-1}}{Q} - \frac{\rho(\alpha-1)}{\sigma}\sum_{i=1}^{n}\frac{P}{Q} \\
&= \frac{\partial^2 l(x_i;\boldsymbol{\xi},\boldsymbol{\tau})}{\partial\sigma\partial\kappa}.
\end{aligned}
$$